THESIS

presented to

UNIVERSITE DE PARIS SUD

(Ecole Doctorale MIPEGE, Orsay)
(Institute de Physique Nucléaire, Orsay)

by

Robert Bright Mawuko SOGBADJI

for the award of

Docteur en Sciences Physique Nucléaire de L'Université de Paris Sud XI

NEUTRONIC STUDY OF THE MONO-RECYCLING OF AMERICIUM IN PWR
AND OF THE CORE CONVERSION IN MNSR USING THE MURE CODE

<u>Directeurs de thèse:</u> BERNARD Berthier, DAVID Sylvain IPN, Orsay
        AKAHO Edward, NYARKO Benjamin GSNAS, Legon

Date of thesis defense: 11 July 2012

Composition of jury:

<u>Président du jury:</u> DESESQUELLES Pierre CNRS/IN2P3 IPN Orsay
<u>Rapporteurs:</u>   DESSAGNE Philippe   CNRS/IN2P3 IPHC Strasbourg
       NUTTIN Alexis   INPG LPSC Grenoble
<u>Examinateur:</u>   BACRI Charles-Olivier CNRS/IN2P3 IPN Orsay
       BILLEBAUD Annick   INPG LPSC Grenoble
<u>Co-Directeur de thèse:</u> DAVID Sylvain   CNRS/IN2P3 IPN Orsay

DEDICATION

To my loving father, Christian Yao Sogbadji,

To my sweetheart, Alice Ofosua Asiedu

ACKNOWLEDGMENT

Above all, I thank the Lord God Almighty for His gift of life and all things, His holy name is praised.

TABLE OF CONTENT

ABSTRACT

The MURE code is based on the coupling of a Monte Carlo static code and the calculation of the evolution of the fuel during irradiation and cooling periods. The MURE code has been used to analyse two different questions, concerning the mono-recycling of Am in present French Pressurized Water Reactor, and the conversion of high enriched uranium (HEU) used in the Miniature Neutron Source Reactor in Ghana into low enriched uranium (LEU) due to proliferation resistance issues. In both cases, a detailed comparison is made on burnup and the induced radiotoxicity of waste or spent fuel. The UOX fuel assembly, as in the open cycle system, was designed to reach a burn-up of 46GWd/t and 68GWd/t. The spent UOX was reprocessed to fabricate MOX assemblies, by the extraction of Plutonium and addition of depleted Uranium to reach burn-ups of 46GWd/t and 68GWd/t, taking into account various cooling times of the spent UOX assembly in the repository. The effect of cooling time on burnup and radiotoxicity was then ascertained. Spent UOX fuel, after 30 years of cooling in the repository required higher concentration of Pu to be reprocessed into a MOX fuel due to the decay of Pu-241. Americium, with a mean half-life of 432 years, has high radiotoxic level, high mid-term residual heat and a precursor for other long lived isotope. An innovative strategy consists of reprocessing not only the plutonium from the UOX spent fuel but also the americium isotopes which dominate the radiotoxicity of present waste. The mono-recycling of Am is not a definitive solution because the once-through MOX cycle transmutation of Am in a PWR is not enough to destroy all the Am. The main objective is to propose a "waiting strategy" for both Am and Pu in the spent fuel so that they can be made available for further transmutation strategies. The MOXAm (MOX and Americium isotopes) fuel was fabricated to see the effect of americium in MOX fuel on the burn-up, neutronic behavior and on radiotoxicity. The MOXAm fuel showed relatively good indicators both on burnup and on radiotoxicity. A 68GWd/t MOX assembly produced from a reprocessed spent 46GWd/t UOX assembly showed a decrease in radiotoxicity as compared to the open cycle. All fuel types understudy in the PWR cycle showed good safety inherent feature with the exception of the some MOXAm assemblies which have a positive void coefficient in specific configurations, which could not be consistent with safety inherent features. The core lifetimes of the current operating 90.2% HEU UAl fuel and the proposed 12.5% LEU UOX fuel of the MNSR were investigated using MURE code. Even though LEU core has a longer core life due to its higher core loading and low rate of uranium consumption, the LEU

core will have it first beryllium top up to compensate for reactivity at earlier time than the HEU core. The HEU and LEU cores of the MNSR exhibited similar neutron fluxes in irradiation channels, negative void coefficient but the LEU is more radiotoxic after fission product decay due to higher actinides presence at the end of its core lifetime.

CHAPTER ONE

1 GENERAL INTRODUCTION

1.1 INTRODUCTION

When a relatively large fissile atomic nucleus (usually uranium-235 or plutonium-239) absorbs a neutron, a fission of the atom often results. Fission splits the atom into two or more smaller nuclei with kinetic energy (known as fission products) and also releases gamma radiation and free neutrons. A portion of these neutrons may later be absorbed by other fissile atoms and create new fission, which release other neutrons, and so on. This nuclear chain reaction can be controlled by using neutron poisons and neutron moderators to change the portion of neutrons that will go on to cause more fission. Nuclear reactors generally have automatic and manual systems to shut the fission reaction down if unsafe conditions are detected.

A cooling system removes heat from the reactor core and transports it to another area of the plant, where the thermal energy can be harnessed to produce electricity or to do other useful work. Typically the hot coolant will be used as a heat source for a boiler, and the pressurized steam from that boiler will power one or more steam turbine driven electrical generators [1]. There two main types of fission reactors, power reactors and research reactors.

In this work, both types of reactors are understudy for mainly two reasons;

- the mono-recycling of americium in the UOX once-through cycle of the Pressurized Water Reactor (PWR), (standard French power reactor). All water-cooled reactors store spent nuclear fuel, once it has been unloaded from the reactor, at the reactor site in an underwater pool. Originally it was planned that spent fuel would be shipped off site after some years of cooling; the fuel would then go for reprocessing or direct disposal. In practice, reprocessing is currently carried out in France, and permanent disposal of spent fuel has not yet taken place. The need for storage has thus increased. The cooling time before the heat generation of spent fuel has declined to a level suitable for disposal in a geological repository is between 30 and 50 years. In current reprocessing facilities, used fuel is separated into its three components: uranium, plutonium, which both can be recycled into fresh fuel, and waste containing fission products and minor actinides (Am, Np, Cm). The plutonium can either be

stored or made directly into mixed oxide (MOX) fuel, in which uranium and plutonium oxides are combined. The waste is then treated to produce vitrified blocks incorporating most of the highly radioactive materials and other low- and intermediate-level radioactive technological wastes. Am combined in the glasses is produced essentially during the cooling period after irradiation by the decay of Pu-241. Am-241is responsible for the high mid-term residual heat, this is the main dimensioning parameter for geological waste repository. Hence, it will be very interesting to reprocess the Am together with the Pu to minimize the mid-term residual heat and also radiotoxicity of the waste. The vitrified waste is a high-quality standardized product well suited for geological disposal. The technological waste is of much lower activity, and much of it can go to near-surface disposal sites. However, there are problems associated with each output stream. Plutonium in MOX are unstable in storage because of the buildup of Am-241. After conversion and enrichment, the uranium from reprocessing can be reused as fuel, if necessary.

- the core convention of the High Enriched Uranium (HEU) fuel to a Low Enriched Uranium (LEU) fuel of the Miniature Neutron Source Reactor (MNSR), (research reactor). Many of the world's nuclear reactors are used for research and training, materials testing, or the production of radioisotopes for medicine and industry. They are basically neutron factories. These are much smaller than power reactors or those propelling ships, and many are on university campuses. There are about 240 such reactors operating, in 56 countries. Some operate with high-enriched uranium fuel, and international efforts are underway to substitute low-enriched fuel. Some radioisotope production also uses high-enriched uranium as target material for neutrons, and this is being phased out in favour of low-enriched uranium. Since 1978, various national and international activities have been underway to convert research and test reactors from the use of HEU to LEU fuel. These activities support the objective of reducing and eventually eliminating the civil use of HEU. Achieving the conversion of all MNSR reactors would be a helpful step forward in this international effort to reduce and eventually eliminate the civil use of HEU.

1.2 REACTORS TYPES CONSIDERED

There are many different reactor designs, utilizing different fuels and coolants and incorporating different control schemes. Some of these designs have been engineered to meet a specific need. Reactors for nuclear submarines and large naval ships, for example, commonly use highly

enriched uranium as a fuel. This fuel choice increases the reactor's power density and extends the usable life of the nuclear fuel load, but is more expensive and a greater risk to nuclear proliferation than some of the other nuclear fuels.

In the relatively short history of nuclear power, many types of reactors have been proposed for the production of steam. Power reactor systems consist primarily of five types of reactors: (a) pressurized water and boiling water reactors, which produce steam directly in the core and are the mainstay of the nuclear power industry; (b) evolutionary pressurized water reactors, which have the basic elements of pressurized water reactors but with many significant improvements; (c) evolutionary boiling water reactors; (d) heavy-water moderated reactors; and (e) gas-cooled reactors. The reactors considered in this work are the Pressurized Water Reactor (Power Reactor) and the Miniature Neutron Source Reactor (Research reactor).

1.2.1 Pressurized Water Reactor (PWR)

There are basically two types of light-water reactors now in use: the pressurized-water reactor (PWR) and the boiling-water reactor (BWR). Both of these types of reactors are well established in the Europe and abroad, and both produce power about as cheaply as comparable coal-fired plants. Pressurized Water Reactors comprise a majority of all western nuclear power plants and are one of two types of light water reactor (LWR), the other type being boiling water reactors (BWRs).

In a PWR the primary coolant (superheated water) is pumped under high pressure to the reactor core, then the heated water transfers thermal energy to a steam generator. In contrast to a boiling water reactor, pressure in the primary coolant loop prevents the water from boiling within the reactor. All LWRs use ordinary light water as both coolant and neutron moderator. PWR's were originally designed to serve as nuclear submarine power plants and were used in the original design of the first commercial power plant at Shippingport Atomic Power Station.

Light water is used as the primary coolant in a PWR. It enters the bottom of the reactor core at about 275 °C (530 °F) and is heated as it flows upwards through the reactor core to a temperature of about 315 °C (600 °F).

Pressure in the primary circuit is maintained by a Pressurizer, a separate vessel that is connected to the primary circuit and partially filled with water which is heated to the saturation temperature

(boiling point) for the desired pressure by submerged electrical heaters. Pressure transients in the primary coolant system manifest as temperature transients in the pressurizer and are controlled through the use of automatic heaters and water spray, which raise and lower pressurizer temperature respectively.

Pressurized water reactors (PWR), like other thermal reactor designs, require the fast fission neutrons to be slowed down (a process called moderation or thermalization) in order to interact with the nuclear fuel and sustain the chain reaction. In PWRs the coolant water is used as a moderator by letting the neutrons undergo multiple collisions with light hydrogen atoms in the water, losing speed in the process.
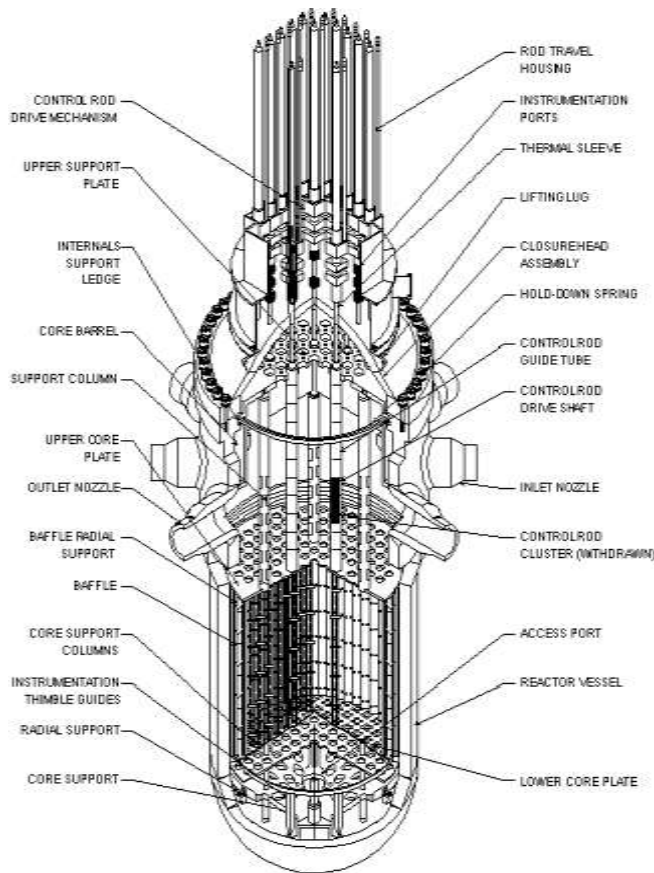
Figure 1.1 PWR reactor vessel   **Figure 1.2** PWR fuel assembly
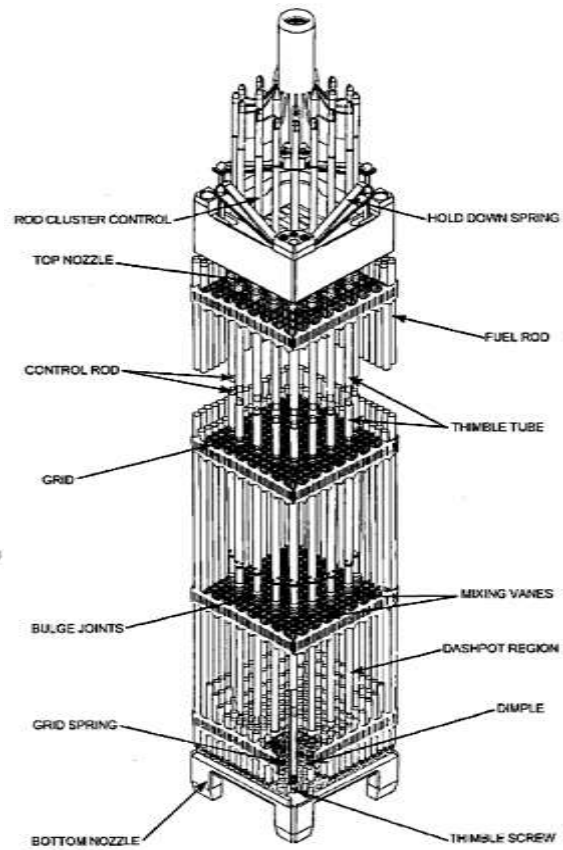
PWRs are designed to be maintained in an under moderated state, meaning that there is room for increased water volume or density to further increase moderation, because if moderation were near saturation, then a reduction in density of the moderator/coolant could reduce neutron absorption significantly while reducing moderation only slightly, making the void coefficient

positive. Also, light water is actually a somewhat stronger moderator of neutrons than heavy water, though heavy water's neutron absorption is much lower.

The PWR uses UO_2 or MOX as fuels. After enrichment, the uranium dioxide (UO_2) powder is fired in a high-temperature, sintering furnace to create hard, ceramic pellets of enriched uranium dioxide. The cylindrical pellets are then clad in corrosion-resistant zirconium metal alloys (Zircaloy) which are backfilled with helium to aid heat conduction and detect leakages. Zircaloy is chosen because of its mechanical properties and its low absorption cross section. The finished fuel rods are grouped in fuel assemblies, called fuel bundles, which are then used to build the core of the reactor. A typical PWR has fuel assemblies of 200 to 300 rods each, and a large reactor would have about 150–250 such assemblies with 80–100 tonnes of uranium in all. Generally, the fuel bundles consist of fuel rods bundled 14×14 to 17×17. A PWR produces on the order of 900 to 1,500 MW_e. PWR fuel bundles are about 4 meters in length [2] [3] [4].

Refueling for most commercial PWRs is on an 18–24 month cycle. Approximately one third of the core is replaced each refueling, though some more modern refueling schemes may reduce refuel time to a few days and allow refueling to occur on a shorter periodicity.

The larger proportion of plutonium in the core shifts the neutron spectrum towards higher energy levels, thereby reducing the efficiency of the control systems. This has led to improve the control rods pattern, to increase boron concentration of the boron make-up storage tank and to increase boron concentration of the refueling water storage tank.

The fuel design of MOX rods, together with all components of the MOX fuel assembly (FA), are designed to meet the same mechanical and thermo hydraulic conditions as UOX ones. A MOX FA contains only mixed oxide rods. The plutonium is mixed with depleted uranium (0.25% 235U). The Pu content is adjusted to take account of its isotopic composition (63 to 70% fissile Pu). Energy equivalence to 3.25% enriched UOX is obtained with an average content of about 7% total Pu in MOX. Currently, ''hybrid'' management is implemented with 3-batch for MOX and 4-batch for 3.70% UOX. The average MOX BU is maintained at around 38 GWd/t [5] [6].

In PWRs reactor power can be viewed as following steam (turbine) demand due to the reactivity feedback of the temperature change caused by increased or decreased steam flow. Boron and control rods are used to maintain primary system temperature at the desired point. In order to

decrease power, the operator throttles shut turbine inlet valves. This would result in less steam being drawn from the steam generators. This results in the primary loop increasing in temperature. The higher temperature causes the reactor to fission less and decrease in power. The operator could then add boric acid and/or insert control rods to decrease temperature to the desired point.

Reactivity adjustment to maintain 100% power as the fuel is burned up in most commercial PWRs is normally achieved by varying the concentration of boric acid dissolved in the primary reactor coolant. Boron readily absorbs neutrons and increasing or decreasing its concentration in the reactor coolant will therefore affect the neutron activity correspondingly. The reactor control rods, inserted through the reactor vessel head directly into the fuel bundles, are moved for the following reasons:

- To start up the reactor.

- To shut down the reactor.

- To accommodate short term transients such as changes to load on the turbine.

The control rods can also be used:

- To compensate for nuclear poison inventory.

- To compensate for nuclear fuel depletion.

But these effects are more usually accommodated by altering the primary coolant boric acid concentration.

1.2.2 Miniature Neutron Source Reactor (MNSR)

The MNSR is a compact, thermal and low power research reactor. It adopts tank-in-pool type structure, fuel element of high-enriched uranium, and light water as moderator, coolant and shield. The core is surrounded by annulus, bottom and top beryllium reflectors that reduce the critical mass and provide neutron flux peak inside the reflectors where the irradiation sites are situated. The reactor is designed by the Chinese Institute of Atomic Energy for the purposes of neutron activation analysis (NAA), some short-lived radioisotope preparation, and personnel training in nuclear technique applications [7].

The High Enriched Uranium (HEU) and proposed Low Enriched Uranium (LEU) of the MNSR which is simulated in this work is a 30kW and 34kW tank-in-pool reactor respectively (see Figure 1.3). The description of the MNSR in this chapter is basically the parameters of the HEU core of Ghana Research Reactor-1 (GHARR-1) which uses 90.2% enriched U-Al alloy as fuel. The diameter of the fuel meat is 4.3 mm and the thickness of the aluminium cladding material is 0.6 mm. The total length of the element is 248 mm and the active length is 230 mm. The percentage of U in the UAl_4 dispersed in Al is 27.5% and the loading of U-235 in the core with 344 fuel element is 990.72 g. In order to reduce the thermal resistance between fuel pellet and the cladding tube, after the fuel meat has been loaded into the cladding tube, the cladding is drawn to obtain mechanical close attachment between the cladding and the fuel meat. The clearance between pellet and end plug is 0.5 mm, which is allowed for the thermal expansion of the pellets. To ensure fuel stability in the core, the lower end of the fuel rods is designed to have a tapered structure which enables a self-lock fit between the fuel end and the lower grid plate and thus the fuel rods and dummy elements are tightly locked to the lower grid plate while its upper end is free in the upper grid plate.

The reactor is designed to be compact and safe and it is used mainly for neutron activation analysis, production of short-lived radioisotopes and for education and training. The maximum

Figure 1.3 3D diagram of Miniature Neutron Source Reactor (MNSR)

thermal neutron flux at its inner irradiation site is $1 \times 10^{12} n \cdot cm^{-2} \cdot s^{-1}$. It is cooled and moderated with light water, and light water and beryllium act as reflectors. The fuel cage consists of 344 fuel pins, 4 tie and 6 dummy rods, a central control rod guide tube, upper and lower grid plates. The fuel pins, tie and dummy rods are concentrically arranged in 10 rings of the fuel cage. The core has a central guide tube through which a cadmium control rod cladded in stainless steel moves to cover the active length of 230 mm of the core. The single control rod is

used for regulation of power, compensation of reactivity and for reactor shutdown during normal and abnormal operations. The fuel cage is placed on a 50 mm thick beryllium reflector of diameter 290 mm and it is surrounded by another 100 mm thick metallic beryllium reflector of height 238.5 mm as shown in Figure 1.3. The bottom beryllium plate and the side beryllium annular reflectors form the inlet orifice and the supporting plate and the side beryllium annular reflectors form the outlet orifice. On top of the core is placed an aluminium tray which may contain certain thickness of beryllium plates required for adjustment of core excess reactivity for compensation of fuel depletion and fission product poisoning. The reactor core is located in the lower section of a sealed aluminium alloy vessel of diameter 0.6m which is hanged on a frame across a stainless steel lined water pool of diameter 2.7m and depth 6.5m.

Since heat generation is not useful for the intended purpose of the MNSR, the heat generated by fission is removed via in an upward direction through approximately 4metres column of water in the tank. The heated water, which moves to the upper section of the reactor tank, is transferred to the upper section of the water in the tank. The core is cooled by natural convection and under normal operation conditions, the flow regime is single phase but nucleate boiling is expected under abnormal condition when power excursion occurs due to large reactivity insertion. There are two pairs of NiCr-NiAl thermocouples, which are fixed in the inlet and outlet of the core coolant for measuring the temperature difference between the inlet and the outlet of the coolant. A platinum resistance thermometer is used for measuring the inlet temperature of the coolant. The reactor which is under moderated with atomic ratio of H/U-235 as 197 possesses the non-sufficient natural circulation feature. Due to the suction, part of the hot outlet coolant is taken into the core by the coolant near the inlet orifice [7] [8].

The Ghana MNSR has currently been utilized extensively in the field of neutron activation analysis (NAA) which is a nuclear process used for determining the concentrations of elements in a vast amount of materials. NAA allows discrete sampling of elements as it disregards the chemical form of a sample, and focuses solely on its nucleus. The method is based on neutron activation and therefore requires a source of neutrons. The sample is bombarded with neutrons, causing the elements to form radioactive isotopes. The radioactive emissions and radioactive decay paths for each element are well known. Using this information, it is possible to study spectra of the emissions of the radioactive sample, and determine the concentrations of the

elements within it. A particular advantage of this technique is that it does not destroy the sample, and thus has been used for analysis of works of art and historical artifacts. NAA can also be used to determine the activity of a radioactive sample. Neutron activation analysis is a sensitive multi-element analytical technique used for both qualitative and quantitative analysis of major, minor, trace and rare elements. The Ghana MNSR has used this technique for several scientific works such, to measure neutron absorption cross sections of different isotopes [9] [10], environmental pollution and health monitoring [11] [12], to investigate hazardous exposure of industrial workers [13], elemental analysis of soil for mineral exploration purposes and etc.

1.3 THE FRENCH NUCLEAR FUEL CYCLE

The nuclear fuel cycle, also called nuclear fuel chain, is the progression of nuclear fuel through a series of differing stages. It consists of steps in the *front end*, which are the preparation of the fuel, steps in the *service period* in which the fuel is used during reactor operation, and steps in the *back end*, which are necessary to safely manage, contain, and either reprocess or dispose of spent nuclear fuel. If spent fuel is not reprocessed, the fuel cycle is referred to as an *open fuel cycle* (or a once-through fuel cycle); if the spent fuel is multi-reprocessed, it is referred to as a *closed fuel cycle* [14].

In this work, the open cycle of the UOX fuel is integrated in a partially closed cycle of the French MOX cycle fuel. The spent fuel from the UOX fuel is fabricated into a MOX fuel to be re-used in the reactor at various burn-up. It concentrates partially on the in-core fuel management and the backend of the fuel cycles considered.

1.3.1 In-Core Fuel Management

The cycle begins with the mining of uranium ore. This ore contains uranium in the form of a number of complex oxides, and is reduced to the oxide U_3O_8, also called yellow cake, at mills located in the vicinity of the uranium mines. The U_3O_8 is then converted to uranium hexafluoride, UF_6, the form in which uranium is accepted at current isotope enrichment plants. Approximately 0.5 percent of the uranium is lost in the conversion to UF6. The UF_6 is converted to UO_2. Finally, the UO_2 is fabricated into PWR or BWR fuel assemblies, and, in time, loaded into the reactor. Fuel fabrication is accompanied by about 1 percent loss of uranium.

In the reactor core, the fabricated fuel assemblies are irradiated to produce fission energy. During irradiation, the changes in properties of a nuclear reactor over its lifetime are determined by the changes in composition due to fuel burnup and the manner in which these are compensated.

At any given time, the fuel in a reactor core will consist of several batches that have been in the core for different lengths of time. The choice of the number of batches is made on the basis of a trade-off between maximizing fuel burnup and minimizing the number of shutdowns for refueling, which reduces the plant capacity factor. At each refueling, the batch of fuel with the highest burnup is discharged, the batches with lower burnup may be moved to different locations, and a fresh or partially depleted batch is added to replace the discharged batch. The analysis leading to determination of the distribution of the fuel batches within the core to meet the safety, power distribution and burnup, or cycle length constraints for fuel burn cycle is known as fuel management analysis [2].

Typically, a PWR will have three fuel batches, and a BWR will have four fue1 batches in the core at any given time and will refuel every 12 to 15 months. A number of different loading patterns have been considered, with the general conclusion that more energy is extracted from the fuel when the power distribution in the core is as flat as possible. In the in-out loading pattern, the reactor is divided into concentric annular regions loaded with different fuel batches. The fresh fuel batch is placed at the periphery, the highest burnup batch is placed at the center, and intermediate burnup batches are placed in between to counter the natural tendency of power to peak in the center of the core. At refueling, the central batch is discharged, the other batches are shifted inward, and a fresh batch is loaded on the periphery. The in-out loading pattern has been found to go too far in the sense that the power distribution is depressed in the center and peaked at the periphery. An additional difficulty is the production of a large number of fast neutrons at the periphery that leak from the core and damage the pressure vessel.

In the scatter loading pattern the reactor core is divided into many small regions of four to six assemblies from different batches. At refueling, the assemblies within each region with the highest burnup are discharged and replaced by fresh fuel assemblies. This loading pattern has been found to produce a more uniform power distribution and to result in less fast neutron leakage than the in-out pattern.

Since the pressure vessel damage by fast neutrons became recognized as a significant problem, a number of different loading patterns have been developed with the specific objective of minimizing neutron damage to the pressure vessel. These include placement of only partially depleted assemblies at the core periphery, placement of highly depleted assemblies near welds and other critical locations, using burnable poisons in peripheral assemblies, replacing peripheral fuel assemblies with dummy assemblies, and others.

Better utilization of resources argues for the highest possible fuel burnup consistent with materials damage limitations, and a new higher enrichment fuel has been developed that can achieve burnups of up to 50,000MWd/T in LWRs. The higher fuel burnup produces more actinides and fission products with large thermal neutron cross sections, which compete more effectively with control rods for thermal neutrons and reduces control rod worth, and which produces larger coolant temperature reactivity coefficients. The higher-enrichment higher-burnup fuel also provides the possibility of longer refueling cycles, which improves plant capacity factor and reduces power costs [2].

The economics of nuclear power is strongly affected by the efficiency of fuel utilization to produce power, which in turn is affected by these long-term changes associated with fuel burnup.

1.3.1.1 Burnup

The initial composition of a fuel element will depend on the source of the fuel. For reactors operating on the uranium cycle, fuel developed directly from natural uranium will contain a mixture of U-234, U-235 and U-238, with the fissile U-235 content varying from 0.72% (for natural uranium) to more than 90%, depending on the enrichment. Recycled fuel from reprocessing plants will also contain the various isotopes produced in the transmutation-decay process of uranium [15]. A typical PWR uses enriched uranium fuel of about 3.0% − 4.5% of U-235.

During the operation of a nuclear reactor a number of changes occur in the composition of the fuel. The various fuel nuclei are transmuted by neutron capture and subsequent decay. For a uranium-fueled reactor, this process produces a variety of transuranic elements in the actinide series of the periodic table. For a thorium fueled reactor, a number of uranium isotopes are produced. The fission event destroys a fissile nucleus, of course, and in the process produces two intermediate mass fission products. The fission products tend to be neutron-rich and

subsequently decay by beta or neutron emission (usually accompanied by gamma emission) and undergo neutron capture to be transmuted into a heavier isotope, which itself undergoes radioactive decay and neutron transmutation, and so on. The fissile nuclei also undergo neutron transmutation via radiative capture followed by decay or further transmutation [15]. Figure 1.4 shows a simplified diagram of transmutation of nuclei in the uranium series. Actinides of interest are marked with thick borders.
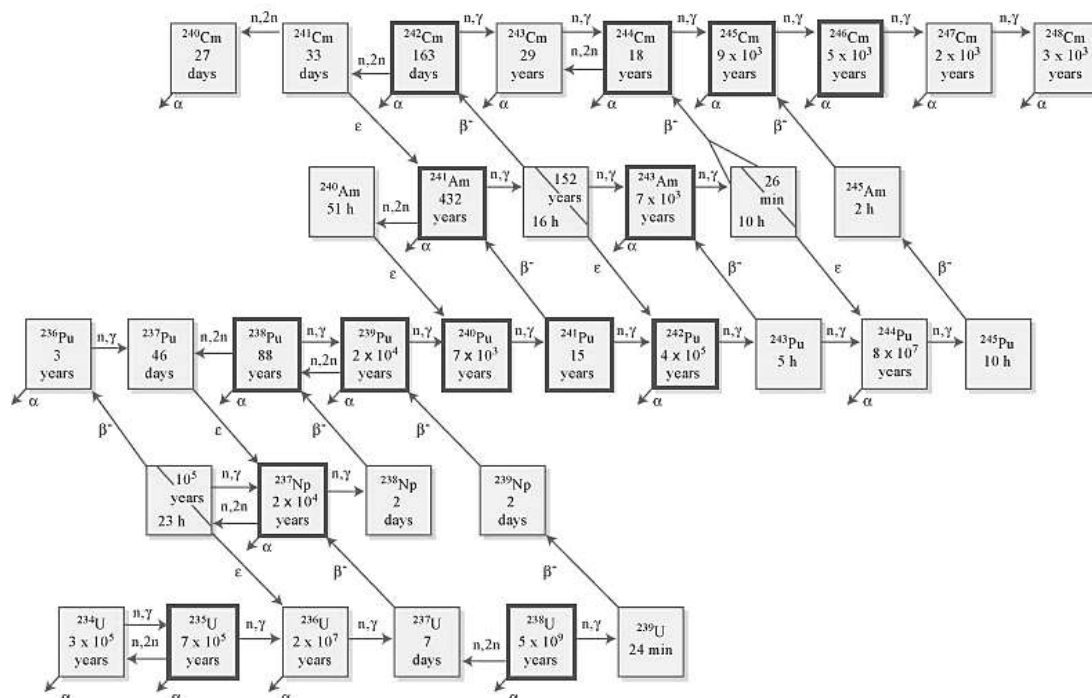
Figure 1.4 The most important actinide nuclides and their relations, via α-decay, β-decay and neutron capture reactions

The buildup of actinides in the U-238 transmutation-decay process introduces a fuel reactivity penalty because some of actinides act primarily as parasitic absorbers. While Pu-239 and Pu-241 are fissionable in a thermal reactor, and Pu-240 transmutes into Pu-241(fissile), Pu-242 transmutes into Pu-243 with a rather small cross section and thus build up in time. Pu-243 decays immediately towards Am-243(non-fissile). Pu-242 is effectively a parasitic absorber. The Am-243 also accumulates and acts primarily as a parasitic absorber. Whereas the Am-243, which is produced by the decay of Pu-243, can be separated readily, it is quite impossible to separate the different plutonium isotopes from each other by chemical means, so the negative Pu-242 reactivity effect is exacerbated if the plutonium is recycled with uranium [15].

In nuclear power technology, burn-up is a measure of the number of fuel atoms that underwent fission. It is normally quoted in megawatt–days per metric ton of heavy metal (MWd/THM), or

its equivalent gigawatt–days/T (GWd/tHM). The unit GWd/tHM is the (average) thermal output, multiplied by the time of operation, and divided by the mass of heavy involved. This gives a rough measure of the number of nuclear fission events that have taken place within the fuel.

The actual fuel may be uranium, plutonium, or a mixture of these or of either or both of these with thorium. This fuel content is often referred to as the *heavy metal* (the only nuclei which can fission to produce energy) to distinguish it from other elements present in the fuel, such as oxygen of an oxide fuel or those used for cladding. The heavy metal is typically present as either metal or oxide, but other compounds such as carbides or other salts are possible. In a power station, high fuel burn-up is desirable for:

- Reducing downtime for refueling
- Reducing the number of fresh nuclear fuel elements required and spent nuclear fuel elements generated while producing a given amount of energy
- Reducing the potential for diversion of plutonium from spent fuel for use in nuclear weapons, for short BU, the plutonium produced is essentially Pu-239 which highly fissile. Alpha decay of this isotope also leads to the formation of U 235. Below is a table showing the dominance of Pu with BU.

It is also desirable that burn-up should be as uniform as possible both within individual fuel elements and from one element to another within a fuel charge [16]. In reactors with online refueling (as in the case of CANDU reactor), fuel elements can be repositioned during operation to help achieve this. In reactors without this facility, fine positioning of control rods to balance reactivity within the core, and repositioning of remaining fuel during shutdowns in which only part of the fuel charge is replaced may be used, this type of fuel management is incorporated in this work with four fractionating cycles for the study of mono-recycling of the americium.

Generation II reactors were typically designed to achieve about 40GWd/t. With newer fuel technology, and particularly the use of nuclear poisons, these same reactors are now capable of achieving up to 60GWd/t. Some more-advanced reactor designs are expected to achieve over 90GWd/t of higher-enriched fuel, and eventually over 200GWd/t [16]. PWR cores designed in this work were made to reach 46GWd/t and 68GWd/t for both UOX and MOX fuel assemblies.

1.3.2 Reprocessing and Backend of the Nuclear Fuel Cycle

When the spent fuel is removed from the reactor, it is hot and very radioactive. It must be cooled and shielded from people. It is put into storage ponds at the reactor site. The storage ponds are steel-lined concrete tanks, about 8 meters deep and filled with water. The water cools the spent fuel rods and acts as a shield. The heat and radioactivity decrease over time - after about 40 years they are down to about 1/1000 of what they were when taken from the reactor. The longer they are stored, the easier they are to deal with.

In France, the spent fuel is sent for reprocessing. This means that the most highly radioactive waste, about 3% by mass, is separated, concentrated and made into a special glass (vitrification). The unused uranium and plutonium are then recycled into fresh reactor fuel.

1.3.2.1 Reprocessing

A substantial amount of plutonium is produced by neutron transmutation of U-238 in LWRs. About 220kg of fissionable plutonium (mainly Pu-239 and Pu-241) is present in the spent fuel discharged from an LWR at a burnup of 45MWd/T. The spent fuel can be reprocessed to recover the plutonium (and remaining enriched uranium) for recycling as new fuel [15]. This process is utilized in this work to reprocess the Pu and Am in the once through cycle of the UOX just as in the French case of MOX fuel fabrication.

Table 1.1 Typical Isotopic Compositions of Pu in Spent Fuel at Discharge from Power Reactors[16]

Reactor type	Fuel burn-up GWd/t	Isotopic composition, %			
		Pu-239	*Pu-240*	*Pu-241*	*Pu-242*
GCR	3.6	77.9	18.1	3.5	0.5
PHWR	7.5	66.4	26.9	5.1	1.5
AGR	18.0	53.7	30.8	9.9	5.0
RBMK	20.0	50.2	33.7	10.2	5.4
BWR	27.5	59.8	23.7	10.6	3.3
PWR	33.0	56.0	24.1	12.8	5.4

In an LWR fuel cycle or in any breeder reactor cycle it is necessary to *reprocess* the spent fuel in order to recover the plutonium or uranium. Several methods have been developed over the years

to do. However, virtually *all* reprocessing plants that have been built since the 1950s utilize the Purex *solvent extraction process* [15].

1.3.2.2 Plutonium extraction from spent UOX

The Purex process is based on the fact that uranium and plutonium can exist in a number of valence (oxidation) state and because of differences in their oxidation and reduction potentials, it is possible to oxidize or reduce one of these elements without disturbing the other. Furthermore, the compounds of uranium and plutonium in different states have difference solubilities in organic solvents.

The batch of spent fuel is then dissolved in a concentrated solution of nitric acid (HNO_3). This aqueous solution of uranium and plutonium both of which at this point are in high states of oxidation, together with the fission products and dissolved and the remnants of the fuel assemblies passes through a filter to remove the undissolved components of the assemblies.

Organic solvent tributylphosphate (TBP), diluted in the kerosene-like substance, is used for the extraction of uranium and plutonium from the aqueous solution. The plutonium is separated and often purified and concentrated by the method of ion exchange. This process involves passing the plutonium solution into an ion exchange resin and then eluting the plutonium with dilute acid. The concentration of the purified plutonium can then be increased by partially evaporating the solution, taking care not to approach criticality: This is the usual form of the plutonium output from a fuel reprocessing plant-a highly purified solution of plutonium nitrate. It is an easy matter to transform the plutonium to the oxide PUO_2 [15].

1.3.2.3 Americium Extraction form spent fuel

In this work, not both plutonium and americium extraction from the spent UOX fuel of the once through is considered. Americium which also has different oxidation sates can also be extracted using the PUREX method. After Pu and U extraction, the lanthanides and remaining actinides are then separated from the aqueous residue (raffinate) by a diamide-based extraction, to give, after stripping, a mixture of trivalent actinides and lanthanides. Americium compounds are then selectively extracted using multi-step chromatographic and centrifugation techniques with an appropriate reagent.

A large amount of work has been done on the solvent extraction of americium. For example, a recent EU funded project codenamed "EUROPART" studied triazines and other compounds as potential extraction agents [17] [18] [19]. Bis-triazinyl bipyridine complex has been recently proposed as such reagent as highly selective to americium (and curium). Both Am and Cm are mostly present in solutions in the +3 valence state; whereas curium remains unchanged, americium oxidizes to soluble Am(IV) complexes which can be washed away.

Metallic americium is obtained by reduction from its compounds. Americium(III) fluoride was first used for this purpose. The reaction was conducted using elemental barium as reducing agent in a water- and oxygen-free environment inside an apparatus made of tantalum and tungsten [20] [21]:

$$2AmF_3 + 3Ba \rightarrow 2Am + 3BaF_2$$
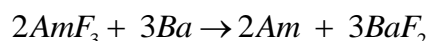
An alternative is the reduction of americium dioxide by metallic lanthanum or thorium [22]:

$$3AmO_2 + 4La \rightarrow 3Am + 2La_2O_3$$
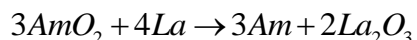
In this work, the simulation of the extracted Am and Pu is used irrespective of the chemical method which would be practically used. Am and Pu are treated together.

1.3.2.4 Residual Heat, Storage and disposal

Radioactive wastes in several different forms are produced at various points in the fuel Cycle of a nuclear power plant: during the mining of uranium, the manufacture of the fuel, the operation of the reactor, and the reprocessing and recycling of the fuel (if this is part of the cycle).

The actinides produced in the transmutation-decay of the fuel isotopes and the fission products are the major contributors to the radioactive waste produced in nuclear reactors, although activated structure and other materials are also present. In fact, the radioactivity of the spent fuel decreases substantially within the first 6 months after removal from the reactor. The more troublesome fission products from the waste management point of view are those with long half-lives like Tc-99 ($T_{1/2} = 2.1 \ x \ 10^5$ years), I-129 ($T_{1/2} = 1.59 \ x \ 10^7$ years) and Cs-135($T_{1/2} = 2.3 \ x \ 10^6$ years) and those that are gamma emitters, such as Sr-90, Cs-137 and alpha emitting Am-241 which are responsible for the dimensioning of the waste repository, produce substantial decay

heating for decades. The actinides constitute a relatively small part of the total radioactivity at reactor shutdown but become relatively more important with time because of the longer half-lives of Pu-239 and Pu-240 and dominate the radioactivity of spent fuel after about 1000 years [2] [15].

1.3.2.5 Potential Hazard of permanent fuel disposal

In order to compare the radiological hazard of different nuclides, the concept of radiotoxicity has been introduced. Radiotoxicity is hypothetical dose, expressed in Sieverts (Sv). Different types of radiation yield quite different radiotoxicities due to large variations in their effect on the human body. Further, the radiotoxicity of a particular nuclide varies depending on whether it is inhaled or ingested and depending on the age of the recipient, small children being more sensitive to radiation than are adults [23].

The International Commission on Radiological Protection, ICRP, issues coefficients for calculating the radiotoxicity of different nuclides from their activities, in units of Sv/Bq. Table 1.2 presents dose conversion coefficients as recommended by ICRP in 1996 for some important nuclides appearing in spent fuel [24]. The large differences between doses for ingestion and inhalation are clear. Especially for the actinides, inhalation poses a much greater hazard than does ingestion. However, assuming a scenario where actinides from a repository are dispersed in the biosphere, ingestion seems more likely. Especially this is true in the long run and therefore in this work, only radiotoxicity by ingestion is taken into account when comparing the radiotoxicity of nuclides, rather than its inhalation equivalent.

In Table 1.2 the transuranic nuclides exhibit dose coefficients significantly larger than most of the important fission products. The major exceptions are Pu-241 and Cm-242 which cause comparatively low damage, and I-129 which, on the contrary, poses a considerable threat in comparison to other fission products due to its concentration in the thyroid, where it remains. The β-decay of Pu-241 is far less harmful than α-decays once the source is within the body. Cm-242 has a half-life much shorter than most of the actinides. It decays to Pu-238 with a much longer half-life and lower activity. In conclusion, the radiotoxicity is dependent not only on the activity and quality of the emitted radiation, but also on whether the nuclide accumulates and on its residence time in the body [23] [24].

Table 1.2 Dose coefficients for important nuclides in spent nuclear fuel given for intake by ingestion and for inhalation in adult humans

Transuranic Elements (nSv/Bq)			Long-lived Fission Products (nSv/Bq)		
Nuclide	Ingestion	Inhalation	Nuclide	Ingestion	Inhalation
^{237}Np	110	23000	^{79}Se	2.9	2.6
^{238}Pu	230	46000	^{90}Sr	28	36
^{239}Pu	250	50000	^{93}Zr	1.1	10
^{240}Pu	250	50000	^{99}Tc	0.64	4.0
^{241}Pu	4.8	900	^{107}Pd	0.037	0.085
^{242}Pu	240	48000	^{126}Sn	4.7	28
^{241}Am	200	42000	^{129}I	110	15
^{242m}Am	190	37000	^{135}Cs	2.0	3.1
^{243}Am	200	41000	^{137}Cs	13	9.7
^{242}Cm	12	5200			
^{243}Cm	150	31000			
^{244}Cm	120	27000			
^{245}Cm	210	42000			

Processing of spent UO_2 fuel to recover the residual U and Pu reduces the potential long-term radiotoxicity of the remaining High Level Waste (minor actinides, fission products, activated structure, etc.) by a factor of 10 and reduces the volume by a much larger factor, and processing technology (PUREX) capable of 99.9% efficient recovery of U and Pu is commercially available in a number of countries (United Kingdom, France, Japan, India, Russia, and China). At present a number of commercial reactors are operating with recycled Pu in Western Europe [15].

Note that, the Pu contained in MOX spent fuel is not currently considered as waste. In case the MOX spent fuel becomes a waste, the mono-recycling of Pu would lead to the same amount of waste as in the once-through cycle.

CHAPTER TWO

2 ANALYTICAL TOOLS AND METHODOLOGY

2.1 INTRODUCTION

The problem of a radiotoxicity of long-lived radioactive wastes produced in various nuclear fuel cycles is important from the viewpoint of ecological danger of these cycles; Separation of the most important nuclides and extracting them from storage with subsequent transmutation permits to reduce radiological danger of wastes staying in storage. Removal of nuclides with increased decay heat power from storage permits to ease requirements to heat removal systems at long-term storage of wastes.

A major issue to secure the development of nuclear energy in future is the radioactive waste minimization, both inside the fuel cycle and in a deep geological storage. Neutronics plays a most important role in the assessment of the transmutation potential of nuclear power (NP). For example, long lived fission products (LLFP) incineration is directly defined by the neutron surplus available in the given nuclear system. Every nuclear fission produce a fraction of long lived nuclei but the same fission can produce some neutron surplus for elimination of these long lived nuclei.

Quantitative comparison of the radiological characteristics of minor actinides produced in various fuel cycles is of interest.

2.2 STATIC NEUTRONIC CALCULATION

This work concerns the simulation of the operation cycle, irradiation, cooling time and fabrication, essentially from the neutronic point of view. Neutronic behavior of neutrons in the core is dictated by the Boltzmann equation, which can be solved only for the simplest problems. For realistic, multidimensional, energy-dependent problems, it is necessary to calculate numerical solutions as accurately and efficiently as possible. This can be an extremely daunting task. Research on computational methods for the Boltzmann transport equation has been actively pursued from the 1950s up to the present [25] [26].

During this time, the speed and memory of computers has increased by many orders of magnitude. Nonetheless, it has been argued that the gains in efficiency of simulations of particle transport problems, due to improvements in computational algorithms, exceed the gains due to improvements in computer hardware. Here, we give a brief overview of the major advances in computational neutron transport algorithms. For details, we refer the reader to previous publications [27].

The history of computational transport methods is basically the history of two fundamentally different approaches, commonly called *stochastic* and *deterministic*. Stochastic (or *Monte Carlo*) methods are based on a probabilistic interpretation of the transport process. In this approach, the random *histories* of individual particles are calculated using pseudo random number sequences and the results are averaged over a large number of histories. Stochastic methods have no really need of a Boltzmann transport equation; they rely only on the detailed physics of interactions between individual neutrons and nuclei. Deterministic methods instead are based on (i) discretizing the Boltzmann transport equation in each of its independent variables, resulting in a (typically very large) algebraic system of equations, and then (ii) solving this algebraic system.

For the past 50 years, Monte Carlo and deterministic algorithms have been developed independently. The two approaches were viewed as being incompatible, and two basically disjoint technical communities evolved to develop codes for them. Major technical advances for one type of method (e.g., acceleration techniques for deterministic methods, variance reduction techniques for Monte Carlo methods) had no impact on the other method. Except for specialized applications, the two methods were not implemented in the same (production) computer code. Monte Carlo and deterministic methods became viewed as complementary: one approach was advantageous for certain problems, the other advantageous for different problems. Because of their complementarity, both methods have survived and matured.

However, during the past 10 years, it has become fairly widely understood that *hybrid* methods – which combine aspects of both Monte Carlo and deterministic methods – can be used to enhance the strengths and overcome the weaknesses of the individual approaches. Although hybrid methods are in the early stages of their development and implementation, they have already demonstrated that they can yield major improvements in efficiency and accuracy for difficult problems. It now appears that hybrid methods represent a promising third approach, offering a

way to significantly improve the efficiency and ease of simulations for difficult practical particle transport problems [26].

2.2.1 Monte Carlo Methods

In the physical process of *particle transport*, typically a *very* large number of particles undergo random and independent histories. Each element of an individual particle's history (distance to collision, probability of scattering, post-scattering energy, and direction of flight) has a specific probability distribution function. Because of this, the collective behavior of the particle population is predictable, with a statistical noise that decreases as the number of particles $N \to \infty$.

Stochastic or *Monte Carlo* methods model this process by applying the known distribution functions to simulate the random histories of N_{MC} fictitious *Monte Carlo particles*, and averaging the results over the histories [28] [27]. Monte Carlo simulations usually have orders of magnitude more statistical noise than the actual physical process. This is a significant issue when Monte Carlo methods are used to estimate *rare events*, such as the response rate in a detector located far from a source.

Nonetheless, Monte Carlo methods have certain basic advantages. If the geometry of the System and its cross sections are known, then the results of the Monte Carlo simulation contain only statistical errors. By processing a sufficient number of Monte Carlo particles, it is possible to reduce the probable statistical error below any specified level [26].

According the *central limit theorem*, for any Monte Carlo simulation, the statistical error in the estimation of a given quantity is, with probability 0.68, bounded by:

$$\text{Statistical error} \leq \frac{\sigma}{\sqrt{N_{MC}}} \tag{2.1}$$

where σ (the *standard deviation*) is specific to the given problem and the quantity estimated, and (2.1) holds only for N_{MC} sufficiently large. The positive feature of (2.1) is that as N_{MC} increases, the statistical error will, with high probability, also decrease. The negative feature is that the rate of decrease of the statistical error is slow. For instance, equation (2.1) shows that to decrease the statistical error by a factor of 10, it is necessary to increase N_{MC} (and hence the computational expense) by a factor of 100.

Monte Carlo methods are widely used because of their relative ease of implementation, their ability to treat complex geometries with great fidelity, and their ability to solve problems accurately with cross-sectional data that can have extremely complex energy dependence. However, Monte Carlo simulations can be costly, both to set up and to run. In particular, when attempting to calculate a rare event, such as a detector response far from a source, such a small fraction of the physical particles participate in this event that the number of Monte Carlo particles that create a "score" is *very* small - and the resulting statistical error is unacceptably large. In this situation, the "rules" of the Monte Carlo "game" can be altered so that Monte Carlo particles are "encouraged" to travel from the source to the detector region. The result is that the desired response is estimated with smaller statistical error and computational effort. In effect, the Monte Carlo process is changed so that the estimate of the response is preserved, but the standard deviation in this estimate (the constant σ in equation (2.1)) is reduced.

To accomplish this alteration of the Monte Carlo process, the code user must input a (generally) large number of *biasing parameters* that successfully "encourage" Monte Carlo particles to migrate from the source to the specified detector region. These parameters are strongly problem-dependent, and generating them can be a slow and laborious task. For difficult problems, a lengthy process of trial and error may be necessary, and there is no guarantee that at the end of this process, the code user will have been successful.

Another difficulty with Monte Carlo simulations is that they operate most efficiently when calculating limited information, such as a single detector response. If several detector responses are desired, and the detectors are located far from the source and far from each other, then often the best solution is to run several different Monte Carlo simulations, each with its own specially defined set of biasing parameters. Thus, while Monte Carlo codes are widely used, running these codes efficiently is problematic for complex problems. In these situations, Monte Carlo codes are not a "black box" into which a user can simply specify the problem, press the "start" button, and expect reliable answer in a short time. *In addition to specifying the physical problem, the user must also specify the problem-dependent biasing parameters*, and this can be a formidable task [26].

Historically, research on Monte Carlo methods has focused on new approaches that show hope of alleviating the major difficulties associated with the method. For example, different biasing

methods to encourage Monte Carlo particles to travel toward specified detector regions have been developed and tested. Also, methods have been developed to obtain, via the Monte Carlo process itself, the biasing parameters for difficult problems. In addition, sophisticated statistical methods have been developed to analyze Monte Carlo simulations and better determine the magnitude of the statistical errors. (For example, obtaining accurate estimates of the standard deviation σ, and hence of the true statistical error, can be problematic, particularly for eigenvalue problems.).

During the past 50 years, many significant advances in Monte Carlo techniques have been developed and implemented in large-scale codes. However, the difficulties described above remain significant obstacles to running these codes optimally.

2.2.2 Deterministic and Hybrid Monte Carlo Methods

Because the particle transport process is governed by specified probability distribution functions, the Boltzmann transport equation exists for predicting the *mean* or *average* flux of particles at each location in phase space. *Deterministic*, or *discrete-ordinates*, or S_N methods are based on discretizing the Boltzmann equation in each of its independent variables, and solving the resulting (typically very large) system of algebraic equations.

Because the Boltzmann equation depends on its independent variables in significantly different ways, different methods have been developed for their discretization. For time-dependent problems, the most common method for discretizing the time variable t is the *implicit* or *backward Euler* method. Of all the independent variables in the transport equation, the energy variable E is the most problematic. The reason for this is that typically, the material cross-sections, and hence the particle flux itself, have an extraordinarily complex energy-dependence.

However, the *multigroup* method has been developed to deal with this difficulty, and because of its success, it is almost universally used. From the user standpoint, determining accurate problem-dependent multigroup cross sections is the most challenging and time-consuming aspect of deterministic calculations. The angular or direction-of-flight variable Ω is generally discretized in one of two ways: *discrete-ordinates*, or *collocation* (or S_N) methods, and *spherical harmonic* (or P_N) methods. S_N methods are more commonly used because the structure of the

resulting discrete equations is more closely linked to the innate physical interpretation of particle transport.

The spatial variable x has probably been subjected to a greater variety of discretization methods than any other independent variable in the Boltzmann transport equation. A major issue in discretizing the spatial variable is the number of unknowns that must be calculated (and stored) per spatial cell. Another issue in spatial discretizations concerns accuracy in optically thick, scattering dominated (*diffusive*) regions.

Historically, the research on S_N methods has tended to focus on (i) advanced discretization methods in space, angle, energy, and time, and (ii) advanced iterative methods that converges the iterative solution more rapidly and efficiently. However, a fundamental difficulty remains at the heart of deterministic calculations: the costly and time-consuming task of obtaining adequate multigroup cross sections for a specified difficult problem. This aspect of deterministic simulations remains the most significant obstacle to obtaining useful, accurate deterministic solutions of practical transport problems in a reliable, efficient, and user-friendly manner [26] [25] [29].

In the last 10 - 15 years, it has become understood that the most challenging aspect of difficult Monte Carlo simulations – the determination of problem-dependent biasing parameters - can be done efficiently by a deterministic simulation.

The principal disadvantage is that two separate codes (Monte Carlo and deterministic) must be set up to run the same geometric problem, and the results of the deterministic code must be processed, formatted properly, and then input to the Monte Carlo code. This process can be unwieldy unless a suitable investment has been made in the computing infrastructure, enabling the process to occur automatically.

Most public particle transport codes are either Monte Carlo or deterministic, but a small number of user-friendly hybrid codes are now available. For example, the hybrid code MCBEND [20] uses a multigroup diffusion solver to determine weight windows for Monte Carlo simulation. Also, the recent SCALE 6.0 package from Oak Ridge National Laboratory contains software that enables, with one geometric input deck, deterministically generated multigroup S_N solutions to be calculated, turned into weight windows, and then used in Monte Carlo simulations [30] [31]. The

type of problem for which deterministic methods have been most widely used to derive biasing parameters for Monte Carlo simulations is the classic source-detector problem – in which particles are born in a source, and a single detector response, in a possibly distant detector, is desired.

To date, the term "hybrid" has implied a method in which a deterministic simulation is used to assist – through the calculation of biasing parameters – a Monte Carlo simulation. However, deterministic and Monte Carlo techniques can be merged in different advantageous ways. The principal difficulty with deterministic methods is the laborious calculation of multigroup cross sections. If continuous-energy Monte Carlo simulations could be efficiently run, to automatically determine (problem-dependent) multigroup cross sections, then this would be a way in which Monte Carlo simulations could significantly influence deterministic solutions. Promising work in this area has recently been reported [32] [33].

During the past 50 years, computational methods for performing neutron and coupled neutron/ photon simulations have been an active and vibrant area of research in the nuclear engineering community. Major advances in algorithms for Monte Carlo and deterministic simulations have been made. There is little doubt that, due to the increasing demands on increased realism in simulations, research will continue on different fronts to improve the accuracy and efficiency of these simulations. Also, hybrid methods may become a distinct third approach, which would have its own class of difficult problems for which it is best suited [26].

2.3 EVOLVING NEUTRONIC CALCULATION

2.3.1 Utilization of the MCNP Code

MCNP is a general-purpose continuous-energy, generalized-geometry <u>M</u>onte <u>C</u>arlo <u>N</u>–<u>P</u>article code that can be used for neutron, photon, electron, or coupled neutron/photon/electron transport, including the capability to calculate eigenvalues for critical systems. The code treats an arbitrary three-dimensional configuration of materials in geometric cells bounded by first- and second-degree surfaces and fourth-degree elliptical tori. The user creates an input file that is subsequently read by MCNP. This file contains information about the problem in areas such as: the geometry specification, the description of materials and selection of cross-section evaluations, the location and characteristics of the neutron, photon, or electron source, the type of

answers or tallies desired, and any variance reduction techniques used to improve efficiency. The neutron energy regime is from 10^{-11} MeV to 20 MeV for all isotopes and up to 150 MeV for some isotopes, the photon energy regime is from 1keV to 100GeV, and the electron energy regime is from 1KeV to 1GeV [34].

MCNP uses continuous-energy nuclear and atomic data libraries. The primary sources of nuclear data are evaluations from the Evaluated Nuclear Data File (ENDF) [35] system, Advanced Computational Technology Initiative (ACTI) [36], the Evaluated Nuclear Data Library (ENDL) [37], Evaluated Photon Data Library (EPDL) [38], the Activation Library (ACTL) [39], compilations from Livermore, and evaluations from the Nuclear Physics (T−16) Group at Los Alamos [40]. Evaluated data are processed into a format appropriate for MCNP by codes such as NJOY [41]. The processed nuclear data libraries retain as much detail from the original evaluations as is feasible to faithfully reproduce the evaluator's intent.

A surface source allows particles crossing a surface in one problem to be used as the source for a subsequent problem. The decoupling of a calculation into several parts allows detailed design or analysis of certain geometrical regions without having to rerun the entire problem from the beginning each time. The surface source has a fission volume source option that starts particles from fission sites where they were written in a previous run [34].

The user can instruct MCNP to make various tallies related to particle current, particle flux, and energy deposition. MCNP tallies are normalized to be per starting particle except for a few special cases with criticality sources. Currents can be tallied as a function of direction across any set of surfaces, surface segments, or sum of surfaces in the problem. Charge can be tallied for electrons and positrons. Fluxes across any set of surfaces, surface segments, sum of surfaces, and in cells, cell segments, or sum of cells are also available. Similarly, the fluxes at designated detectors (points or rings) are standard tallies, as well as radiography detector tallies. Fluxes can also be tallied on a mesh superimposed on the problem geometry. Heating and fission tallies give the energy deposition in specified cells. A pulse height tally provides the energy distribution of pulses created in a detector by radiation. In addition, particles may be flagged when they cross specified surfaces or enter designated cells, and the contributions of these flagged particles to the tallies are listed separately. Tallies such as the number of fissions, the number of absorptions, the total helium production, or any product of the flux times the approximately 100 standard ENDF

reactions plus several nonstandard ones may be calculated with any of the MCNP tallies. In fact, any quantity of the form

$$C = \int \emptyset(E) f(E) dE \tag{2.2}$$

can be tallied, where $\emptyset(E)$ is the energy-dependent fluence, and $f(E)$ is any product or summation of the quantities in the cross-section libraries or a response function provided by the user [34].

The basic principle is to follow the propagation of a particle in the cells by applying the laws of its characteristic movement. A wide diversity of neutrons histories in a geometry is simulated in order to raise the average values of useful physical quantities. The average behavior of particles in the real physical system is then deduced from the average behavior of particles simulated using the central limit theorem. Each particle is followed from birth to death, and at each stage of its transport, that is to say, its interactions with matter is also calculated. To do this, the following should be known;

- Whether or not the neutron interacts with the environment;

- If Yes, with what nuclei of the environment did it interacts?;

- What kind of reaction takes place?;

- What are the secondary particles eventually formed?.

The propagation of a particle is consists of several successive operations, performed by MCNP for each neutron monitor [42].

At a given energy *E*, the first step consists of the calculation of the free mean path *λ(E)*, defined by:

$$\lambda(E) = \frac{1}{\sum^{tot}(E)} \tag{2.3}$$

where $\sum^{tot}(E)$ is the effective macroscopic cross-section of the medium, which is expressed for a nucleus *i* as:

$$\sum{}^{tot}(E) = \sum_i N_i \sigma_i^{tot}(E) \tag{2.4}$$

with *Ni* the number of nuclei per cm^3 and $\sigma_i^{tot}(E)$ the total microscopic cross section of interaction of the nucleus *i* in cm^2.

Knowledge of *λ(E)* allows aids the computation of the distance travelled *l(E)* through random sampling before the first interaction by law:

$$l(E) = -\lambda(E)\ln(1-p) \tag{2.5}$$

where p is a random number drawn uniformly in [0 ; 1[.

If point the of interaction is not in the same cell (that is to say if *l(E)* is greater than the distance between the point of emission of the neutron and the edge of the cell), the neutron is at boundary of two cells, the preceding on *λ(E)* and *l(E)* calculations are repeated as well as the total cross section $\sum{}^{tot}(E)$ of the cell in which the neutron is found. If the neutron cell has not changed cell, the nucleus *k* on which the reaction takes place is determined by taking a number p uniformly in interval [0, 1], the nucleus *k* is then selects by the test [42]:

$$\sum_{i=1}^{k-1}\sum{}_i^{tot}(E) \le p \times \sum_{i=1}^{N}\sum{}_i^{tot}(E) < \sum_{i=1}^{k}\sum{}_i^{tot}(E) \tag{2.6}$$

where *N* is the total number of nuclei present, $\sum{}_i^{tot}(E)$ is the total macroscopic cross section of nucleus *i*. The quantity in the center of the inequality, equation (2.6) is always the same for a material and energy data: multiplying it by p, builds a quantity which is lower.

As the interval between the partial sums is proportional to the effective macroscopic cross section k tot (E), the more the interval widens, and the number of *p* values that select the nucleus *k* increases.

Once the nucleus *k* defined, the type of reaction *r* that it undergoes is determined in an analogue manner as:

$$\sum_{i=1}^{r-1}\sigma_i(E) \le p \times \sum_{i=1}^{R}\sigma_i(E) < \sum_{i=1}^{r}\sigma_i(E) \tag{2.7}$$

where $\sigma_i(E)$ is the microscopic cross section of reaction *i* for the previously determined nucleus *k*, R the number of possible reactions for the nucleus k, and p a new random number drawn uniformly in [0, 1 [.

The neutron history can follow different paths: in the case of radiative capture, the neutron is absorbed and indefinitely stops the histories and in the manner most of the other reactions (diffusion, fission reaction (n, 2n) ...), the neutron survives, or, one or more neutrons are emitted. Their energy and direction are randomly drawn according to laws depending on the type of reaction that has been created [42].

During a transport calculation, the neutron is followed from birth to death. In the case of a critical system, the fission reactions are considered as death for neutrons. The neutrons are followed generation by generation and the source of each generation is formed by the fission sites of previous generation.

MCNP can be used to calculate the neutron multiplication constant (eigenvalue) of the reactor, k_{eff}. The k_{eff} is the ratio of the number of neutrons in successive generations, with the fission process regarded as the birth event that separates generations of neutrons. To run a criticality problem, in addition to the geometry description and material cards, all that is required is a KCODE card and an initial spatial distribution of fission points. In a calculation of criticality (KCODE in MCNP), a cycle corresponds to N neutrons belongs to the same generation. The transition to the calculation of the next cycle is initiated by MCNP once all the neutrons of the current generation have disappeared. Each site of fission is kept in memory, to start the fission source of the next generation. A large number of neutrons are spread each cycle, and several inactive cycles are necessary for a convergence of the fission source, and several active cycles to have an acceptable precision. Inactive cycles are cycles in which neutrons are propagated in the geometry, but none of the results obtained for transport is used for the calculation of the tallies. They are used to skip the first states which are not sufficiently convergence and would also introduce bias into the calculation. If the fission source has enough converges, this means that the neutron source is completely "forgotten", then we can safely use neutrons to calculate the tallies (Flux...) [42].

2.3.1.1 Flux Calculation in MCNP

Between two interactions, a neutron has a constant energy E and its contribution to the average flux of the cell is $\dfrac{l(E)}{V}$, where l is the distance travelled by the neutron between two interactions and V the volume of the cell or occur interactions. In each cell or isotopic volume *V*, MCNP estimated the average flux in the cell, integrated on energy and normalizes by simulated neutron source N_S (in a criticality calculation, it comes from the fissions neutron), with k the number of the track which has energy E_k, as:

$$\Phi_c = \frac{1}{N_s} \frac{\sum_k l(E_k)}{V} \qquad (2.8)$$

It should be noted that one can assign a weight for the particle MCNP to explore more remote areas from the neutron source, and therefore that may be less populated neutron. For example, one can define a reaction as an absorbent reaction rather than the particle disappearance, the particle continues to be propagated, but with a weight less than or about 1, which corresponds to the probability that the particle has not been absorbed. If *X* is the probability of the particle to be absorbed, then the particle continues to move with probability (1-*X*). Hence, for all the reactions that are meant to lead to the disappearance of the particle, taking into account the particle weight ω, the flux can be written as [42]:

$$\Phi_c = \frac{1}{N_s} \frac{\sum_k l(E_k)\omega}{V} \qquad (2.9)$$

This definition is equivalent to that of equation (2.8) in which the weight is taken equal to 1.

2.3.1.2 Average reaction rate

Reaction rates calculations are essential for resolving the Bateman equations, and thus achieve the evolution of fuel. This calculation is made by MCNP on request from the user (multiplier tally). In a given cell, microscopic reaction rate induced by energy neutron E is $\dfrac{\sigma(E)l(E)}{V}$ for a

reaction and considered isotope. The average microscopic reaction rate in a given cell is expressed as:

$$\left\langle \sigma\Phi \right\rangle_c^{i,j} = \frac{1}{N_s} \frac{\sum_k \sigma_i^j(E_k)l(E_k)}{V} \tag{2.10}$$

with $\left\langle \sigma\Phi \right\rangle_j^i$ the average microscopic reaction rate of nuclei i for reaction j in a cell, and $\sigma_i^j(E_k)$ reaction cross section j of nucleus i, being treated in a continues manner. Reaction rate is obtained by multiplying the microscopic reaction rate by N_i which is the number of nuclei i per cm^3. It should be noted that with MCNP, the calculation of rates of reaction can be realized on materials that are not present in the geometry (materials perturbation). This feature allows MCNP to implement the calculation of evolution of the fuel. Indeed, it is necessary to know the rate of reaction of nuclei that will appear during the evolution, even if they are not all present in the original geometry. From this it follows that the statistical error on the rate of reaction of a given nucleus depends somewhat on its concentration in the first approximation, since each track contributes to the calculation of the rate of reaction of each nucleus [42].

2.3.1.1 Power Normalization

MCNP provides raw tallies normalized by source neutron. For reactor applications, in order to simulate constant reactor power, one must normalize all tallies by the equivalent number of neutrons per second for a user-given power value. This normalization factor will change as the isotopic composition of the material evolves with time and therefore needs to be calculated at the lowest level of time discretization, i.e., at every Runge-Kutta(RK) step.

Total power delivered by total number of fissions in a given instant (in MCNP raw units) is given by the double sum as:

$$P_{MCNP} = \sum_j \sum_i N_i^j \sigma_i^j \phi_{MCNP}^j \xi \tag{2.11}$$

where N_i^j is the number of nuclei i present in cell j.

σ_i^j is the average fission cross-section of nucleus i in cell j.

ϕ_{MCNP}^j is MCNP's neutron flux track-length estimation for cell j.

ξ is the average energy delivered in one fission, taken by default to be 200 MeV.

The sum is to be carried out over all cells and all nuclei belonging to each cell's material.

P_{MCNP} can be thought of as power delivered per source particle transported in the global geometry considered: If ϕ^j is in standard MCNP flux tally output units (particles per unit surface per source particle) then P_{MCNP} will be normalized too by source particle.

Therefore, the scaling factor α, by which tallies will be normalized and which has to be taken into account in order to simulate constant burn-up at the desired power P_{user}, is given as:

$$\alpha \equiv \frac{P_{user}}{1.6 \times 10^{-19} P_{MNCP}} = \frac{P_{user}}{1.6 \times 10^{-19} \sum_{j} \sum_{i} N_i^j \sigma_i^j \phi_{MCNP}^j \xi} \tag{2.12}$$

where P_{user} is provided in watts and ξ in eV.

2.3.1.2 Evolution of Nuclei

Different routes are possible to create or destroy nuclei under irradiation neutron beam. Basically, neutron capture, of fissions, of radioactive disintegrations and of (n, 2n) reactions. The Bateman equations reflect the variation of the number of nuclei of isotope gives, depending on what produced and what is destroyed. These are equations of the first order of differential in a given cell if as follows [43]:

$$\frac{dN_i}{dt} = \underbrace{-\sigma_i^{abs} \Phi N_i + \sum_{j \neq i} \sigma_{j \to i} \Phi N_j}_{reaction} \underbrace{- \lambda_i N_i + \sum_{j} \lambda_{j \to i} N_j}_{decay} \tag{2.13}$$

where N_i is the number of nuclei for isotope i

$\sigma_i^{abs} \Phi$ is the average reaction rate of absorption of the nuclei i

$\Phi \sigma_{j \to i}$ is the average rate of reaction of the nuclei j of the reaction producing i

λ_i is the total decay constant of nuclei i

$\lambda_{j \to i}$ is the decay constant of nuclei j to produce nuclei i

The first two terms correspond to the neutron reactions (capture, fission, ...) and the last two in the natural decay of the nuclei. The general approach for the resolution of these equations,

representing the evolution of a set or nuclei, implies the definition of a matrix of evolution for each evolving isotope. To simulate the evolution fuel, one needs to solve digitally the Bateman equations system in each evolving isotope. A Runge-Kutta method of order 4 was chosen for the purpose of efficiency.

These equations can has to be written in matrix form, as a matrix B of dimension n, where n is the number of nuclei in the evolving isotope,

$$\frac{d\vec{N}(t)}{dt} = B\vec{N}(t) \tag{2.14}$$

with $\vec{N}(t)$ the vector of the number of nuclei in the cell

$$\vec{N}(t) = \begin{pmatrix} N_1(t) \\ \dots \\ N_j(t) \\ \dots \\ N_{n-1}(t) \\ N_n(t) \end{pmatrix} \tag{2.15}$$

The elements of the matrix are;

$$B_{ii} = -\lambda_i - \sigma_i^{abs}\Phi \tag{2.16}$$

$$B_{ij} = \sigma_{j \to i}\Phi + \lambda_{j \to i} \tag{2.17}$$

where B_{ii} represents disappearance of the nuclei i and B_{ij} the formation of the nuclei i by nuclear reaction of nuclei J $\left(\sigma_{j \to i}\Phi\right)$ and by natural decay $\left(\lambda_{j \to i}\right)$ [44].

Because of the evolution of the fuel, the shape of the spectrum will be amended, and by such medium-sized sections will also change. Over time, the spatial distribution of the flow will also vary, therefore σ and Φ are not constant with time and equation (2.13) becomes

$$\frac{dN_i}{dt} = \underbrace{-\sigma_i^{abs}(t)\Phi(t)N_i + \sum_{j\neq i}\sigma_{j\to i}(t)\Phi(t)N_j}_{reaction} \underbrace{-\lambda_i N_i + \sum_j \lambda_{j\to i}N_j}_{decay} \qquad (2.18)$$
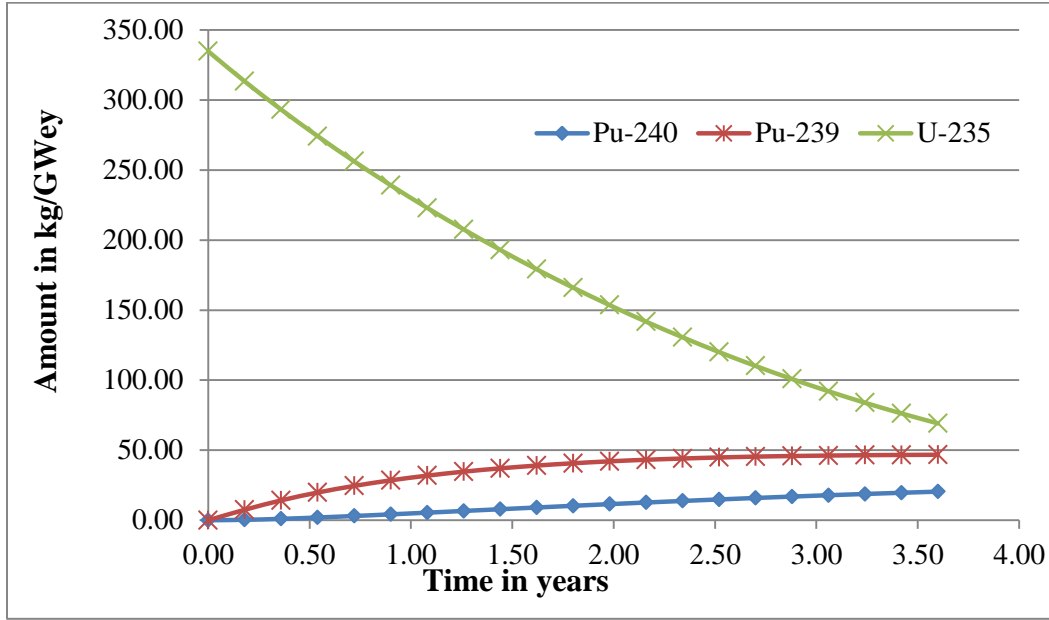
Figure 2.1 Evolution of the main actinides in a PWR-UOX fuel to reach 46GWd/t using the MURE code

MCNP input file with the composition at the initial time t_i is built and an MCNP calculation is executed (all tallies necessary for calculating average flux and reaction rate of evolving cells are constructed automatically). The mean flux over all or selected evolving cell i of volume V is calculated as:

$$\bar{\phi} = \frac{\sum_i \phi_i V_i}{\sum_i V_i} \qquad (2.19)$$

Bateman equations are solved in the interval Δt_i, with a Runge-Kutta method of the 4th order and using the flux and reaction rates calculated by MCNP, a new MCNP file with new compositions has a $t_{i+1} = t_i + \Delta t_i$, is created.

There are 3 levels of time discretization:

  • The first level is the MCNP step, i.e., the number of Δt_i or MCNP runs. These steps are user-defined and are generally not regular. This is indicated by the various points in Figure 2.1.

• The second level is the discretization within a Δt_i. Each Δt_i is divided in N_{RK} equally spaced Runge-Kutta(RK) δt steps (which we'll also refer to as RK steps). At each $t_k = k\delta t$, Bateman equations are built with given cross-sections.

• Then the last discretization step is performed automatically by the adaptive step size RK method. During this step (discretization of δt in dt_{rk}) cross-sections as well as fluxes are kept constant [45].

2.3.1.3 Average Cross-section

Flux-weighted average microscopic fission and capture cross sections are calculated according as:

$$\overline{\sigma_{x,i}} = \frac{\int \sigma_{x,i}(E)\phi(E)dE}{\int \phi(E)dE} \tag{2.20}$$

x and i representing the type of reaction and the nuclide, respectively. The integrations are performed up to the maximum energy of the flux considered.
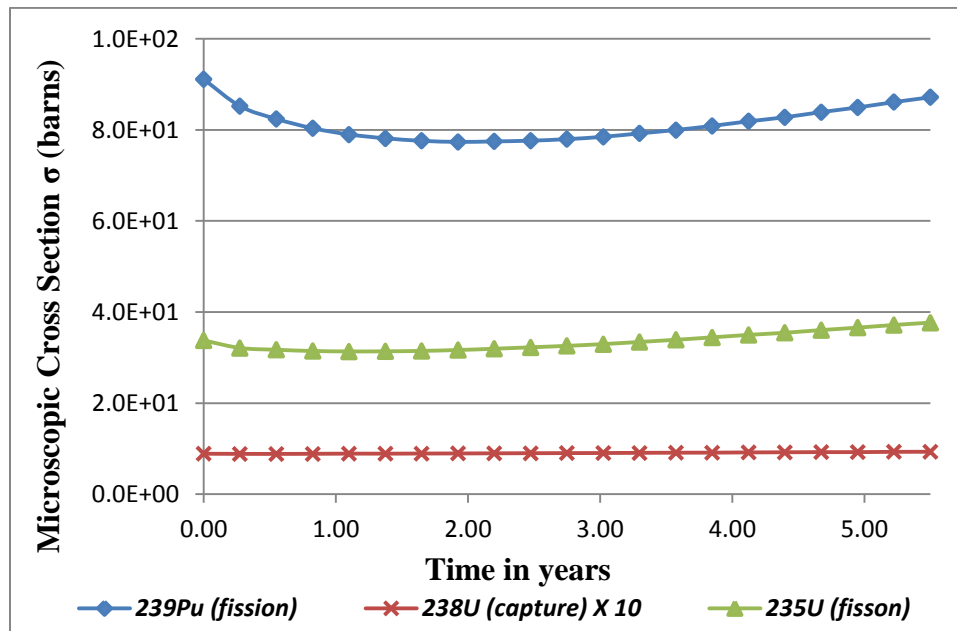
Figure 2.2 MURE update of microscopic cross sections during evolution of 68GWd/t UOX fuel

In Figure 2.2, each point represents a static MNCP calculation where σ_i is calculated. The evolution of microscopic cross section is the key to the burnup simulation of the evolving

material considered. This parameter is updated after each static MCNP cycle for every burnup step.

One group microscopic cross sections are useful as indicators of the hardness of the neutron spectrum. Flux-weighted average macroscopic cross sections are calculated according to

$$\overline{\sum}_x = \sum_i \left(\overline{\sigma_{x,i}} \cdot n_i \right) \tag{2.21}$$

where n_i is the atom density for nuclide i.

It should be noted that to simulate the neutron transport, MCNP calculates the value of the total macroscopic cross section of material at a given energy. The values of the average cross sections for each nucleus in each material, is extracted by MCNP at the request of the user (Tally application).
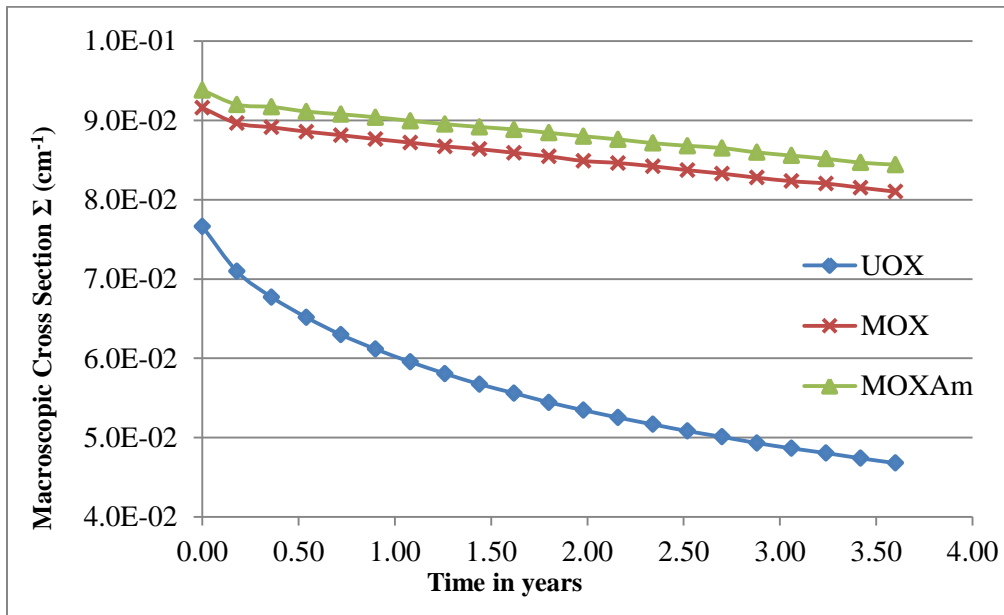
Figure 2.3 Evolution of macroscopic cross section of the different fuels to reach 46GWd/t

2.3.1.4 Thermal dependence of cross section

Due to the sensitive nature of the MNSR cores to reactivity and the high percentage of the core surrounding materials being water and beryllium (moderators) the S(α,β) Thermal tables of the MCNP were used because they are absolutely essential to get correct answers in problems

involving neutron thermalization when very low energies are present. Where α,β are variables which are energy and momentum dependent respectively.

A collision between a neutron and an atom is affected by the thermal motion of the atom, and in most cases, the collision is also affected by the presence of other atoms nearby. The thermal motion cannot be ignored in many applications of MCNP without serious error. The effects of nearby atoms are also important in some applications. MCNP uses a thermal treatment based on the free gas approximation to account for the thermal motion. It also has an explicit S(α,β) capability that takes into account the effects of chemical binding and crystal structure for incident neutron energies below about 4eV, but is available for only a limited number of substances and temperatures [34]. When a particle (representing any number of neutrons, depending upon the particle weight) collides with a nucleus, the following sequence occurs:

1. the collision nuclide is identified;

2. either the S(α,β) treatment is used or the velocity of the target nucleus is sampled for low-energy neutrons;

3. photons are optionally generated for later transport;

4. neutron capture (that is, neutron disappearance by any process) is modeled;

5. unless the S(α,β) treatment is used, either elastic scattering or an inelastic reaction (including fission) is selected, and the new energy and direction of the outgoing track(s) are determined;

6. if the energy of the neutron is low enough and an appropriate S(α,β) table is present, the collision is modeled by the S(α,β) treatment instead of by step 5.

The microscopic cross-section of a particular isotope is temperature dependent. This is taken into account when a particle (say a neutron) moves from cell into another cell with very varying temperatures. This property shown in Figure 2.4 enables the simulation of safety features in terms temperature coefficients and investigations of Doppler broadening. In this work, the Evaluated Nuclear Data file (ENDFB6.8) is used. It has a wide temperature range from $300^{o}K$ to $2000^{o}K$ which is good isotopic evolution and upgrade of cross-section which simulates special effect like the Doppler broadening of U-238.
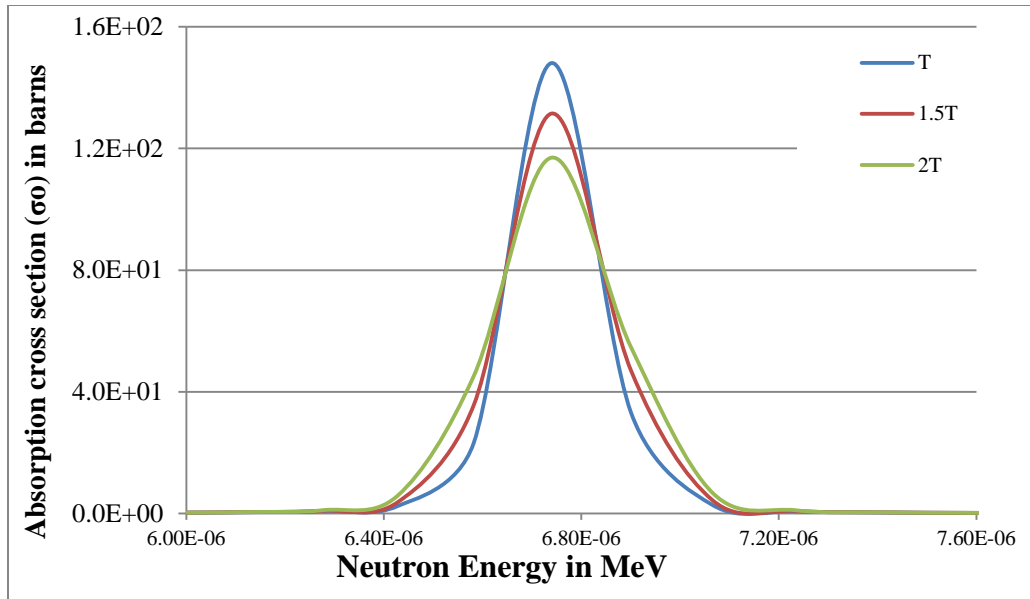
Figure 2.4 microscopic absorption cross section (σ_o) of U-238 at different temperatures (T=1500K) at the energy of the first resonance.

2.3.1.5 Reflecting surfaces

A surface can be designated a reflecting surface based on what one hopes to achieve. Any particle hitting a reflecting surface is specularly (mirror) reflected. Reflecting planes are valuable because they can simplify a geometry setup (and also tracking) in a problem.

They can, however, make it difficult (or even impossible) to get the correct answer. The user is cautioned to check the source weight and tallies to ensure that the desired result is achieved. Any tally in a problem with reflecting planes should have the same expected result as the tally in the same problem without reflecting planes [34].

The geometry can be modeled by half its height and a reflecting surface. All dimensions remain the same except the distance from the tally surface to the opposite surface (which becomes the reflecting surface). This property of the MCNP was employed in this work to model the fuel assemblies simulated to mimic the infinite medium of the reactor.

2.3.2 The MURE Code

MURE is an acronym for <u>M</u>CNP <u>U</u>tility for <u>R</u>eactor <u>E</u>volution. MURE is based on C++ objects allowing a great flexibility in it use. The code seeks to perform nuclear reactor time-evolution

using the widely-used particle transport code MCNP (The Monte Carlo Code discussed in the previous section).

Many depletion codes exist for determining time-dependent fuel composition and reaction rates. These codes are either based on solving Boltzmann equation using deterministic methods or based on Monte-Carlo method for neutron transport. Among them one has to cite, MCNPX/CINDER 90 [46], MONTEBURN [47], KENO/ORIGEN [48], MOCUP [49], MCB [50], VESTA/MORET [51], which provide neutron transport and depletion capabilities. However, the way to control (or interact with) the evolution are either limited to specific procedure and/or difficult to implement [45].

In MURE, due to the Object-oriented programming, any user can defined its own way to interact with evolution. Moreover, MURE provides a simple graphical interface to visualize the results. It also provides a way to couple the neutronics (with or without fuel burn-up) and thermal-hydraulics using either an open source simple code developed in MURE (Simplified Approach of Thermal Hydraulics) or to use a sub-channel 3D code, COBRA-EN. But MURE can also be used just as an interface to MCNP to build geometries (e.g. for neutronics experiments simulation) [52] [53].

2.3.2.1 Evolving with MURE code

There are 3 main parts of the MURE Code:

a)   Definition of the geometry, materials, neutron source, tallies, etc.;

This can be used independently of the 2 others, it allows "easy" generation of MCNP input files by providing a set of classes for describing complex geometries. The ability to make quick global changes to reactor component dimensions and the ability to create large lattices of similar components are two important features that can be implemented by the C++ interface. It should be noted that some knowledge of MCNP is very useful in understanding the geometry generation philosophy [45].

b)   Construction of the nuclear tree, the network of links between neighboring nuclei via radioactive decays and nuclear reactions;

This part of the code builds the specific nuclear tree from an initial material composition containing the list of nuclei. The nuclei tree of each evolving nucleus is created by following the links between neighbours via radioactive decay and/or reactions until a self-consistent set of linked nuclei is extracted. Nuclei with half-lives which are very much shorter than the evolution time steps could be removed from the tree and their parents and daughters re-linked in the correct way. This part can also be used independently of the other two parts to process cross-sections for MCNP at the wanted temperature [45].

c)   Evolution of some materials, by solving the corresponding Bateman's equations.

Simulation of the evolution of the fuel within a given reactor over a time period of up to several years, by successive steps of MCNP calculation and numerical integration of Bateman's equations is achieved in this section of the code. Each time MCNP is called, the reactor fuel composition will have changed due to the fission/capture/decay process occurring inside. Changes in geometry, temperature, external feeding or extraction during the evolution can also be taken into account. This is illustrated in Figure 2.5 and Figure 2.1 below
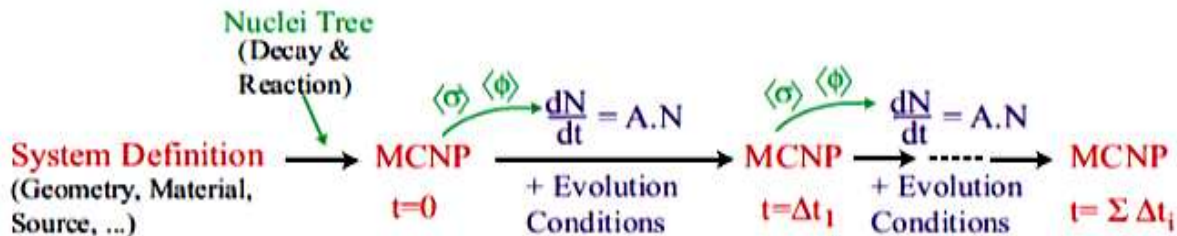
Figure 2.5 Principle of fuel evolution in MURE [45].

Once all the materials originally present in the geometry are defined, the list of nuclei that will appear during the evolution is built once and for all at the beginning of evolution; this is called the nuclei tree. This tree takes into account the different relationships of filiation, lineage and ancestry, or by reaction nuclear or by decay, which may exist for the different types of nuclei. The nuclear tree can be simplified to reduce the number of nuclei in other to reduce the computation time [42].

d)   Thermal-hydraulics: it couples neutronics, thermal-hydraulics and, if needed, fuel evolution.

This part consists of the coupling of the Oak Ridge National Laboratory code COBRA-EN (<u>C</u>oolant <u>B</u>oiling in <u>R</u>od <u>A</u>rrays) with MURE. COBRA is a sub-channel code that allows steady-

state and transient analysis of the coolant in rod arrays. The simulation of flow is based on three or four partial differential equations: conservation of mass, energy and momentum vector for the water liquid/vapor mixture (optionally a fourth equation can be added which tracks the vapor mass separately). The heat transfer model is featured by a full boiling curve, comprising the basic heat transfer regimes: single phase forced convection, sub-cooled nucleate boiling, saturated nucleate boiling, transition and film boiling. Heat conduction in the fuel and the cladding is calculated using the balance equation [45]. This part of the code was not utilized in this work.

2.4 BURNUP ANALYSIS

One of the most important and difficult problems in reactor design is the prediction of the properties of a reactor core throughout its life. How these properties change in time must be known to ensure that the reactor will operate safely throughout the lifetime of the core. The changing reactor properties also determine the length of time that a given reactor core will remain critical, producing power at the desired level. This is an important practical consideration also for waste and spent-fuel characterization, as well as natural resource consumption. It obviously makes little sense for a public utility to purchase a reactor that must be shut down every month for refueling, if it can obtain one that needs to be refueled every 2 years, except for power reactors that can be fueled online such as the CANDU system. However, it makes equally little sense to buy a core that has fuel enough to remain critical for 20 years when radiation damage is known to compromise the fuel elements in 3 or 4 years [2].

In a typical UOX fueled thermal reactor, as energy is removed from a reactor, the fuel composition changes as a result of loss of fissionable material due to fission, buildup and decay of fission products, and transmutation of other reactor materials due to neutron capture. These composition changes occur over a relatively long period of time [54]. All fission products absorb neutrons to some extent, so they are known as reactor poisons. Most fission product poisons simply build up slowly as the fuel burns up and are accounted for as a long-term reactivity. The neutron absorbing fission products such as Xe-135 have particular operational importance. Their concentrations can change quickly, producing major changes in neutron absorption on a relatively short time scale. Each arises from the decay of a precursor fission product, which controls their production rate, but, because they have large absorption cross-sections, their removal changes quickly with changes in flux [8]. Notwithstanding, U-235 in a UOX fuel

fissions into other fission products and minor actinides while the fertile isotopes U-238 undergoes neutron capture to build up fissile isotope Pu-239. All these phenomenon and transmutations tend to modify the core parameters during the core-lifetime of the fuel.

Computations of changing reactor properties are known as burnup calculations or lifetime calculations [2].

2.4.1 Linear Assumption

In view of the above, in a standard PWR core using an enriched uranium fuel (typically 3% or 4% of U-235), the reactivity of one assembly decreases with time because the buildup of fissile Pu-239 is unable to compensate for the U-235 consumption by fission and capture. The irradiation of used assemblies brings about lowering the criticality, k, of the core. k<1 is not desirable in reactor operation, k=1 if these irradiated assemblies are compensated by fresh ones, with k>1.

G. T. Parks in 1989, presented a technical note on linear reactivity fuel cycle model, it was reported that the flux and fuel behavior within a reactor are energy, space and time-dependent, hence certain basic core characteristics may be adequately represented through a simple 'lumped' model, which considers only variations with time (or, equivalently, burnup). The parameter most commonly chosen to describe the state of the core is its reactivity, which is conceptually the difference between the neutron production rate and the removal rate normalized relative to the production rate. It was stated that the linear reactivity model(LRM) does not satisfactorily represent the characteristics of reactors using fuel containing burnable poisons, which are beginning to play an increasingly important role in fuel management, hence the piecewise linear reactivity model was developed by G. T. Park, 1989, to correct the defect in the LRM [55].

This part of the work explains the linear assumption based on evolution of criticality. Let's assume first a linear evolution for k_∞,

$$\text{then} \quad k_\infty = k_\infty^o - \alpha t \tag{2.22}$$

where k_∞^o depends on the initial UOX enrichment in U-235, typically 1.3 for a 3.5% enriched UOX fuel assembly.

Let T = cycle length and N = number of fractionation, so an assembly is used in a core during a total time NT.

Then burn-up at the end of the fractionating cycle, i=1, 2, 3 …N, is T, 2T, 3T … NT

For the whole core average $\left\langle k_\infty^{EOC} \right\rangle$ is defined as the mean of the $k_\infty^{EOC,i}$ of each cycle and can be written as;

$$\left\langle k_\infty^{EOC} \right\rangle = \frac{k_\infty^{EOC_1} + k_\infty^{EOC_2} + k_\infty^{EOC_3} + \cdots + k_\infty^{EOC_N}}{N} = \frac{1}{N}\sum_{i=1}^{N}\left(k_\infty^o - \alpha iT\right) \tag{2.23}$$

Using the formula $S_N = \frac{nN}{2}[2a + (N-1)d]$, where $a = -\propto T$, $d = -\propto T$, one obtains

$$\left\langle k_\infty^{EOC} \right\rangle = \frac{1}{N}\sum_{i=1}^{N}\left(k_\infty^o - \alpha iT\right) = k_\infty^o - \alpha\frac{N+1}{2}T \tag{2.24}$$

To operate the reactor, the effective multiplication factor at the end of irradiation should be to equal to one, $\left\langle k_{eff}^{EOC} \right\rangle = 1$, which can be written using the infinite multiplication factor as $\left\langle k_\infty^{EOC} \right\rangle = 1.03$, this is done in order to compensate for the typical neutron leakage in a PWR.

This gives a period of cycle, T, which corresponds to the time of the reactor operation between two refueling process

$$T = \frac{2}{N+1}\frac{k_\infty^0 - \left\langle k_\infty^{EOC} \right\rangle}{\alpha} \xrightarrow{N=1} \frac{k_\infty^0 - \left\langle k_\infty^{EOC} \right\rangle}{\alpha} \tag{2.25}$$

hence total time an assembly remains in the core (τ) is then obtained as

$$(\tau) = NT = \frac{2N}{N+1}\frac{k_\infty^0 - \left\langle k_\infty^{EOC} \right\rangle}{\alpha} \xrightarrow[N\to\infty]{(NT)_{max}} 2\frac{k_\infty^0 - \left\langle k_\infty^{EOC} \right\rangle}{\alpha} \tag{2.26}$$

From equations (2.25) and (2.26), it can be concluded that the maximum burn-up for an infinite fractionating cycle (N) is twice the burn-up when N=1. Thus, $\tau_{N\to\infty} = 2\tau_{N=1}$
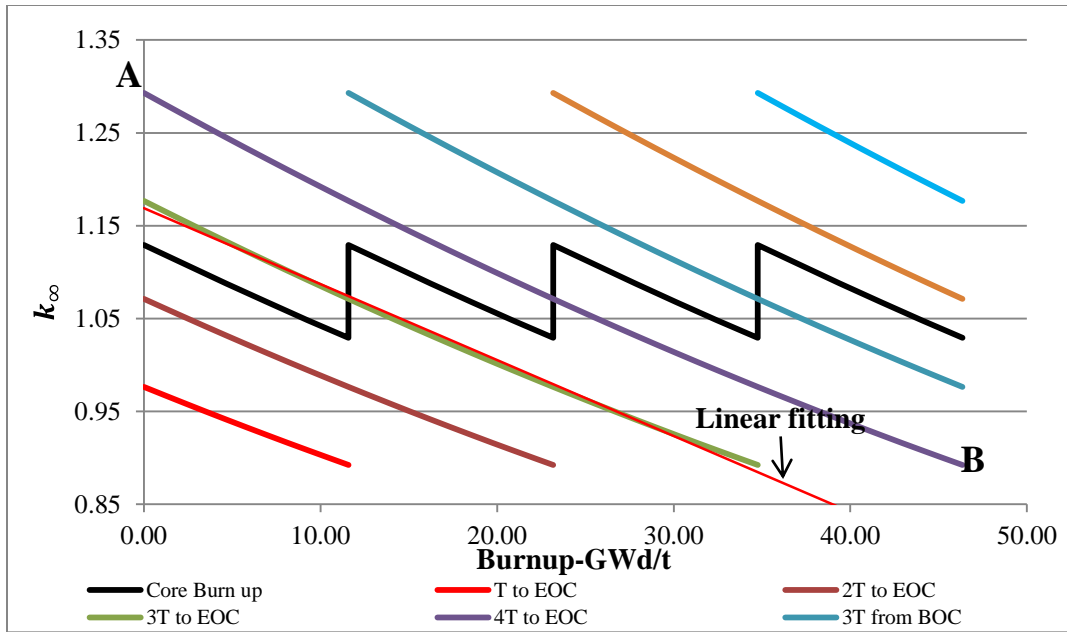
Figure 2.6 Illustration of this calculation for a typical UOX fueled core enriched at 4.3%, with N=4, k_∞^o =1.13 and $\left\langle k_\infty^{EOC} \right\rangle$ = 1.03

The line $\overrightarrow{AB}$ is the burnup for a fraction of assemblies while the thick lines show the total burn-up in the core, at point **A**, fresh fraction of assemblies has been introduced into the core so as to adjust the global k_∞ of the core.

However, in situations where results obtained from simulations do not strictly follow the linear assumption, the quadratic approach can be adopted.

2.4.2 Quadratic Assumption

The linear models, while adequately describing the behavior of higher enrichment reactors, such as the PWR, do not satisfactorily represent the characteristics of reactors which contain burnable poisons to reduce initial fuel reactivity or of the natural uranium reactors. The relationships between reactivity and burnup for such reactors, if operated without partial reloading, are typically quadratic. The reactivity of a natural uranium fueled reactor rises briefly due to plutonium production after the initial samarium dip. G. T. Parks and J. D. Lewins in 1987 developed a quadratic fitting model which included initial reactivity increases [56].

Due to the higher concentration of plutonium utilized in the MOX assembly based on the concept of reaching higher burnup and the low fuel quality as a result of addition of americium

to the MOX fuel, such quadratic burnup curves is expected, hence a quadratic approach is developed in this work.

Thus assuming a quadratic fitting of the form $k_\infty = k_\infty^0 + \alpha t + \beta t^2$ (2.27)

$$\left\langle k_\infty^{EOC} \right\rangle = \frac{\left(k_\infty^0 + \alpha T + \beta T^2\right) + \left(k_\infty^0 + \alpha 2T + \beta (2T)^2\right) + \cdots k_\infty^0 + \alpha NT + \beta (NT)^2}{N}$$ (2.28)

And we have

$$\frac{k_\infty^{EOC_1} + k_\infty^{EOC_2} + k_\infty^{EOC_3} + \cdots + k_\infty^{EOC_N}}{N} = \frac{1}{N}\sum_{i=1}^{N}\left(k_\infty^o + \alpha iT + \beta (iT)^2\right) = k_\infty^o + \alpha \frac{N+1}{2}T + \frac{\beta T^2}{N}\sum_{i=1}^{N}(i)^2 \quad (2.29)$$

but $T^2 \sum_{i=1}^{N}(i)^2 = (T)^2 + (2T)^2 + (3T)^2 + \ldots + (NT)^2 = \left(\dfrac{N^3}{3} + \dfrac{N^2}{2} + \dfrac{N}{6}\right)T^2$ (2.30)

therefore $\left\langle k_\infty^{EOC} \right\rangle = k_\infty^o + \alpha \dfrac{N+1}{2}T + \beta T^2\left(\dfrac{N^2}{3} + \dfrac{N}{2} + \dfrac{1}{6}\right)$ (2.31)

To solve for T using the quadratic formula $T = \dfrac{-b \pm \sqrt{b^2 - 4ac}}{2a}$ for $aT^2 + bT + c = 0$, it becomes

$$T = -\frac{3}{2}\frac{\alpha}{\beta}\frac{(N+1)}{\Omega} \pm \left\{\left(\frac{3}{2}\frac{\alpha}{\beta}\frac{(N+1)}{\Omega}\right)^2 - \frac{6}{\Omega}\frac{K_\infty^0 - \left\langle K_\infty^{eoc}\right\rangle}{\beta}\right\}^{\frac{1}{2}}$$ (2.32)

Hence for a quadratic fit with $(\alpha < 0)$ and $(\beta > 0)$ equation (2.26) becomes

$$T = -\frac{3}{2}\frac{\alpha}{\beta}\frac{(N+1)}{\Omega} - \left\{\left(\frac{3}{2}\frac{\alpha}{\beta}\frac{(N+1)}{\Omega}\right)^2 - \frac{6}{\Omega}\frac{K_\infty^0 - \left\langle K_\infty^{eoc}\right\rangle}{\beta}\right\}^{\frac{1}{2}} \xrightarrow{N=1} -\frac{1}{2}\frac{\alpha}{\beta} - \left\{\left(\frac{1}{2}\frac{\alpha}{\beta}\right)^2 - \frac{K_\infty^0 - \left\langle K_\infty^{eoc}\right\rangle}{\beta}\right\}^{\frac{1}{2}}$$ (2.33)

where $\Omega = \left(2N^2 + 3N + 1\right)$, as $N \to \infty$, $\dfrac{N(N+1)}{\Omega} = \dfrac{1}{2}$

$$(\tau) = NT = -\frac{3}{2}\frac{\alpha}{\beta}\frac{N(N+1)}{\Omega} - \left\{\left(\frac{3}{2}\frac{\alpha}{\beta}\frac{N(N+1)}{\Omega}\right)^2 - \frac{N^2}{\Omega}\frac{6}{\beta}\left(K_\infty^0 - \left\langle K_\infty^{eoc}\right\rangle\right)\right\}^{\frac{1}{2}} \xrightarrow[N\to\infty]{(NT)_{max}} -\frac{1}{2}\frac{\alpha}{\beta} - \left\{\left(\frac{1}{2}\frac{\alpha}{\beta}\right)^2 - 2\frac{K_\infty^0 - \left\langle K_\infty^{eoc}\right\rangle}{\beta}\right\}^{\frac{1}{2}}$$ (2.34)

for $(\alpha < 0)$ and $(\beta > 0)$, the burnup is of the form,
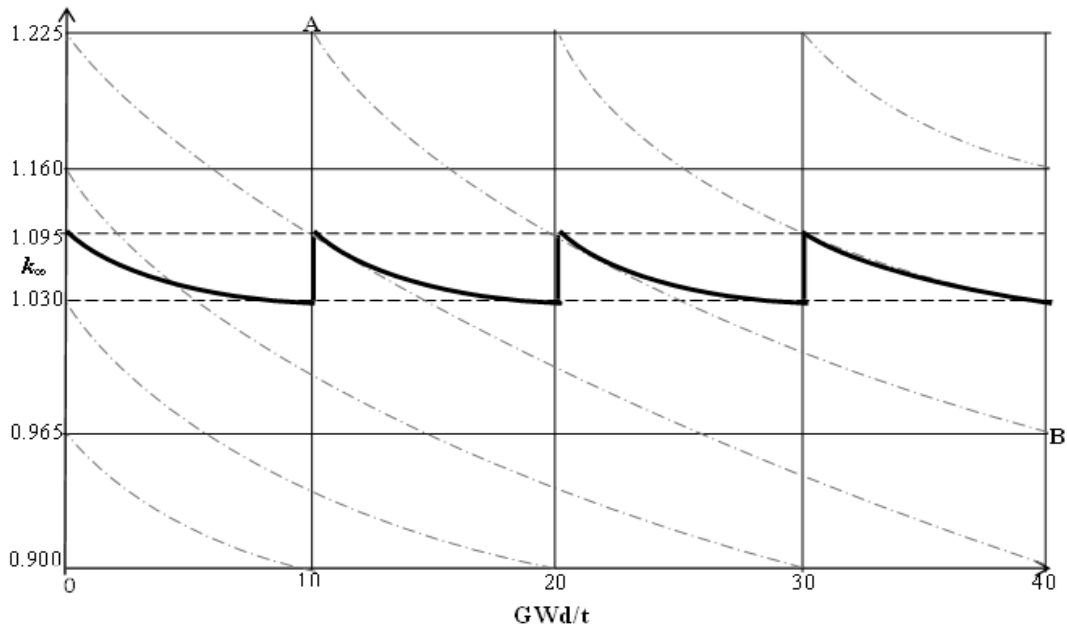
Figure 2.7 Schematic representation of evolution of nuclear fuel using the quadratic assumption with N=4

For a quadratic fit with $(\alpha < 0)$ and $(\beta < 0)$, the burnup is of the form,
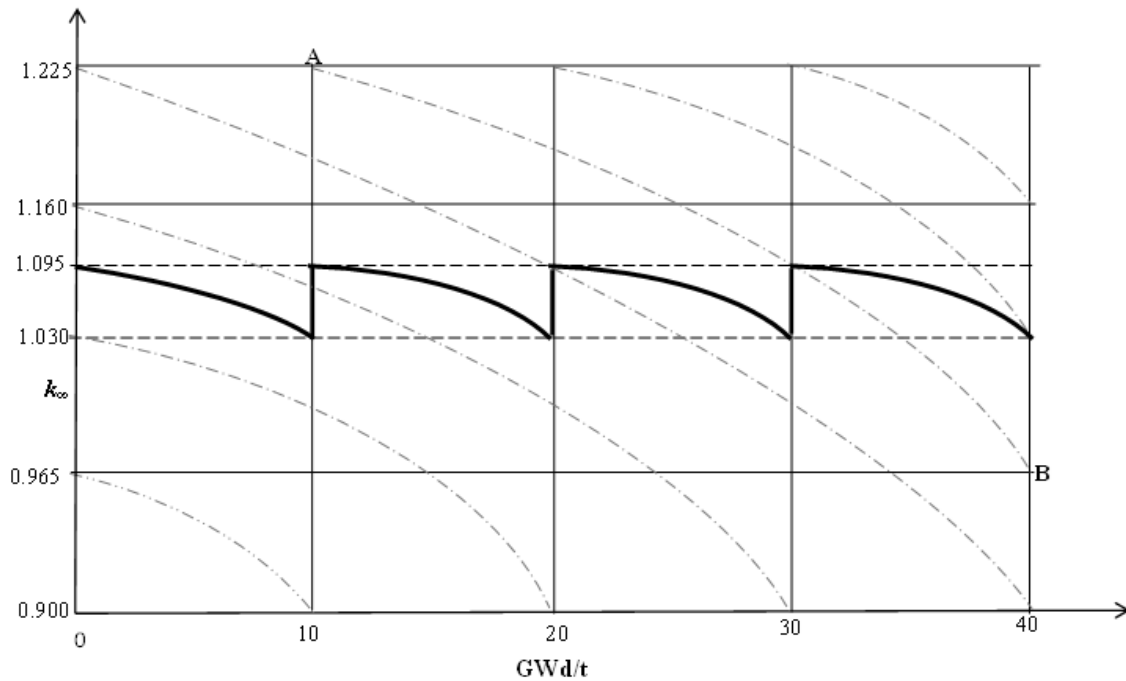
Figure 2.8 Schematic representation of evolution of nuclear fuel using the quadratic assumption with N=4

From equation (2.26), T becomes

$$T = -\frac{3}{2}\frac{\alpha}{\beta}\frac{(N+1)}{\Omega} + \left\{\left(\frac{3}{2}\frac{\alpha}{\beta}\frac{(N+1)}{\Omega}\right)^2 - \frac{6}{\Omega}\frac{K_\infty^0 - \langle K_\infty^{eoc}\rangle}{\beta}\right\}^{\frac{1}{2}} \xrightarrow[N=1]{} -\frac{1}{2}\frac{\alpha}{\beta} + \left\{\left(\frac{1}{2}\frac{\alpha}{\beta}\right)^2 - \frac{K_\infty^0 - \langle K_\infty^{eoc}\rangle}{\beta}\right\}^{\frac{1}{2}} \quad (2.35)$$

$$(\tau) = NT = -\frac{3}{2}\frac{\alpha}{\beta}\frac{N(N+1)}{\Omega} + \left\{\left(\frac{3}{2}\frac{\alpha}{\beta}\frac{N(N+1)}{\Omega}\right)^2 - \frac{N^2}{\Omega}\frac{6}{\beta}\left(K_\infty^0 - \langle K_\infty^{eoc}\rangle\right)\right\}^{\frac{1}{2}} \xrightarrow[N\to\infty]{(NT)_{max}} = -\frac{1}{2}\frac{\alpha}{\beta} + \left\{\left(\frac{1}{2}\frac{\alpha}{\beta}\right)^2 - 2\frac{K_\infty^0 - \langle K_\infty^{eoc}\rangle}{\beta}\right\}^{\frac{1}{2}} \quad (2.36)$$

For burnup in Gigawatts day per tonne of heavy metal (GWd/t), it was calculated as follows;

$$BU(GWd/T) = \frac{\tau(days) \times Power(GWatts)}{Mass\ of\ heavy\ metal(Tonnes)} \quad (2.37)$$

The linear and quadratic fitting for these cores simulated in Table 2.1 has the same K_∞^{EOC} of 1.03 and fractionating cycle, N, is 4. Clearly, it can be seen that there is variation in the output of the both the irradiation time and the burnup of both approaches which is due to the sensitivity of K_∞^{BOC} which varies depending on the chosen fitting. For shorter enrichment, either approach is suitable since the variation is not very significant due to difference in K_∞^{BOC} in the third or fourth decimal number.

Table 2.1 Comparison of the linear and quadratic fitting for UOX fuel at different enrichments

U-235 Enrichment of UOX	Linear Fitting		Quadratic fitting	
	Irradiation time (years)	*Burnup (GWd/t)*	*Irradiation time (years)*	*Burnup (GWd/t)*
2.0%	0.70	8.95	0.69	8.94
4.0%	3.14	40.38	3.22	41.41
6.0%	5.19	66.76	5.32	68.45
8.0%	7.06	90.86	7.25	93.32
10.0%	8.84	113.78	9.04	116.39
12.0%	10.55	135.78	10.82	139.33

However, higher enrichment with its associate longer burnup calculations shows significant variation in their values using both approaches. In Figure 2.6, the linear fitting shows the

variation of K_{∞}^{BOC} from simulated curve of a 6.0% UOX assembly, hence the quadratic fitting is quite suitable for this work since high concentrations of plutonium is also involve.

2.5 Evolution of Radioactivity and Radiotoxicity

2.5.1 Introduction

Separation of the most important nuclides and extracting them from storage with subsequent transmutation permits to reduce radiological danger of wastes staying in storage. Removal of nuclides with increased decay heat power from storage permits to ease requirements to heat removal systems at long-term storage of wastes and to minimize the size of the high activity waste.

2.5.2 Radioactivity

Radioactivity is defined as the spontaneous nuclear transformation of an unstable element which results in the formation of a new one. The process of radioactive decay is statistical and therefore random in its nature. Radioactivity is a nuclear process that originates in the nucleus and is therefore not determined by the chemical or physical states of the atom [57]. A radioactive nucleus has no age, that means that the probability to decay in the coming second is constant with time, and does not depend on the previous time spent. This probability is the decay constant, λ, so the probability for a nucleus to decay in time dt is λdt. Then from the total number of nuclei N, in time dt, the number of nuclei that will decay, dN, can be calculated as

$$dN = -N\lambda dt \tag{2.38}$$

Since the decay constant is not dependent on, the solution of the above equation is simply

$$N = N_o e^{-\lambda t} \tag{2.39}$$

where N_o is the starting number (amount) of nuclei and N represents the amount of nuclei that did not decay after time t [57].

Activity, **A**, is the number of nuclei decaying per unit time. If the probability for a nucleus to decay is λ, and there are N nuclei present, the average number of decaying nuclei is $N\lambda$, and is defined as activity

$$\mathbf{A} = N\lambda \tag{2.40}$$

Thus, from equation (2.39), $A \equiv N\lambda = N_o \lambda e^{-\lambda t} = A_o e^{-\lambda t}$ (2.41)

Hence the total activity due different nuclei at time t is expressed as;

$$A(t) = \sum_i A_i = \sum_i \lambda_i N_i(t) \tag{2.42}$$

Let's consider the decay of an unstable mother nucleus as follows; $N_1 \rightarrow N_2 \rightarrow N_3$

Assuming that half- lives of the isotopes in the decay chain are as follows;

$N_1 \rightarrow T_1 = 5$ $N_2 \rightarrow T_2 = 2$ $N_3 \rightarrow T_3 = 1000$

then
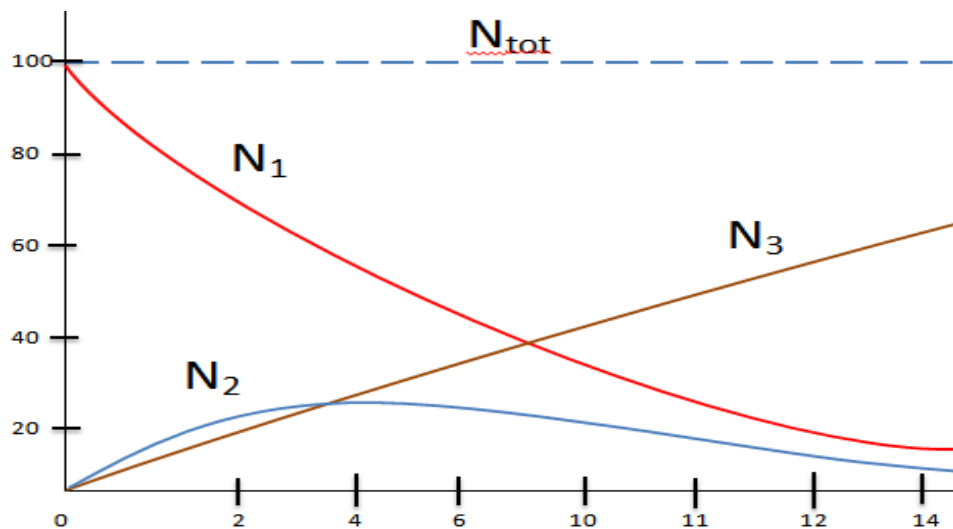
Figure 2.9 Schematic representation of contribution of daughter and precursor nuclide to the total radioactivity.

For N number of nuclei in a spent nuclear fuel, the time considered for the calculation of the evolution of the radioactivity and radiotoxicity extends to millions of years. On such time scales, the Runge-Kutta method cannot be used for resolving the Bateman equations (equation 2.13); Indeed, to be stable, this method implies that the *dt* to obtain *N(t + dt)* with *N(t)* is of a very small order of time compared to their half-life. The equations of Bateman presented under matrix form in equation (2.14) are then resolved by diagonalization of the evolution matrix **B** [42].

The matrix in equation (2.14) is diagonalised by calculating the transition matrices P and P^{-1} as:

$$B = P^{-1}\Delta P \tag{2.43}$$

P is the transition matrix from $\boldsymbol{B}$ to Δ, where Δ is a diagonal matrix which constitutes the eigenvalues of $\boldsymbol{B}$. Then equation (2.14) can be written as:

$$\frac{d\vec{N}(t)}{dt} = P^{-1}\Delta\vec{P}(t) \tag{2.44}$$

Multiplying through equation (2.44) by P, and letting $\vec{N} = P\vec{N}$ the equation (2.44) becomes

$$\frac{d\vec{N}(t)}{dt} = \Delta\vec{N}(t) \tag{2.45}$$

This system is integrated easily (from the fact that Δ is diagonal):

$$\vec{N}(t) = e^{\Delta t}\vec{N^o}(t) \tag{2.46}$$

Hence,
$$\vec{N}(t) = P^{-1}e^{\Delta t}\vec{N^o}(t) = P^{-1}e^{\Delta t}P\vec{N^o}(t) \tag{2.47}$$

Let
$$\Gamma(t) = P^{-1}e^{\Delta t}P \tag{2.48}$$

Then
$$\vec{N}(t) = \Gamma(t)\vec{N^o} \tag{2.49}$$

Therefore $N_i(t)$ in equation (2.45) can be written as:

$$\vec{N}_i(t) = \sum_j \Gamma_{i,j}(t)\vec{N}^o_j \tag{2.50}$$

2.5.3 Radiotoxicity

Radioactivity is not sufficient to describe the risk one human being takes when he ingests radioactive material. The concept of radiotoxicity by ingestion tries to distinctively quantify the effect of the different types of radiotoxicity to build a quantitative evaluation of the risk.

The problem of a radiotoxicity of long-lived radioactive wastes produced in various nuclear fuel cycles is important from the viewpoint of ecological danger of these cycles. Emitted Particles do not have the same effects.

The radiotoxicity of a radionuclide is influence by the following factors;

- Energy of the rays (nuclear properties)

- Location of Absorption in the organism (chemical properties)

- Residence time in the body (chemical properties)

For the radiotoxicity, $R(Sv)$, analyses of each radio-nuclide, the contribution dose is proportional to the integral activity **A** (in Bq), where the coefficient is called as the Dose Factor (F_d) "via ingestion" or "via inhalation" (in Sv/Bq):

$$R(Sv) = F(Sv/Bq) \times A(Bq) \tag{2.51}$$

For waste characterization in a geological storage, most of the time radiotoxicity by ingestion is used, because radionuclides are supposed to migrate from the disposal towards the biosphere. However, a complete risk analysis must take into account the difference of migration characteristics of the different elements present in the disposal, which is not performed in this work.

Table 2.2 Period and factor of dose "via ingestion" [58].

Nuclides	Life period (years)	F	Emission
Tc-99	2×10^5	0.64×10^{-9}	β-
I-129	1.6×10^7	0.11×10^{-6}	β-
Pu-238	88	0.23×10^{-6}	α
Pu-239	2.4×10^4	0.25×10^{-6}	α
Am-241	432	0.20×10^{-6}	α
Am-243	7.4×10^3	0.20×10^{-6}	α
Cm-244	18	0.16×10^{-6}	α

Hence, the radiotoxicity of each nuclide varies with time as the following:

$$R_i(t) = F(i) \times \lambda_i N_i(t) \tag{2.52}$$

where N_i is defined amount of nuclide present in isotope, i, at time t.

As we have seen with the equation (2.52), the potential radiotoxicity for a geological time t is expressed as a function of the activity **A** and dose factor f, hence the total radiotoxicity for different nuclei i in Sv is expressed as:

$$R(t) = \sum_i f_i \lambda_i N_i(t) \tag{2.53}$$

where f_i factor dose of the nuclei i , λ_i the decay constant of the nucleus i, and $N_i(t)$ is the number of nuclei i. The origin is the separation of the isotopes considered as waste and recoverable materials from the spent fuel considered.

Hence, with reference to equation (2.50), equation (2.53) becomes

$$R(t) = \sum_i \sum_j f_i \lambda_i \Gamma_{i,j}(t) \overrightarrow{N}_j^o \tag{2.54}$$

The sum over the index j corresponds to a sum over the nuclei initially present in the inventory of which the radiotoxicity is calculated. The sum over the index i, it corresponds to the sum of all nuclei present at time t at which radiotoxicity is calculated. This leads to two different physical descriptions when one looks at the radiotoxicity contributions of each isotope [42]. If one wants to determine the contribution of each of the evolving isotopes present at time t, then:

$$R(t) = \sum_i R_i(t) \tag{2.55}$$

where
$$R_i(t) = f_i \lambda_i \overrightarrow{N}_i(t) = f_i \lambda_i \sum_j \Gamma_{i,j}(t) \overrightarrow{N}_j^o(t) \tag{2.56}$$

In this case, $R(t)$ represents the radiotoxicity induced by nuclei i present at time t.

To determine the nuclei present at the initial time responsible for the radiotoxicity time t, even if they disappeared for a long time, a nuclei representation by mother is used. If one knows the radiotoxicity induced by the nuclei j present at the initial time t, then it can be written as:

$$\overrightarrow{N^0} = \begin{pmatrix} 0 \\ 0 \\ \dots \\ N_j \\ \dots \\ 0 \\ 0 \end{pmatrix} \tag{2.57}$$

Then $\overrightarrow{N_i}(t)$ becomes;
$$\overrightarrow{N_i}(t) = \Gamma_{i,j}(t)\overrightarrow{N_j^o} \tag{2.58}$$

The induced radiotoxicity at time t by the nuclide j present at the time $t = 0$ is:

$$\tilde{R}_j(t) = \sum_i f_i \lambda_i \Gamma_{i,j} \vec{N}_j^o \tag{2.59}$$

The induced radiotoxicity at the time t by several nuclei j presents initially is given as [42]:

$$R(t) = \sum_j \tilde{R}_j(t) \tag{2.60}$$

This equation represents all the set of coupled differential equations for the decays which is solved by the matrix diagonalization procedure discussed. Inventory composition over time is then directly obtained from the initial composition [45].

2.6 MURE TREATMENT

2.6.1 Radiotoxicity

In this work, the graphic user interface (GUI) of MURE has the capability to analyze the radiotoxicity of the evolution of a nuclear fuel. The ROOT graphical tools develop at CERN is necessary if one want to use the post treatment GUI tools. In the GUI, radiotoxicity of fuel/waste can be calculated and plotted.

In the Radiotoxicity Tab, shown on Figure 2.10, decay calculations can be performed for the final inventory, after an evolution has been done. Determination of total and partial radiotoxicities, heat released and activities as a function of time can be computed for a given system.

The "Built Mat" button will compute the Material and the Matrices. The material is based on the material defined in the DATA files where all the nuclei are copied, and all their decay children.
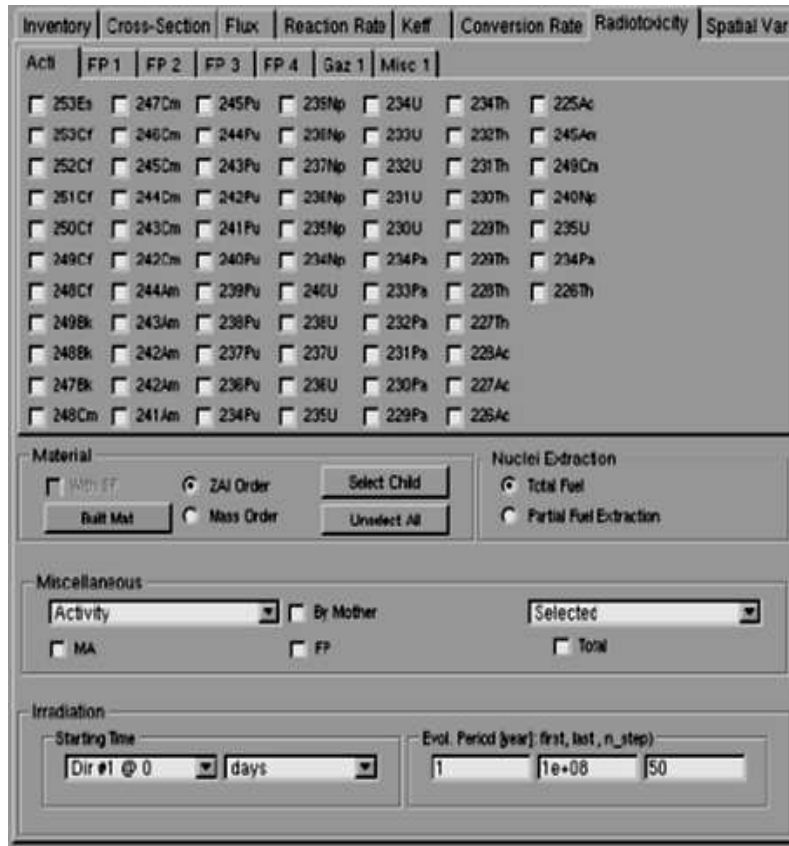
Figure 2.10 Mure Graphic User Interface (MureGui), the radiotoxocity tab [43]

In this work, the partial radioactivities "by mother" will be used essentially to analyse the radiotoxicity of the spent fuels. The because we are interest of this study lies in the long-term impact in the geological disposal of a minor actinide (Am) to verify the possibility of reprocessing it in a MOX fuel, from spent UOX fuel.

2.6.2 Residual heat

When the reactor is shut down, the accumulated fission products continue to decay and release energy within the reactor. This fission product decay energy can be quite sizable in absolute terms. The β- and γ-radiation emitted from decaying fission products amounts to about 7% of the total thermal power output of the reactor.

Consider a reactor that has been operating at a constant thermal power P_o long enough for the concentrations of the radioactive fission products to come to equilibrium. Since the rate of

production of the fission products is proportional to the reactor power, it follows that the activity, **A**, of the fission products at any time after the reactor has been shut down is also proportional to P_o. The waste in MURE heat is calculated according to the calculation of activity as shown in equation (2.42).

The evolution of the activity is calculated in the same manner as that of the radiotoxicity (equation 2.45). To calculate the residual heat, the nuclei heat factors, *f* are incorporated in place of dose factors in radiotoxicity, which are expressed in watts per Curie (W/Ci).

For the contribution to the residual heat of individual nuclei, once the activity is calculated, either by daughter or mother mode, the value of the activity simply multiply by the heat factor (W/Bq). The residual heat in watts is then obtained. The method of resolution of *N(t)* is exactly the same as that of previously written for the calculation of radiotoxicity. However, the time scales are different, while the radiotoxicity is described on geological periods up to several million years, residual heat from nuclear waste is designed for underground storage site for a few hundreds of years [42].

2.7 SYSTEM DESIGN of AMERICIUM MONO-RECYCLING IN PWR

Based on a large program of experimentations implemented during the 90s, the industrial achievement of new Fuel Assemblies (FAs) designs with increased performances opened up new prospects. The currently Uranium Oxide (UOX) fuels used on the 58 Electricite´ De France (EDF) PWR units are now authorized up to a maximum FA Burn-Up (BU) of 52GWd/t with a large experience from 45 to 50GWd/t for current management modes.

Regarding the back end of the fuel cycle, from the origin EDF strategy has focused on ''closing the fuel cycle'' (reprocessing and the recycling of valuable materials). This strategy led EDF to decide in 1984 to recycle plutonium (Pu) in the PWR 900MW units. By October 2005, 20 reactors have been loaded with 1,100 tons of Mixed Oxide (MOX), corresponding to the recycling of 58 tHM (tons of heavy metal) of plutonium [6].

In this work, the open cycle of the UOX fuel strategy of the fuel cycle is integrated in the closed cycle of the MOX fuel with the aim of reducing radiotoxicity of waste by reprocessing Americium together with Plutonium. Various burnups of UOX is simulated and the spent fuel from the UOX strategy is cooled for different years, reprocessed and fabricated into a MOX

(Plutonium and Uranium) fuel or MOXAm (Plutonium, Uranium and Americium) to be re-used in the reactor to achieve various burnups. The Radiotoxicity of the spent fuel from both the closed, open and the integrated system are analysed with and without specific isotopes such Americium, Plutonium and Uranium. The availability of Americium for incineration in fast reactors is important in this integrated cycle. This nuclear fuel strategy used is shown in below;
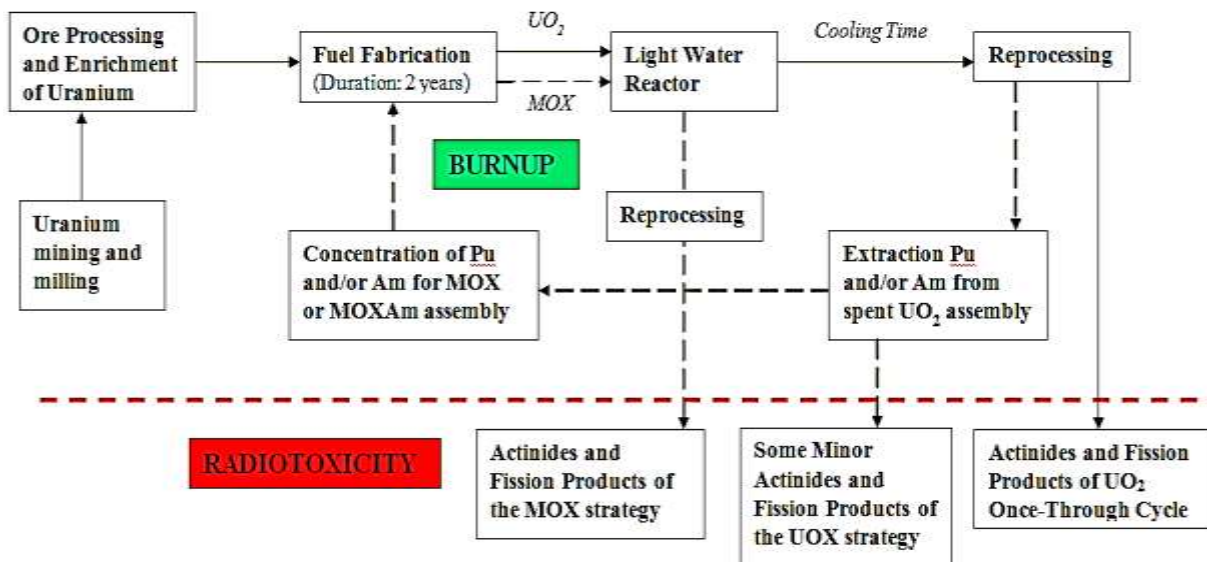
Figure 2.11 The Nuclear cycle of the integrated system of closed UOX and MOX fuel cycle (Dash black line showing the path of reprocessed Plutonium and/or Americium strategy).

In this integrated system, the UOX used in a light water reactor. After the fuel has been utilized, wet storage is done for cooling before reprocessing and fabrication into a new fuel. All that period after the fuel burnup in the core constitutes the cooling time of the spent fuel. This area is well monitored due to isotopic changes by radioactive decay during this period. In Figure 2.11, the solid line depicts the open system where all fission products minor actinides ends up in permanent storage. The broken arrow lines shows the part of the system where the UOX spent fuel from the light water reactor is reprocessed into a standard MOX or MOXAm fuel to be fed back in to a lighter water reactor.

A complete assembly of a Pressurised Water Reactor (PWR) was modeled for this work using the MURE code. Reflective surface were put at the boundaries of the assembly design to mimic the performance of a fuel assembly in the core of a PWR (see Table 2.3 and Figure 2.12).

With the MURE code, the burnup performance and the radiotoxicities of fuels and waste are compared and analysed with respect to varying cooling times when the spent UOX assembly came out from the reactor core. The basic safety features of these fuels, in terms of moderator void co-efficient, fuel and moderator temperature co-efficient were also considered using the MCNP by changing moderator densities and temperature and fuel temperatures accordingly.

2.7.1 Fuel Assembly Design Consideration

Table 2.3 shows the parameters incorporated in the design of the fuel pins and assemblies for the various type of fuel used in the N4 type French pressurized water reactor. This assembly was design by Framatome ANP (Areva NP, previously Framatome Advanced Nuclear Power - until March 1, 2006 - , is a French company of supply for the nuclear industry founded in 2001, by the French company Framatome and the German company Siemens).

The MOX FA of the current operating French reactor contains plutonium mixed with depleted uranium (0.25% 235U). The Pu content is adjusted to take account of its isotopic composition (63 to 70% fissile Pu). Energy equivalence to 3.25% enriched UOX is obtained with an average content of about 7% total Pu in MOX. Currently, ''hybrid'' management is implemented with 3-batch for MOX and 4-batch for 3.70% UOX. The average MOX BU is maintained at around 38GWd/t. In the simulated assembly of this work, the assembly contains only UOX or MOX fuel pins.

From the origin of the MOX use in EDF PWRs, some 1,800 MOX Fuel Assemblies (Fas) have been unloaded after 3 annual cycles. Only 4 failed MOX FAs have been identified from the beginning (probably caused by debris), which gives a very satisfactory level of reliability to MOX, same or better than UOX fuel.

The larger proportion of plutonium in the core shifts the neutron spectrum towards higher energy levels, thereby reducing the efficiency of the control systems. This has led to improve the control rods pattern, to increase boron concentration of the boron make-up storage tank and to increase boron concentration of the refueling water storage tank. In view of this, the boron concentration in the PWR fuel assembly in this work is set to 600ppm [6].

EDF is now looking to introduce fuels with a higher plutonium content (up to 8.6% total Pu) equivalent to UOX enriched to 3.7%). It is the goal of the MOX Parity core management which

main features are: annual cycles, 3.7% UOX and 8.6% total Pu for MOX, managed in 4 batches. It will also contribute to recycle more plutonium each year, in the goal to stabilize the amount of separated plutonium. Hence high concentrations of plutonium to reach higher burnups were also incorporated in this work as well.

Table 2.3 Design parameter of UOX and MOX assembly for Pressurised Water Reactors

Materials	*Parameters*
Number of fuel pins	264
Number of lattice points	17 X 17
Fuel material	UOX and MOX
U-235 Enrichment of UOX	variable for required BU
U-235 Enrichment of MOX	Depleted Uranium (0.25%)
Concentration MOX	variable for required BU
Fuel diameter	8.20mm
Clad material	Zircaloy
Clad diameter	9.50mm
Clad thickness	0.57mm
Distance between pins	12.60mm
Simulated Length of Fuel Pin	213.35mm
Simulated Length of Assembly	224.4mm
Moderator	H2O + 600ppm of Boron
Simulated Thermal Power	0.982MWth

The MURE code which works together with the MCNP code generates the input file of the MCNP code to be utilised. The fuel assembly simulated has about 4.75% the height of the normal fuel assembly with reflected surface at it boundaries. Below is the cross-section view of the whole assembly design from the visual editor, with a zoom on one of the fuel pins.
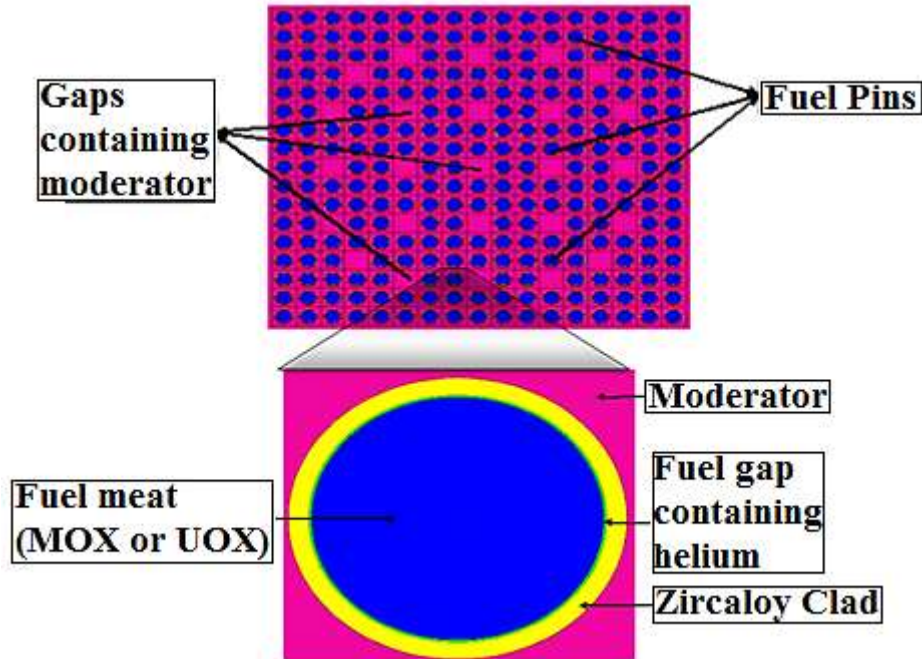
Figure 2.12 MCNP Schematic diagram of fuel assembly used in the simulation with a zoom on a fuel pin

As shown in Figure 2.1, the burnup steps are indicated. Each point represents an MCNP simulation (2.3 x 10^6 particle histories), hence to reach the required burnup with prcission, several burnup steps are simulated. It takes about 5hours 30mins to complete one fuel burnup assembly which consist of 20 burnup steps (MCNP runs) on 6 processors of 2.9GHz CPU. Hence burnup calculations are expensive in time. During each MCNP calculation, the fuel is evolved and the input file is updated as shown in Figure 2.5.

2.8 FUEL CYCLE STRATEGIES EMPLOYED

2.8.1 Reprocessing of spent UOX

In this work, all the results are considered for an equilibrium theoretical scenario, where all the spent UOX are reprocessed the same way to produce a MOX fuel or a MOXAm fuel. Waste characterization takes into account the normalization by the factor *R*, which is dependent on indices such as the cooling time, isotopic concentration and fuel quality. Every fuel cycle strategy considered in this work has its own *R* factor.

$$R = \left(MOX_{Assembly} \middle/ UOX_{Assembly} \right) \tag{2.61}$$

where

$MOX_{Assembly}$ is the mass of plutonium (and americium) at BOC needed for MOX or MOXAm assembly to reach a specific burnup.

$UOX_{Assembly}$ is the mass of plutonium (and americium) extracted form spent UOX assembly specific after cooling time.

This **R** factor is taken into account in all normalization to compare the various individual strategies considered.

The spent UOX fuel was allowed to cooling for a period of 5 years and 30 years before reprocessing to study the effect of short and long cooling times respectively. For all cases, a fabrication period of 2 years follows the separation process. During this period outside the core, the fuel continues to evolve by radioactive decay. The main contributor of the fuel evolution is the beta- decay of Pu-241 into Am-241, within a period 14.32 years. The composition of the new MOX or MOXAm assembly is determined to reach 46GWd/t and 68GWd/t, with and without americium from the spent UOX fuel.

Table 2.4 Extracted actinides from UOX spent fuel to fabricate MOX and MOXAm fuel

Actinides in spent UOX after 46GWd/t	Mass in kg/GW$_e$y per simulated assembly		
	At discharge	*After 5+2 years of cooling*	*After 30+2 years of cooling*
Pu-238	6.551	7.829	6.430
Pu-239	155.792	158.407	158.312
Pu-240	68.057	70.866	71.686
Pu-241	43.148	35.596	10.675
Pu-242	19.193	21.224	21.224
Am-241	1.516	10.540	34.458
Am-243	4.635	5.377	5.365

2.8.2 Burnup and Radiotoxicity of MOX

The Plutonium-Uranium Oxide (MOX) fuel assembly was design using spent Uranium Oxide (UOX) fuel burnt at 46GWd/t and 68GWd/t. This was achieved by extracting plutonium from the spent UOX fuel to create a MOX fuel, after a given period of cooling. In the case where Americium was extracted together with Plutonium, the Plutonium-Americium Uranium Oxide (MOXAm) fuel is fabricated. In all the burnup calculations done in this work, the fabrication time of the MOX or MOXAm assembly was set at 2 years and the fractionating cycle, N, was set at four (4) for all burnups in which fuel management was incorporated. The criticality at the end of a fractionating cycle (k_∞^{eoc}) was also set at 1.03 for all PWR assemblies, to simulate the neutron leakage (MCNP calculation are done for an infinite medium).

As shown in Figure 2.13, various burnup calculations were simulated to attain a specific burnup. Each burnup curve consists of 20 burnup steps. With the help of calculations made in Figure 2.14, the burnup calculations and their corresponding enrichment or concentration are finally estimated by further fine tuning simulations.
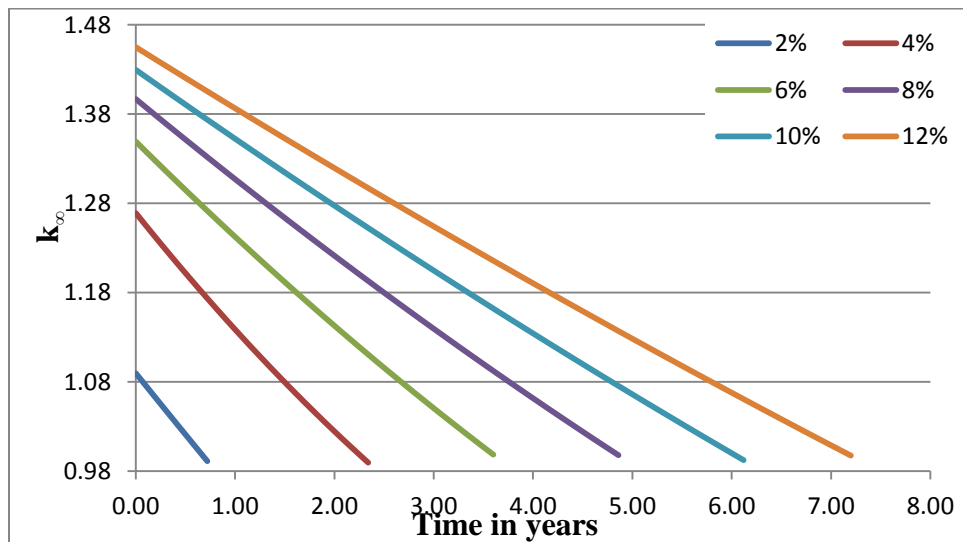
Figure 2.13 Evolution of k_∞ for UOX assembly at various U-235 enrichments.
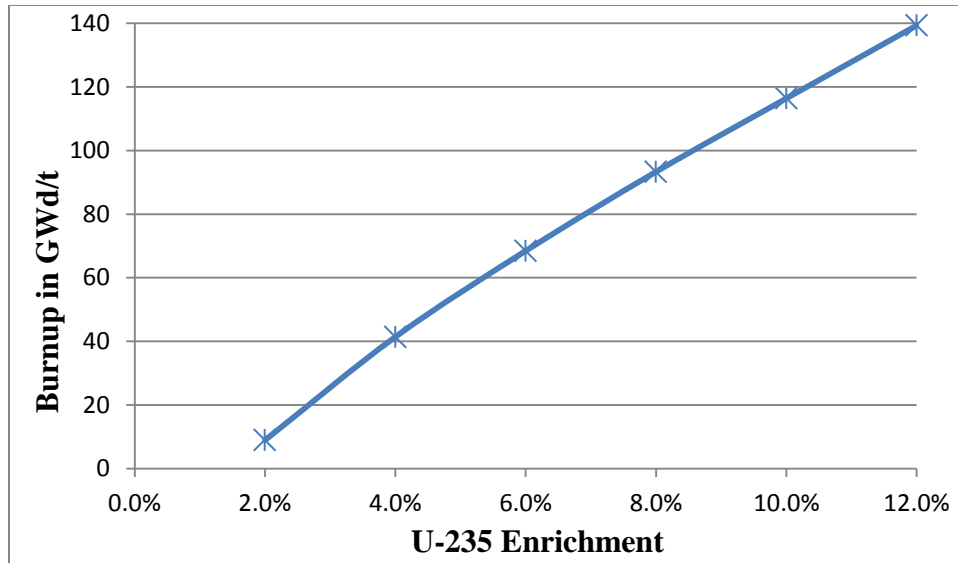
Figure 2.14 Burnup calculations for UOX assembly at various enrichments.

The actinides extracted from the UOX spent assembly, Table 2.4, are added to depleted uranium at various concentrations to estimate the burnup of the MOX and MOXAm assembly. The processes illustrated in Figure 2.13 and Figure 2.14 are also adopted to reach the required burnup of 46GWd/t and 68GWd/t. This process was utilized for all burnup fitting in this work

However, during the curve fitting of the burnup curves, different values were recorded for different fittings. The linear fitting and the quadratic fitting gave different burnup results. Hence there was the need to modify the curve fittings of the simulated burnups.

Equations (2.16) to (2.20) have been widely used to estimate the burnup of simulated nuclear assemblies with acceptable error margin. However, longer burnups simulated in this work did not fit well with the linear assumption, especially for MOX assemblies. In view of this observation, the quadratic approach is used, equations (2.18) to (2.29), to fit the long burnup curves which had significant curve during the evolution period.
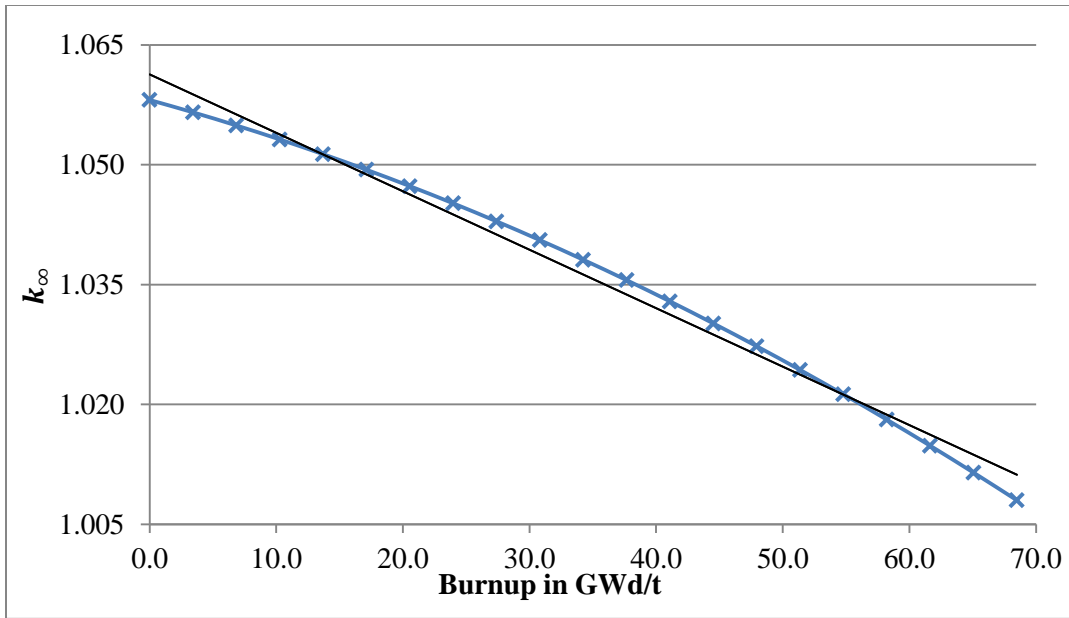
Figure 2.15 Burnup curve fitting of MOXAm assembly to reach 68GWd/t not in agreement with linear fitting

In Figure 2.15, the burnup curve, when fitted with the quadratic equations was calculated to be 68GWd/t but a 80.73GWd/t burnup value was calculated when a linear fitting was used. However, both approaches report similar values for short burnups. This quadratic approach can also be used to precisely predict burnups cases where significant breeding is observed, such as in a CANDU reactors. Hence, the quadratic fitting was used to analyse all burnup simulations unless stated otherwise.

The radiotoxicity and decay heat of the spent assemblies were also calculated for the UOX and MOX strategies using the MureGui console (as described in section 2.6) which works hand in hand with the MURE code. The radiotoxicities of the spent fuel were analysed from the point of fuel discharge to millions of years for all the fuel assemblies. In the case of reprocessed spent fuels, chemical losses were estimated to be 1.0% of the original mass of the particular isotope.

The radiotoxicities of the MOX or MOXAm strategies were compared to the UOX strategy to see which strategy performed well in terms of radiotoxicties. This was also repeated for the decay heat analysis. The formula below was used for the comparison to enable good comparison;

$$MOX^{Total} = \left(MOX^{At\ Discharge} \right) + \left\{ (UOX^{glasses}) \times R \right\} \qquad (2.62)$$

$UOX^{glasses}$ is processed waste of the UOX assembly where specific isotopes such as Plutonium and/or Americium have been extracted after specific years of cooling, leaving chemical losses of 1.0% .

Equation (2.62) was developed to calculate the total radiotoxicity of the MOX or MOXAm strategy so as to truly compare it to the UOX strategy. The comparison of radiotoxic analyses where done in Sievert per terawatt hour electric (Sv/TWe), this mode of comparison was done to link the electrical power of the assembly to its radiotoxicity and hence present a good comparison for each assembly.

2.8.3 Safety parameters

In the preliminary and final safety analysis reports (PSAR and FSAR), an applicant for a reactor license must analyze a set of postulated, severe accidents to show that the facility can be operated without undue risk to the health and safety of the public. These are called design basis accidents (DBA). For the purpose of evaluating the safety of the plant, these accidents are analyzed within the framework of highly conservative assumptions that tend to exaggerate the consequences of each accident. They are used as a basis for the design of plant safety features.

Any unexpected decrease in coolant flow through a reactor core can lead to serious consequences for the plant as a whole. Such a drop in flow can be caused by anything from a leak in a small coolant pipe to the complete severance of a major coolant pipe. It is the latter that is the starting point of a design basis of Loss of Coolant Accident [2]. Decrease in coolant flow can also be caused by malfunctioning of the primary pumps that circulate the coolant causing temperatures to rise in the coolant or moderator and fuel materials as well.

In view of this, all the fuel assembly types being analyzed in the work were tested in terms of Coolant Void Reactivity, moderator and fuel temperature coefficient. The calculations were made for infinite medium because the variation of neutron leakage due to the loss of moderator was not taken into account. Therefore, in real terms, the safety parameters are better when the leakage term is factored into their calculation.

The density of the moderator was reduced at a rate of 10% to mimic loss of coolant. The MCNP code was the utilized to check for fuel behavior in case of a hard spectrum. The k-effectives were

then recorded check for a negative or positive moderator void co-efficient. During the onset of LOCA, temperature feedback effect also plays a role in the k-effective of the core, hence the fuel and moderator temperature coefficient were also measured by increasing the fuel and moderator temperature at rate of 10% of the nominal temperature. The MCNP code was sole used in this calculation. The safety assessment of these fuel assembly were conducted both at beginning of assembly cycle (BOC) and at end of assembly cycle (EOC). This is to also see the effect that fuel depletion and other fission product together with actinides play on safety parameters.

Decay heat analysis were done by simulated the decay of 3,457 isotopes to see the effect few seconds after shutdown and also long term effect. The contributions of fission product and the minor actinides were the major concern. This was achieved by interlacing the isotopic inventory to the MureGui interface.

2.9 SYSTEM DESIGN of CORE CONVERSION IN MNSR

The China Institute of Atomic Energy (CIAE) has designed a new reactor called the In Hospital Neutron Irradiator (IHNI). This reactor is similar in physics and design to the present MNSR and is expected to operate with LEU fuels in hospitals. Many MNSR operating countries including Ghana, Nigeria and China have been studying conversion of existing MNSR cores to LEU. It is generally accepted that conversion of the MNSRs is feasible and it is likely that China or other fuel fabricators will be able to produce LEU cores for MNSR reactors in the near future. Hence at a Technical Meeting of the International Atomic Energy Agency (IAEA) held in May 2005, all the participating MNSR operators indicated their desire to convert to LEU fuel. It was acknowledged that to successfully carry out MNSR core conversions, a number of preparatory steps, including additional analysis and various calculations have to be made, in order to confirm the feasibility of conversion [59].

In this work, the MNSR fuel cycle is design as a once-through cycle where the one assembly core will be put permanent storage after the fuel is spent. The burnup of both the HEU and LEU cores were simulated using the MURE code and the appropriate equation was used for the burnup based on whether the simulation obeys the linear or quadratic curve. The core-life times of the simulated cores calculated based on the operations of the currently operating Ghana Research Reactor-1(GHARR-1) MNSR. The radiotoxicity of the HEU core is compared to LEU core after their core-lifetime using the MUREGUI. This is to investigate the impact of the spent

cores, especially the HEU which due for storage, on exposure in terms of radiotoxicity. The LEU core is proposed to be house in the same location of the HEU core without a complete change in the nuclear structure material. Hence, there is the need to compare their basic safety inherent feature in terms of moderator void coefficient, fuel and moderator temperature coefficient using the MCNP by changing moderator densities and temperature and fuel temperatures accordingly.

2.9.1 MNSR Assembly Design Consideration

Odoi H.C et al, 2011, performed neutronic analysis on the proposed LEU core at 12.6% enrichment to investigate neutronic parameters based on change in reflector thickness of the MNSR [7]. In a private conversation with Henry Cecil Odoi in 2011, it has been agreed at an RERTR (Reduces Enrichment of Research and Test Reactors) meeting that the enrichment of the proposed LEU fuel should be 12.5% UOX which is readily available on the market. In this work, the LEU core is designed based on this enrichment and the designed parameters of Odoi H.C et al 2011.

The proposed LEU core of the MNSR has all component of the HEU except the following which has been presented in a tabular form in Table 2.5 below;

Table 2.5 Difference between the HEU and LEU MNSR cores

Parameter	HEU	LEU
Rated thermal Power	30kW	34kW
Fuel	U-Al dispersed in Al	UO_2
Enrichment	90.2%	12.5%
No. of fuel pins	344	348
Fuel Clad	Aluminium	Zircaloy
U-235 loading	~1kg	~1.357kg
Num. of Dummy Rods	6	2

Just as the PWR, The MURE code was used together with the MCNP code to generate the input file of the MCNP code to be utilised. But due sensitivity of the MNSR to reactivity, reflected

surface were not employed in modeling the MNSR. The whole core together with the main structural material were modelled and this was very expensive in time.

Below are the cross-sectional views of the whole core design from the visual editor of the MCNP.
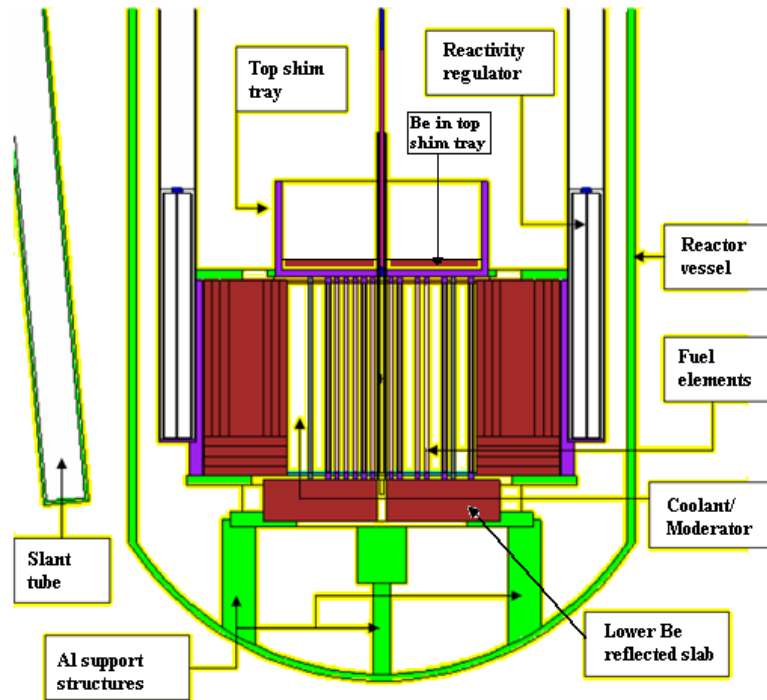
Figure 2.16 MCNP plot of vertical cross section of GHARR-1 reactor (control rod in full withdrawn position) showing structural supports

Due to the sensitive nature of the MNSR cores, the MCNP simulations were run at 200 active with 20 in-active with initial particle of 10,000, this is to make sure that there is enough neutron distribution the core and decrease statistical error before the KCode is calculated. This large number of particle histories caused the burnup calculation of the MNSR to last longer than the PWR with same burnup steps.
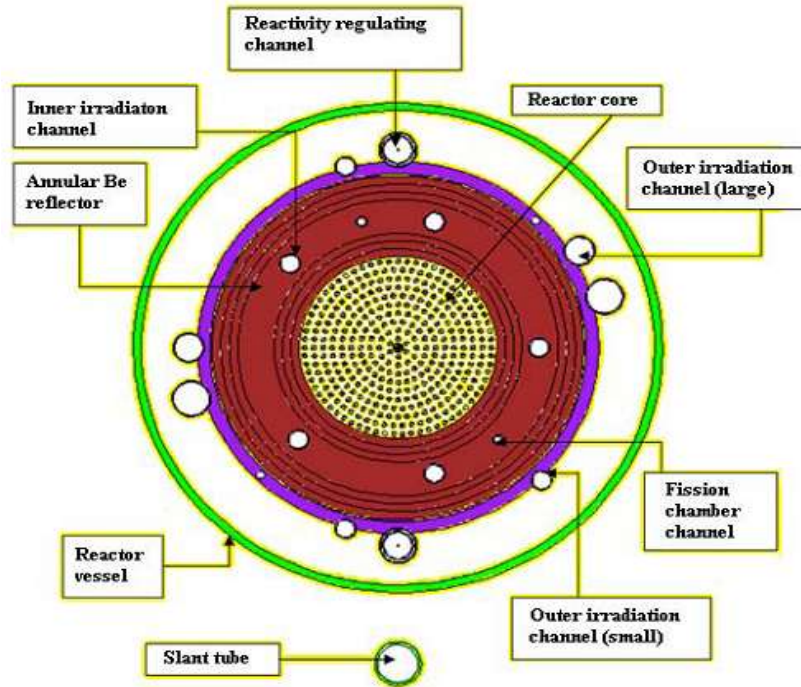
Figure 2.17 MCNP plot of GHARR-1 core configuration showing fuel region (reactor core), channels for irradiation, fission chamber, regulating, slant and annular beryllium reflector

2.9.2 Method employed for MNSR Analysis

Boafo E.K. et al, 2012, performed burnup analyses of the GHARR-1 using the computer code BURNUPPRO. The analyses were based on the rate of change of each fuel isotope density in the GHARR-1 core given by first order differential equations. These equations were solved based on the three energy group model (fast, resonance and slow). The paper concluded that the actinide inventory provided indicated that about 1% of initial U-235 loading of the HEU core has been depleted after 18,00hrs of reactor operation [60].

2.9.2.1 Burnup of cold clean core

The MNSR cannot operate for the more the 5hours due to the buildup of reactor poisons. This is mostly due to fission products, especially xenon-135 which does not even reach equilibrium concentration before the core excess reactivity of the MNSR approaches 2.5mk (i.e. k_{eff} of 1.0025). At this point the reactor is shut down for xenon-135, whose half-life is 9.14hrs, to decay to an appreciable concentration before reactor operation commences again. This makes it very difficult to simulate the burnup of the MNSR with MURE due to the extremely short burnup steps and sensitivity of the MNSR core. The evolution of all fission product cross section are

significant to the sensitivity of the core burnup which introduces lots of statistical error hence the following approach was adopted.

The reactivity regulators of the MNSR enable the core to operate at its licensed excess reactivity of 4mk. These regulators which insert a negative reactivity of about 7.5mk were removed from the simulated core to enable xenon-135 to reach equilibrium. The worth of the reactivity regulators were later incorporated in the estimation of the burnup of the fresh core before the addition of the first beryllium shim. For a fresh MNSR core, there are no beryllium shims in the shim tray.

2.9.2.2 MNSR Core lifetime

Since fuel management of the MNSR was done by the addition of beryllium shims in the shim tray of the core (see figure 2.16), the burnup of the MNSR in this work was simulated by depleting the whole fuel in the core by filling the shim tray with the beryllium shims and removing the reactivity regulators. This was done to estimate the core lifetime of the MNSR at both full thermal power and half thermal power of reactor operation of the HEU and LEU cores.

2.9.3 Radiotoxicity of HEU and LEU of MNSR

The MNSR HEU core is due for replacement with the proposed LEU core. In view of this, the radiotoxicity of HEU core was estimated at the end of its core lifetime and also its current state of operation where 9mm of beryllium has been added in the shim tray. This is to estimate the radiotoxicity of the HEU core if the LEU core is put in place before the addition of the next beryllium shim. These results were compared to the LEU core at the end of its core lifetime.

All these were achieved using the MURE code and the MureGui interface which has been discussed earlier in this chapter.

2.9.4 Safety Parameters of MNSR Cores

Even though there are cooling coils around the tank housing the MNSR core, most MNSR cores are cooled by natural convection and boiling is not allowed to take place. The nominal operating temperature of the MNSR ranges between 30°C to 60°C. Basic safety parameters discussed in this chapter for the PWR were repeated for the MNSR to investigate the safety of the LEU core vis-à-vis the HEU core. Parameters investigated include; Coolant Void Reactivity, fuel and

moderator temperature coefficient, Doppler broadening of U-238 of both fuel and the decay heat which is most important for the HEU.

CHAPTER THREE

3 RESULTS OF MONO-RECYCLING OF AMERICIUM IN PWR

3.1 INTRODUCTION

The engineering designs of nuclear reactors are largely governed by materials properties. The choices of nuclear fuels and designs are limited by the characteristics of the reactor cores, namely, the fuel enrichment, the nature of the moderators and coolants selected, the operating temperatures and pressures in the core, the fuel burnup and exposure time, and the average neutron energy and fluence.

The low fuel-cycle costs and the high reliability of the fuel elements allow nuclear reactors to compete with other energy sources, in spite of the high capital costs for their construction. Above all, the fuel must meet the regulatory requirements for safety in the operation of the plants. The fuel elements must accommodate power cycles and meet the design objectives, such as adequate heat transfer, nuclear reactivity, retention of fission products, inherent safety under accident conditions, and retention of structural and mechanical integrity [61].

In other to consider fuel reprocessing and operational safety, the amounts and activities of individual fission products are important in reactor design because:

- it is necessary to evaluate the potential hazards associated with an accidental release of fission products into the environment
- it is necessary to determine a proper cooling time for the spent fuel (before it becomes ready for reprocessing), which depends on the decay times of fission products
- it is necessary to estimate the rate at which heat is released as a result of radioactive decay of the fission products after the shut-down of a reactor.
- it is necessary to calculate the poisoning effect of the fission products (the parasitic capture of neutrons by fission products that accumulate during the reactor operation)
- the rate at which the concentration of a nuclear species (N_i) in a reactor core changes with time.

Therefore, this chapter reports and discusses result findings on reprocessing of plutonium and americium in spent UOX fuels cycle (once-through) to fabricate the MOX cycle and MOXAm cycle and their safety limits

3.2 BURNUP (BU)

Assigned burnup is the appropriate source of burnup for use in waste package loading decisions utilizing criticality loading curves. With appropriate determination and incorporation of the burnup value uncertainties into the criticality loading curves, the reactor record assigned burnup provides the most reliable burnup value.

A commercial power reactor is monitored by a number of detectors that allow measurement of the radial and axial variations of the power produced by the reactor core. The total power produced by the core is tracked as a function of time by means of the core heat output. These measurements are coupled with "core follow" calculations in order to establish the burnup of each assembly when the core is reloaded. These are the reactor record burnup values, which are then used in the design of the new core for the next cycle of operation of the reactor. Before the refueled reactor is allowed to reach a significant power level, a startup physics test is performed to verify that each assembly is loaded in the correct position and has the burnup that was calculated for it value [62].

An issue in operating reactors and hence specifying the fuel for them is fuel burnup. This is measured in gigawatt-days per tonne and its potential is proportional to the level of enrichment. Hitherto a limiting factor has been the physical robustness of fuel assemblies, and hence burnup levels of about 40GWd/t have required only around 4% enrichment. But with better equipment and fuel assemblies, 55GWd/t is possible (with 5% enrichment), and 70GWd/t is in sight, though this would require 6% enrichment. The benefit of this is that operation cycles can be longer – around 24 months – and the number of fuel assemblies discharged as used fuel can be reduced by one third. Associated fuel cycle cost is expected to be reduced by about 20% [63].

A thermal reactor loaded with 98 metric tons of uranium dioxide (UO_2) fuel in which the uranium 235U is enriched to 3% by weight has a specific burnup of 28.7GWd/t.

The characteristics of LWR-grade plutonium generated from three cycles of operation in a large reactor are as follows: the isotopic composition is 1% Pu-238, 58% Pu-239, 23% Pu-240, 13% Pu-241, and 6% Pu-242. The isotopes Pu-239 and Pu-214 are fissile [61].

RESULTS OF MONO-RECYCLING OF AMERICIUM IN PWR

In this study, we consider typical average Burnup of between 46GWd/t which is consistent with present situation and fuel and cladding damage under irradiation and a higher 68GWd/t for the next generation of MOX fueled reactors.

The burnup calculations of the nuclear fuel assemblies for this work were done based on the following assumptions; the fractionating cycle, N, was set at 4 for all burn-up calculations, the fabrication time of the MOX and MOXAm assembly was set at 2 years and the k_∞ at the end of cycle (EOC) was set at 1.03.

Fuels can be stored during decades before reprocessing due to fact that the spent fuel must be allowed to cool down to appreciable levels in terms of decay or residual heat. In this work, short cooling time of 5 years and long cooling time of 30years was considered due the fact most of the world spent nuclear fuel are still in storage.

3.2.1 UOX Fuel Assembly

Various enrichments of UOX fuel assembly were simulated with the aim of achieving burnups of 46GWd/t and 68GWd/t. The resulting enrichment reached for the required Burnup (BU)s are below.
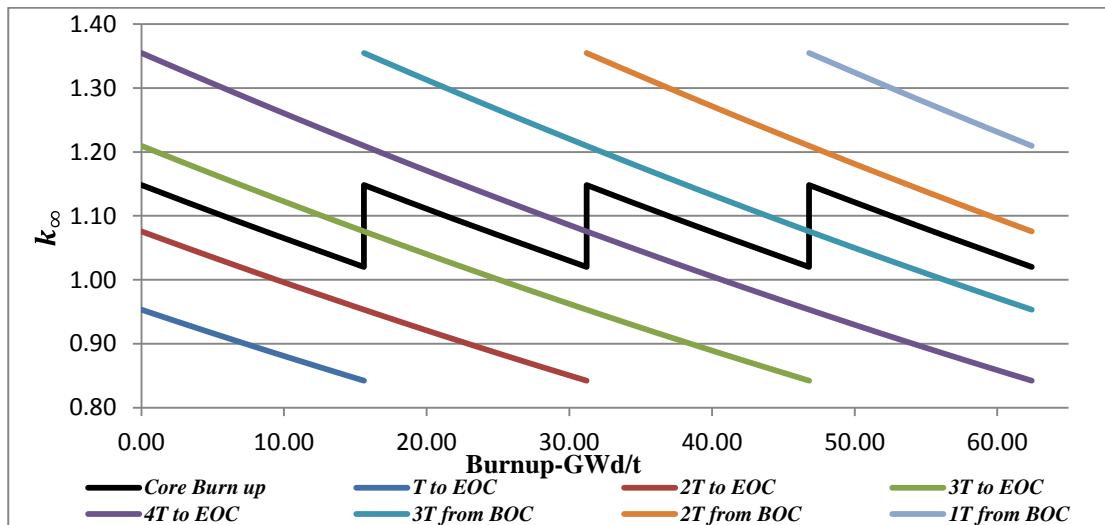
Figure 3.1 UOX fuel assembly core Burnup to reach 46GWd/t

The 46GWd/t and 68GWd/t of burnup of the UOX assemblies were reached at a Uranium-235 enrichment of 4.3% and 6.0% respectively. This is illustrated with the 4 fractionating cycles, in

Figure 3.1 for the 46GWd/t. These enrichments with their corresponding burnup values are comparable to the literature data in section 3.2 of this chapter.

From Figure 3.2 to Figure 3.4 show the evolution of actinides in 46GWd/t and 68GWd/t UOX assemblies during burn-up in the core and after burn-up at various years of cooling. It can be observed in Figure 3.3 that, as the burn-up increases beyond 46GWd/t, the Plutonium-239 curve dips, showing the utilization of Pu-239 beyond this point. Pu-239 under goes fission to support the utilization of Uranium-235 in other to reach a burn-up of 68GWd/t, hence plutonium is being utilized when the burn-up is longer. The formation of Pu-239 is initiated by the neutron capture of Uranium-238 which is abundant isotope in the UOX fuel. $^{238}_{92}U + ^{1}_{0}n \rightarrow ^{239}_{92}U \xrightarrow{\beta^-} ^{239}_{93}Np \xrightarrow{\beta^-} ^{239}_{94}Pu$.
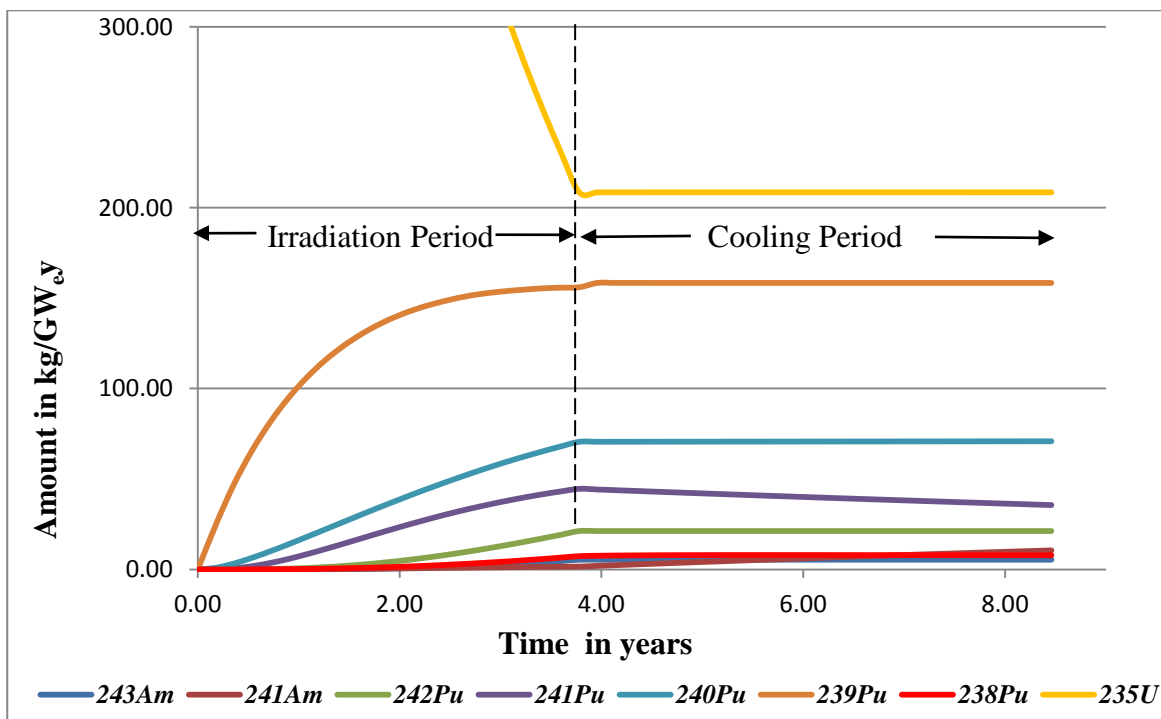
Figure 3.2 Actinides Evolution of a UOX assembly during BU of 46GWd/t and 5 years of cooling
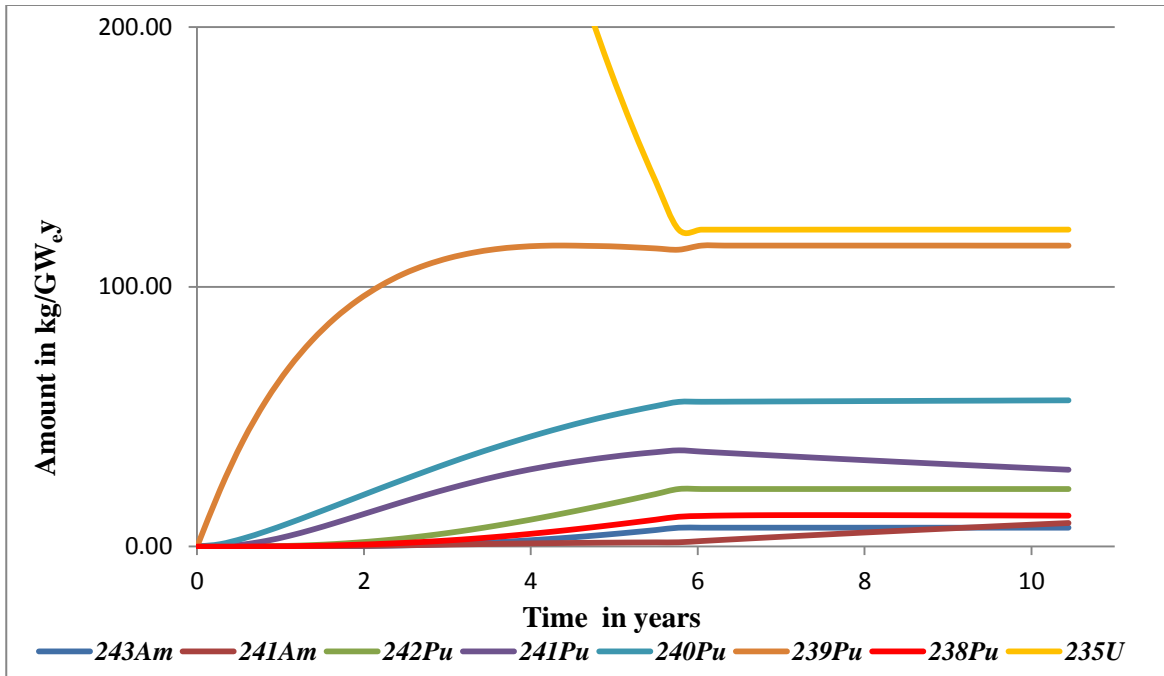
Figure 3.3 Actinides Evolution of a UOX assembly during BU of 68GWd/t and 5 years of cooling

The utilization of Pu-239 reduces the plutonium inventory in the spent fuel which is of much concern to proliferation issues and also the reduction in the radiotoxicity of the spent fuel since comparatively, plutonium has high dose factor (see Table 2.2). However, during the early days of the cooling curves, there is a slight increase in Pu-239. This can be observed as sharp rise in the plutonium-239 inventory after cooling (see Figure 3.2 to Figure 1.4). This Pu-239 slight increase is due the beta decay of Neptunium-239. $^{239}_{93}Np \rightarrow {}^{0}_{-1}\beta + {}^{239}_{94}Pu$ with a half-life of 2.356 days [64], which has reached equilibrium during irradiation after some weeks due the decay of $^{239}_{93}Np$,

at equilibrium, $\dfrac{\phi \sigma_c^{238U}}{\lambda^{239Np}} = \text{Constant}$.

With reference to in Figure 3.4, Americum-241 inventory tends to increase with decreasing Pu-241 during cooling time. Due to the beta decay reaction, $^{241}_{94}Pu \rightarrow {}^{0}_{-1}\beta + {}^{241}_{95}Am$, and the relatively short half-life of about 14.29 years of Pu-241 [64], the Americium-241 inventory tends to increase significantly within a short time.
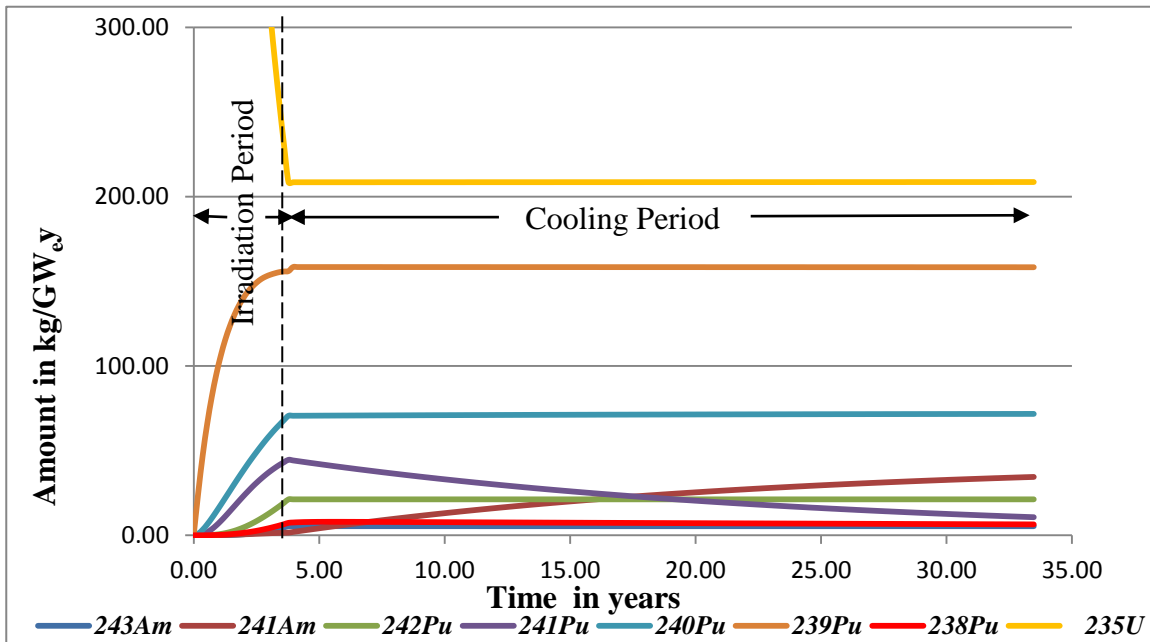
Figure 3.4 Actinides Evolution of a UOX assembly during BU of 46GWd/t and 30 years of cooling

The buildup of Americium-241, with its high radiotoxicity and very long half-life of 432.years [64], will cause a relative increase in the radiotoxicity of the spent UOX fuel for very long period of time, hence the consideration for it reprocessing and or incineration.
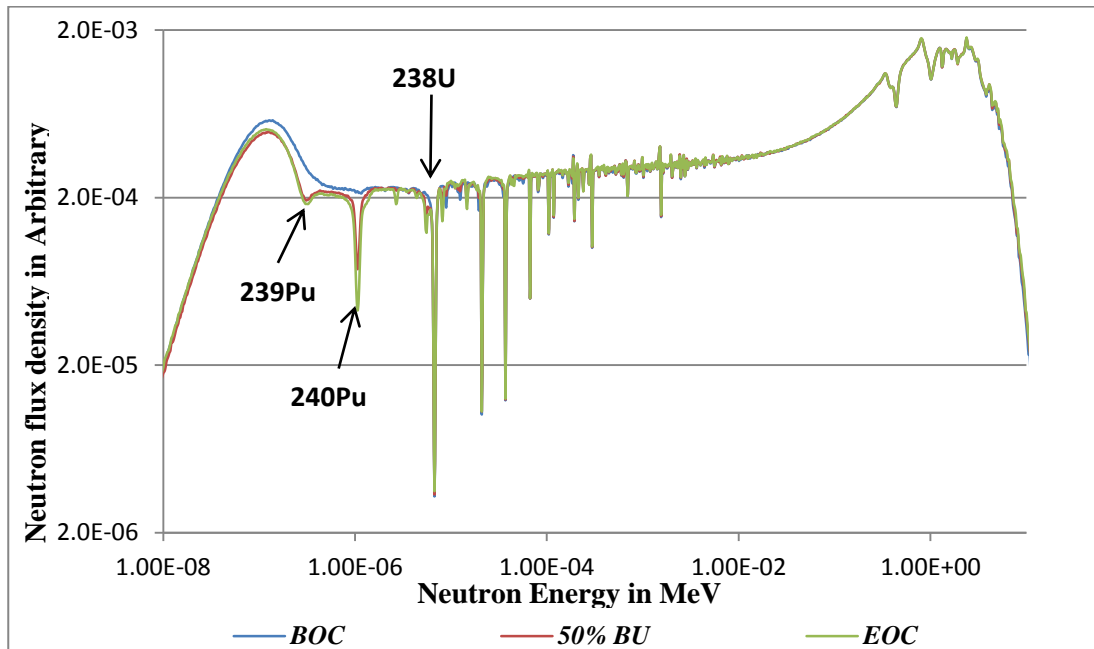
Figure 3.5 Neutron Spectrum of a 46GWd/t UOX assembly at different stages of its Burnup(BU)

The introduction of other actinides in the UOX fuel tends to modify the neutron spectrum in several ways. In Figure 3.5, the introduction of more resonances can be observed with a few nuclei peaks identified. U-238 shows a very large peak due it abundance in UOX fuel. This peak plays an important role in nuclear safety which is discussed later in this chapter.

Table 3.1 Production, consumption and macroscopic absorption cross section of nuclei of interest

Actinides in UOX	46GWd/t UOX Assembly				68GWd/t UOX Assembly			
	Amount (kg/GW_ey)		Macroscopic Cross section(Σ) ($\times 10^{-3} cm^{-1}$)		Amount (kg/GW_ey)		Macroscopic Cross section(Σ) ($\times 10^{-3} cm^{-1}$)	
	BOC	*EOC*	*BOC*	*EOC*	*BOC*	*EOC*	*BOC*	*EOC*
U-235	1122.33	231.76	53.51	10.35	1019.54	140.34	59.37	8.53
U-236	0	145.13	0	0.86	0	141.25	0	1.14
U-238	25297.88	24462.10	23.13	22.71	16177.17	15395.32	22.21	21.88
Np-237	0	17.20	0	0.48	0	19.56	0	0.79
Pu-238	0	6.59	0	0.20	0	10.37	0	0.41
Pu-239	0	156.66	0	20.35	0	114.76	0	20.11
Pu-240	0	68.47	0	23.57	0	54.09	0	23.02
Pu-241	0	43.39	0	0.68	0	36.33	0	1.20
Pu-242	0	19.30	0	43.92	0	20.24	0	43.13
Am-241	0	1.53	0	0.13	0	1.62	0	0.19
Am-243	0	4.66	0	0.19	0	6.38	0	0.37

Approximately 6.5% and 9.7% of Uranium is consumed by mass in a UOX assembly to reach 46GWd/t and 68GWd/t respectively. 27% of the mass of Uranium consumed in the 46GWd/t UOX fuel assembly is converted into actinides of which Plutonium contributes about 17% by mass. For the 68GWd/t UOX fuel assembly, 24% of the mass of Uranium consumed is converted into actinides with Plutonium contributing about 14% by mass. This indicates the utilization and reduction of the amount of actinides produced when fuels are designed to stay longer in the core.

3.2.2 MOX Fuels

Plutonium quality is an important measure for the proliferation-resistance of a nuclear energy system. Degraded plutonium quality decreases its attractiveness for use as nuclear weapons. Civil plutonium discharged from a nuclear reactor with high bum-up and separated from reprocessing has a composition very much different from that of weapons grade (WG). This reactor-grade

(RG) plutonium consists of higher content of heat producing isotopes (e.g., Pu-238) and spontaneous fissionable isotopes (Pu-240, Pu-242) which can significantly complicate its use as nuclear weapons materials [65].

Table 3.2 Plutonium Quality of spent UOX fuel assemblies for this work

Spent UOX	^{238}Pu (wt%)	$\dfrac{^{240}Pu}{^{239}Pu}$	Fissile Plutonium Concentration (wt %)
46GWd/t (*at discharge*)	2.24	0.437	67.96
46GWd/t (*5 year cooling*)	2.66	0.447	66.00
46GWd/t (*30 years cooling*)	2.34	0.452	62.98
68GWd/t (*at discharge*)	4.40	0.471	64.08
68GWd/t (*5 year cooling*)	5.04	0.486	61.68
68GWd/t (*30 years cooling*)	4.21	0.482	59.45

where $Pu\ enrichment = \dfrac{(^{239}Pu + {}^{241}Pu)}{(Total\ Pu\ isotopes)}$

Table 3.2 shows that, for the same spent UOX fuel, as the cooling time increases, plutonium quality at the back end of the UOX cycle decreases. This is due the reduction in the fissile material, Pu-241 which undergoes beta decay with a half-life of 14.29 years and the formation of Pu-240 from the α-decay of Curium-244 with a half-life of 18.1years [3]. Comparatively, the Pu quality decreases for longer burn-ups of spent UOX assemblies due the utilization plutonium-239 and plutonium-241. Values in Table 3.2 follow the general trend of percentage Plutonium production as compared to the values quoted from literature (Chapter 3, in section 3.2) which depicts a burnup of UOX assembly which has undergone 3 cycles, in this work a 4 cycle system was considered, hence the slight variation.

During reactor operation, neutron reactions continuously change the composition of the UOX fuel. U-235 is burnt and fissile Pu-239 and Pu-241 are produced, while neutron absorbing Pu-240 and fission product poisons build up. Reprocessing burnt up reactor fuel, in order to recycle it, by fissioning more of the plutonium created from uranium-238 capture, increases greatly the quantity of energy produced relative to the mass of long half-life radioactive waste created [66].

Due to the high contribution of Pu to radiotoxicity in the spent UOX assembly (see section 3.3.1, Figure 3.15) and its energetic content, the reprocessing and utilization of Pu is considered in this work. The Mixed Oxide (MOX) fuel assemblies were fabricated to utilize the Pu in other to analyze its effect on radiotoxicity and decay heat as compared to the once-through of the UOX.

Figure 3.6 and Figure 3.7 show the utilization and buildup of some actinides in the MOX fuel assembly during burnup. It was ascertained that Pu-239 is consumed in higher burnups, 56.5% consumption at 68GWd/t as compared to 51.6% consumption at 46GWd/t, even though these assemblies were fabricated from the same isotopic ratio of composition from spent UOX assemblies. However, Pu quality increases slightly for spent MOX fuel fabricated from 30 years cooled UOX. This was due to the significant breeding of the Pu-241 isotope during the time spent in the reactor core (compare Figure 3.6 and Figure 3.7), though Pu-241 had least Pu ratio at BOC.
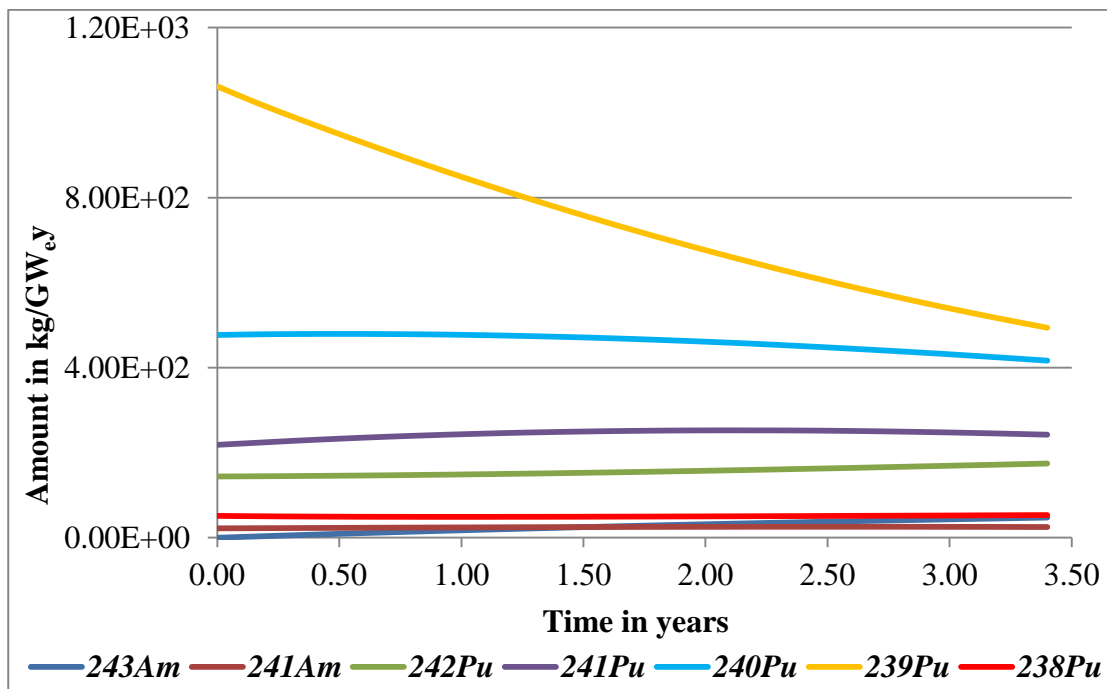
Figure 3.6 Actinides Evolution of a MOX assembly to reach 46GWd/t, 5 years of pre-cooling
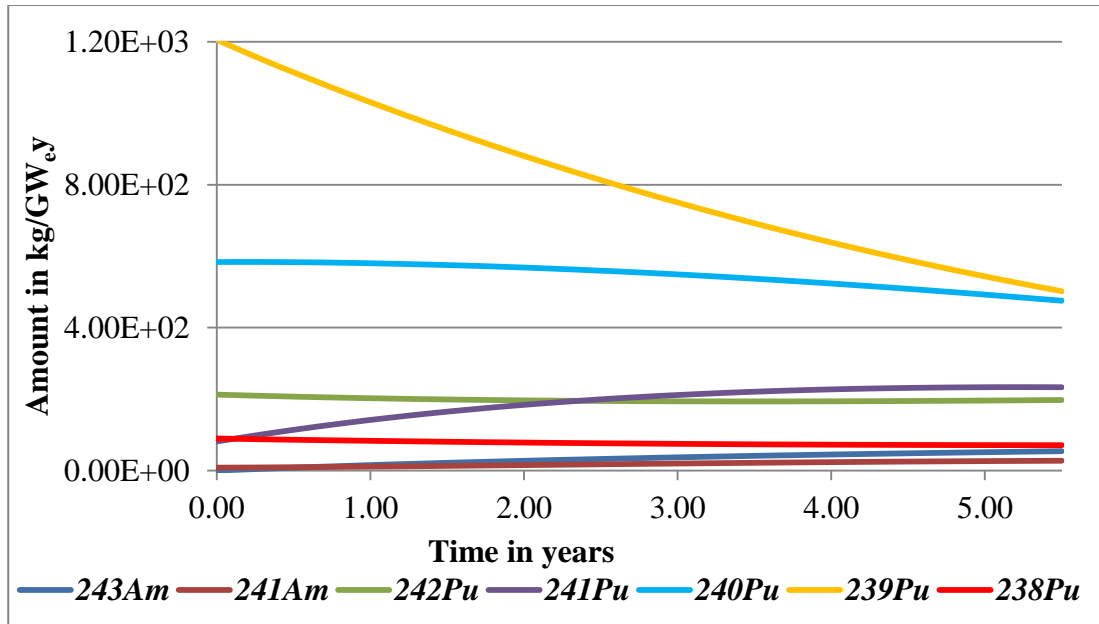
Figure 3.7 Actinides Evolution of a MOX assembly to reach 68GWd/t, 30 years of pre-cooling

The concentration of Pu to reach the various burnups is shown in Table 3.4 and Table 3.5. MOX assemblies fabricated from spent UOX after 30years of cooling had higher concentration than lower cooling times. After 30 years of cooling Plutonium-241 isotope is virtually consumed through beta decay into Americium-241, hence there is a reduction in the quality of Pu (see Table 3.2).

Table 3.3 Plutonium Quality of spent MOX fuel assemblies for this work

	Spent MOX	^{238}Pu (wt%)	$\dfrac{^{240}Pu}{^{239}Pu}$	Fissile Plutonium Concentration (wt %)
Fabricated from spent 46GWd/t UOX	**46GWd/t** *(5 years UOX cooling)*	3.86	0.84	53.33
	46GWd/t *(30 years UOX cooling)*	2.79	0.86	53.71
	68GWd/t *(5 years UOX cooling)*	4.88	0.92	50.69
	68GWd/t *(30 years UOX cooling)*	3.42	0.96	51.40
Fabricated from spent 68GWd/t UOX	**46GWd/t** *(5 years UOX cooling)*	4.31	0.85	51.91
	46GWd/t *(30 years UOX cooling)*	5.88	0.83	51.22
	68GWd/t *(5 years UOX cooling)*	6.74	0.91	48.68
	68GWd/t *(30 years UOX cooling)*	4.80	0.95	49.70

Undoubtedly, for the same Pu quality, an increase in Pu concentration leads to an increase in assembly burnup. Table 3.3 shows that there is reduction in Pu quality after the MOX fuel burnup, which implies that multi-plutonium reprocessing will demand high concentration of plutonium to achieve a good burnup.

3.2.3 The MOX-Americium fuel (MOXAm)

Isotopes with long half-lives are of concern for waste disposal, for those with half-lives of a few years or less are easily stored until their radioactivity is exhausted. The more persistent fission products have half-lives of several decades, and these must be isolated for hundreds of years. The actinides—plutonium, neptunium, **americium**, and others produced by successive capture of neutrons in uranium and its by-products during reactor operation - present the truly long-term challenges in waste disposal [66].

Plutonium-241, having a large fission cross section, also decays into americium-241 which has a large thermal capture cross section and a large capture resonance integral. Americium-241 also decays into daughter products which are energetic gamma emitters. Stored plutonium loses its potency as a fuel over time because of the decay of ^{241}Pu into ^{241}Am. Plutonium from spent LWR fuel at a typical burnup of about 35,000 MWd/T must be utilized within 3 years after discharge or it will be necessary to reprocess it again to remove the ^{241}Am and daughter products [15]. This is to reduce the production of recycled MOX fuel with high concentration of Pu which exceeds the permissible concentration.

However, with the aim of reducing the radiotoxic contribution of MOX fuel due to americium, americium impregnated MOX fuel assembly, MOXAm, simulated using the MURE code are discussed below based on neutronic performance and change of americium inventory in the whole cycle.
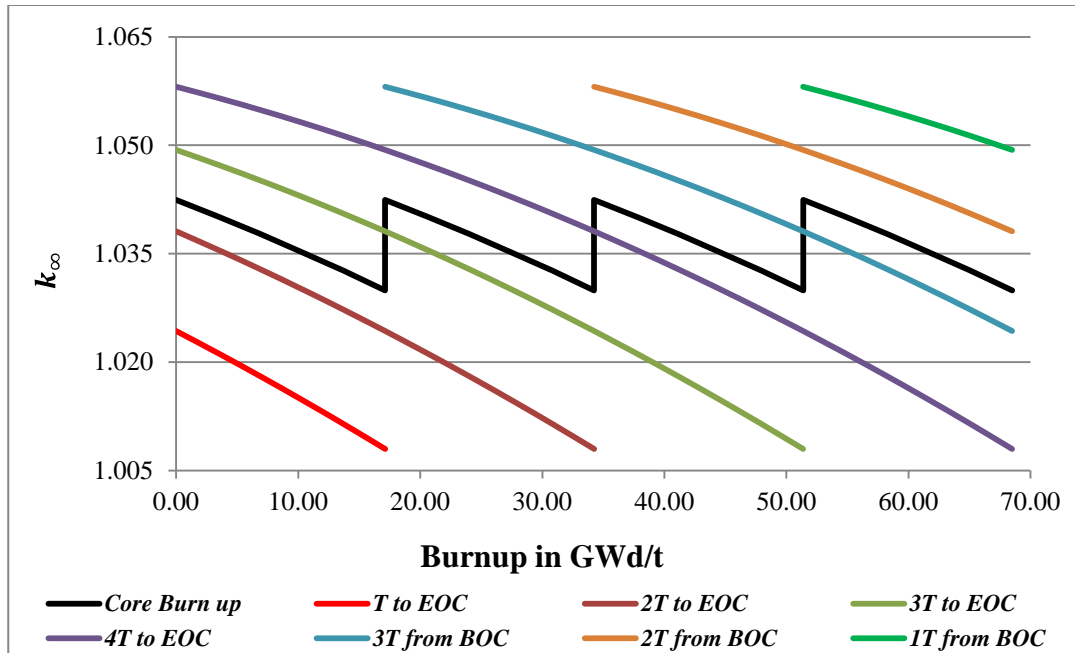
Figure 3.8 MOXAm fuel assembly Burn-up to reach 68GWd/t, 30 years of pre-cooling

The presence of americium in the MOX fuel assembly degrades the Pu quality significantly; hence higher Pu concentrations are needed to achieve the same burnup as in the MOX. The MOXAm spectrum is much harder for thermal neutrons, Figure 3.8, which had the highest percentage of americium in the types of fuel considered, tends to have a burnup curve which deviates from all the fuel assembly types considered. Even though the k_∞^o of the MOXAm assembly from the 30 years pre-cooled UOX is very small as compared to the 5 years pre-cooled, the breeding and utilization of the fissile isotope, Pu-241, sustains the k_∞ at an appreciable level just above criticality. Am-241 undergoes transmutation during fuel irradiation in the core, while Am-243 inventory is fairly stable, hence americium reduction has been achieved. The breeding of Pu-241 and transmutation of Am can be observed in Figure 3.10.
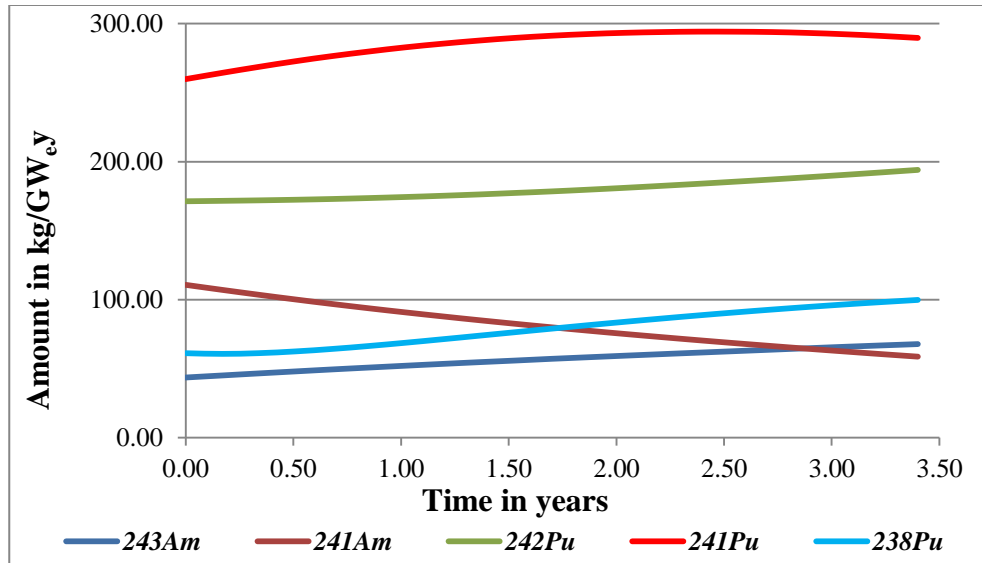
Figure 3.9 Actinides Evolution of a MOXAm assembly to reach 46GWd/t 5 years of pre-cooling
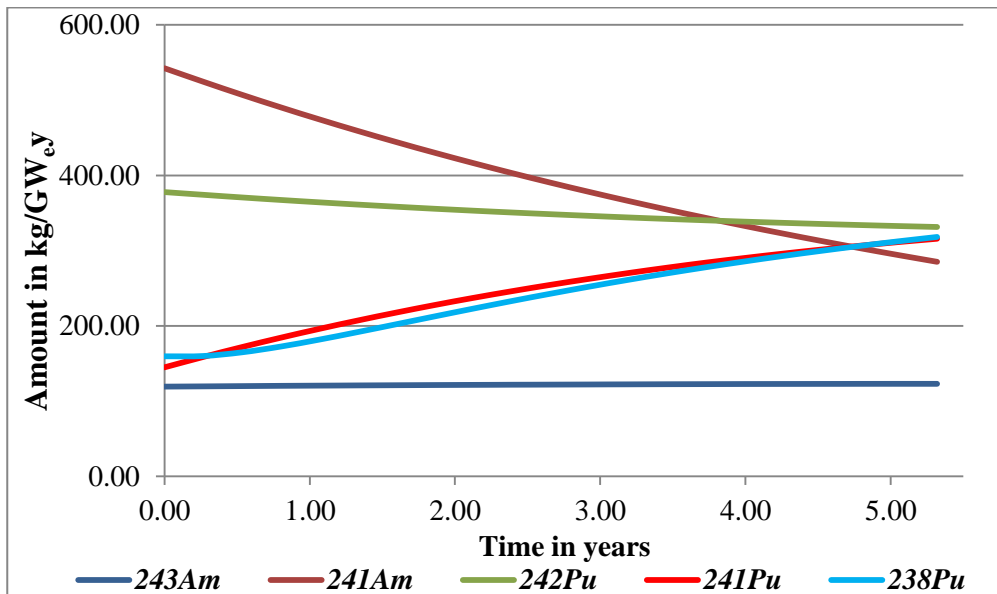
Figure 3.10 Actinides Evolution of a MOXAm assembly to reach 68GWd/t, 30 years of pre-cooling

3.2.4 Comparison of burnup of MOX and MOXAm strategies to the UOX strategy

MOX fuel assemblies have come to stay in French pressurized water reactors due to extensive research and comparison to the well-established UOX fuel assemblies. The MOX and MOXAm fuel assemblies are compared to the well-established UOX fuel. This is to ascertain the performance of these two types of fuels understudy.

The factor **R** which is defined in equation (2.61) is introduced to quantify the amount plutonium and/or americium need for a MOX assembly and/or a MOXAm assembly respectively and also for the fair comparison of the various fuel cycles considered in this work as compared the UOX (once-through) cycle. The **R** of the MOX fuel consists of the amount of plutonium needed to for one MOX assembly as compared to the amount of plutonium produced at EOC in a UOX cycle. In the case of the MOXAm **R** factor, the americium (Am) coming from the spent UOX assemblies are included, this implies increasing the non-fissile inventory in the fresh MOXAm fuel which degrades the neutron balance. It can be expected that mono recycling of Am leads to an increased concentration of Pu to compensate for this neutron poisoning, and hence an increase of spent UOX assemblies needed to produce one MOXAm fresh assembly as compared to one fresh MOX assembly.

Table 3.4 Plutonium concentrations of MOX and MOXAm cycle with respect to spent 46GWd/t UOX cycle and years of cooling time

Burn-up of MOX Assembly GWd/t	Plutonium concentration in MOX fuel %		$R = \dfrac{MOX_{Assembly}}{UOX_{Assembly}}$	
	Cooling period of a spent UOX assembly after 46GWd/t			
	5 years	*30 years*	*5 years*	*30 years*
46	7.66	8.85	6.28	8.00
46 (with Am)	9.60	19.93	7.55	15.74
68	10.84	12.18	8.88	11.01
68 (with Am)	12.30	25.55	11.10	18.44

As observed in Table 3.4 and Table 3.5, plutonium concentrations increase with the cooling time as a result of loss of fissile material in the spent UOX assemblies needed for the recycled fuel fabrication. Indeed, the longer the cooling time is, the higher the concentration of Pu of the MOX assembly should be. It was observed in Table 3.2 that the plutonium quality decreases with increase in cooling time. It can then be deduces that, the longer the cooling period of spent UOX assembly waiting to be reprocessed, the more fissile isotopes are lost due to decay, which causes

an increase in Pu concentration to achieve the same burnup. Such phenomenon is consistent for all MOX fuels assemblies considered in this work. For the MOXAm fuels, the cooling time affects the fuel quality in two ways; loss of fissile material (Pu-241) and the buildup of capturing material (Am-241).

Table 3.5 Plutonium concentrations of MOX and MOXAm cycle with respect to spent 68GWd/t UOX cycle and years of cooling time

Burn-up of MOX Assembly GWd/t	Plutonium concentration in MOX fuel %		$R = \dfrac{MOX_{Assembly}}{UOX_{Assembly}}$	
	Cooling period of a spent UOX assembly after 68GWd/t			
	5 years	*30 years*	*5 years*	*30 years*
46	8.90	10.20	5.95	7.71
46 (with Am)	14.12	23.35	7.78	16.63
68	12.40	13.70	8.29	10.36
68 (with Am)	17.20	28.40	10.88	18.48

In relation to Table 3.4 and Table 3.5, it can be observed that, MOX assemblies which are fabricated from a 5 years of cooled spent 46GWd/t UOX assemblies have the least plutonium concentration at 46GWd/t and 68GWd/t. Hence it has the best plutonium quality for MOX fuels production. The worst plutonium quality fuel was fabricated from a 68GWd/t spent UOX fuel with 30 years of cooling time. It recorded the highest plutonium concentration in the MOX fuel to achieve a burnup of both 46GWd/t and 68GWd/t. This high Pu concentration in this MOX fuel was due the utilization of fissile Pu-239 in the UOX during burnup and the almost complete decay of fissile Pu-241(see Figure 3.6). With the addition of americium to the MOX fuel for form the MOXAm fuels, the trend is still the same but worse.

Factor R allows quantifying the uranium savings resulting from the Pu reprocessing. One has to notice that the introduction of americium degrades deeply the performance of the recycled plutonium as well as higher cooling times which decrease the quantity of fissile Pu-241. However, the disadvantage of a large R value is that, as plutonium concentration increases with

larger **R** values, there is a need for more natural uranium to be enriched to manufacture more UOX assemblies to manufacture one MOX or MOXAm assembly, thus increasing the utilization of the natural resource uranium. This effect makes the multi-reprocessing of Pu in a PWR to look environmentally unfriendly due to the increase in factor **R** after each cycle.

Americium and plutonium which are not present in a UOX fuel, build up during the fuel core lifetime. Such isotopes increase the radiotoxicity of the spent fuel due to their high dose factors. 6.152Kg/GW$_e$y and 8.915Kg/GW$_e$y of americium are present in spent UOX assemblies at discharge after 46GWd/t and 68GWd/t respectively. As cooling time increases, these values increase exponentially, hence increasing radiotoxicity. As shown if Figure 3.11, there is a buildup of Americium in the UOX assemblies during their core-lifetime.
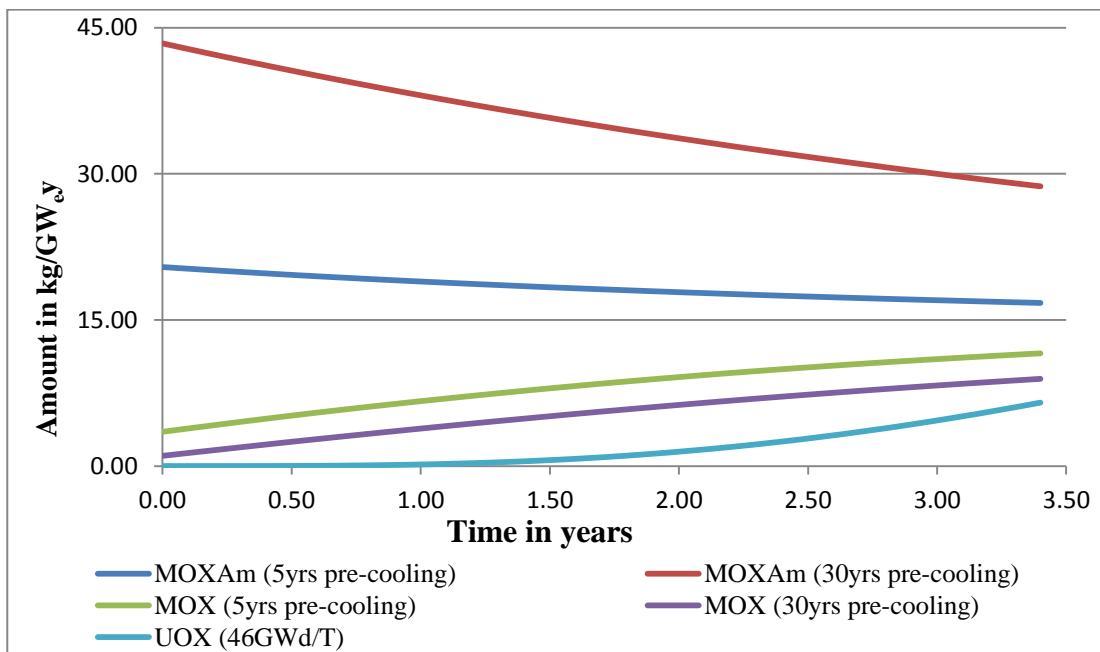
Figure 3.11 Change in Americium concentration during burnup to reach 46GWd/t

In other to compare the mass of americium produced at EOC in both the MOX and MOXAm cycles, the final mass of Am in the MOX cycle per assembly is added to Am from the assemblies of spent UOX cycle from which it was fabricated from, but the MOXAm fuel Am inventory at EOC still has no additional Am from its UOX cycle glasses. But after 5years and 30years of cooling time of the UOX fuel, the americium inventory increases to 15.847Kg/GW$_e$y and 27.072Kg/GW$_e$y respectively for spent 46GWd/t assembly. High amount of Am production due to long decay time of the UOX cycle makes it difficult for reprocessing or transmutation.

Comparing the americium transmutation in the MOX and MOXAm cycles (Figure 3.11), the Am inventory at EOC is much higher for MOXAm fuel than the MOX fuel after 30years of pre-cooling, but for 5years of cooling time, both the MOX and MOXAm fuels exhibit closeness in the mass of the Am at EOC. Hence, the amount of americium has relatively been maintained without being the UOX glasses.

Table 3.6 Ratio of Americium composition at discharge in spent MOX and MOXAm assemblies to UOX assemblies after cooling time

Burn-up of MOX Assembly GWd/t	$R_{Am} = \dfrac{MOX_{cycle}}{UOX_{46GWd/T}}$		$R_{Am} = \dfrac{MOX_{cycle}}{UOX_{68GWd/T}}$	
	Cooling period of a spent UOX assembly			
	5 years	*30 years*	*5 years*	*30 years*
46	1.69	1.21	1.56	1.19
46 (with Am)	0.67	0.64	0.70	0.69
68	1.76	1.24	1.62	1.15
68 (with Am)	0.61	0.56	0.64	0.59

Table 3.6 compares the amount of americium produced in the various MOX strategies at discharge. The americium present in the glasses coming from the reprocessed UOX used to fabricated the MOX and MOXAm assemblies where incorporated in the MOX and MOXAm cycle analysis. The factor R_{Am} was calculated as follows;

For the MOX fuel assembly,

$$R_{Am}^{MOX} = \frac{UOX_{glasses}^{Am} + (MOX_{spent\,fuel}^{Am}/R)}{UOX_{glasses}^{Am}} \qquad (3.1)$$

For the MOXAm fuel, the total UOX glasses in incorporated in the fuel hence equation (3.1) becomes

$$R_{Am}^{MOXAm} = \frac{(MOXAm_{spent\ fuel}^{Am}/R)}{UOX_{glasses}^{Am}} \tag{3.2}$$

where

$UOX_{glasses}^{Am}$ is the mass of americium present in UOX fuel that is intended to be in the UOX glasses after cooling

$MOX_{spent\ fuel}^{Am}$ and $MOX_{spent\ fuel}^{Am}$ are the masses of americium present in MOX and MOXAm fuel assembly respectively at discharge

The americium inventory in the MOX cycle produced from 5years cooled spent UOX increases by an average of 66% with respect to its UOX cycle as compared to an average increase of 20% fabricated from the 30years cooled spent UOX with respect to its UOX cycle. At the BOC, this assembly fabricated from the 5years cooled spent UOX has a better Pu quality than that of the 30 years cooled (see Table 3.2). The 5 years cooled MOX has Pu-241 higher concentration in the fuel at BOC than the 30years cooled UOX, hence beta decay of Pu-241 will produce substantial amount of Am-241. Higher burnup of the MOX increase the Am concentration at EOC due to longer core life of the assembly which enables more Pu-421 to Am-241 transmutation. Across Table 3.6, the Am increment decreases slightly for the MOX fuel fabricated from spent 68GWd/t UOX due less better Pu quality compared to spent 46GWd/t UOX.

However, MOXAm assemblies sustained the concentration of Am-243 from BOC to EOC while there was an appreciable decrease in Am-241 during their core-lifetime (*see* Figure 3.10). From Table 3.6, the MOXAm cycle, fabricated from 5 years pre-cooled UOX assemblies, shows a decrease in americium concentration by an average of about 35% with respect to its once through UOX cycle. Whiles the MOXAm fuel, fabricated from 30 years pre-cooled UOX assemblies, shows an average decrement of 38% Am concentration at EOC. However, The MOX fuel fabricated from 5 years and 30years pre-cooled UOX assemblies shows increment of about 73% and respectively as compared to americium in their once through UOX cycle at discharge. Contrary to the MOX cycle, the higher the burnup of the MOXAm fuel assembly the lower the Am concentration.

However, it can be globally concluded for both MOX and MOXAm assembly that, the better the plutonium quality at BOC, the higher the americium concentration at EOC.

3.3 RADIOTOXICITY

In order to compare the radiological hazard of different nuclides, the concept of *radiotoxicity* has been introduced. Radiotoxicity is expressed in a hypothetical dose called *sieverts* (Sv).

There are scenarios where the releases of radioactive material are considerable through human intrusion into the repository, intentional or unintentional, serves as an example. In fact, human intrusion constitutes the greatest threat to long-term integrity [67].

The long term perspective of the storage of nuclear material arises from the long half-lives of a small set of nuclides. The nuclides that give the largest contribution to the radiological hazard for the first one million years are all nuclides with atom numbers higher than 92, and are so called *transuranium nuclides* (TRU).

The fission products constitute a third group of nuclides, making up about five percent of the spent fuel by mass. In general, the half-lives of the fission products are much shorter than for the transuranic nuclides. Thus, they are more radioactive and are responsible for both the main radiological issue and the main part of the heat production immediately after discharge. Only few of the fission products have half-lives long enough to be of interest for the long-term management perspective. The half-lives of these are given in Table 3.8 together with the half-lives of some of the actinides. Two nuclides, 90Sr and 137Cs have semi-long half-lives, 28.90years and 30.05years respectively. These will be responsible for an important part of the heat generation during the first period in repositories. Gradually, their role as the main heat producer is taken over by the more long-lived actinides [23]. After 90Sr and 137Cs have decayed, the actinides dominate the radiological hazard completely and can dominate the dose coming back to biosphere after several millions of years.

Different types of radiation yield quite different radiotoxicities due to large variations in their effect on the human body. Further, the radiotoxicity of a particular nuclide varies depending on whether it is inhaled or ingested and depending on the age of the recipient, small children being more sensitive to radiation than are adults. Radiotoxicity by ingestion is used in this work,

because radionuclides are supposed to migrate from the disposal in geological storage towards the biosphere. The radiotoxicity analyses in the work consist of eighteen (18) different fuel types, two (2) UOX, eight (8) MOX and eight (8) MOXAm, due the large number of fuel being considered, radiotoxic analyses is discuss based on more interesting cycles.

3.3.1 Radiotoxicity of the reference UOX cycle

Even though some countries recycle nuclear material, the dominating nuclear fuel strategy in the world today is the once-through cycle.

The once-through nuclear fuel cycle is often referred to as an *open fuel cycle* in the respect that it produces long-lived nuclear material beside the desired commodity. A typical annual discharge from a large nuclear power plant is 20 tons of spent fuel, most of which is uranium, around 5% being fission products and 1% transuranium elements. Moreover, some 170-190 tons of depleted Uranium, a by-product of the enrichment process, has to be dealt with [64]. Unless this material finds some use, it has to be considered waste and be treated as such. But in France, the depleted Uranium is re-used in the fabrication of the MOX fuel.

The radiotoxicity of the UOX cycle considered in the work is analysed and compared in terms of their burnups at 46GWd/t and 68GWd/t after time of discharge. Major isotopic contribution to the total radiotoxicity and strategies adopted to reduce the total radiotoxicity of the UOX cycle is discussed.

In other to analyze the effect of radiotoxicity of a spent fuel, this radiological hazard is analyse based on the decay of the mother isotopes in Figure 3.12. This is to observe the total contributions to radiotoxicity of the lifetime of particular nuclei in the spent fuel so as to present a good advice on actinide reprocessing.
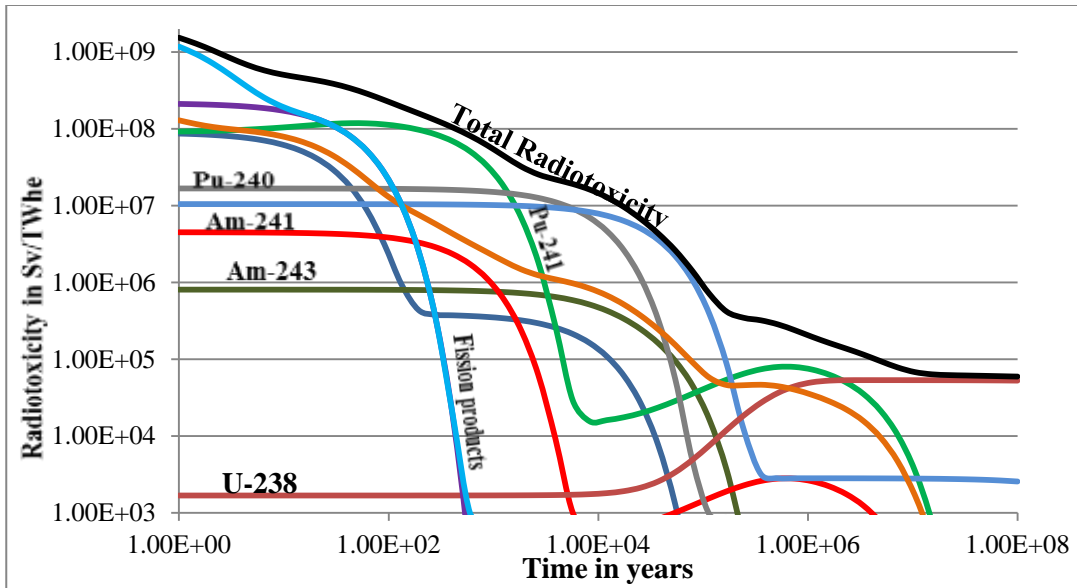
Figure 3.12 Radiotoxicity curve by mother nuclei after discharge of spent 46GWd/t UOX

In Figure 3.12, plutonium is seen to have dominated total radiotoxicity of the spent UOX fuel after the fission product decays in a thousand years. The Minor actinides will be the next major contributors to the total radiotoxicity with americium playing a major role after the extraction of Pu from this spent fuel.

As shown in Figure 3.13, long burn of 68GWd/t or a relatively short burnup of 46GWd/t does not significantly affect the radiotoxicity of the spent UOX assembly. The significant variation at the tail end of the radiotoxicity curve is at the result of uranium-238 contribution.
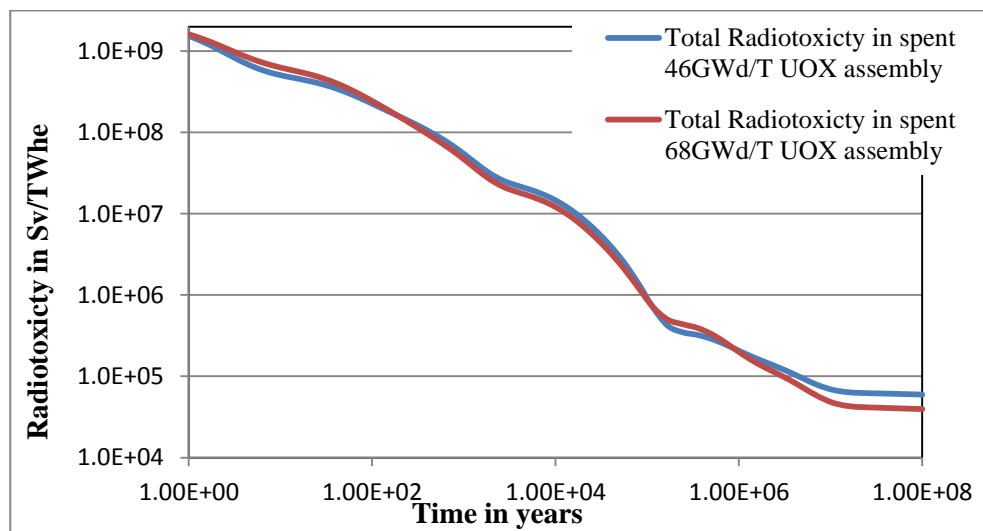
Figure 3.13 Effect of burnup on radiotoxicity on the UOX cycle

The major contributor to the first thousand years of radiotoxicity of the spent UOX is the fission product with Cs-137 and Sr-90 playing major roles.

The role of the daughter nuclei evolution cannot be missed since the mother nuclei decay into the daughter nuclei which quantify the amount and type of isotopes produced by the mother nuclei. This information is very necessary for long term extractions such as 30 years of cooling time. At this times, some mother nuclei with short half-life, such as Pu-241, would have decayed into their daughter nuclei, hence it would be fruitless the extract the mother nuclei after this decay time. In Figure 3.14, the radiotoxicity of daughter nuclei shows that the minor actinides take over from the fission product after thousand years by virtually sustaining the intensity of the radiotoxicity. Americium-241 builds up by the action of β-decay of plutonium-241, $^{241}_{94}Pu \xrightarrow{\beta} {}^{241}_{95}Am$. Due to the long half-life of about 432 years for Am-241, the radiotoxicity contribution from this isotope is high for thousands of years.
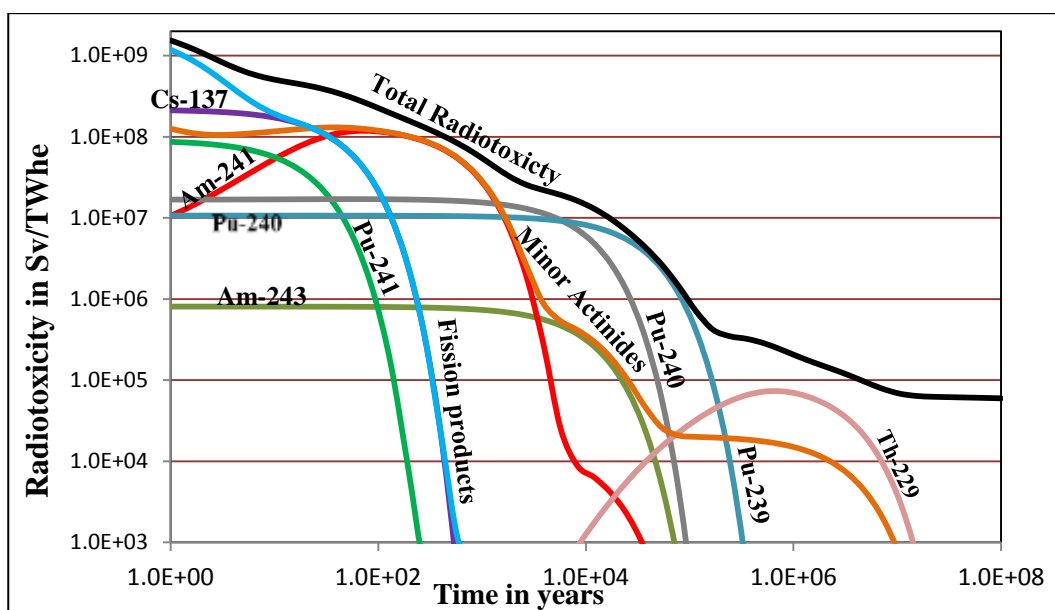
Figure 3.14 Radiotoxicity curve by daughter nuclei after discharge of spent 46GWd/t UOX

It can be observed in Figure 3.14 that americium is the major contributor of radiotoxicity to the overall contribution by minor actinides. Plutonium, however, dominates when it comes to contributions to radiotoxicity. Pu-241 as a precursor for the formation of Am-241, Pu-239, Pu-240 and all the other isotopes of plutonium with their long half-lives and high dose factors, continue to give significant contribution to the total radiotoxicity for tens of thousands of years.

With reference to Figure 3.12 and Figure 3.14, it can be concluded that, the isotopes that contribute to high amount of radiotoxicity for a long period of time are plutonium and americium. Hence the recycling of these nuclei in the attempt to reduce the radiotoxicity in the UOX spent fuel is considered. The reprocessing of spent nuclear fuel involves the use of extractants and diluents (solvent) for separation of the reusable actinides from the unwanted fission products. The most widely used processes employ tributyl phosphate (TBP) diluted with normal-paraffin hydrocarbon. Long-term irradiation of the solvent induces very complex radiolytic chemical reactions, reducing extraction efficiency. In this work, the chemical loss was estimated at 0.1% by weight of the extracted nuclei. The spent fuel is dissolved in nitric acid, and the plutonium is obtained as a nitrate in the solution. Precipitation of the plutonium is obtained as the hydroxide by adding ammonia, as the peroxide (Pu_2O_7) by addition of hydrogen peroxide, or as the oxalate with oxalic acid. PuO_2 is obtained by heating the hydroxide, peroxide, or oxalate in hydrogen at 500–800°C. The PuO_2 is mixed with UO_2 for use as the thermal reactor fuels [26].

In Figure 3.15, the extraction of Pu generally lowers the radiotoxicity of the spent UOX fuel assembly by about 73% - 56% within the first 10years. However, the effect of cooling time before reprocessing and fabrication and plays a role in radiotoxicity reduction. Due to the decay of fission products and alpha decay of Cm-244 into Pu-240, extraction of Pu at 5years after discharge of the spent UOX assembly has higher radiotoxicity within the first10years than when the extraction is done after 30years because the half-life of Cm-244 alpha decay is 18.10 years and a high percentage of fission products decay with this 30 years of cooling.

Furthermore, in the long term, Pu extraction after 5 years performs better after thousand years as compared to when the extraction is done after 30 years. Clearly the effect of americium manifests itself here in terms of increase in radiotoxicity. If Pu is extracted before 5 years after discharge, the formation of Am-241 is completely minimized because the precursor isotope, Pu-241, whose half-life of 14.35 years has been extracted. Due to the α-decay of Am-241, $^{241}_{95}Am \xrightarrow{\alpha} {}^{237}_{93}Np$, the americium effect contributes to further increase in radiotoxicity between the periods of tens of thousands of years to millions of years by the action of neptunium decay.

Due the short and long term effect of americium in the UOX glasses, americium extraction together with plutonium is also considered. The extraction of americium and plutonium lowers

the radiotoxicity much further in the UOX (once-through) spent fuel. The effect of the cooling time on the radiotoxicity within the first 10years follows the same trend as when Pu nuclei alone was extracted but much lower. The average radiotoxicity reduction in the UOX spent fuel in these extractions is about 88% - 81% within the first decade. This is comparatively low for the radiotoxicity in the UOX reference glasses for geological storage.
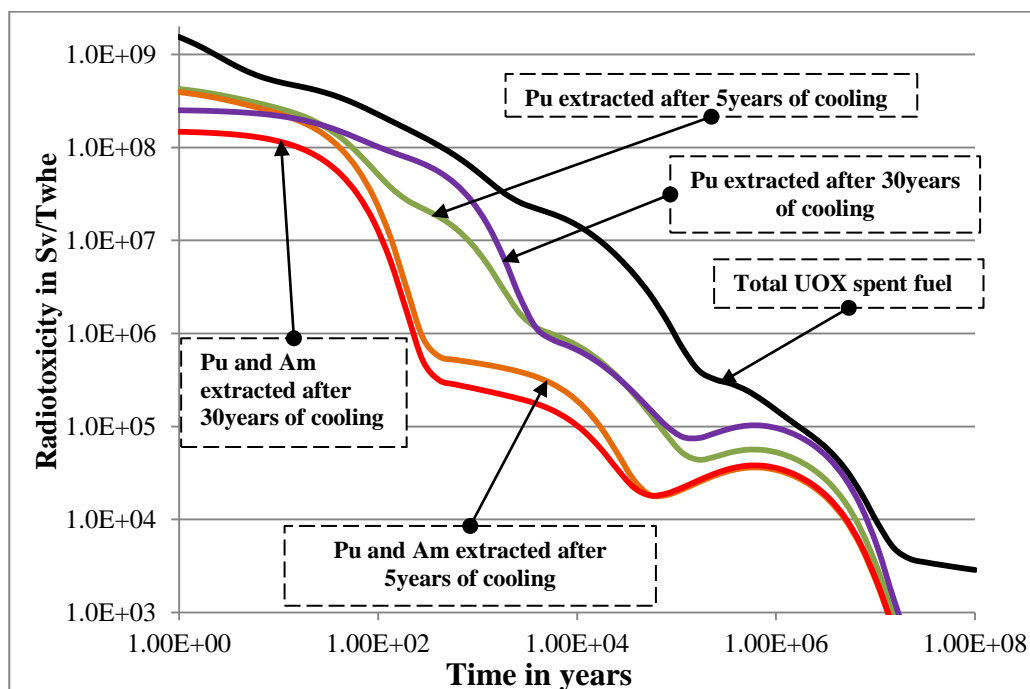
Figure 3.15 Effect of Pu and/or Am extraction on radiotoxicity of UOX glasses produced after reprocessing of spent fuel Assembly after 46GWd/t

This brings about the long term effect, when plutonium and americium are extracted from the spent UOX fuel at 5 after discharge, the radiotoxicity is slightly higher as compared to the extraction after 30 years, this is due the effect of minor actinides like Cm-244 with a half-live of about 18.10 years undergoing α-decay, $^{244}_{96}Cm \xrightarrow{\alpha} {}^{240}_{94}Pu$, into plutonium-240. Hence, Pu-240 is seen to manifest itself between the periods thousands years to tens of thousands of years. After 30 years of cooling, almost all the Pu-241 has converted into Am-241 and that of Cm-244 has also converted to Pu-240, hence the extraction of such isotopes from UOX glasses is very timely leaving the major contributors of radiotoxicity to be fission products and other minor actinides which are not in significant quantity. 0.1% of Am by weight present in the UOX glasses due chemical loses is higher when extraction is done after 30 years of cooling than after 5years of cooling, hence by the action of the α-decay chain of $^{241}_{95}Am \xrightarrow{\alpha} {}^{237}_{93}Np \xrightarrow{\alpha} {}^{233}_{91}Pa$, the radiotoxicity

of UOX glasses of the 30 years extraction slightly increases than that of the 5 years extraction after several millions of years.

Figure 3.14 shows comparative assessment of the cooling effect vis-à-vis burnup of the reference once-through cycles. It confirms that if no actinide is extracted from the spent UOX assembly, their radiotoxicity is quite comparable for the first decade and subsequent ten thousand years as seen in the label "Reference glasses at discharge".
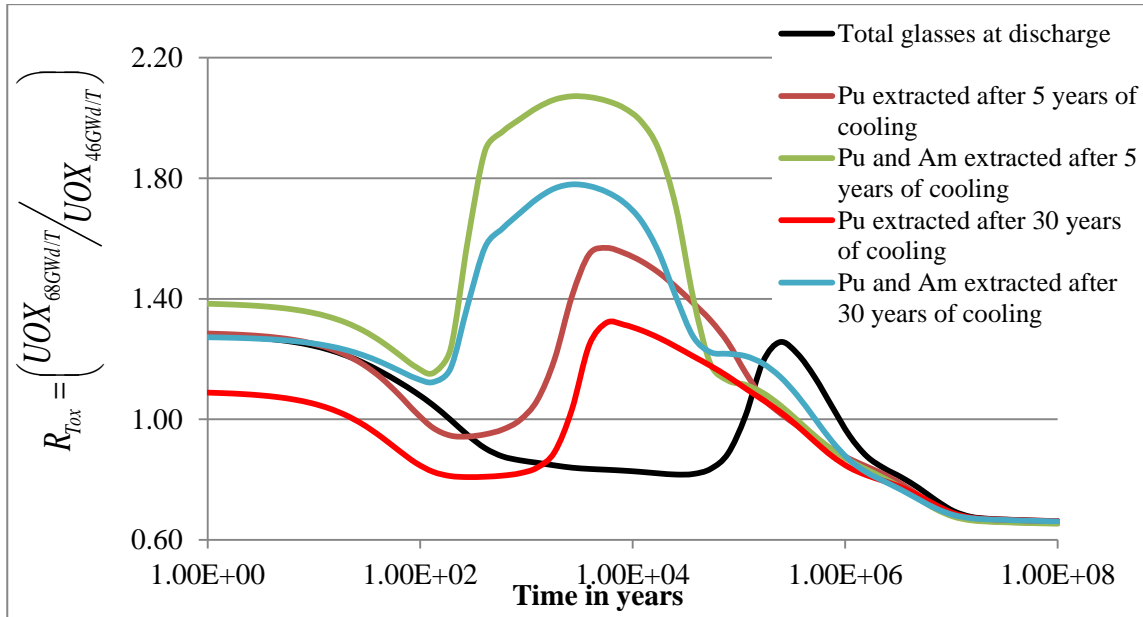
Figure 3.16 Comparison of cooling effect of Pu and/or Am extraction on radiotoxicity with respect to burnup of spent UOX assembly

All indications in Figure 3.16 point to the fact that, extraction of actinides from spent fuel of UOX assembly is better in terms of radiotoxicity of the once-through UOX glasses when the fuel assembly had a shorter burnup. This is because, there will be less production of minor actinides such as curium and americium since the fuel assembly is removed from the core before plutonium, which increases the production of Am (see Figure 3.11), gets utilized in the core.

Generally, the extraction of Pu and Am from the glasses of UOX after 30 years is much better in terms of radiotoxicity when considering permanent storage than all the other considerations (Figure 3.15). Just that Figure 3.16 concludes that it much better when the spent UOX assembly had a shorter burnup. Residual heat production from spent fuel which is a major factor in spent fuel storage is discussed in section 3.4 of this chapter.

3.3.2 Radiotoxicity of MOX and MOXAm recycled Fuels

A fully *closed fuel cycle*, on the contrary, implies that fissionable material is not left behind. In reality, there will always be radioactive material left from the utilisation of nuclear technology for the benefit of mankind. Even though a fully closed fuel cycle is somewhat utopian, it is reasonable to achieve a situation where the potential radiological hazards are reduced within an acceptable timescale so as to reduce the size of a geological storage.

A common goal for the closure of the fuel cycle and for the transmutation effort is to reduce the fraction of long-lived material enough to make the radiotoxicity of the fission products and the losses of actinide material from the fuel cycle to fall below the natural uranium reference level within 1000 years.

Figure 3.17 and Figure 3.18 shows the radiotoxicity curves of a typical MOX spent fuel simulated in this work by daughter and mother nuclei respectively. This MOX fuel was fabricated with the Pu coming from 46GWd/t spent UOX fuel assemblies and depleted U, which has been cooled for 5years.

Decay by mother nuclei shows the significant contribution of Pu to the total radiotoxicity. In case of multi-recycling of Pu, Figure 3.18 presents a good case but this is not considered in this work.
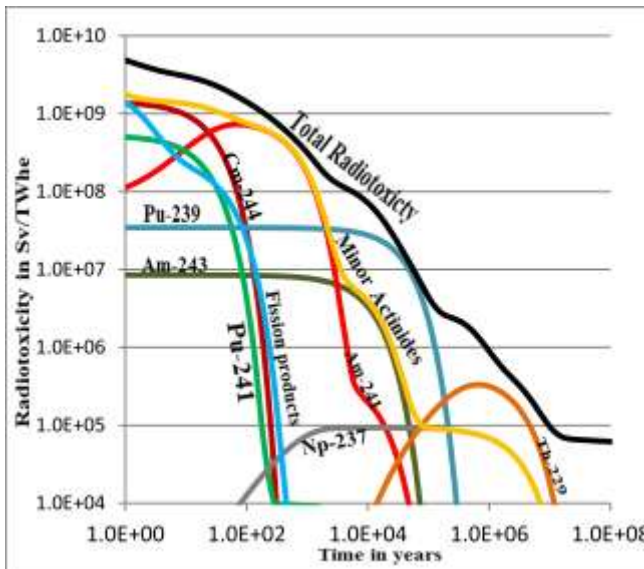
Figure 3.17 Radiotoxicity curve **by daughter nuclei** of spent 46GWd/t MOX assembly after discharge
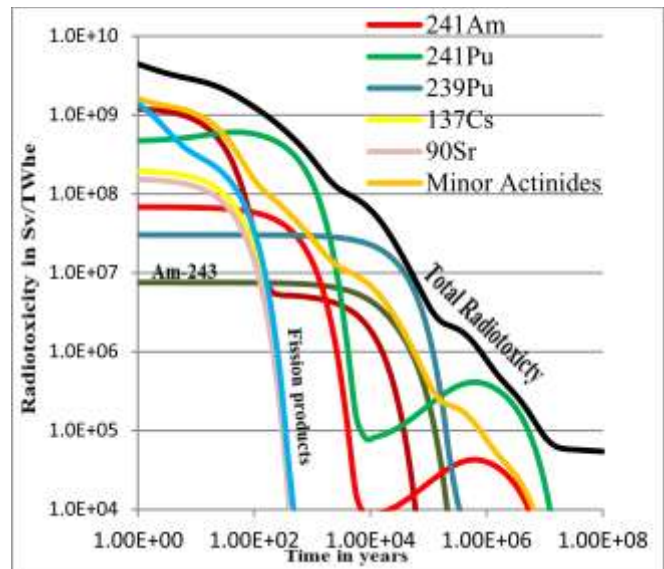
Figure 3.18 Radiotoxicity curve **by mother nuclei** of spent 46GWd/t MOX assembly after discharge

When the radiotoxicity of the spent MOX fuel is analyze as in a geological storage, i.e., by daughter (Figure 3.17), unlike the radiotoxicity of the reference UOX spent assembly whose first 10 years of radiotoxicity is dominated by the fission products, the MOX fuel has Cm-244 dominating the first thousand years through its α-decay into Pu-240 with a half-life of 18.1 years.

For the first 50 years, the radiotoxicity is greatly contributed by the minor actinides with heavy contribution form Am-241 whose precursor isotope is Pu-241. Just like the UOX spent assembly, the remaining part of the radiotoxic curve is contributed by plutonium, neptunium and thorium.

By visual inspection, the radiotoxicity of the MOXAm fuel is comparable to that of the MOX fuel. Major contribution of the total radiotoxicity of the MOX fuel applies to the MOXAm fuel.
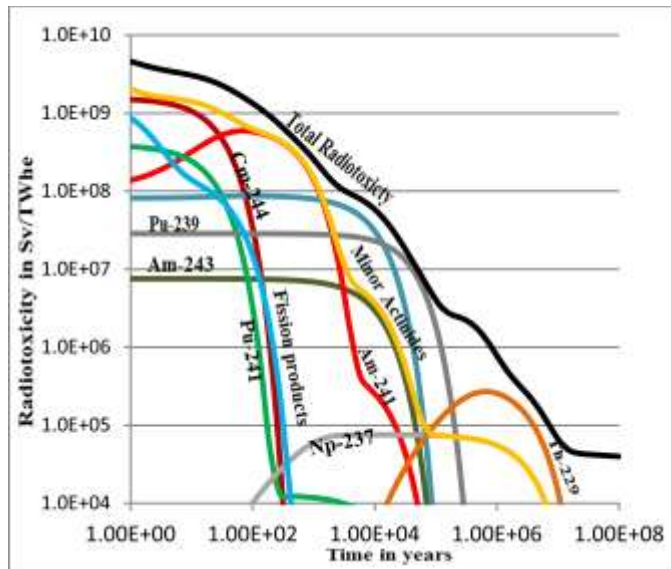
Figure 3.19 Radiotoxicity curve **by daughter nuclei** of spent 46GWd/t MOXAm assembly after discharge
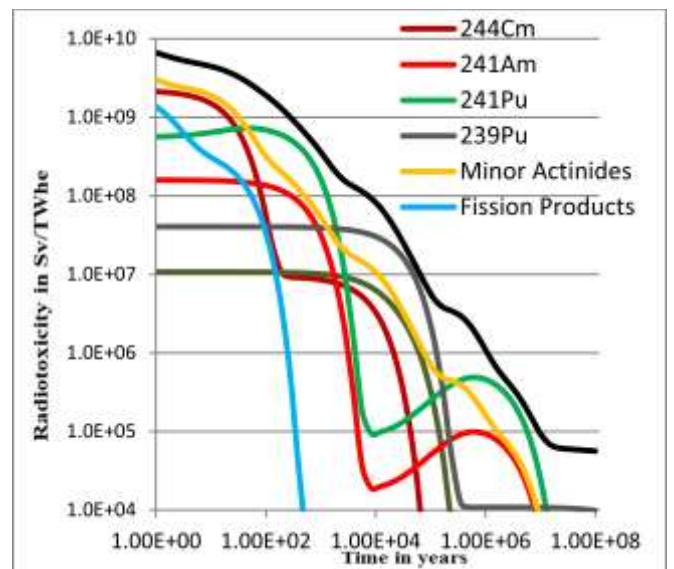
Figure 3.20 Radiotoxicity curve **by mother nuclei** of spent 46GWd/t MOXAm assembly after discharge

Due to the high concentration of Am-241 in the MOXAm fuel and the breeding of Pu-241 by neutron capture on Am-241 that occur during the fuel burnup in the core of this fuel type (see Figure 3.10), the initial contribution of Am-241 to the total radiotoxicity in the MOXAm increase slightly as compared to the MOX fuel.

3.3.1 Comparison of Radiotoxicity of MOX and MOXAm strategies to the UOX strategy

Over the years, a large number of studies have been performed on potential fuel cycles. In the seventies, a main focus was to design fuel cycles guaranteeing the fissile inventory to grow faster

than the expected growth in electricity consumption. This may be achieved through efficient breeding in fast spectrum reactors. By then, electricity consumption had, historically, doubled every twelve years in the western world.

The issue of long-lived nuclear material and nuclear waste is complex, as there are no simple "solutions" or even "right answers". To start with, the term *nuclear waste* has quite different meanings depending on the fuel cycle strategy chosen. In the light water reactor once-through fuel cycle, the fuel elements are by definition waste after irradiation, and should be treated as such. The waste form is ceramic uranium oxide. However, if the MOX-strategy is applied to recycle plutonium, the waste definition is different. In this case, waste is produced at the reprocessing facility, as well as at the reactor. The waste from reprocessing is glass, in which fission products and actinides are dissolved. The irradiated MOX-fuel assemblies are also considered as waste, unless multi-recycling is applied, in which case they are considered a resource [23].

Due to the quest to reduce radiotoxicity using different fuel cycles, the MOX and MOXAm cycles are compared to their respective UOX cycles from which they were fabricated from to check the effect of radiotoxicity as compared to these UOX cycles.

In Figure 3.18 and Figure 3.19, the radiotoxicity of the MOX cycles are compared the radiotoxicity of the spent UOX cycles from which they were fabricated taking into accounts the years of cooling of the spent UOX assemblies. The total radiotoxicity at time t of the MOX cycles were computed as:

$$Rad^{Total}_{MOX\ at\ t} = Rad_{MOX\ at\ t} + \left(Rad_{UOX\ glasses\ at\ t}\right) \times R \qquad (3.3)$$

The comparison of the radiotoxicity of the MOX cycle to the UOX cycle, $R_{cycle\ at\ t}$, for a specific burnup from which the MOX was fabricated is presented in the ratio;

$$R_{cycle\ at\ t} = \left(Rad^{Total}_{MOX\ at\ t} \middle/ Rad^{Total}_{Spent\ UOX\ at\ t} \right) \qquad (3.4)$$

Whereas variables expressed in equations (3.4) are cumulative, variables expressed in equation (3.6) and equation (3.7) are instantaneous at time t.

MOX cycles in Figure 3.21 and Figure 3.22 are compared the UOX cycle in which the burnup of the UOX was 46GWd/t and 68GWd/t respectively. During the first hundred (100) years, all MOX cycles show relative increase radiotoxicity as compared to the UOX cycle with the MOX assembly cycle of shorter cooling time contributing the most. Such assemblies have high plutonium quality which produces relatively more fission products.
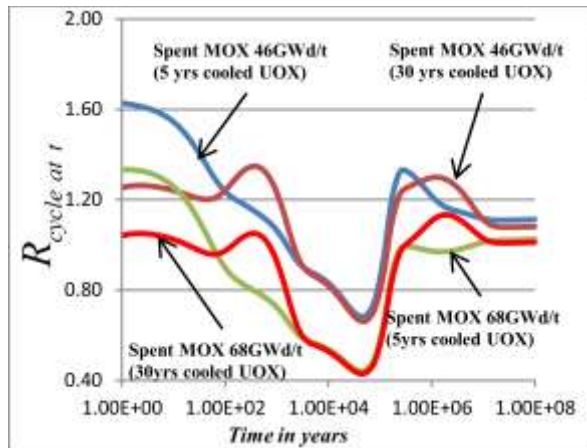
Figure 3.21 Comparison of Radiotoxicity of MOX Strategies to spent **46GWd/t UOX Strategy**
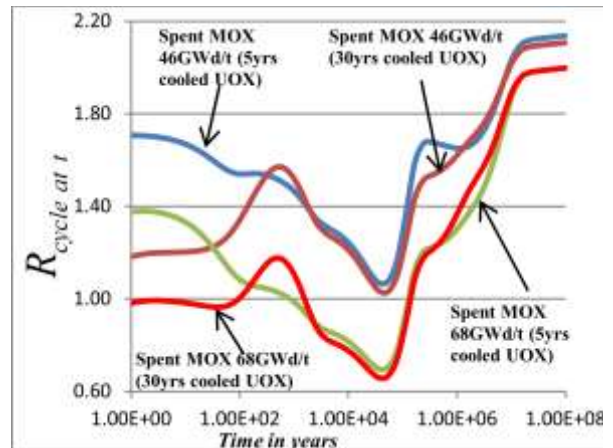
Figure 3.22 Comparison of Radiotoxicity of MOX Strategies to spent **68GWd/t UOX Strategy**

Due to the high concentration of Pu in the MOX fabricated from the 30 years cooled UOX, the decay of Am-241 from the precursor isotope Pu-241 increases radiotoxicity of the MOX cycle as observed between a hundred years to a thousand years. The effect of Cm-244 can also be observed as it contributes to the Pu-240 inventory in the through α-decay. The α-decay of Pu-240 into U-236 together with the α-decay of Np-237 from Am-241causes a little hump between at ten thousand to ten million years as these isotopes have long half-lives. The utilization and relative reduction of pu-239 in the MOX glasses show a deep valley in the ratios of the radiotoxicity of the MOX cycles to the UOX cycle.

Independent of the burnup of the UOX cycle, all MOX cycles fabricated from 30 years cooled UOX fuel assemble show relative reduction in radiotoxicity as compared to those fabricated from the shorter years of cooling of the spent UOX assembly. It is not advisable to fabricate a MOX cycle whose burnup is lower than the UOX cycle from which it was fabricated from. The bad quality of Pu from which such assemblies were fabricated (see Table 3.3), enables the breeding of

fissile isotope Pu-241(see Figure 3.8) which is not utilized before reaching EOC. Figure 3.19 shows that radiotoxicity values will relatively increase after a million years due to the decay chain of Pu-241 which is highly present at discharge.

Conclusively, 68GWd/t MOX cycle, fabricated from 30 years cooled spent 46GWd/t UOX assemblies, relatively maintains radiotoxicity in the first 100 years and further reduces it in the long term.

The MOXAm cycles in Figure 3.23 and Figure 3.24 are also compared the radiotoxicity of the UOX cycle in which the burnup of the UOX at which the extraction was done is 46GWd/t and 68GWd/t respectively. All stages of radiotoxicity of the MOXAm cycle exhibits high radiotoxicity. Though generally, the reduction in americium at EOC is responsible for the decrease radiotoxicity between the periods of hundred (100) years and ten thousand (10,000), it is not good enough to be below the radiotoxicity of the UOX cycle within the same period, except for the MOXAm cycles whose burnup at EOC was more than that of the spent UOX from which they were fabricated. This shows that the longer the fuel stayed in the core the more americium will undergo reduction.
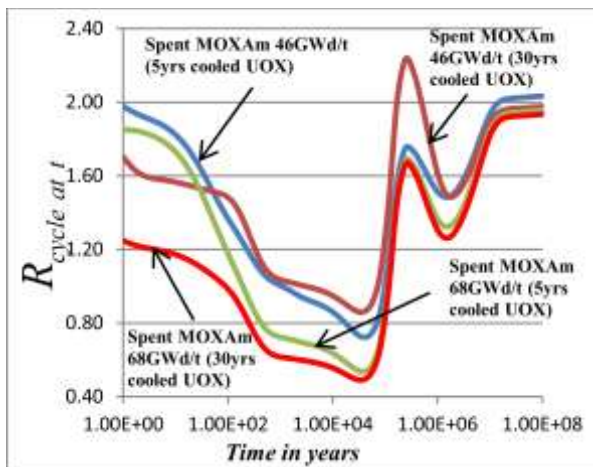
Figure 3.23 Comparison of Radiotoxicity of MOXAm Strategies to spent **46GWd/t UOX Strategy**
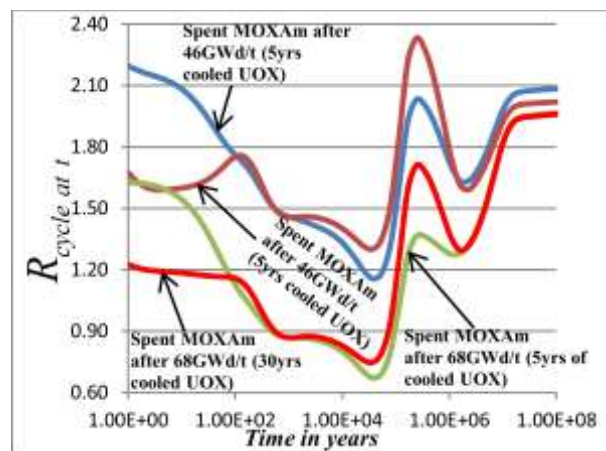
Figure 3.24 Comparison of Radiotoxicity of MOXAm Strategies to spent **68GWd/t UOX Strategy**

MOXAm cycles with shorter cooling time and shorter burnup contributing the most radiotoxicity because their core lifetime is too short to reduce the americium content in their fuel makeup. Also high radiotoxicity contributions from the spent UOX glasses is a factor, since they still contain

relatively short-lived Cm-244 isotope, which decays into Pu-240 to relatively increase the radiotoxicity of their spent UOX glasses.

Though Pu-240 is responsible for the high peaks of radiotoxicity between the periods of ten thousand to ten million years due to it α-decay, the high concentration of Cm-244 at discharge, which is a precursor isotope of Pu-240 through an α-decay is a big contributory factor. However, the effect of Am-241 also contribute tremendously to this peak due to the breeding of about 90% by mass Pu-241with respect to its initial mass at BOC (see Figure 3.10).

Generally, apart from the relative maintenance of radiotoxicity of the 68GWd/t MOXAm fuel fabricated from the 30years cooled spent UOX fuel as compared to its UOX cycle in the first 1000years, the rest of the MOXAm cycles do not necessarily decrease radiotoxicity as compared to its UOX cycle, the high breeding if Pu-241 and the high concentrations of Cm-244 do not make it favorable to reduce radiotoxicity. However, americium concentrations are drastically reduced (see Table 3.6).

Table 3.7 Comparison of in cumulative radiotoxicity of MOX and MOXAm cycles to their respective UOX cycles (Once-through cycle)

MOX and MOXAm Cycle	$R_{cycle} = \left(\dfrac{Rad_{UOX\ cylce}^{Total} - Rad_{MOX\ cylce}^{Total}}{Rad_{UOX\ cylce}} \right)$			
	Cooling period of a spent UOX assembly			
	5 years cooled spent 46GWd/t UOX	30 years cooled spent 46GWd/t UOX	5 years cooled spent 68GWd/t UOX	30 years cooled spent 68GWd/t UOX
46GWd/t MOX	70.09%	72.01%	-24.09%	-19.76%
46GWd/t MOXAm	-8.56%	-5.28%	-21.94%	-18.23%
68GWd/t MOX	81.94%	81.68%	-4.90%	-4.14%
68GWd/t MOXAm	3.92%	4.24%	-1.87%	-1.64%

The overall radiotoxicity of a particular cycle determines its potency over millions of years after discharge. The period considered is from one year to hundred million years, by then most of the actinides would have decayed to low levels. All negative values in Table 3.7 show increase

cumulative radiotoxicity of the MOX or MOXAm cycle with respect to its UOX once-through cycle whereas the positive values states the decrease which we hope to achieve in geological period.

All the MOX cycles show high reduction in cumulative radiotoxicity with the higher burnup showing better reduction. The 68GWd/t MOX cycles fabricated from a lower burnup of spent 46GWd/t UOX cycle show relatively equal and best reduction irrespective of their cooling times. This can also be confirmed with Figure 3.18 that, most of the radiotoxicity evolution of these MOX cycles lies below the 1.0 line. The longer burnup of this MOX cycle which further utilized the fissile plutonium and transmutes other minor actinides, reduces the amount of actinides present in these spent MOX cycle at discharge.

In the same frame, MOXAm cycles from better plutonium quality show better cumulative radiotoxicity values. Higher burnup of the MOXAm cycle show a slight improvement on cumulative radiotoxicity as compared to their originated lower burnup UOX cycle. Even though **Error! Reference source not found.** shows that it is not advisable to have a MOX or MOXAm ycle's burnup lower or equal to that of the UOX cycle it originate from, the 68GWd/t MOXAm cycles fabricated from the spent 68GWd/t UOX cycles irrespective of their cooling times, show relative similar amount of cumulative radiotoxicity. This is good for the availability of americium for incineration (transmutation) in fast reactors when they are fully operational.

3.4 DECAY HEAT (GEOLOGICAL STORAGE)

Decay heat is the heat produced by the decay of radioactive fission products and actinides after a nuclear reactor has been shut down. Decay heat is the principal reason of safety concern in Light Water Reactors (LWR). It is the source of 60% of radioactive release risk worldwide. It is also responsible of the dimensioning of the geological disposal for nuclear waste. For reactor safety, the period concerns are in days or months, for geological disposal, a few decades or centuries. A few decade of geological storage is considered for this work.

In an international conference of nuclear energy for new Europe in September 2008, Gašper Žerovnik et al reported on the decay heat of the Krško NPP whose 4.0% UOX fuel assembly was simulated with ORIGEN 2.1 to reach 46GWd/t. Gašper Žerovnik et al recoded a decay heat of

about $2.0 \times 10^5 Watts$ at 3155.76sec after shutdown which is equivalent to $1.3 \times 10^7 W/GW_e y$. Below is the plot of decay heat of the Krško NPP by Žerovnik et al, 2008.
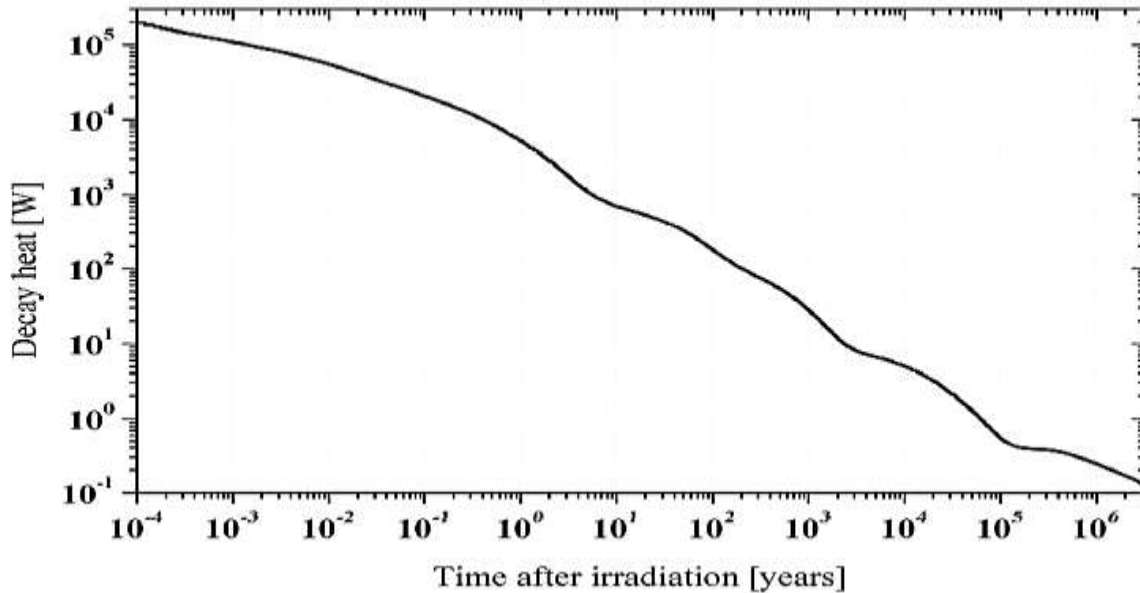
Figure 3.25 Decay heat of Krško NPP 46GWd/t UOX assembly simulated with ORIGEN 2.1 by Žerovnik et al, 2008 **[68]**

In this work, the decay heat was simulated taking into account the build and decay of all fission products available in the MURE heat data file. 3457 number of nuclides (fission products and actinides) were involved in the analyses. The MureGui console, which has inbuilt series of functions of analyses is used to analyse the decay heat.

Due to the heavy dependence of decay heat on fission products, there will be an indirect dependence of burnup and reactor fuel composition. This work seeks to establish the relationship between decay heat of the simulated assembly and burnup and also pre-cooling effect of before fabrication of the MOX and MOXAm which is linked to the fuel composition.

3.4.1 UOX

As shown in Figure 3.26 the decay heat of the UOX assembly is typically dominated by the fission products up to almost a thousand years. The dominance of fission product contribution to decay heat is typical for all LWR. The actinides and minor actinides do not influence the decay heat even in hundreds of years after shutdown.
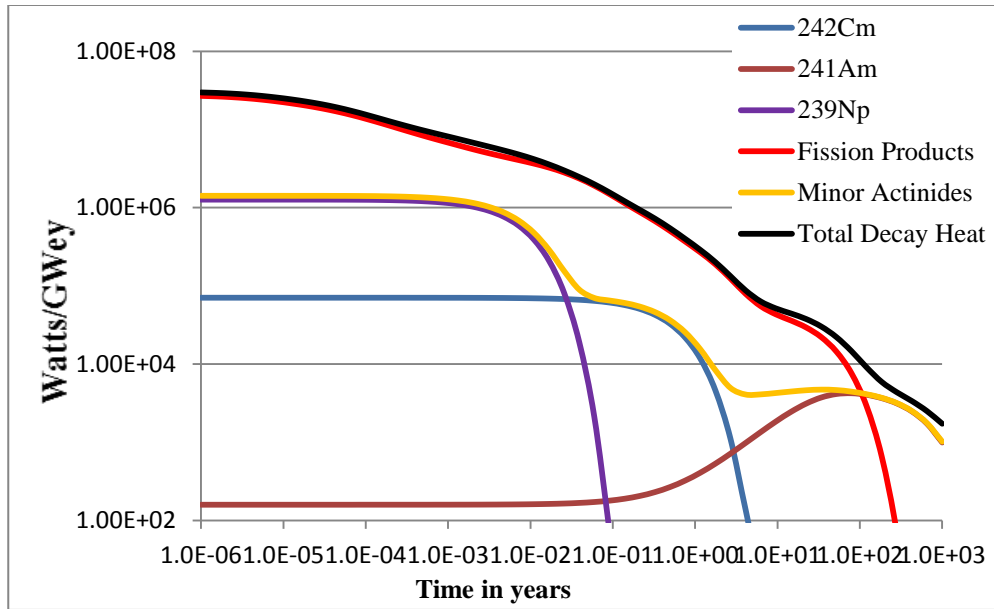
Figure 3.26 Decay heat of UOX after 46GWd/t

Comparing Figure 3.25 and Figure 3.26, the value of decay heat for the 46GWd/t UOX simulated in this work is $1.5 \times 10^7 W/GW_e y$ at 1.0e-04years (3307sec) which is comparable to Žerovnik et al, 2008 discussed earlier.

Error! Reference source not found. shows that, higher burnup of UOX fuel assembly relatively owers the decay heat for almost 9months as compared to shorter burnup. The longer burnt fuel has the capacity to incinerate some of the fission products produced thereby achieving this effect.
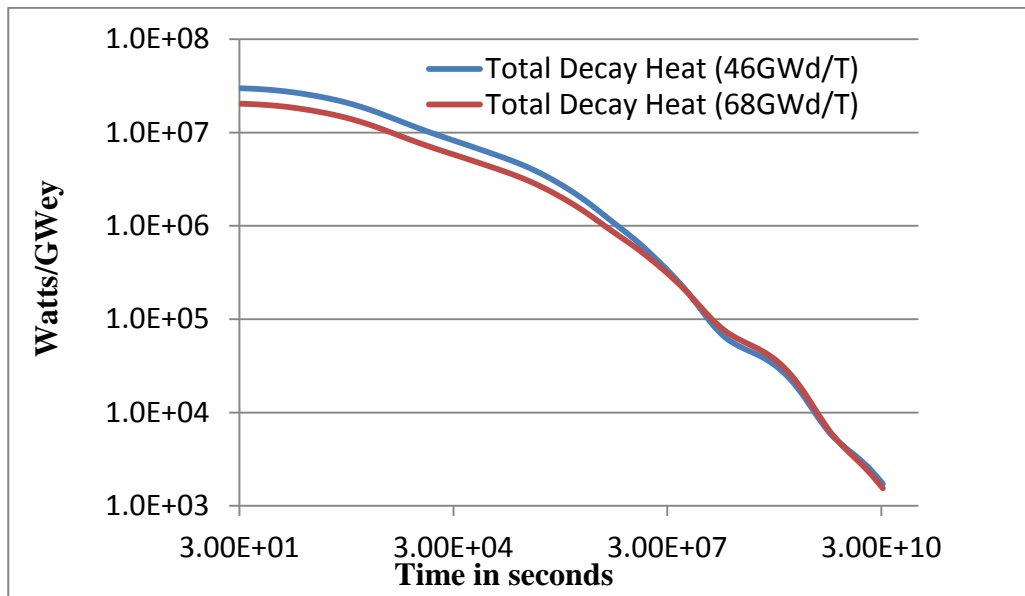
Figure 3.27 Comparison of burnup effect on Decay heat of UOX Assemblies

Due to the extraction of Pu and/or Am from the spent UOX assembly to fabricate the MOX and MOXAm fuel in this work, it will be prudent to compare the geological decay heat performance of the various UOX glasses to the once-through cycle. In **Error! Reference source not found.**, it s observed that after the decay of the fission products, the UOX glasses without Pu and Am has the lowest decay heat, with reference to Figure 3.26, the contribution of Pu-241 in the dominance of the minor actinides at 1000years shows that the UOX glasses without Pu would reduce the decay heat as observed in **Error! Reference source not found.**.
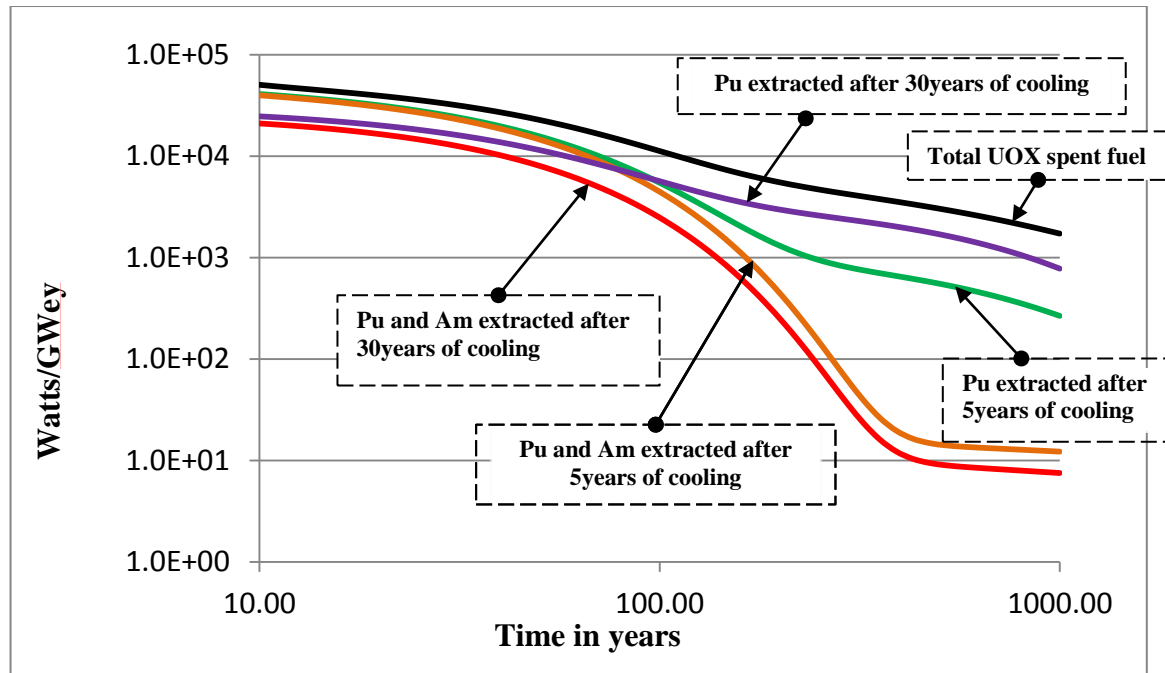
Figure 3.28 Effects of Actinide extraction on decay heat of spent UOX assembly and glasses in geological storage

This reduction relative to the once-through cycle has the tendency to reduce the size of its geological storage at least after 100 years of temporary storage of the UOX glasses. It should be noted that all these analyses do not take into account delayed fission induced by delayed neutrons and the decay of structural and cladding materials in the reactor that may have become radioactive.

3.4.2 MOX

The decay heat of MOX assembly, even though is dominated by the decay of the fission products, the minor actinides contributes significantly after one year. Curium and Neptunium are major contributors to the effects of the minor actinides on MOX decay heat. Actinides such as

plutonium isotopes and uranium isotopes do not make significant contributions to the decay heat (Figure 3.29).

The effect of burnup on decay heat curve of the MOX fuel follows the trend of the UOX fuel, but does not merge even in a thousand years after shutdown. During this period, the UOX decay heat solely rely on the fission product, but the MOX fuel decay heat rely significantly on the minor actinides in the spent assembly (Figure 3.29). The minor actinides concentration in the MOX assembly in a shorter burnup is more than that of the longer burnup, hence these actinides dictates the decay heat production after one year of shutdown.
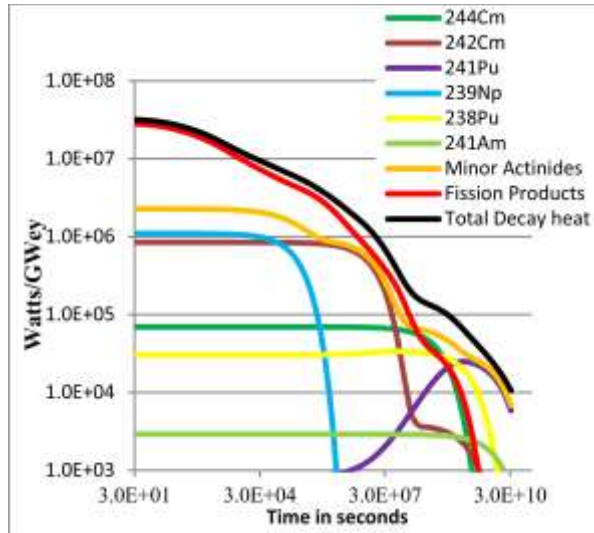
Figure 3.29 Decay heat of MOX Assembly after 46GWd/t
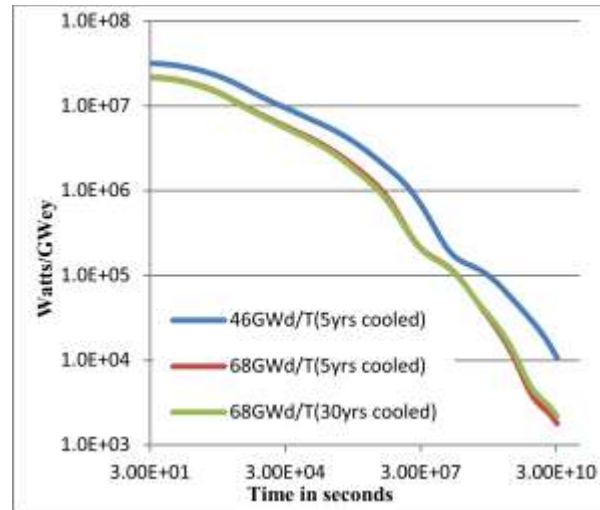
Figure 3.30 Comparison of burnup and cooling effect on Decay heat of MOX

All MOX fuels in Figure 3.30 were fabricated form the spent UOX but have different cooling times. In the MOX fuel, cooling time does not affect decay heat provided the MOX fuels reach the same burnup. Longer cooling periods of the spent UOX tends to increase the plutonium concentration in the MOX during fabrication due to bad Pu quality, however Figure 3.18 shows that this type of MOX assembly has lower fission products and high concentration of Pu-241 concentration at EOC, hence Pu-241 does dictate the decay heat after hundreds of years which makes the cooling effect not to significantly affect decay heat of a MOX fuel assembly few years after shutdown.

3.4.3 MOXAm

Decay heat of MOXAm fuel assembly is similar to that of the MOX assembly based on the elements that dictate the total decay heat. The MOXAm fuel decay heat however, is heavily dependent on minor actinides present in the core. The effect of minor actinides dominates the control of the decay heat just 22days after shutdown with curium-242 being the major contributor (Figure 3.31). Due to long half-lives of the minor actinides, this development is not desirable for spent fuel storage since the spent fuel has to spend long years in wet storage and longer times of cooling if reprocessing is considered.
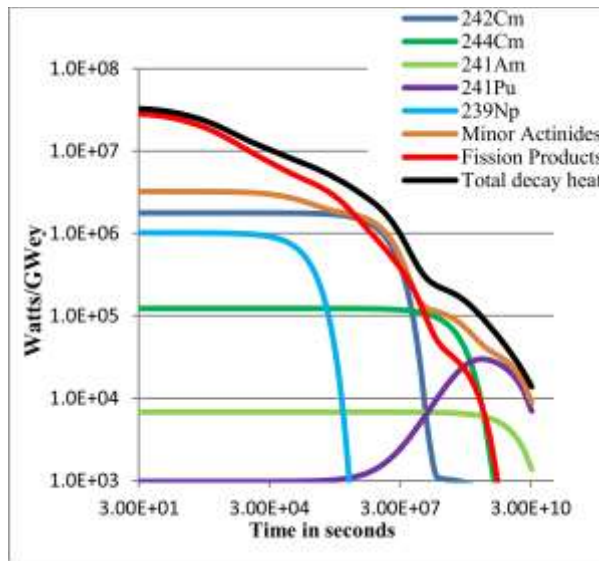
Figure 3.31 Decay heat of MOXAm Assembly after 46GWd/t
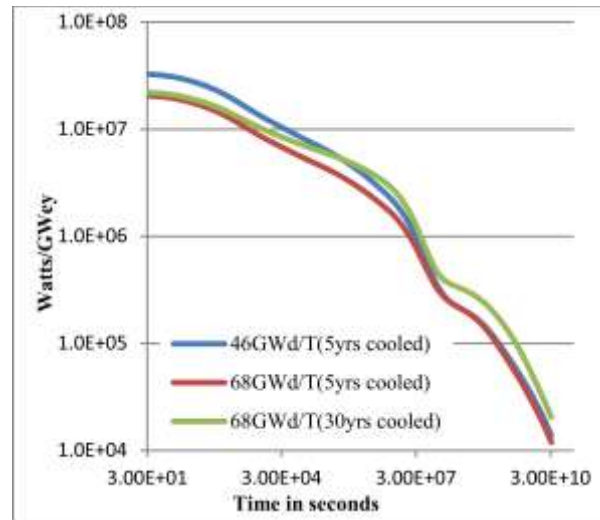
Figure 3.32 Comparison of burnup and cooling effect on Decay heat of MOXAm Assembly

Burnup effect of MOXAm fuel is dependent on cooling time of the spent UOX from which the MOXAm assembly was fabricated, which is directly dependent on the amount of americium present in the fuel at BOC. For MOXAm assembly fabricated from the same pre-cooled time of spent UOX, the decay heat of the shorter MOXAm fuel burnup dominated the amount of heat after shut down due to only fission products effect, this is the same phenomenon observed for all the fuel types. After a significant amount of the fission products have undergone decay, the minor actinides in both short and long burnup spent fuel produce similar amount of decay heat after one year, this is similar to the MOX fuel decay heat curve. However, the amount of Cm-242 in the spent MOXAm fuel at EOC increases with increasing amount of americium in the fuel at BOC. Therefore, MOXAm fuels produced from 30yrs pre-cooled spent UOX has higher decay heat as

compared to shorter pre-cooling, 20days after shutdown during which fission products dominated the decay heat contribution, the Cm-242 rich MOXAm spent assembly lowers the rate of decay heat removal from the spent core due to its high americium concentration at BOC. This is not also desirable as compared to the other fuels cycles considered in this work.

3.5 FUEL SAFETY ANALYSES

Inherent, prompt, negative feedback to reactivity following a temperature increase or a loss of coolant is the most important parameter to assure stable operation of a nuclear core. Without such feedback, minor deviations from the desired operation condition might escalate, threatening core safety [23]. In this work, basic safety coefficient was performed (detailed transient studies not included) to classify the fuel inherent safety. All safety analyses made in this work does not take into consideration the leakage term of the neutron diffusion equation. In thermal reactors, neutron leakage occurs when moderator void increase due to lack of lighter nuclides in the core to slow down the fast neutrons. This increases the fast neutrons population in the core there by gaining the energy to leak out from the core, which in effect further lowers the reactivity of the thermal core under consideration.

3.5.1 Decay Heat (After Reactor Shutdown)

The β- and γ-radiation emitted from decaying fission products amounts to about 7% of the total thermal power output of the reactor. When the reactor is shut down, the accumulated fission products continue to decay and release energy within the reactor while actinides continue to dictate the heat in the long term out of the core. The amount of decay heat produced in the reactor will exponentially decrease as more and more of the radioactive material decays to some stable forms. Decay heat may decrease to about 2% of the pre-shutdown power level within the first hour after shutdown and to about 1% within the first day. Decay heat will continue to decrease, but at a much slower rate due to contribution from minor actinides. Decay heat is significant, weeks and even months after the reactor is shut down. Failing to cool the reactor after shutdown results in core heat up and possibly core meltdown just like what happen to the Daiichi nuclear power plants at Fukushima, Japan in March, 2011.
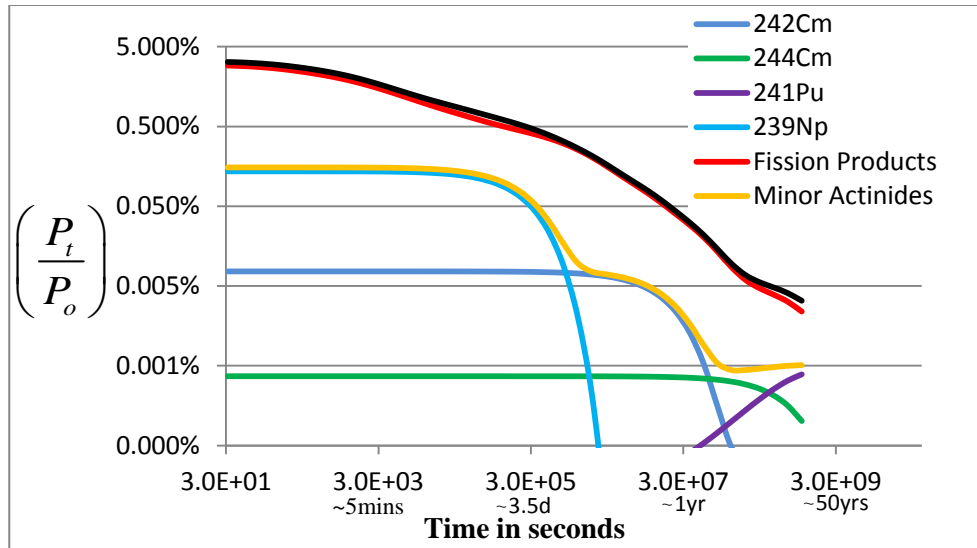
Figure 3.33 Decay heat of UOX after 46GWd/t

About 4% of the nominal operating power of the UOX core is experienced as decay heat 30seconds after shutdown with fission product dominating the decay heat contribution while 3.1% ratio of decay heat to nominal power of the MOX fuel assembly is recorded, which is a better value of decay heat than the UOX fuel for the same time interval.
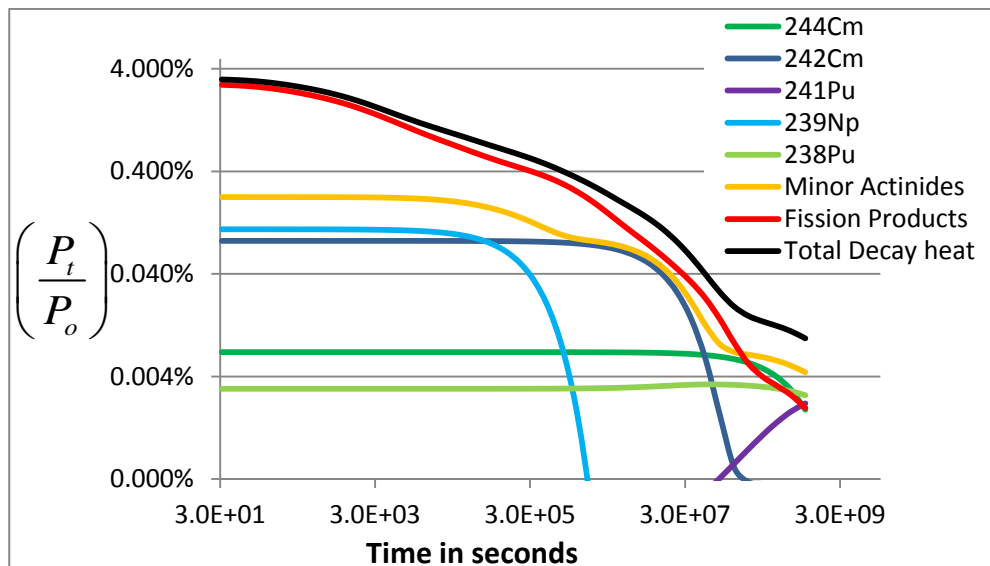
Figure 3.34 Decay heat of MOX Assembly after 46GWd/t

The MOX and MOXAm cores also exhibit relatively good percentage of their nominal operating power as decay heat. Even though the decay heat of these assemblies are dominated by fission products, the contribution from the minor actinides cannot be down played as they take over the domination of contribution of decay at most one years after shutdown.
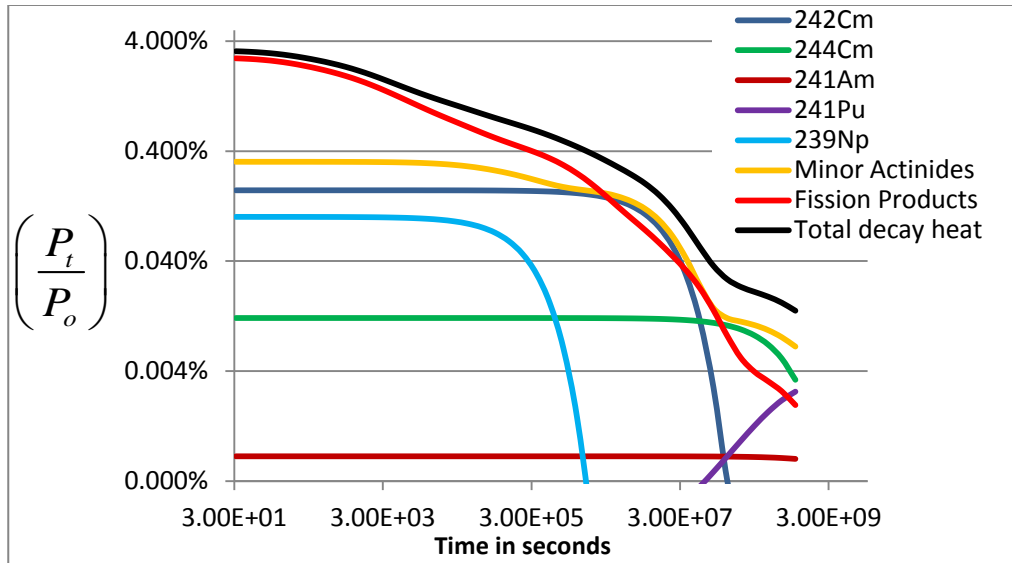
Figure 3.35 Decay heat of MOXAm Assembly after 46GWd/t
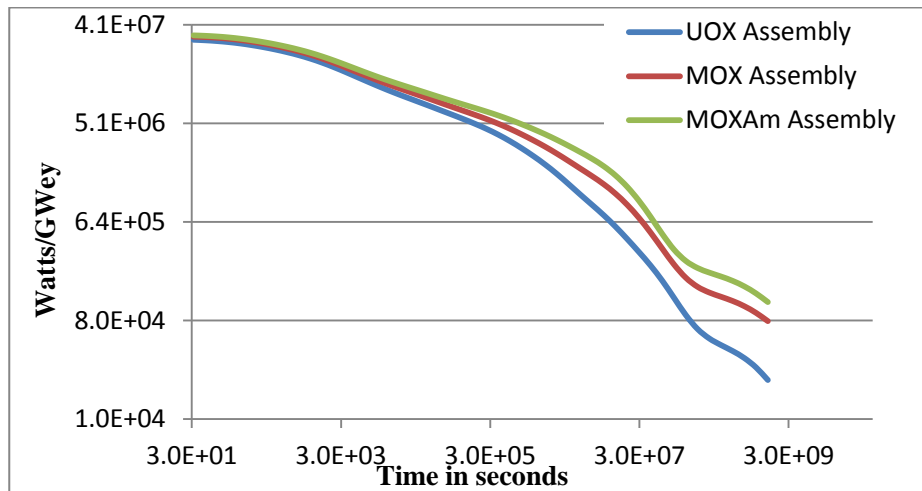
Figure 3.36 Comparison of Decay heat of consider fuel cycles after 46GWd/t

Figure 3.36 shows the comparison of decay heat of some of the various cycles considered in this work. It can be observed that, 3 days after reactor shutdown, the uniform dominance of the fission products contribution to decay comes to an end for the MOX and MOXAm fuels and the minor actinides with their relatively long half-lives tends to dictate rate of reduction of the decay heat. This is responsible for the relative slow rate of reduction of decay heat of the MOXAm assembly due to its high content of minor actinides at EOC.

Table 3.8 Some significant Isotope contribution to decay heat per assembly few seconds after shutdown

Nuclei in Spent Fuel	Half – Life	UOX (Watts/GWey)		MOX (Watts/GWey)		MOXAm (Watts/GWey)	
		46GWd/t	*68GWd/t*	*46GWd/t*	*68GWd/t*	*46GWd/t*	*68GWd/t*
Fission Products	(β-decay)	3.00e+05	3.88e+05	3.40e+05	4.20e+05	3.38e+05	4.08e+05
Sr-90	28.90*y*	1.69e+04	2.59e+04	7.97e+03	1.24e+04	7.94e+03	1.19e+04
Cs-137	30.05*y*	3.02e+04	4.77e+04	3.05e+04	4.81e+04	3.05e+04	4.66e+04
Ru-106	373.59*d*	8.05e+04	1.01e+05	1.52e+05	1.68e+05	1.52e+05	1.67e+05
Ce-144	284.91*d*	1.10e+05	1.11e+05	9.18e+04	9.58e+04	9.16e+04	9.54e+04
Minor Actinides	(α-, β- decay)	1.87e+04	2.95e+04	2.53e+05	3.67e+05	4.67e+05	6.05e+05
Cm-242	162.80*d*	1.52e+04	2.05e+04	1.82e+05	1.73e+05	3.83e+05	2.77e+05
Cm-244	18.1*y*	3.29e+03	8.71e+03	6.70e+04	9.21e+04	1.18e+05	1.26e+05
Np-239	2.36*d*	4.31e+00	2.98e+00	3.75e+00	2.42e+00	3.47e+00	1.98e+00
Am-241	432.2*y*	1.58e+02	1.85e+02	2.92e+03	3.17e+03	6.79e+03	6.44e+03

where *h, m, d* and *y* in the table above represent hours, minutes, days and years respectively.

Note that Table 3.4 and Table 3.5 should be taken into consideration when comparing the isotopic contribution to the decay heat of the individual cycles.

3.5.2 Coolant Void Reactivity

3.5.2.1 UOX

The void coefficient of reactivity is defined as a rate of change in the reactivity of a water-moderated reactor resulting from any modification of the density of the coolant as the power level and temperature changes. A negative void coefficient is desirable because an accidental increase in void fraction will reduce the reactivity and automatically shut down the chain reaction. This condition tends to return the reactor to its initial state.
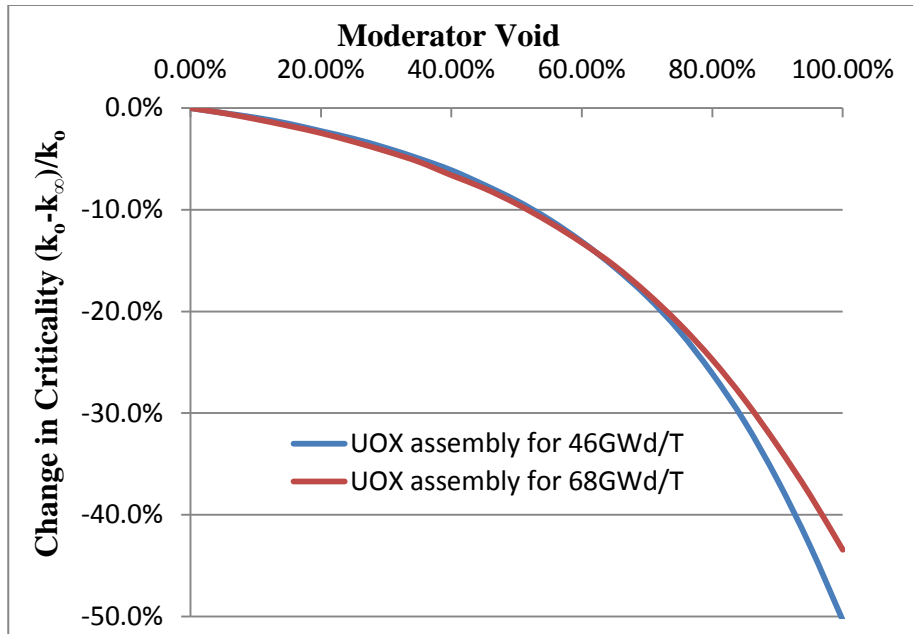
Figure 3.37 Moderator Void for UOX Assembly at BOC

The UOX fuels assemblies simulated in this work to reach their required burnups have desirable Coolant Void Reactivity at all stages of moderator void (see Figure 3.37). The UOX fuel which was designed to operate in the thermal spectrum goes subcritical due to loss of thermal neutrons. The loss of thermal neutron is as a result of loss in light element in the core and hence leads to loss of thermal fission to sustain the nuclear chain reaction (see Figure 3.38).
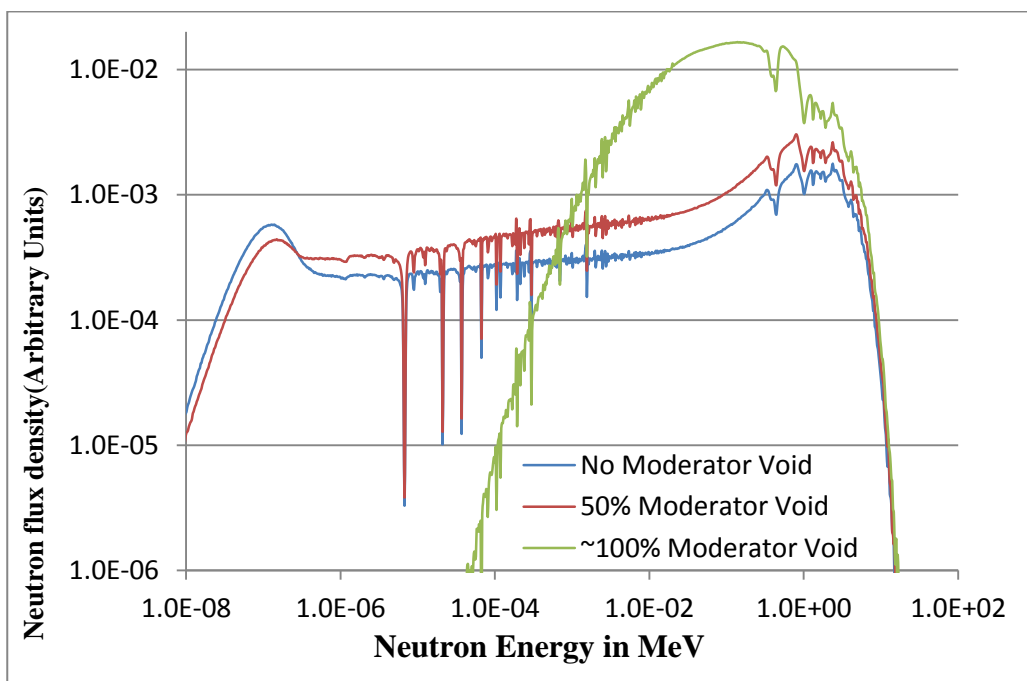
Figure 3.38 Neutron spectra of different percentage loss of Coolant of a 46GWd/t UOX assembly

3.5.2.2 MOX

In practice there is always a tradeoff between the need for a hard neutron spectrum and other aspects, such as core safety. Pu-240 and Pu-242 has high fission cross section for high energy neutrons which makes it necessary to draw a line on plutonium concentration in thermal reactors. High concentrations of fast fission nuclides in the core of a thermal reactor will affect its safety in terms of moderator void.

All moderator voids co-efficient of the MOX assembly fall below the operating criticality of the core hence a good signal for safety inherent feature of the MOX assembly. The MOX fuel assembly with higher burnup of 68GWd/t has higher plutonium concentration which eventually contains high pu240 and Pu-242 isotopes, which fissions with high energy neutrons (Figure 3.43).
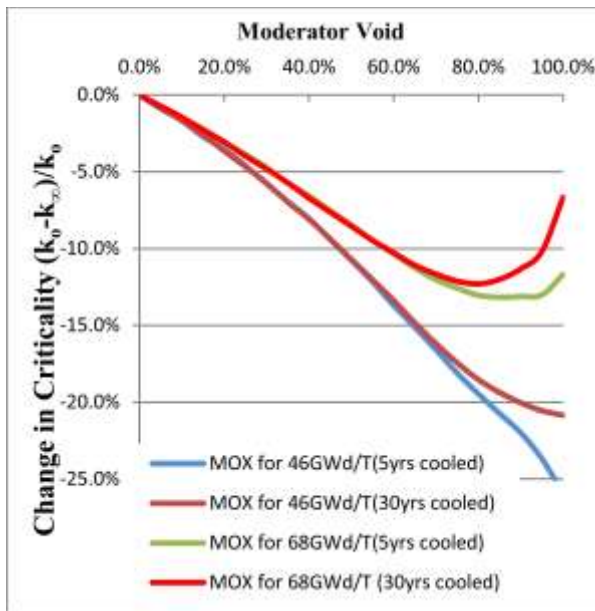
Figure 3.39 Coolant Void reactivity for MOX Assemblies at BOC, all fuels from reprocessed spent 46GWd/t UOX
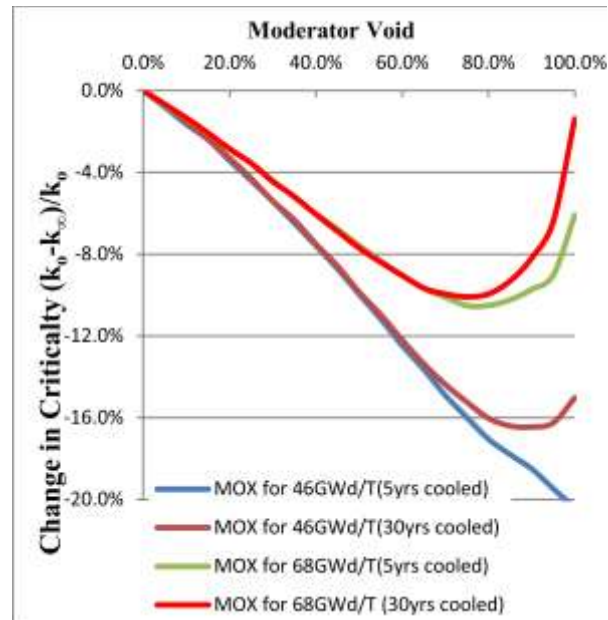
Figure 3.40 Coolant Void reactivity for MOX Assemblies at BOC, all fuels from reprocessed spent 68GWd/t UOX

As the core gets dominated by high energy neutrons due to lack of moderation by increasing moderator void, the fast neutrons dominate the core (Figure 3.41) and hence fission with the plutonium. This phenomenon is responsible for the curving and positive void co-efficient at about 75% of moderator void (see Figure 3.39 and Figure 3.40) however, the global void coefficient

(between 0% and 100% of void moderator) remains negative in all cases, for the mono-recycling of Pu strategy (MOX cycle).
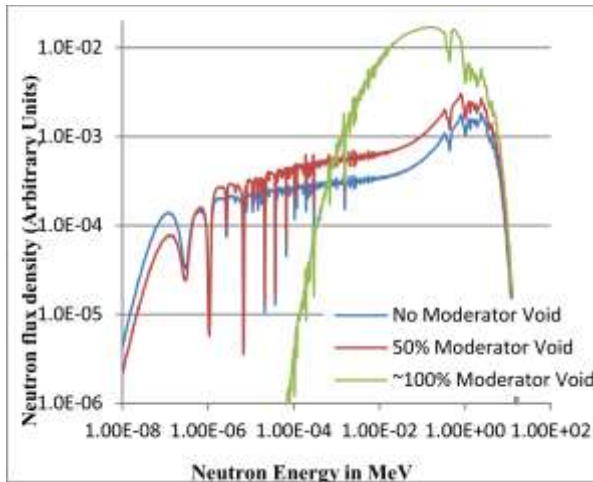
Figure 3.42 Neutron spectra of different percentage loss of Coolant of a 46GWd/t MOX assembly
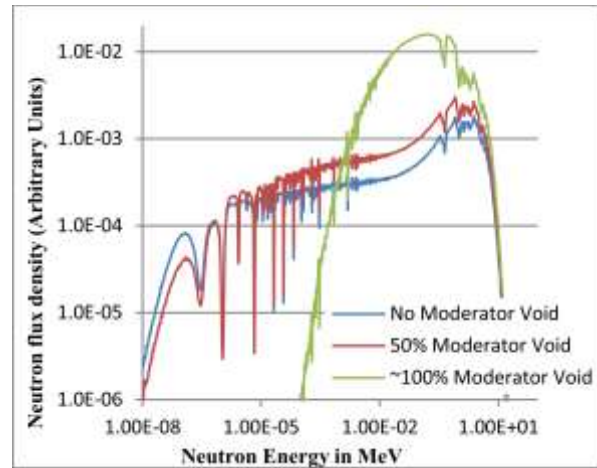
Figure 3.43 Neutron spectra of different percentage loss of Coolant of a 68GWd/t MOX assembly

Though the MOX fuel has high amount of U-238, the presence of plutonium introduces lots of

resonance peaks in the spectrum due to their high absorption cross sections at such energies. The average flux contribution from high energy neutrons gets higher with increasing plutonium concentration whiles there is a reduction in thermal flux to achieve the same operating power (compare the thermal flux region in Figure 3.41 and Figure 3.42). Even though at an almost no moderator in the core, the flux is dominated by fast neutrons, the reactor still remains subcritical

Figure 3.41 (n.f) cross section of Pu-242 from JEFF 3.1

because the amount of fast fission nuclide in the core is below the critical mass to sustain a fast fission chain reaction.

3.5.2.3 MOXAm

The presence of Am (a neutron poison) requires an increase the Pu concentration at the beginning of cycle to balance the neutron ratio, this leads to degrade the performance of the Coolant Void

Reactivity of the MOXAm fuel. It is expected this effect may create positive Coolant Void Reactivity some configurations.

Americium also exhibits fission with fast neutrons (see Figure 3.46) which may have a negative effect on moderator void coefficient as it combines with plutonium in the MOXAm assembly.
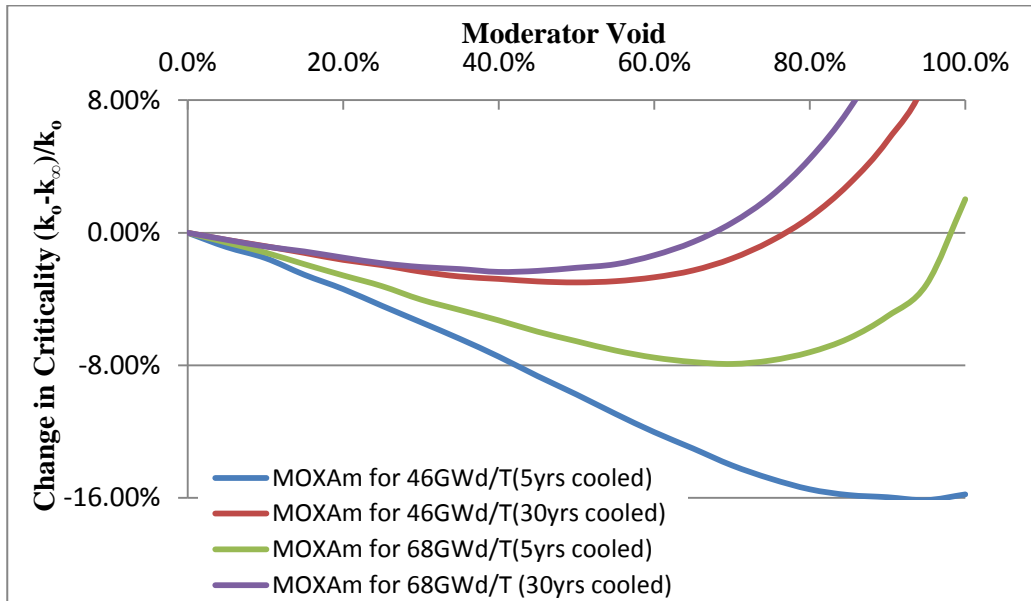
Figure 3.44 Coolant Void of reactivity for MOXAm Assemblies at BOC, all fuels from reprocessed spent 46GWd/t UOX
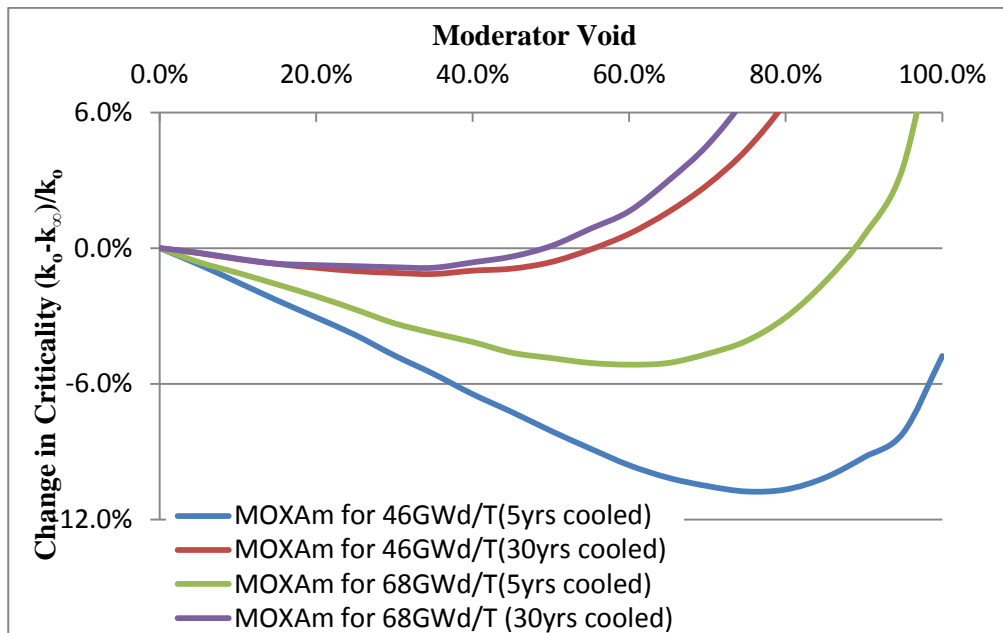
Figure 3.45 Coolant Void reactivity for MOXAm Assemblies at BOC, all fuels from reprocessed spent 68GWd/t UOX

Even though the majority moderator void co-efficient of the MOXAm fuel assemblies fell below the initial k_∞, the moderator void co-efficient of the MOXAm fuel is dependent not only on plutonium concentration but also depends on the concentration of some fast fission nuclides like Am-241 and Pu-242 (Figure 3.46). The americium content in the 68GWd/t MOXAm fuel fabricated from 30yrs cooled spent UOX is more than the other fuels, however, the 46GWd/t MOXAm fuel fabricated from 30yrs cooled spent UOX has the highest ratio of fast fission nuclide to thermal fission nuclides. These two mentioned fuels above, even though were fabricated from the same spent

Figure 3.46 (n.f) cross section of Am-241 from JENDL 2007

UOX, the 68GWd/t MOXAm assembly has high plutonium concentration thereby decreasing the ratio of the amount of americium to plutonium in the assembly. The MOXAm fuels fabricated form high burnup of spent UOX fuel contains relatively high americium and plutonium and hence has fission rate in the fast spectrum.
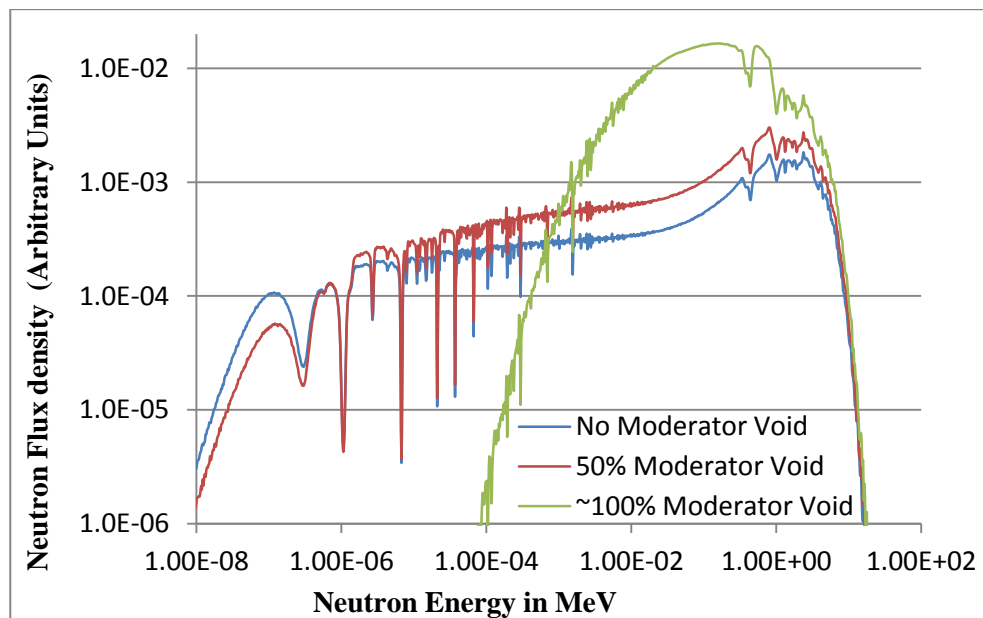
Figure 3.47 Neutron spectra of different percentage loss of Coolant of a 46GWd/t MOXAm assembly fabricated from reprocessed spent 5 years cooled 46GWd/t UOX fuel.

Similar to the MOX spectrum, the MOXAm spectrum has its fast nuclides totally dominating the neutronics of the core at an almost total moderator void of the core. The americium in MOXAm assembly introduces more resonance peaks as it can be observed clearly in Figure 3.48 within the energy region of 1.8e-07MeV to 1.5e-05MeV. Americium introduction in the MOX fuel to form the MOXAm fuel has two negative effects, increasing the Pu concentration, and also high concentration of it leads to positive moderator void co-efficient.
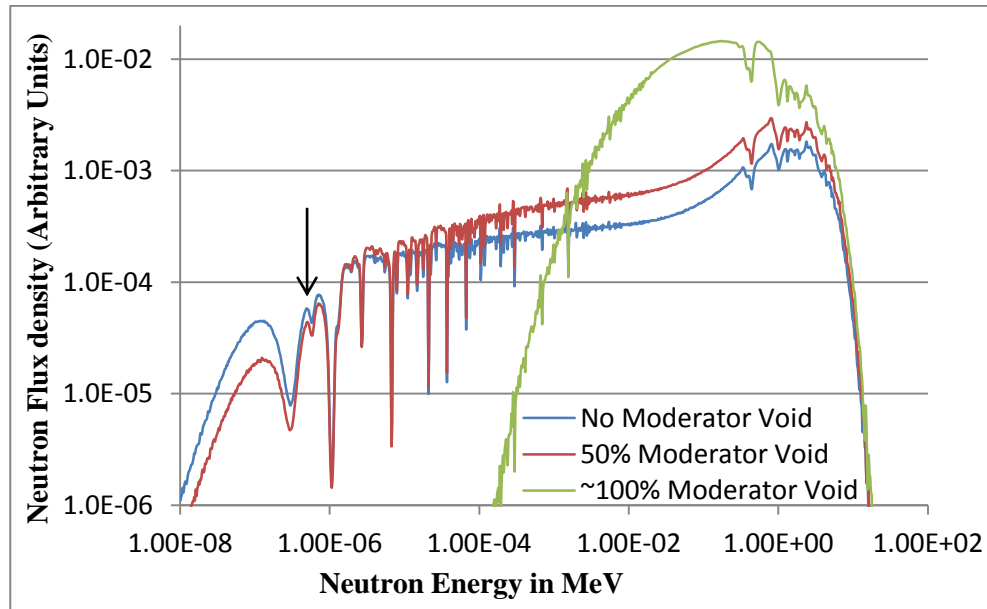
Figure 3.48 Neutron spectra of different percentage loss of Coolant of a 46GWd/t MOXAm assembly fabricated from reprocessed spent 30years cooled 46GWd/t UOX fuel.

3.5.3 Temperature Coefficient

The change in reactivity per degree change in temperature is called the temperature coefficient of reactivity. Because different materials in the reactor have different reactivity changes with temperature and the various materials are at different temperatures during reactor operation, several different temperature coefficients are used. Usually, the two dominant temperature coefficients are the moderator temperature coefficient and the fuel temperature coefficient.

Globally, the temperature coefficients of the all fuels under study were negative between changes in increasing temperature of 0% to 100% of the nominal operating temperature of 575K and 1500K for moderator and fuel temperature respectively. All coefficient values have 10% MCNP statistical error. The reference UOX fuel for 46GWd/t have moderator and fuel temperature coefficients as $(-4.473 \times 10^{-6})\Delta k/K$ and $(-1.953 \times 10^{-5})\Delta k/K$ respectively and that for UOX

68GWd/t have moderator and fuel temperature coefficients as $(-3.233 \times 10^{-6})\Delta k/K$ and $(-1.456 \times 10^{-5})\Delta k/K$ respectively. Table 3.9 shows the global temperature coefficient of the MOX and MOXAm fuel. In the MOX or MOXAm fuels assemblies which have low moderator temperature coefficient, they are balanced with relatively high fuel temperature coefficient and vise-versa. This is good for reactor operation since high values of these indicators will bring lots of perturbations in the excess reactivity and very low values will have adverse effect on inherent safety.

Table 3.9 Temperature Coefficients of MOX and MOXAm fuels considered in this work

Burn-up of MOX Assembly (GWd/t)	Temperature Coefficient ($\Delta k/K$) $\times 10^{-5}$							
	Sources of MOX and MOXAm fuel fabrication							
	5 years cooled spent 46GWd/t UOX		*30 years cooled spent 46GWd/t UOX*		*5 years cooled spent 68GWd/t UOX*		*30 years cooled spent 68GWd/t UOX*	
	Mod	Fuel	Mod	Fuel	Mod	Fuel	Mod	Fuel
46	-1.233	-2.277	-0.974	-2.169	-1.426	-2.183	-1.213	-2.119
46 (with Am)	-1.457	-2.075	-1.502	-1.608	-1.437	-1.932	-1.435	-0.949
68	-1.211	-2.274	-1.049	-2.065	-1.379	-2.238	-1.106	-2.013
68 (with Am)	-1.415	-2.019	-1.049	-2.065	-1.376	-1.859	-1.182	-1.392

The column Mod in Table 3.9 represents moderator temperature coefficient while Fuel represents temperature coefficient. Detailed fuel performance in the different cycles in terms of the various temperature coefficients is discussed in the next section.

3.5.3.1 Moderator Temperature coefficient

The change in reactivity per degree change in moderator temperature is called the moderator temperature coefficient of reactivity. A negative moderator temperature coefficient is desirable because of its self-regulating effect [69].
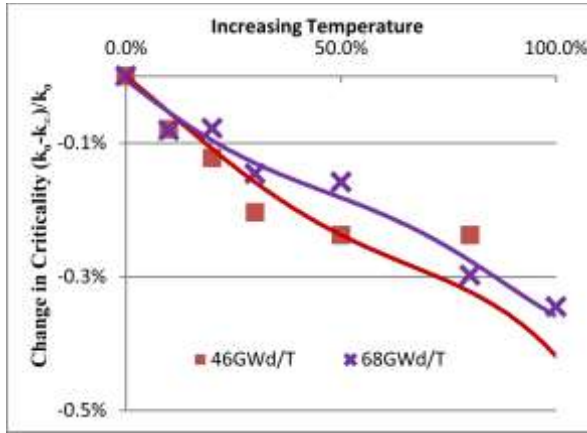
Figure 3.49 Moderator Temperature coefficient for UOX Assembly at BOC
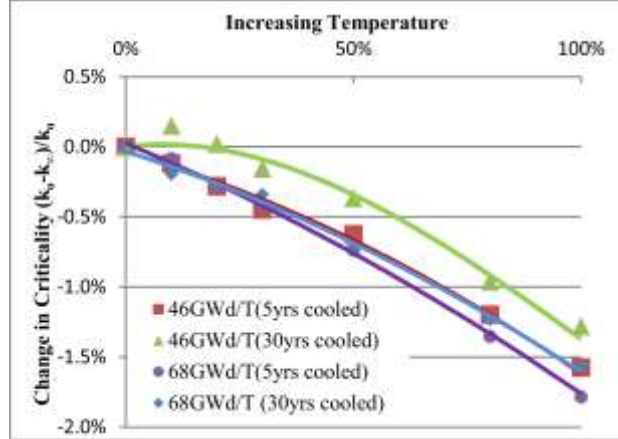
Figure 3.50 Moderator Temperature coefficient for MOX Assemblies at BOC (*fuels from reprocessed spent 46GWd/t UOX*)

The moderator temperature coefficient of all fuel cycles considered are desirable since the k_{∞} decreases with increasing moderator temperature. This increase in moderator temperature makes the core under moderated due the increase in energy of the lighter nuclides that cause moderation.
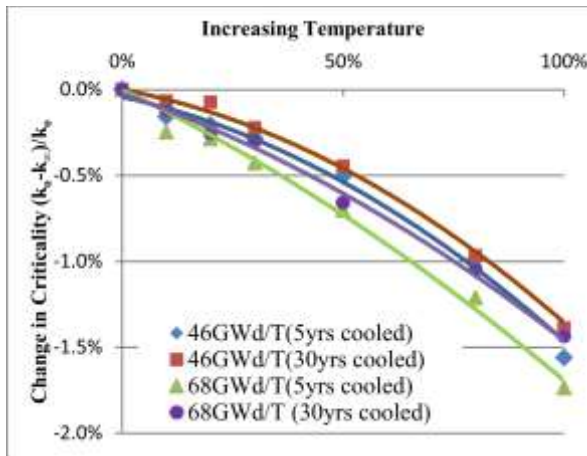
Figure 3.51 Moderator Temperature coefficient for MOX Assemblies at BOC (*fuels from reprocessed spent 68GWd/t UOX*)
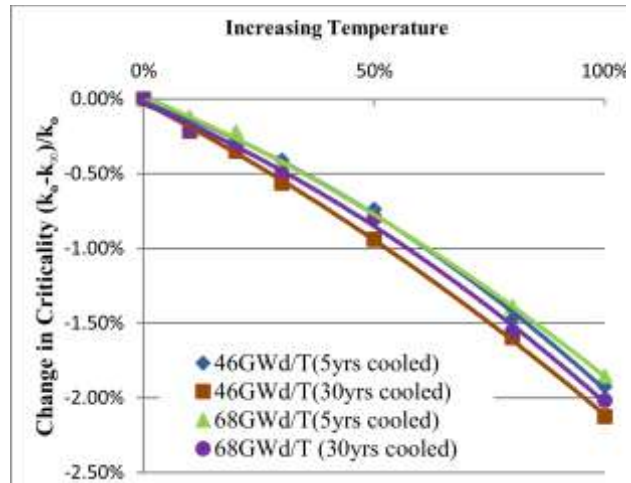
Figure 3.52 Moderator Temperature coefficient for MOXAm Assemblies at BOC (*fuels from reprocessed spent 46GWd/t UOX*)

If a reactor is under moderated, it will have a negative moderator temperature coefficient. If a reactor is over moderated, it will have a positive moderator temperature coefficient.
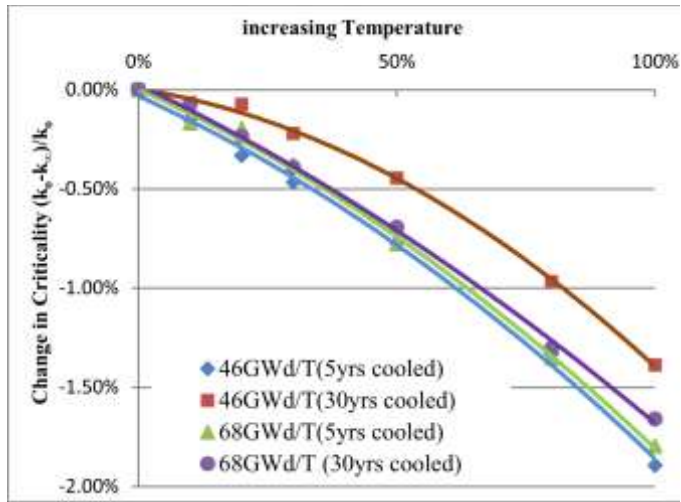
Figure 3.53 Moderator Temperature co-efficient for MOXAm Assemblies at BOC (*fuels from reprocessed spent 68GWd/t UOX*)

The MOX and MOXAm cycles showed better moderator temperature coefficient as compared to the once through cycle of the UOX. During moderator void or loss of coolant in the core, the moderator or coolant temperature tend to increase as well. The negative reactivity feedback of the moderator temperature coefficient tends to compliment the negative feedback of the Coolant Void Reactivity in the previous section.

3.5.3.2 Fuel Temperature Coefficient

Another temperature coefficient of reactivity, the fuel temperature coefficient, has a greater effect than the moderator temperature coefficient for some reactors. The fuel temperature coefficient is the change in reactivity per degree change in fuel temperature. This coefficient is also called the "prompt" temperature coefficient because an increase in reactor power causes an immediate change in fuel temperature, where the fission heat is generated before the extra energy is transferred to coolant. A negative fuel temperature coefficient is generally considered to be even more important than a negative moderator temperature coefficient because fuel temperature immediately increases following an increase in reactor power [69].
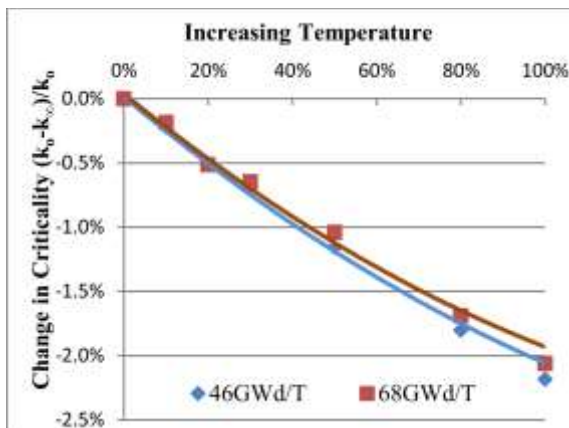
Figure 3.54 Fuel Temperature coefficient for UOX Assembly at BOC
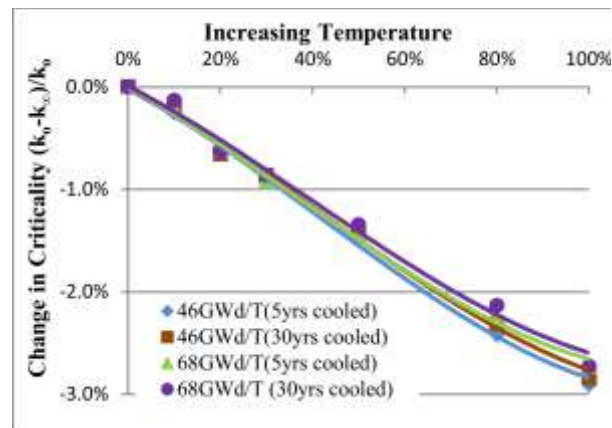
Figure 3.55 Fuel Temperature coefficient for MOX Assemblies at BOC (*fuels from reprocessed spent 46GWd/t UOX*)
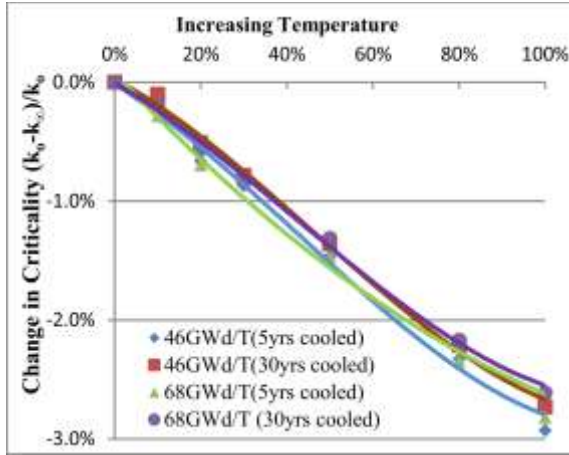
Figure 3.56 Fuel Temperature coefficient for MOX Assemblies at BOC (*fuels from reprocessed spent 68GWd/t UOX*)
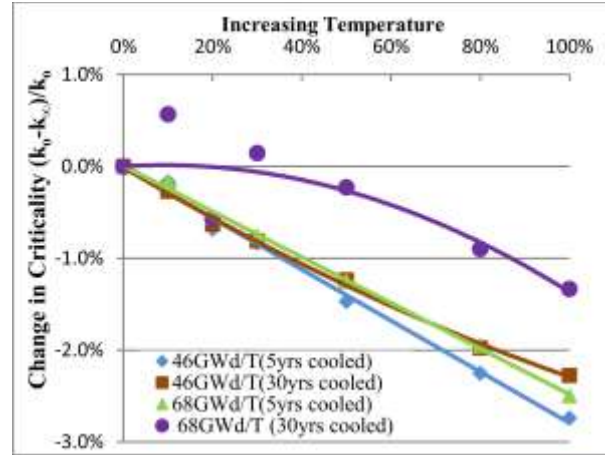
Figure 3.57 Fuel Temperature coefficient for MOXAm Assemblies at BOC (*fuels from reprocessed spent 46GWd/t UOX*)

It can be observed that all fuel show negative fuel temperature coefficient which is desirable for reactor operations. The time for heat to be transferred to the moderator is measured in seconds. In
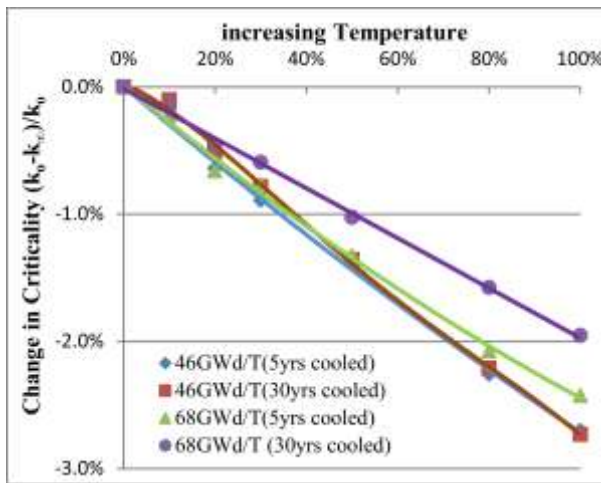
Figure 3.58 Fuel Temperature coefficient for MOXAm Assemblies at BOC (*fuels from reprocessed spent 68GWd/t UOX*)

the event of a large positive reactivity insertion, the moderator temperature cannot turn the power rise for several seconds, whereas the fuel temperature coefficient starts adding negative reactivity immediately. The fuel temperature coefficients simulated in these analyses is observed to be dependent on fuel quality. The 68GWd/t MOXAm fuel fabricated from 30years cooled spent UOX assemblies has the least performance in terms this safety inherent index. This fuel has the highest plutonium concentration and the highest

americium content at BOC due to the total decay of Pu-241, hence the worse fuel quality at BOC. However, due to the transmutation of americium and buildup of Pu-241 during core irradiation, this behavior is expected to change for a better index.

3.5.4 Doppler Broadening of U-238

Another name applied to the fuel temperature coefficient of reactivity is the fuel Doppler reactivity coefficient. This name is applied because in typical low enrichment, light water moderated, thermal reactors. Their fuel temperature coefficient of reactivity is negative and is the result of the Doppler Effect, also called Doppler broadening. The phenomenon of the Doppler Effect is caused by an apparent broadening of the resonances due to thermal motion of nuclei.

Stationary nuclei absorb only neutrons of energy a specific energy, say E_o. If the nucleus is moving away from the neutron, the velocity (and energy) of the neutron must be greater than E_o to undergo resonance absorption. Likewise, if the nucleus is moving toward the neutron, the neutron needs less energy than E_o to be absorbed. Raising the temperature causes the nuclei to vibrate more rapidly within their lattice structures, effectively broadening the energy range of neutrons that may be resonantly absorbed in the fuel. Two nuclides present in large amounts in the fuel of some reactors with large resonant peaks that dominate the Doppler Effect are uranium-238 and plutonium-240 [69].
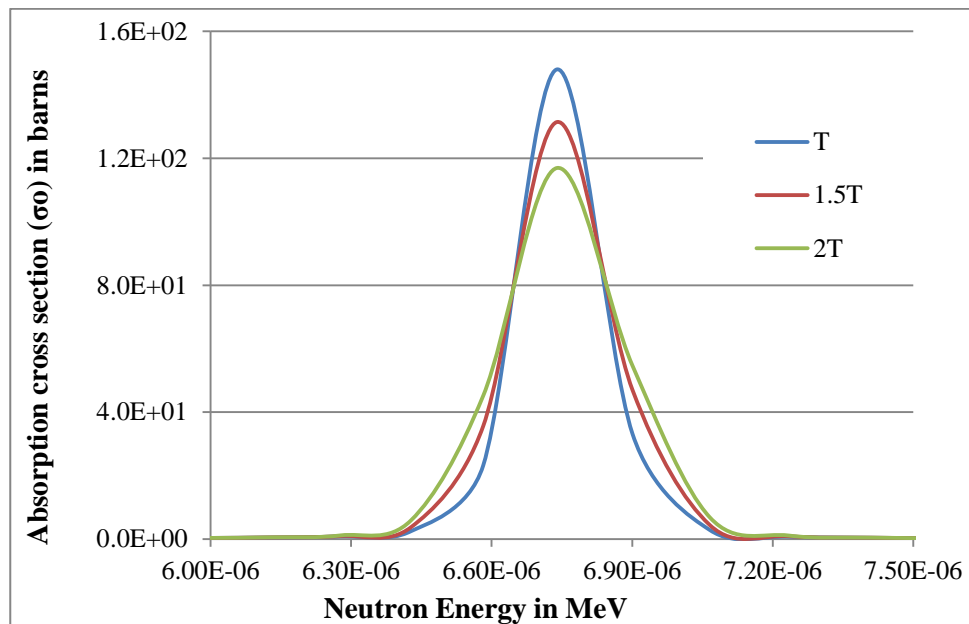
Figure 3.59 Doppler broadening in 46GWd/t UOX

The Doppler broadening effect is observed in the UOX fuel. As observed in Figure 3.59, increasing temperature increases the broadening of the U-238 peak. Since about 80% - 90% of the fuel fabricated in this work contains U-238, this effect is replicated in all these fuels. If Figure

3.59 is compared to Figure 3.60 and Figure 3.61, they look similar even though these simulations were done for MOX and MOXAm assemblies respectively.
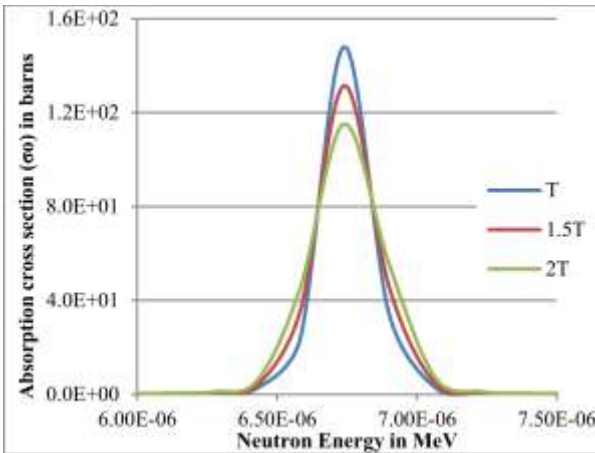
Figure 3.60 Doppler broadening in 46GWd/t MOX fuel
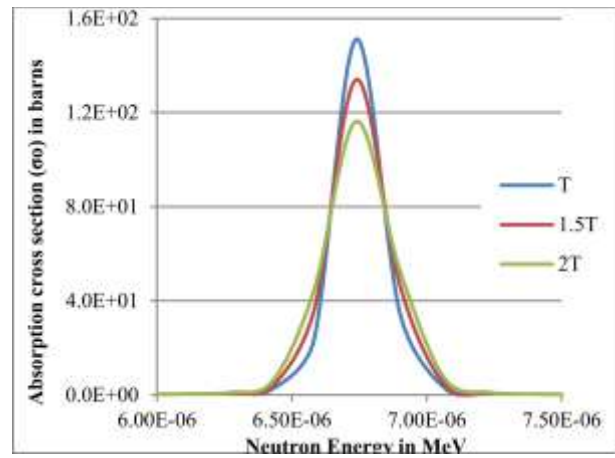
Figure 3.61 Doppler broadening in 46GWd/t MOXAm fuel

Hence the presence of americium in the fuel does not have any adverse effect on the Doppler broadening of the fuel. This effect of Doppler broadening is one of the factors responsible for the negative fuel temperature coefficient of the fuels recorded in Table 3.9.

CHAPTER FOUR

4 RESULTS OF CORE CONVERSION IN MNSR

4.1 BURNUP of MNSR

The neutron spectrum at BOC of both HEU and proposed LEU fuel pin of MNSR shown in Figure 4.1 shows variation in neutron flux distribution with respect energy. There are more resonance peaks in the LEU than the HEU with a high U-238 resonance peak of the LEU fuel due to high capture cross section at that energy. In view of this, the burnup analysis of both fuels is discussed in this section.
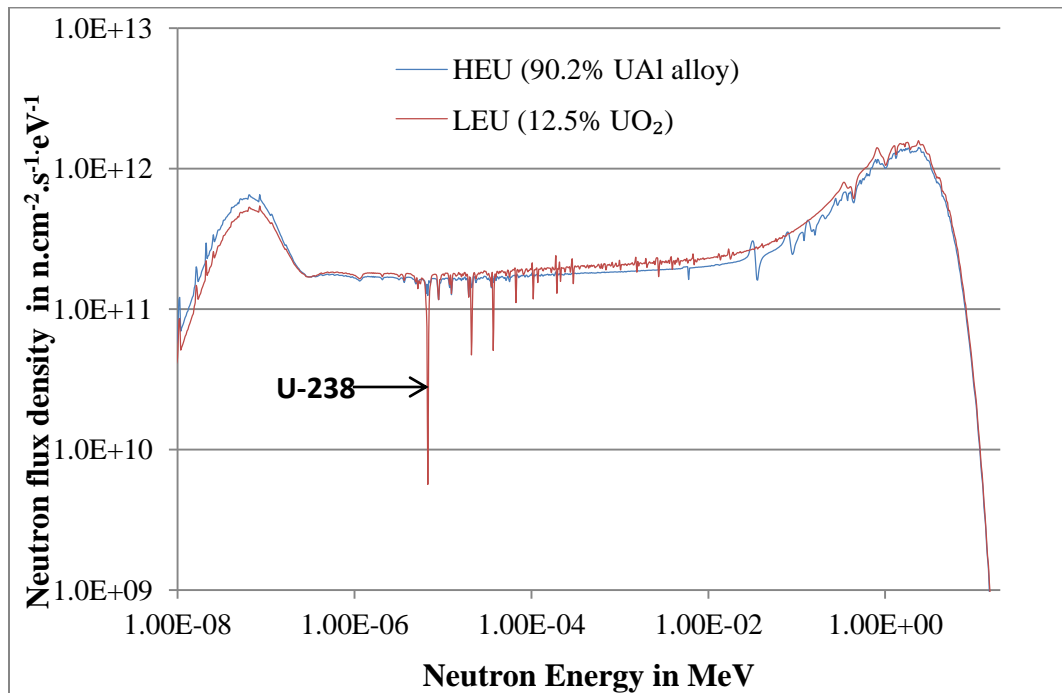
Figure 4.1 Neutron spectrum of HEU and proposed LEU cores of MNSR

4.1.1 Burnup of clean core of MNSR

The phrase clean core was adopted because this is the point where the research reactor nuclear chain reaction commences for the first time. The burnup of this clean core is investigated to estimate the duration of core operation before it first addition of beryllium reflectors in the shim tray.

In Figure 4.2, the burnup of the fresh clean is analyzed without reactivity regulators to estimate the lifetime before the addition of the first beryllium shim. It can be observed that the LEU clean core will operate longer than the HEU core at both half power and full power. The burnup curve of the cores without reactivity regulators and no beryllium in the shim tray obeys the quadratic burnup which gives an extension its operational life time of the cores. In Figure 4.2, the licensed operating reactivity of the core was not considered hence there were no reactivity regulators. In this mode, the proposed LEU core will operate up to a burnup of about 20GWd/t at thermal power and the HEU core has a burn of about 12GWd/t. It is expected that, the MNSR cores will have the same burnup at full power and at half power. However, Figure 4.2 shows some difference in their which can be attributed to fission product not reach equilibrium before reactor shutdown. At full power, the core lifetimes of the LEU and HEU cores before the first addition of beryllium in their shim tray are 1.8years and 1.2years respectively. However, this is cannot be since it core excess reactivity in this operational mode exceeds that of the licensed operational mode of 4mk.
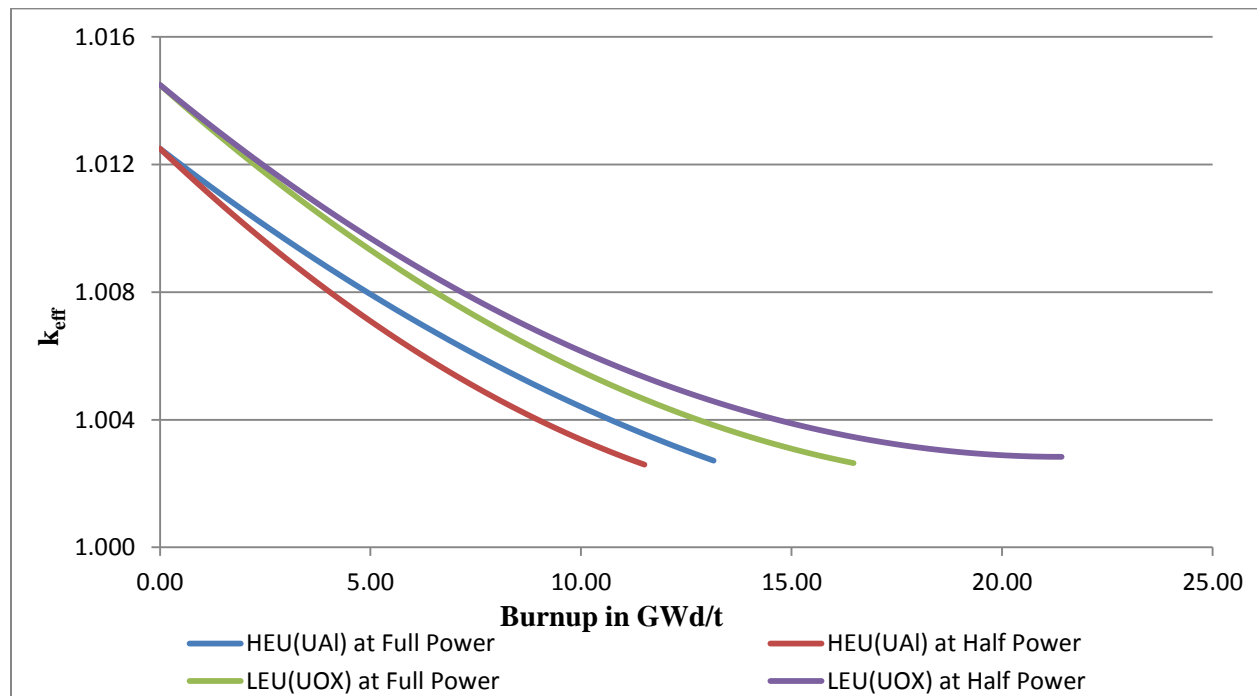
Figure 4.2 Burn up of fresh MNSR without reactivity regulators

In the subsequent simulations, the burnups were estimated taking into consideration the reactivity regulators of the HEU which has a reactivity worth of 7.5mk (i.e negative reactivity of -0.0075, using GHARR-1 as a case study). In Figure 4.3 and Figure 4.4, the burnup of the HEU

and LEU cores were simulated with the reactivity regulators, it was realized that core excess reactivity of the LEU MNSR does not reach the operational licensed excess reactivity of 4mk (i.e. k_{eff} = 1.004).
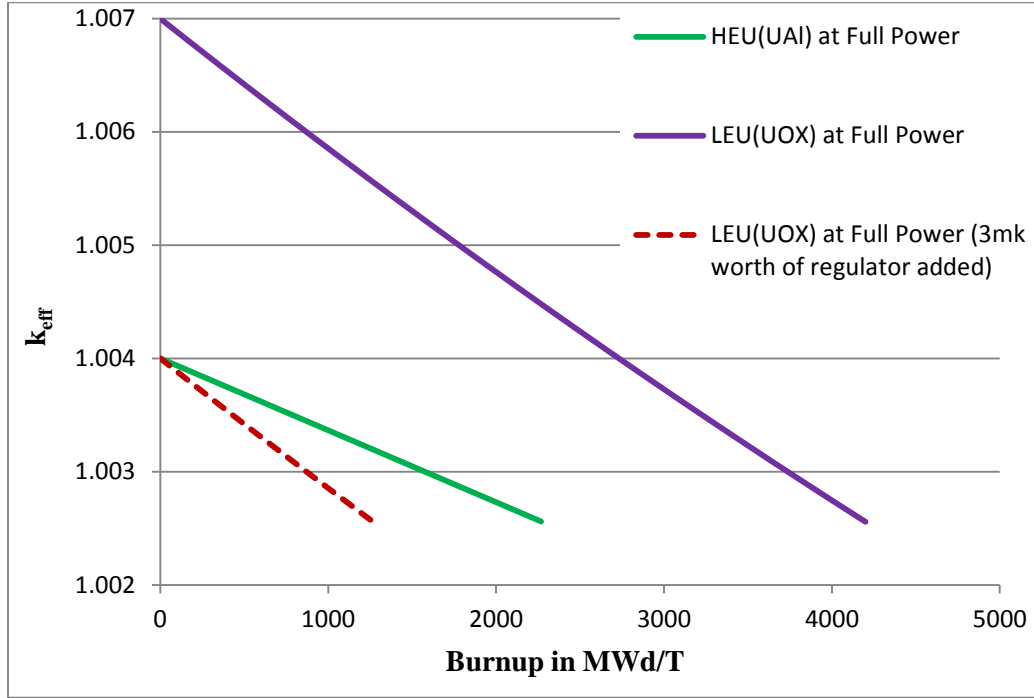
Figure 4.3 Burn up of fresh MNSR with reactivity regulators at full thermal power

In view of this, and additional negative reactivity of -3mk is needed for the LEU core excess reactivity to fall within the maximum licensed excess reactivity of 4mk. Figure 4.2 and Figure 4.3 show that, the addition of extra negative reactivity drastically reduces the core operational time of the LEU before the addition of it first beryllium shim. The burnup of both HEU and LEU cores indicates that, at simulated at full power of 30kW and 34kW respectively where the negative reactivity regulator worth of -7.5mk for the HEU and the proposed reactivity regulator worth of a -10.5mk for the LEU are incorporated, the LEU will undergo fuel management by addition of beryllium shim at an earlier time than the HEU.

If S_{CL} represents the simulated core life time in hours and W is the operational working hours/day then working core life time W_{CL} is expressed as;

$$W_{CL} = \frac{S_{CL}(hrs)}{W(hr/day) \times 365.25(days/yr)} \ years \qquad (4.1)$$

If f_{CL} represents the non-working core life time factor of the MNSR, then the total non-working core life time is expressed as;

$$f_{CL} = \frac{(M + H + \varpi)\, days\,/\, yr}{365.25\, days\,/\, yr} \tag{4.2}$$

where

M, H and ϖ represent maintenance days, holidays and weekend days respectively.

Hence the operational core lifetime of the MNSR is expressed as follows;

$$O_{CL} = \left\{ \left(f_{CL} \times W_{CL} \right) + W_{CL} \right\} = \left(f_{CL} + 1 \right) W_{CL} \quad years \tag{4.3}$$

The burnup of the HEU and LEU at full power is 2268MWd/T and 1263MWd/T. Considering the Xe-135 effect which causes a daily operation of 4hrs of the HEU at half power or 2hrs of the HEU at full power, 4days per week, and considering 60days of annual maintenance and public holidays. The operational core life before the addition of the first beryllium shim in years at full power for the HEU and LEU core are 3.96yrs and 2.64yrs respectively.

At half thermal power operational mode in figure 4.4, both cores have burnups of 1759MWd/T and 1644MWd/T for HEU and LEU respectively. Taking all the operational condition discussed above into consideration, this burnups give equivalent operational time of 3.06years and 2.87years for both HEU and LEU respectively at an EOC k_{eff} of 1.0026. Since the HEU core of GHARR-1 does not operate at its maximum 4hrs period at all time, but operates for between 1hr/day to 4hrs/day, for an average operational time of 2hrs/day, the core life before beryllium addition for the HEU is extended to 6.13 years.
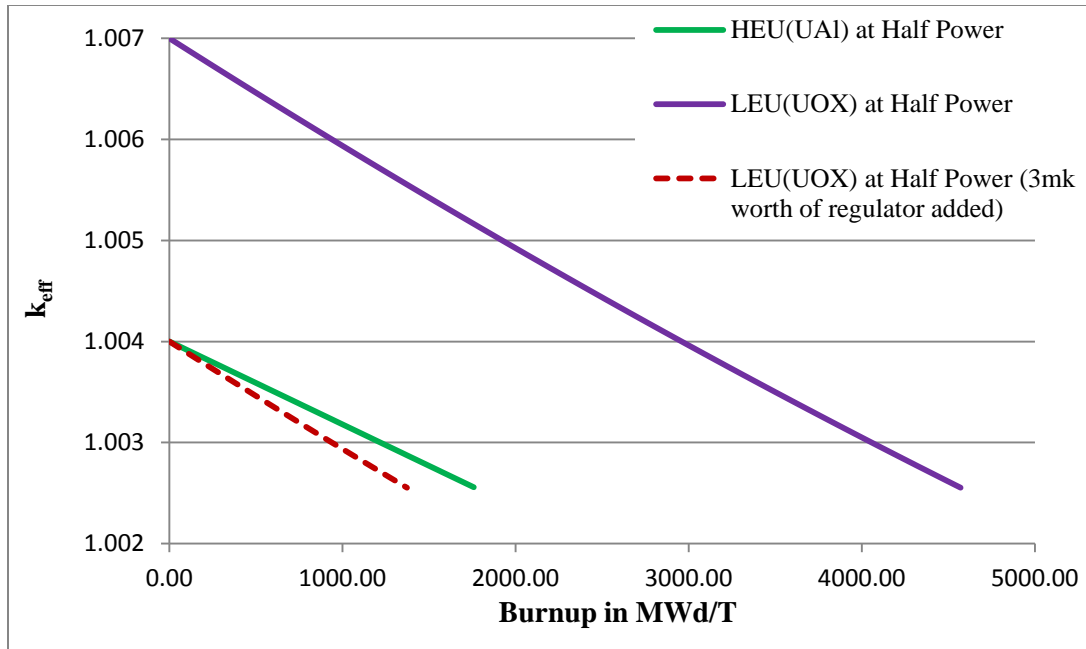
Figure 4.4 Burn up of fresh MNSR with reactivity regulators at half Power (thermal)

Javad Ebadati et al in 2006 reported 7 years for the Syrian MNSR [70]. This operational period are prone to change based on the extensive utilization of the MNSR and the number of non-operational days.

It can be concluded that, the proposed LEU core undergo the addition of beryllium in its tray for the first time at earlier time than the HEU when operated either in full thermal power or half thermal power mode.

4.1.2 Estimated Core Life Time of MNSR

In countries where there is an ongoing public discussion about a nuclear power phase-out, you often hear the phrase 'the life expectancy of the nuclear power plant'. Strictly speaking however, nuclear power stations do not have a fixed life expectancy. The initial design lifespan is usually 30 to 40 years. This is the figure used for the financial depreciation of the investment in the plant. However, nearly all elements in a nuclear power plant can be replaced except for the reactor vessel. This is consequently the crucial element in determining the true life expectancy of the plant.

In this work the life expectancy of the HEU and LEU MNSR core are calculated in various modes of power and fuel management and compared. The k_{eff} is at EOC was set at 1.0023 and

the operational time of the core is set as in section 4.1.1 in this chapter. These times were chosen based on the operational data of the GHARR-1 MNSR.

The total core life times of both the LEU and HEU cores were simulated without reactivity regulators fill up the 109mm shim tray of the reactor with beryllium. This was done to completely deplete the core in other not be able to sustain a meaningful chain reaction.
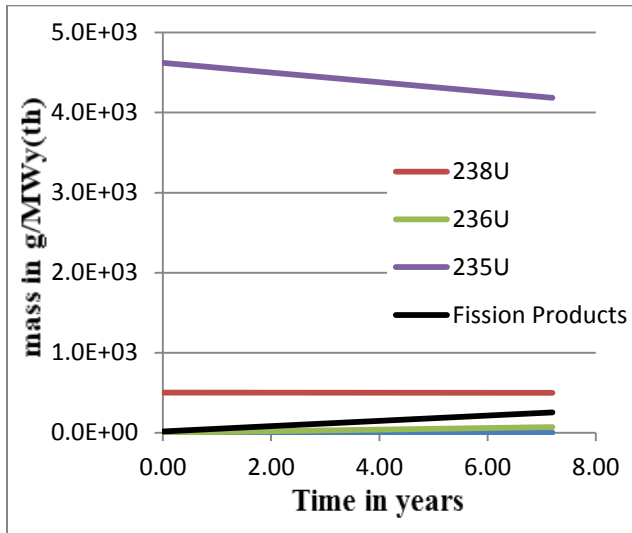
Figure 4.5 Fuel depletion of HEU core at full power
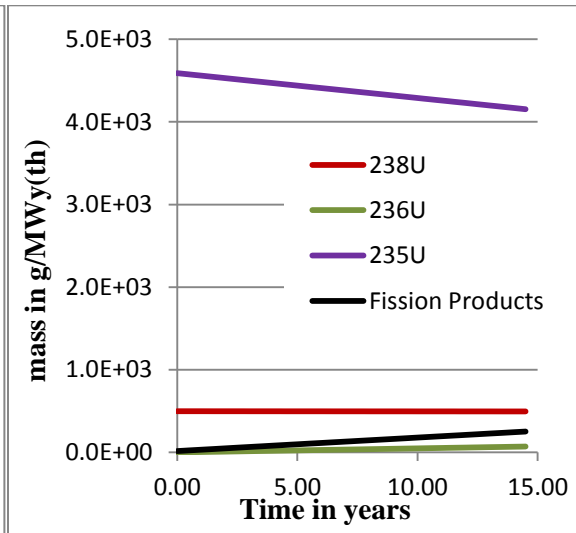
Figure 4.6 Fuel depletion of HEU core at half power
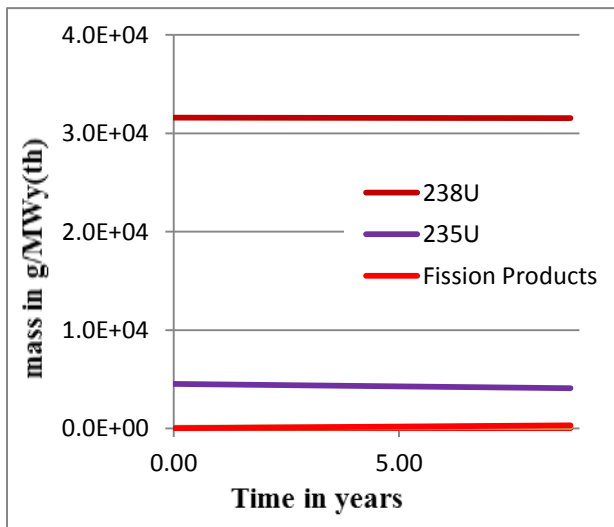
Figure 4.7 Fuel depletion of LEU core at full power
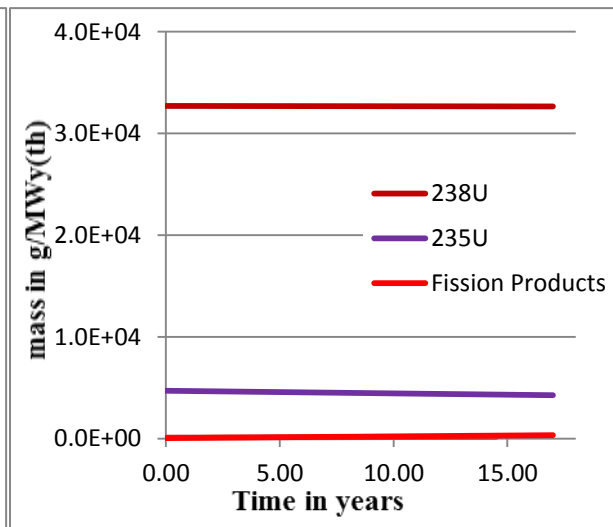
Figure 4.8 Fuel depletion of LEU core at half power

Operating both HEU and LEU continously at full or have power does not change the amount of uranium consumed. The Cosumption U-235 in the HEU core is at a higher rate since it domiates

the fuel uranium composition. The high core loading of the LEU provides enough U-235 to sustain the fission chain reaction. Massive uranium depletion is not observed in the LEU core. The production of neutron poisons such as neuton capturing U-236 and fission product are minimal in the LEU as compared to the HEU, (*see* Figure 4.5 to Figure 4.8).

The HEU and LEU core has identical burnup values over their total core life and thermal power as shown in fig. this makes the two cores quite identical in terms of energy dissipated over their corelifetime.
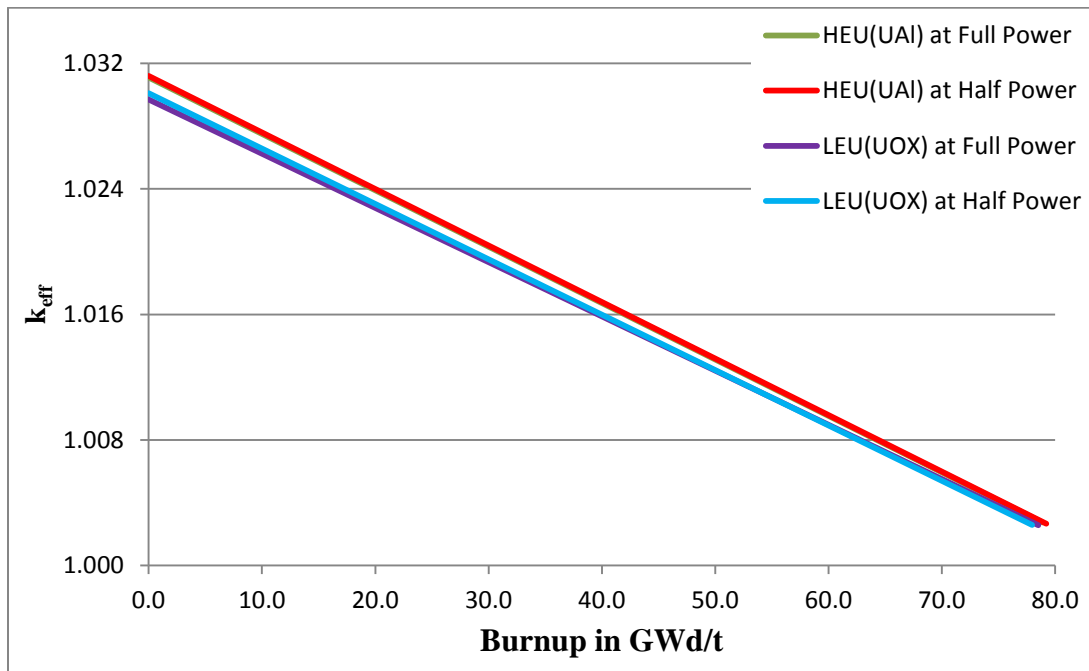
Figure 4.9 Burnup of HEU and LEU during core lifetime

However, the core lifetimes of both fuel vary based the rate of uranium consumption and core loading of both the HEU and the LEU. From Figure 4.3 and Figure 4.4, the LEU core will have it first beryllium top up in it shim earlier than the HEU core, but due to the core loading and lower rate of uranium consumption of the proposed LEU, the LEU core will stay longer in the containment than the HEU. The core burnup in years is shown in Figure 4.10.
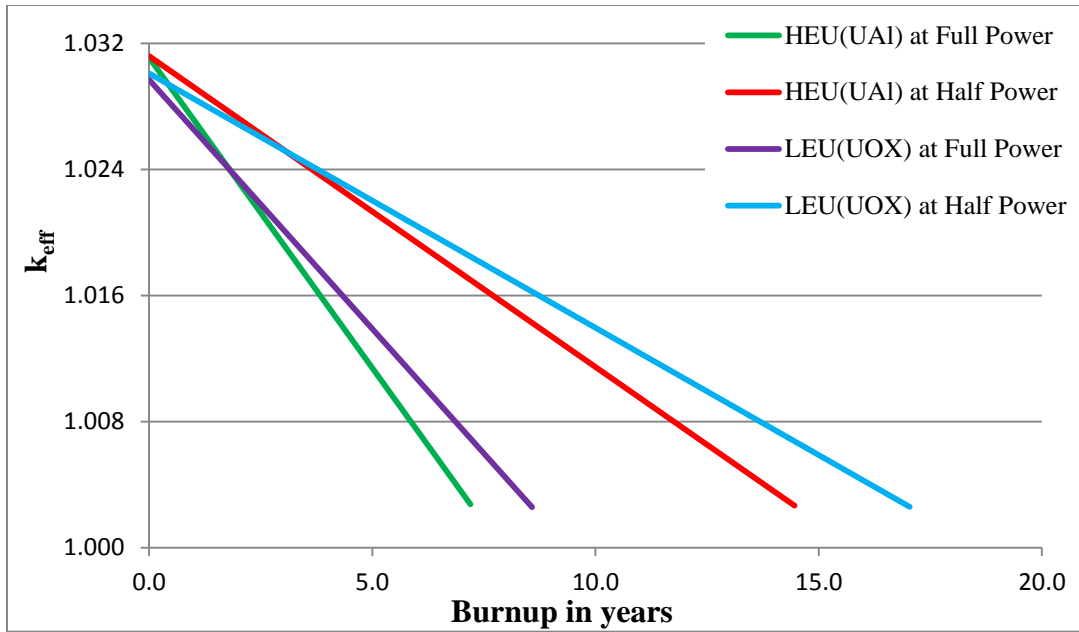
Figure 4.10 Core lifetime of HEU and proposed LEU MNSR

In both the half power and full power mode, figure to figure shows that the rate of uranium consumption does not change, hence the LEU core has higher core lifetime than HEU. Using the same operational assumption of 4hrs/day at half power and 2hrs/day at full power, the operational core lifetimes of the HEU and LEU at half power are shown in Table 4.1 below.

Table 4.1 The core lifetimes and estimated operational lifetimes of the HEU and proposed LEU core of the MNSR (2hr/d at full power and 4hr/d at half power)

MNSR Core Burnup	HEU Core (90.2% UAl fuel)				Proposed LEU Core (12.5% UOX fuel)			
	Simulated Core lifetime (days)		Operational Core Lifetime (years)		Simulated Core lifetime (days)		Operational Core Lifetime (years)	
	Half Power	*Full Power*	*Half Power*	*Full Power*	*Half Power*	*Full Power*	*Half Power*	*Full Power*
Addition of Beryllium Shim	117.2	75.6	3.06	3.96	109.6	50.4	2.87	2.64
Core Replacement	5.3×10^3	2.6×10^3	138.55	135.94	6.2×10^3	3.1×10^3	162.08	160.08

However, these values can either increase or decrease based on the utilization of the core. Some experiment analyses during the core lifetime may require operation in either half power or full power. Note that the operational hours per day is determined by Xe-135 production in the core

which dependent on the power of operation. In view of this, fuel consumption per day is partially constant in the MNSR which makes the operational core lifetime at both half power and full power the almost the same.

4.2 FLUX IN IRRADIATION CHANNELS

Research reactors are basically design to utilize their neutron flux, the MNSR is no exception. Since the MNSR is extensively used for neutron activation analysis which is technique to determine the quantitative and qualitative method of high efficiency for the precise determination of a number of main-components and trace elements in different types of geological, environmental and biological samples, knowledge of the expected neutron flux of the proposed LEU core of the MNSR would be very vital to scientists who utilize the irradiation channel neutron flux for their research.

Table 4.2 Average thermal neutron flux ration of MNSR irradiation channels

Irradiation Channels	Thermal Neutron flux ratio
$\dfrac{(Inner)_{LEU}}{(Inner)_{HEU}}$	0.963 ± 0.017
$\dfrac{(Outer)_{LEU}}{(Outer)_{HEU}}$	0.936 ± 0.0194
$\dfrac{(Outer)_{HEU}}{(Inner)_{HEU}}$	0.524 ± 0.017
$\dfrac{(Outer)_{LEU}}{(Inner)_{LEU}}$	0.567 ± 0.018

In Table 4.2, the average thermal neutron flux ratios, of both HEU and LEU irradiation channels are tabulated. Neutron energy range of $0.0001eV - 0.625eV$ tallies were simulated because 98% of thermal neutrons exist within this energy range, hence 0.625eV serves as an upper limit for thermal energy neutron [71]. Thermal neutrons are the main neutron energy group of concern in NAA. Almost half of the thermal neutrons flux in the inner irradiation of the HEU is found in the outer channel. This is comparable to what was reported my Sogbadji et al 2011 for the GHARR-

1 reactor which reported a ratio of 0.588 [9]. The LEU which shows similar thermal flux ratio has a reduction in neutron flux in both the inner channel and the outer of the proposed LEU core. This reduction can be seen to manifest itself as the inner and outer channels of the both the LEU and HEU cores are compared. The high amount of U-238 in the proposed LEU core is expected to capture some thermal neutron and higher energy neutron which would be moderated into the outer channel as thermal neutron. This has slightly decreased the thermal neutron flux both in the outer and inner irradiation channels of the proposed LEU MNSR which is vital for neutron activation analysis.

4.3 RADIOTOXICITY OF HEU AND LEU

The radiotoxicity of the HEU and LEU fuel are of importance to the backend of their fuel cycle. Currently, the HEU core would be replace with the LEU core, hence radiotoxicity of the HEU core needs to be investigated. However, most HEU cores in operation have not reached half of their core lifetime, the GHARR-1 HEU, which has only 9mm thickness of beryllium in its shim tray, is used as a reference case to compare the radiotoxicity of at its current burnup and after its core lifetime.
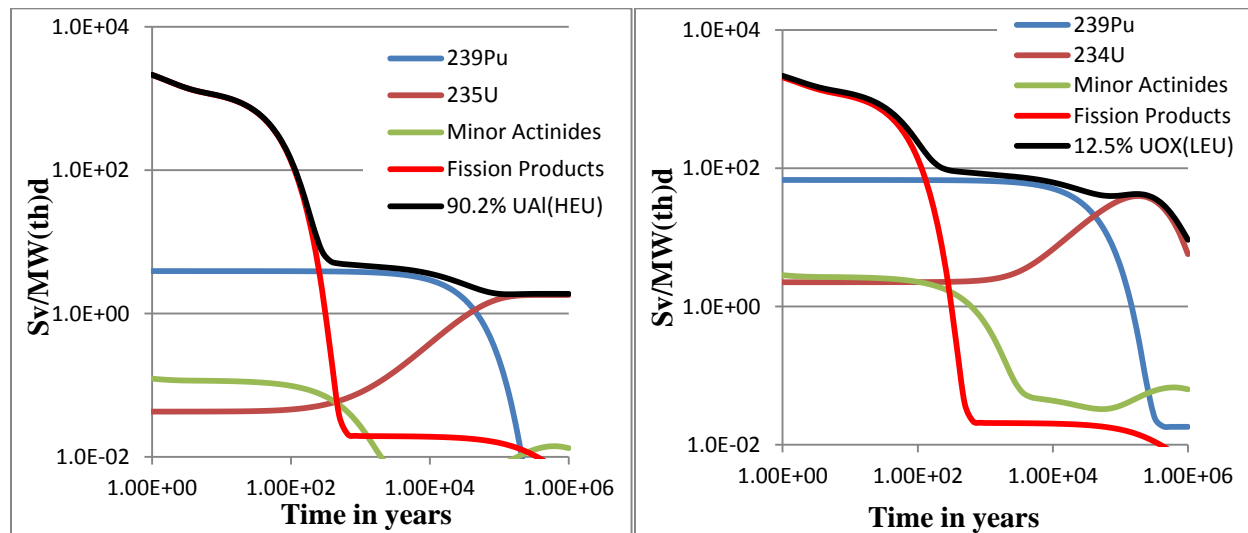
Figure 4.11 Radiotoxicity of HEU core after discharge   **Figure 4.12** Radiotoxicity of LEU core after discharge

Fission products, basically Cs-137, dominate the total radiotoxicity in both cores for the first 600yrs. Both HEU and LEU core seems to have similar amount fission products contribution the total radiotoxicity. Production of minor actinides in both the HEU and LEU cores do not have significant influence on their total radiotoxicity. Comparing Figure 4.11to Figure 4.12, the

production of Pu-239 is higher in the LEU core due to neutron capture on U-238 hence its contribution to total radiotoxicity to the spent LEU core is more than that of the HEU core.

In figure 4.13, the HEU core and the LEU core is compared to the current state of the GHARR-1 after discharge. Fission product are high in the current state of the GHARR-1 due to it relatively short burnup. Comparing the current state of the GHARR-1 to the spent HEU and LEU core, fission product in this GHARR-1 core has not fully accumulated as compared the whole core lifetime of the HEU core. In view of this, the current core of GHARR-1, when replaced, will have a lower radiotoxicity than both the HEU and LEU spent core at the end of their core life time. The current GHARR-1 core overtakes the spent HEU core after about 34,000 years in storage due to the radiotoxicity of the unutilized uranium in its spent fuel.
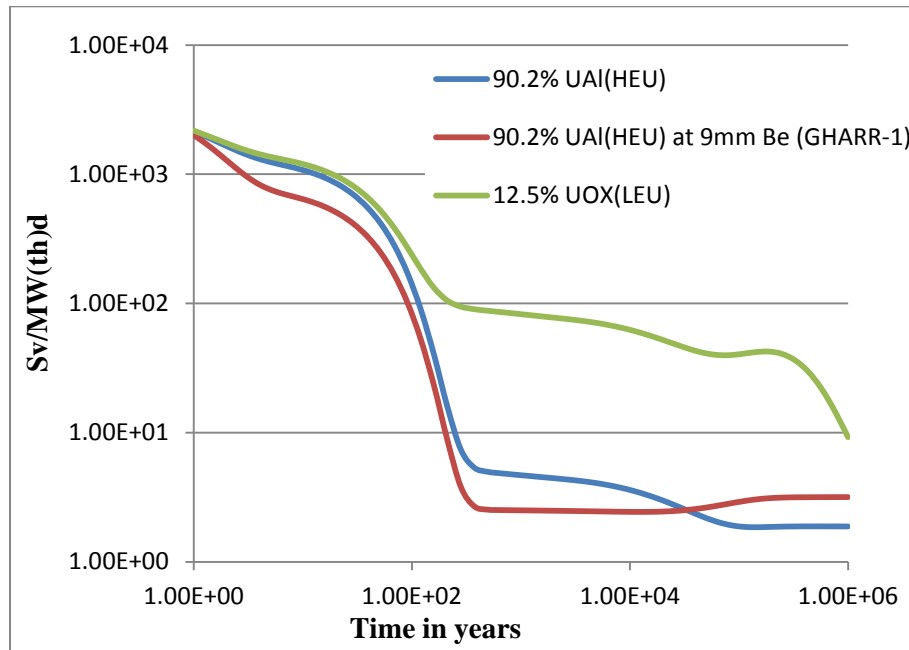
Figure 4.13 Comparison of radiotoxicity of proposed LEU, HEU and current state of GHARR-1 HEU core at discharge

The HEU and LEU core have the same radiotoxicity at discharge after approximately 80GWd/t, but the HEU spent core is dominated by fission product while the LEU spent core has higher contribution to its radiotoxicity form actinides after the decay of its fission product. This makes the LEU spent fuel to have a relative higher radiotoxicity after 100years of discharge.

4.4 SAFETY ANALYSIS

Safety analyses of reactors are not only necessary for new core designs but at every stage for the core life time of the reactor. This is necessary to assure the safety of the reactor operators, the public and the environment. The safety features of the LEU core are investigated vis-à-vis the HEU core in terms of Coolant Void Reactivity. The decay heat analysis, which is necessary for wet storage after shutdown and replacement of the HEU core is also analyzed to aid safety at the backend of the HEU cycle.

4.4.1 DECAY HEAT (AFTER SHUTDOWN)

The decay heat of the MNSR fuels for the first 50year after shutdown is totally dominated by fission products to the extent that the fission products contribution line in Figure 4.14 can hardly be seen. Ce-144 isotope is a major contributor to the decay heat for almost 2year after shutdown. Cs-137 also contributes to the decay heat but takes over the decay heat after approximately 2years in storage.
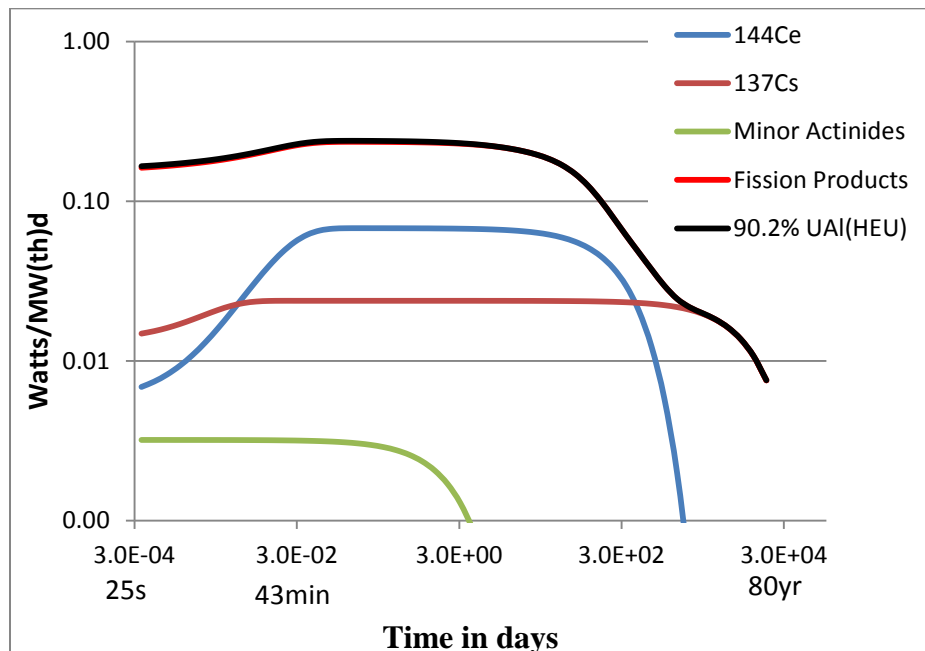
Figure 4.14 Decay heat of HEU core at shutdown after complete core burnup

Ce-144, which has a half-life of 284.9 days, has built up in the current HEU core of the MNSR more done at the end of its core lifetime and more the end of the core lifetime of the proposed LEU core. Therefore, the current HEU core dominates the decay heat after shutdown due to the β-decay of Ce-144 as shown in Figure 4.15.

However, the amount of Cs-137 present at EOC of the HEU and proposed LEU is higher than the current HEU, hence the decay heat of the current HEU lowers after significant decay of Ce-144. The proposed LEU and the HEU, when allowed to reach the end of their core lifetime would exhibit approximately the same amount of decay heat.
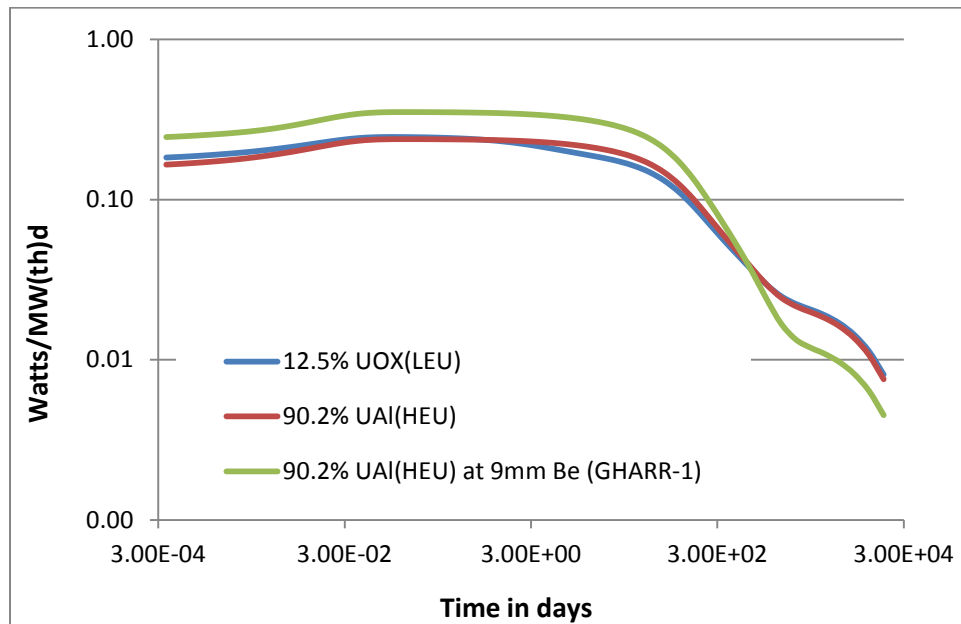
Figure 4.15 Comparison of decay heat of proposed LEU, HEU and current state of GHARR-1 HEU core after shutdown

4.4.2 Coolant Void Reactivity of MNSR

Coolant Void Reactivity, as discussed in chapter 3 is very important for investigation of safety inherent features of every reactor core. In this safety parameter simulation of the MNSR, the leakage term was included, hence change in k_{eff} is measured not k_{inf} as observed in the case of the PWR.
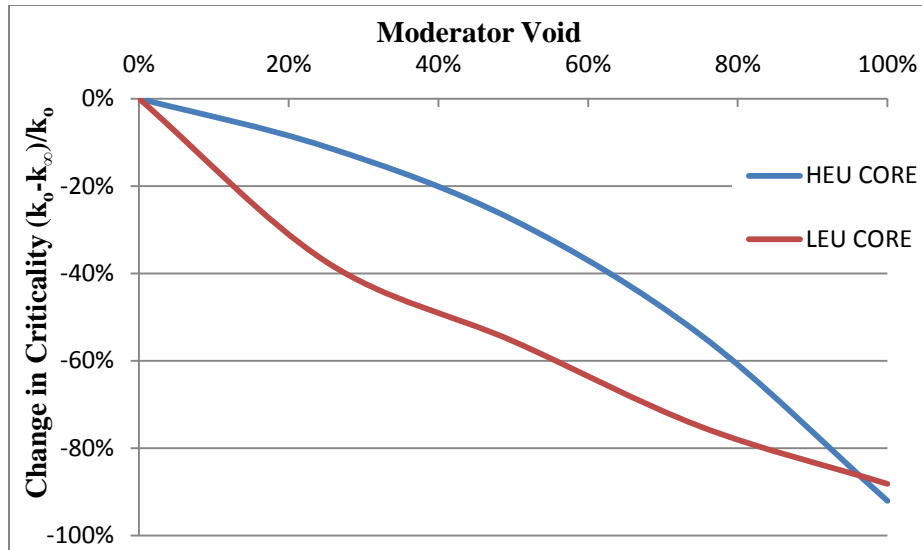
Figure 4.16 Coolant Void Reactivity of HEU and of Proposed LEU MNSR Core at BOC

A simulation of the Coolant Void Reactivity, which represents a void creation during boiling or accident scenario such as loss of coolant for both HEU and LEU, is shown in Figure 4.16. The figure above indicate negative void coefficient for both reactor cores.

However, the spectrum analyses of the MNSR cores at various moderator voids are quite different when compared to that of the PWR. In Figure 4.17 and Figure 4.18, the moderator void spectrum of the HEU and LEU cores are represented respectively.
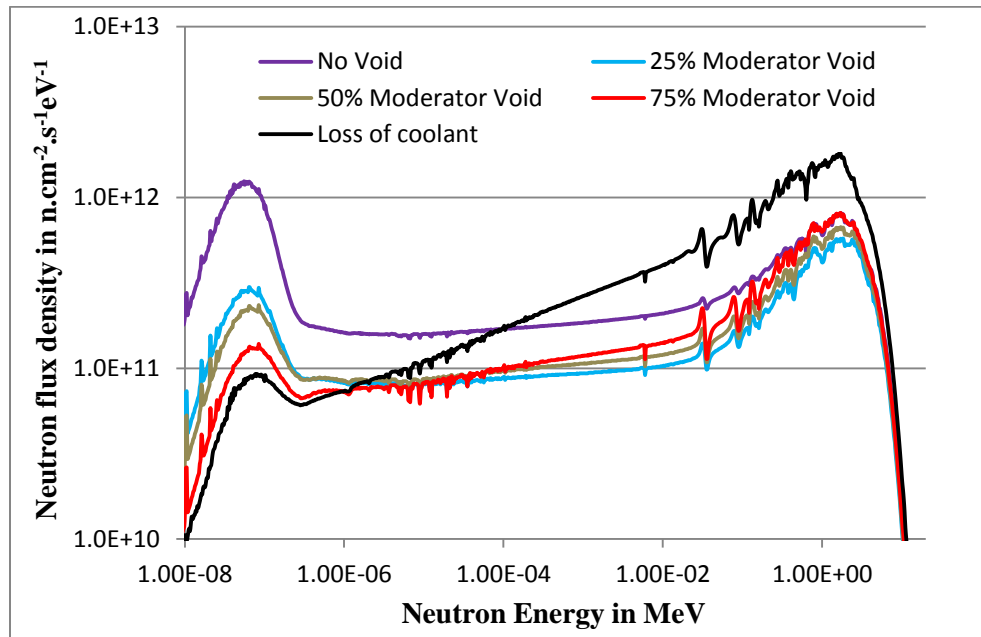
Figure 4.17 Neutron spectra of different percentage loss of Coolant of proposed HEU Core of MNSR

Due to the compact nature of the MNSR core, heavy moderation by means of water and beryllium reflector around and beneath the fuel pins is used. In view of this, moderation of fast neutrons to lower energy neutrons still continued at various moderator voids. Even at approximately 100% moderator void, there are still thermal neutrons present in the core to cause fission. This is possible due the presence of beryllium which is a moderating and a reflector material too.
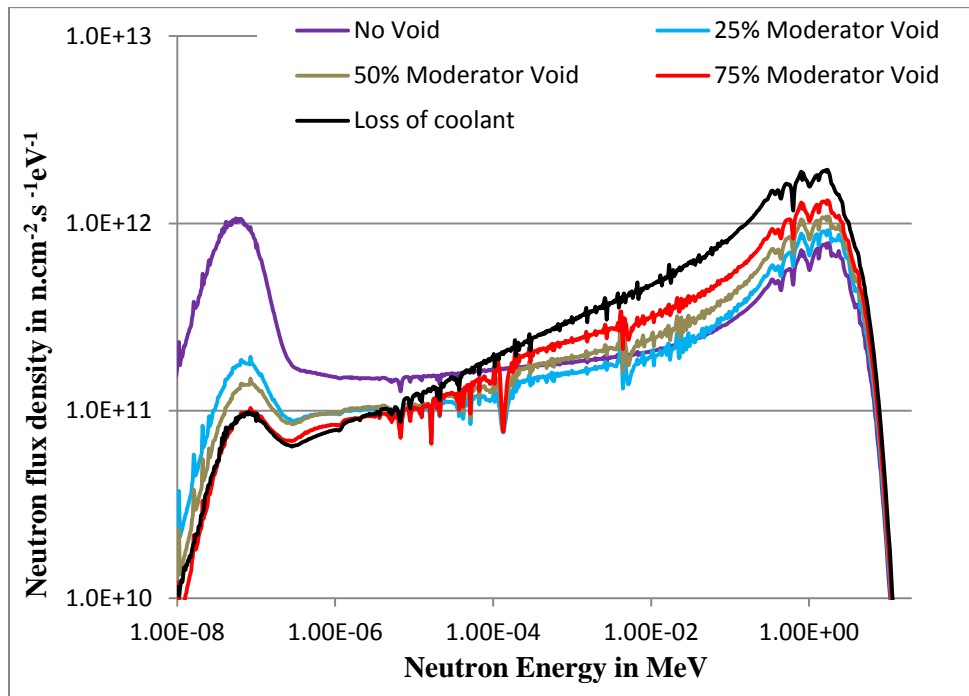
Figure 4.18 Neutron spectra of different percentage loss of Coolant of proposed LEU Core of MNSR

But Figure 4.16 indicated that thermal neutron fission present at loss of coolant is not enough to sustain a fission chain reaction. Hence the MNSR cores are inherently safe despite the presence of thermalisation of neutrons at loss of coolant.

4.4.3 TEMPERATURE COEFFICIENT

Fuel temperature coefficient which is essential to the safety inherent feature of a reactor is simulated for both HEU and LEU core of the MNSR. Fuel temperatures of both cores were simulated at 800K. Even though Figure 4.19 shows a partially no change of reactivity for the HEU core in terms of fuel temperature coefficient between 40% - 100% increase in fuel

temperature, the global value within the simulated temperature range is -5.12E-06Δk/K, this is quite desirable since a negative value is recorded.

The proposed LEU core however, shows a relative high change in reactivity of is -1.49E-05Δk/K within the simulated temperature. This is due to high percentage of the fuel consisting of U-238 which exhibits Doppler broadening as the fuel temperature increases, this characteristic of U-238 is shown in Figure 3.59. This phenomenon has increased the safety margin of the LEU core of the MNSR in terms of core fuel heating up in case of loss of coolant accident.
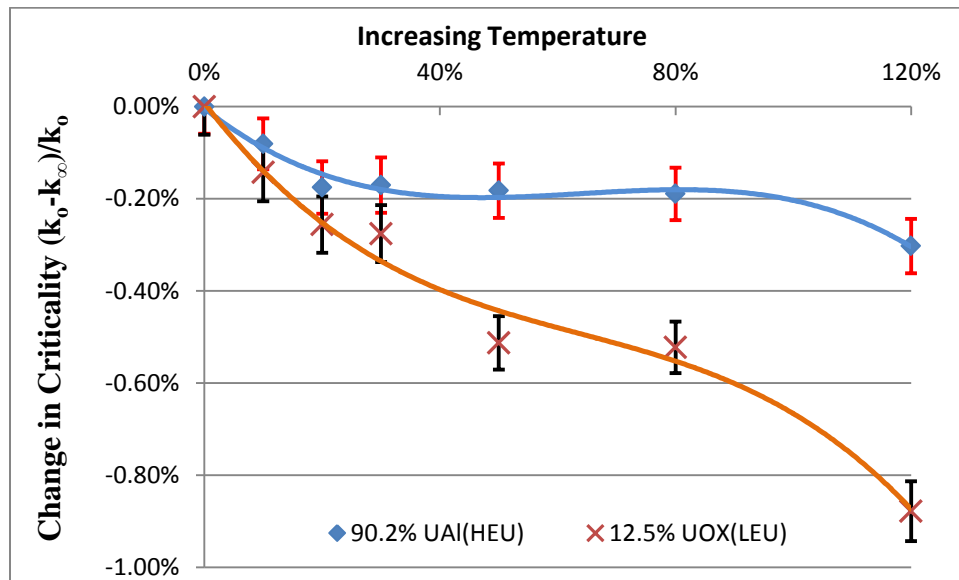
Figure 4.19 Fuel temperature coefficient of HEU and LEU MNSR fuels

The moderator temperature coefficient is simulated to see the effect of increase in moderator temperature on reactivity. Moderator temperatures of both cores were simulated at 500K. It can be observed that, the HEU core has a higher negative moderator temperature of -4.00E-05Δk/K to complement its low negative Coolant Void Reactivity.
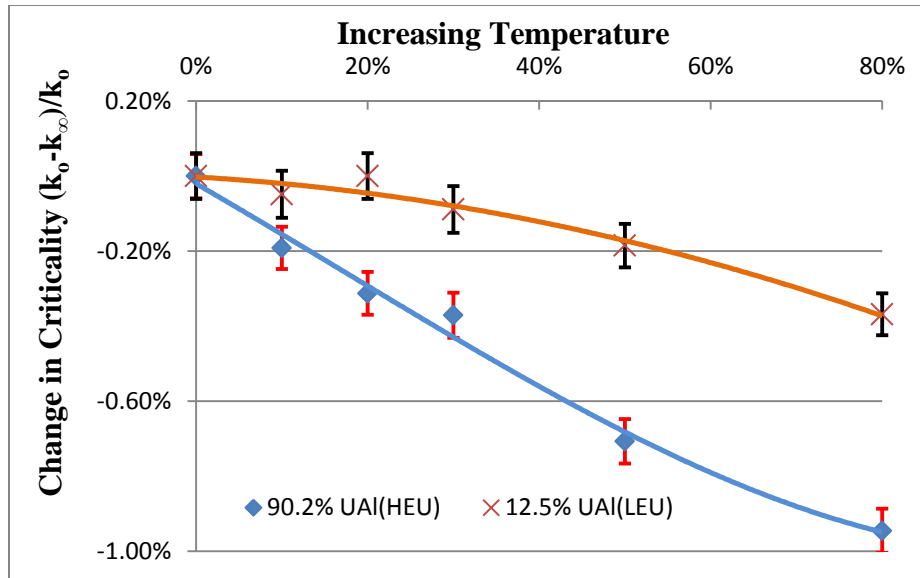
Figure 4.20 Moderator temperature coefficient of HEU and LEU MNSR fuels

On other hand an increase in moderator temperature of the LEU core does not significantly affect the core excess reactivity even though a global value of -9.35E-06Δk/K is recorded. This is due to the high amount of U-238 in the LEU fuel which tends to undergo fission with fast neutrons which dominate the core when moderator temperature increases which affects neutron moderation. However this value is expected to be more negative when coupled with increasing fuel temperature.

Since core heating is controlled by the fuel through fission, moderator temperature coefficient is not as appreciable to core safety as the fuel temperature coefficient. A negative moderator temperature coefficient is acceptable since the Coolant Void Reactivity will complement safety inherent feature of the moderator.

CHAPTER FIVE

5 CONCLUSION AND RECOMMENDATION

5.1 Mono-Recycling of Americium in PWR

The mono-recycling of americium is intended to reduce radiotoxicity in the UOX glasses which is bound for geological storage. Results show that, due to the high concentration of Pu in the MOXAm (mixture of PuO_2, UO_2 and AmO_2) fuel, which is due to americium poisoning of the fuel, the radiotoxicity of the MOXAm fuel from longer cooling time and longer burnup from the UOX cycle from which they were reprocessed from relatively maintain their radiotoxicity as compared to the open cycle from which they were fabricated from. However, this makes americium available for incineration (transmutation) when fast reactors become commercialized.

The decay heat of UOX glasses were also reduced due the extraction of Pu and Am from the UOX spent fuel. This will go a long way to reduce the size of the geological storage needed to permanently store these UOX glasses.

Irrespective of the cooling time, the americium impregnated MOX fuel (MOXAm) performed well in reducing the americium inventory in the MOXAm cycle as compared to the UOX once-through cycle from which they were fabricated from. The MOX (mixture of PuO_2 and UO_2) fuel cycle however, relatively maintain the mass of americium at the end of its core life-time.

All fuel types understudy in the PWR cycle showed good safety inherent feature with the exception of the some MOXAm assemblies which contained high amount of americium showed positive moderator void reactivity in specific configurations, which could not be consistent with basic safety features due to high Pu content in those fuel configurations, however their global void coefficient of the MOX fuels remain negative.

Since the MOXAm fuel is not intended for a whole core but to replace specific number of assemblies of the MOX and UOX core, it is recommended that neutronic study of a whole core of such mixed assembly core will complement this work. These results can be used as a guide to calculate the complete transmutation strategy of Am in the MOXAm fuel just as the Pu strategy used in the MOX fuel of the French PWR.

Complete safety analyses of the MOXAm fuel should be studied, in terms of thermal hydraulics, severe accident scenarios, loss of coolant and control rod efficiency due to the high amount of Pu needed in this type of fuel.

A generalized method can be developed to fix any cooling time and burnup of the UOX fuel need to fabricate the MOXAm fuel. This will make reduce the time of analyses for various scenarios.

The impact of the americium in the MOXAm fuel in terms of radiotoxicity and decay heat should be understudied at each stage of its nuclear cycle; such as transportation, reprocessing, fabrication.

5.2 Core Conversion of MNSR

Even though LEU core has a longer core life due to its higher core loading of Uranium-235 and production of fissionable plutonium, the LEU core will have its first beryllium top up to compensate for reactivity at earlier time than the HEU core. The HEU and LEU cores of the MNSR exhibited similar neutron flux ratios in the irradiation channels, however, there is a slight reduction in thermal neutron flux by a factor of 1.04 and 1.07 of both inner and outer irradiation channel of the proposed LEU MNSR respectively, as compared to the HEU MNSR.

LEU is more radiotoxic after fission product decay due to higher actinides presence in the fuel after its core lifetime. If the HEU core of the MNSR is to be replaced with the proposed LEU core at its current spent time of operation, the decay heat of the current HEU core will be higher than if it is allowed to reach its full core lifetime. In terms of void coefficient, both HEU and LEU core have negative void coefficients despite the presence of thermalisation of fast neutrons by the beryllium reflectors surrounding the MNSR core.

The current reactivity regulator would not be enough to have a safe shutdown margin for the LEU MNSR based on the operating license of the MNSR (see Figure 4.3 and Figure 4.4), it is recommended that the proposed LEU core should increase it control rod worth or reactivity regulators worth by a minimum of -3mk.

Coupled neutronic and thermal hydraulics analysis and severe accident scenarios such fuel clad damage of the new core is needed to update the safety analyses report of the LEU MNSR.

Furthermore, investigations to increase the thermal neutron flux of the irradiation channels of the LEU MNSR needs to be understudied.

BIBLIOGRAPHY

[1]   V. Carter, Advance Nuclear Physics, Chandni Chowk, Delhi: Global Media, ISBN: 9380168926, 2009.

[2]   J. R. Lamarsh and A. J. Baratta, Introduction to Nuclear Engineering, New Jersey 07458: Upper Saddle River, 2001, p. 389.

[3]   J. Cooper and R. Dooley, "Revised Release on Viscosity and Thermal Conductivity of Heavy Water Substance," in *International Association for the Properties of Water and Steam*, Lucerne, Switzerland , 2007.

[4]   S. Glasstone and A. Sesonske, Nuclear reactor engineering, New York, NY: Chapman & Hall, 1994.

[5]   J. J. Duderstadt and L. J. Hamilton, Nuclear Reactor Analysis, Wiley. ISBN04712236, 1076.

[6]   J.-L. PROVOST and M. DEBES, "MOX and UOX PWR Fuel Performances EDF Operating Experience," *Journal of NUCLEAR SCIENCE and TECHNOLOGY,* vol. 43, no. 9, p. 960–962, 2006.

[7]   H. Odoi, E. Akaho, S. Anim-Sampong, S. Jonah, B. Nyarko, R. Abrefah, E. Ampomah-Amoako, R. Sogbadji, I. Lawson, S. Birinkoranga, Y. Ibrahimc and J. Boffie, "Investigative studies on effect of reflector thickness on the performance of low," *Nuclear Engineering and Design,* vol. 241, no. doi:10.1016/j.nucengdes.2011.05.019, pp. 2902-2915, 2011.

[8]   R. Sogbadji, R. Abrefah, E. Ampomah-Amoako, S. Agbemava and B. Nyarko, "Neutron energy spectrum flux profile of Ghana's miniature neutron source reactor core," *Ann. Nucl. Energy,* vol. doi:10.1016/j.anucene.2011.04.017, 2011.

[9]   R. B. M. Sogbadji, B. J. B. Nyarko, A. E. H. K. and R. G. A. Abrefah, "Determination of Neutron Fluxes and Spectrum Shaping Factors in Irradiation Sites of Ghana's Miniature Neutron Source Reactor (mnsr) by Activation Method after Compensation of Loss of Excess Reactivty," *World Journal of Nuclear Science and Technology,* vol. 1, no. doi:10.4236/wjnst.2011.12009 Published Online July 2011, pp. 50-56, 2011.

[10] R. Sogbadji, B. Nyarko, E. Akaho and A. R.G., "Determination of thermal neutron cross-section and resonance integral for the 75As (n, γ)76As reaction by activation method using 55Mn (n, γ)56Mn as a monitor," *Nuclear Engineering and Design,* vol. 240, no.

doi:10.1016/j.nucengdes.2009.12.020 , pp. 980 - 984, 2010.

[11] Y. Serfor-Armah, B. J. B. Nyarko, S. B. Dampare and D. Adomako, "Levels of Arsenic and Antimony in Water and Sediment from Prestea, A Gold Mining Town in Ghana and its Environs," *EARTH AND ENVIRONMENTAL SCIENCE. WATER, AIR, & SOIL POLLUTION,* vol. 175, no. DOI: 10.1007/s11270-006-9127-9, pp. 181 - 192, 2006.

[12] H. Ahiamadjie, Y. Serfor-Armah, J. Tandoh, O. Gyampo, F. Ofosu, S. Dampare, D. Adotey and B. Nyarko, "Evaluation of trace elements contents in staple foodstuffs from the gold mining areas in southwestern part of Ghana using neutron activation analysis," *JOURNAL OF RADIOANALYTICAL AND NUCLEAR CHEMISTRY,* vol. 288, no. DOI: 10.1007/s10967-011-0979-0, pp. 653 - 661, 2011.

[13] R. G. Abrefah, D. K. Adotey, E. Mensimah, E. Ampomah-Amoako, R. B. M. Sogbadji and N. S. Opata, "Biomonitoring of Occupational Exposure to Total Arsenic and Total Mercury in Urine of Goldmine Workers in Southwestern Ghana," *Environmental Research, Engineering and Management,* vol. 2, no. 56, pp. 43 - 48, 2011.

[14] CNSC, "Science and Reactor Fundamentals - Reactor Physics," Technical Training Group, 2003, pp. 85, 111.

[15] S. M. Weston, "Fuel Reprocessing and Recycling," in *Nuclear Reactor Physics*, Weinheim, Wiley-VCH Verlag GmbH & Co., 2007, p. 223.

[16] J. Carlson, J. Bardsley, V. Bragin and J. Hill, "Plutonium Isotopics - Non-Proliferation And Safeguards Issues," Australian Safeguards Office, Canberra ACT, Australia IAEA-SM-351/64.

[17] R. A. Penneman and T. K. Keenan, The radiochemistry of americium and curium, Washington: Subcommittee on Radiochemistry, National Academy of Sciences-National Research Council : available from the Office of Technical Services, Dept. of Commerce , 1960.

[18] Hudson, M. J. et al, "The coordination chemistry of 1,2,4-triazinyl bipyridines with lanthanide(III) elements – implications for the partitioning of americium(III)," Dalton Trans. (9): 1675–1685. doi:10.1039/b301178j, 2003.

[19] C. Hill, D. Guillaneux, X. Hérès, N. Boubals and L. Ramain, "Sanex-BTP Process Development Studies," in *Scientific Research on the Back-end of the Fuel Cycle for the 21st Century. Commissariat à l'énergie atomique.*, Atalante, 24–26 October 2000.

[20] D. Magnusson, B. Christiansen, M. Foreman, A. Geist, J. Glatz, R. Malmbeck, G. Modolo, D. Serrano-Purroy and l. C. Sore, "Demonstration of a SANEX Process in Centrifugal Contactors using the CyMe4-BTBP Molecule on a Genuine Fuel Solution," *Solvent Extraction and Ion Exchange,* vol. 27, no. doi:10.1080/07366290802672204, p. 97, 2009.

[21] E. F. Westrum, Eyring and Leroy, "The Preparation and Some Properties of Americium Metal," *Journal of the American Chemical Society,* vol. 73, no. 7, doi:10.1021/ja01151a116, p. 3396, 1951.

[22] W. Wade, "Preparation and some properties of americium metal," *Journal of Inorganic and Nuclear Chemistry,* vol. 29, no. 10, doi:10.1016/0022-1902(67)80183-0, p. 2577, 1967.

[23] D. WESTLÉN, "Why Faster is Better - On Minor Actinide Transmutation in Hard Neutron Spectra," in *Doctoral Thesis*, Stockholm, Sweden, KTH School of Engineering Sciences, 2007, p. 37.

[24] ICRP Publication 72, "Age dependent doses to members of the public from intake of radionuclides," in *Part 5 - compilation of ingestion and inhalation dose coefficient*, Annals of the ICRP, 26:1, 1996.

[25] M. L. Adams and E. W. Larsen, "Fast iterative methods for discrete-ordinates particle transport calculations," *Prog. Nucl. Energy,* vol. 40, p. 3, 2002.

[26] D. G. Cacuci, Handbook of Nuclear Engineering, LLC 233 Spring Street, New York, NY 10013, USA: Springer Science+BusinessMedia,, 2010.

[27] L. L. Carter and E. D. Cashwell, Particle transport simulation with the Monte Carlo method, TID-26607, National Technical Information Service, U.S. Department of Commerce, 1975.

[28] X-5 Monte Carlo Team, "MCNP – a general Monte Carlo N-particle transport code, Version 5," in *LA-UR-03-1987* , Los Alamos National Laboratory, 2003.

[29] R. Sanchez and N. McCormick, "A review of neutron transport approximations," *Nucl Sci Eng,* vol. 80, p. 481, 1982.

[30] A. Haghighat and J. Wagner, "Monte Carlo variance reduction with deterministic importance functions," *Prog Nucl Energy,* vol. 42, p. 25, 2003.

[31] H. P. Smith and J. C. Wagner, "A case study in manual and automated Monte Carlo variance reduction with a deep penetration reactor shielding problem," *Nucl Sci Eng,* vol. 149, p. 23, 2005.

[32] Wolters, E.R. et al, "A hybrid Monte Carlo-S2 method for preserving neutron transport effects. In: Proceedings of the 2009 international conference on advances in mathematics, computational methods, and reactor physics," Saratoga Springs, New York, 3 – 7 May, 2009.

[33] J. Yang and E. Larsen, "Application of the "functional Monte Carlo" method to estimate continuous energy k-eigenvalues and eigenfunctions.," in *Proceedings of the 2009 international conference on advances in mathematics, computational methods, and reactor physics*, Saratoga Springs, New York, 3 – 7 May 2009.

[34] X-5 Monte Carlo Team, "MCNP — A General Monte Carlo N-Particle Transport Code, Version 5," in *LA-UR-03-1987*, Los Alamos National Laboratory, 2008.

[35] Rose, P. F. Compiler and Editor, "ENDF-201, ENDF/B-VI Summary Documentation," in *BNL-NCS-17541, Brookhaven National Laboratory*, October 1991.

[36] Frankle, S. C. et al, "ACTI An MCNP Data Library for Prompt Gamma-ray Spectroscopy," in *12th Biennial Radiation Protection and Shielding Topical Meeting*, Santa Fe, NM, April 15-19, 2002.

[37] Howerton, R. J. et al, "The LLL Evaluated Nuclear Data Library (ENDL): Evaluation Techniques, Reaction Index, and Descriptions of Individual Reactions," *Lawrence Livermore National Laboratory report UCRL-50400,* Vols. 15, Part A, September 1975.

[38] Cullen, D. E. et al, "Tables and Graphs of Photon Interaction Cross Sections from 10 eV to 100 GeV Derived from the LLNL Evaluated Photon Data Library (EPDL)," *Lawrence Livermore National Laboratory report UCRL-50400,* Vols. 6, Rev. 4, Part A: Z = 1 to 50 and Part B: Z = 51 to 100, 1989.

[39] Gardner, M. A. et al, "ACTL: Evaluated Neutron Activation Cross–Section Library-Evaluation Techniques and Reaction Index," *Lawrence Livermore National Laboratory report UCRL-50400,* vol. 18, October 1978.

[40] Arthur, E. D. et al, "New Tungsten Isotope Evaluations for Neutron Energies Between 0.1 and 20 MeV," *Trans. Am. Nucl. Soc.,* vol. 39, no. 793, 1981.

[41] R. E. MacFarlane and D. W. Muir, "The NJOY Nuclear Data Processing System Version 91," *Los Alamos National Laboratory report LA-12740-M,* October 1994.

[42] Brizi and Julie, Cycles uranium et thorium en réacteurs à neutrons rapides refroidis au sodium. Aspects neutroniques et déchets associés, Orsay, France: Thèse de doctorat,

Université Paris XI, Octobre 2010.

[43] O. Méplan, "MCNP Utility for Reactor Evolution. MURE User Guide – Version, 1.0.," Report LPSC 0912 and IPNO-09-01, Janvier 2009.

[44] F. MICHEL-SENDIS, Contributions à l'étude de la production d'233U en combustible MOX-ThPu en réacteur à eau sous pression.Scénarios de transition vers des concepts isogénérateurs Th/233U en spectre thermique. Développement du code MURE d'évolution du combustible., Orsay: Thèse de doctorat, Université Paris XI, 2006.

[45] O. Méplan, J. Wilson, A. Bidaud, S. David, N. Capellan and a. et, "MURE,MCNP Utility for Reactor Evolution, User Guide - Version 1.0," 2009, pp. 73-74.

[46] J. Hendricks, G. McKinney, H. Trellue, J. Durkee, T. Roberts, H. Egdorf, J. Finch, M.L.Fensin, M.R.James, D.B.Pelowitz and L. Waters, "MCNPX version 2.6.A," Los Alamos National Laboratory report LA-UR-05-8225, 2005.

[47] H. Trellue and D. Poston, "User's Manual, version 2.0 for MONTEBURNS, version 5B," Los Alamos National Laboratory report LA-UR-99-4999, 1999.

[48] "SCALE," in *A Modular Code System for Performing Standardized Computer Analyses for Licensing Evaluations*, ORNL/TM-2005/39, 2006, pp. Version 5.1, Vols. I-III.

[49] R. S. Babcock, D. E. Wessol, C. A. Wemple and S. C. Mason, "The MOCUP Interface: A Coupled Monte Carlo/Depletion System," in *Topical Meeting on Advances in Reactor Physics*, Knoxville, TN, April 11-14, 1994.

[50] J. Cetnar, W. Gudowski and J. Wallenius, "MCB: A continuous energy Monte Carlo Burnup simulation code," in *Actinides and Fission Product Partitioning and Transmutation*, EUR 18898 EN, OECD/NEA, 1999, p. 523.

[51] W. Haeck and B. Verboomen, "An optimum Approach to Monte Carlo Burn-Up," *Nucl. Sci. Eng.,* vol. 156, pp. 180-196, 2007.

[52] N. Capellan, Couplage 3D neutronique thermohydraulique. Développement d'outils pour les études de sûreté des réacteurs innovants., Orsay: Thèse de doctorat en science, Université Paris XI, november 2009.

[53] O. Méplan et al, "Coupled Monte Carlo transport with fuel burnup calculation," in *MCNP Utility for Reactor Evolution*, Data Bank Computer Program Services, OECD Nuclear Energy Agency, http://www.oecd-nea.org/tools/abstract/detail/nea-1845, 2009.

[54] H. W. J. Graves, "Nuclear Fuel Management," New York, Wiley, 1979, pp. 269,143.

[55] G. T. Parks, "TECHNICAL NOTE, A PIECEWlSE LINEAR REACTIVITY FUEL-CYCLE MODEL," *Annals of Nuclear Energy,* vol. 16, no. 8, pp. 417-422, 1989.

[56] G. T. Parks and J. D. Lewins, "QUADRATIC REACTIVITY FUEL-CYCLE MODEL STABILITY," *Annals of Nuclear Energy,* vol. 14, no. 3, pp. 145 - 151, 1987.

[57] T. Jevremovic, Nuclear Principles in Engineering, Second edition, USA: Purdue University School of Nuclear Engineering West Lafayette IN 47907-1290, 2009.

[58] S. I, "Lectures given at the Workshop on Nuclear Data and Nuclear Reactors: Physics, Design and Safety, Trieste," in *Long term radiotoxicity*, Cadarache, France, Department of Reactor Physics, 13 March -14 April 2000, p. 789.

[59] P. ADELFANG and I. N. GOLDMAN, "LATEST IAEA ACTIVITIES RELATED TO RESEARCH REACTOR CONVERSION AND FUEL RETURN PROGRAMMES," Nuclear Fuel Cycle and Materials Section, Division of Nuclear Fuel Cycle and Waste Technology, Vienna, Austria, 2005.

[60] E. Boafo, E. Akaho, B. Nyarko, S. Birikorang and G. Quashigah, "Fuel burnup calculation for HEU and LEU cores of Ghana MNSR," *Annals of Nuclear Energy,* vol. 44, no. doi.10.1016/j.anucene.2011.12.027, pp. 65-70, 2012.

[61] S. T. Massoud, "Nuclear Reactor Materials and Fuels," pp. 128,777,785, 1992.

[62] Office of Civilian Radioactive Waste Management, "Source of Burnup Values for Commercial Spent Nuclear Fuel Assemblies," US. Department of Energy, 2004.

[63] World Nuclear Association, "The Nuclear fuel Cycle," http://www.world-nuclear.org/info/inf03.html, 2011.

[64] T. K. Jagdish, Nuclear wallet cards, National Nuclear Data Center, April, 2005.

[65] J. S. Choi, C. K. Lee and B. B. Ebbinghaus, "Effects of Plutonium Quality on Critical Mass," in *American Nuclear Society Winter Meeting and Nuclear Technology Expo*, Washington DC, United States, November 14 - 18, 2004.

[66] E. L. Elmer, in *Fundamentals of Nuclear Reactor Physics*, 2008, pp. 258, 259.

[67] B. S. Lee, M. J. Sin, Y. H. Kim, W. S. Park and T. Y. Song, in *8th Int. Information Exchange Meeting on Actinide and Fission Product Partitioning and Transmutation*

(OECD/NEA, 2004.

[68] Ž. Gašper, R. Matjaž, S. Luka and K. Marjan, "Isotopic Composition and Decay Heat Calculations of Spent Nuclear Fuel from Krško NPP," in *Nuclear Energy for New Europe*, Portoroz, Slovenia, September 8 -11, 2008.

[69] DOE-HDBK-1019/2-93, "Reactor Theory (Nuclear Parameters)," in *DOE FUNDAMENTALS HANDBOOK NUCLEAR PHYSICS AND REACTOR THEORY*, Washington, D.C. 20585, Volume 2 of 2 U.S. Department of Energy FSC-6910 , 1993.

[70] J. Ebadati, M. Rezvanifard and I. Shahabi, "Calculation and Experiment of Adding Top Beryllium Shims for Iran MNSR," in *14th International Conference on Nuclear Engineering (ICONE14)* , Miami, Florida, USA, July 17–20, 2006 .

[71] J. Weinman, Monte Carlo Cross Section TestinP for Thermal and Intermediate 235U/238U Critical Assemblies, ENDFB-V vs ENDF/B-VI, SCHENECTADY, NEW YORK 12421: KAPL ATOMIC POWER LABORATORY, June 1997.

[72] E. Nichita, "Reactor Physics," University of Ontario Institute of Technology, pp. 120, 147, 173.

[73] South Australian Chamber of Mines and Energy, "The Back End of the Nuclear Fuel Cycle," http://www.uraniumsa.org/fuel_cycle/back_end_nfc.htm, 2001.

TABLE OF FIGURES

TABLE OF TABLES

SYNTHESE EN FRANÇAIS

TITRE: NEUTRONIC STUDY OF THE MONO-RECYCLING OF AMERICIUM IN PWR AND OF THE CORE CONVERSION IN MNSR USING THE MURE CODE

RÉSUMÉ

Le code MURE est basé sur le couplage d'un code Monte Carlo statique et le calcul de l'évolution pendant l'irradiation et les différentes périodes du cycle (refroidissement, fabrication). Le code MURE est ici utilisé pour analyser deux différentes questions : le mono-recyclage de l'Am dans les réacteurs français de type REP et la conversion du cœur du MNSR (Miniature Neutron Source Reactor) au Ghana d'un combustible à uranium hautement enrichi (HEU) vers un combustible faiblement enrichi (LEU), dans le cadre de la lutte contre la prolifération. Dans les deux cas, une comparaison détaillée est menée sur les taux d'irradiation et les radiotoxicités induites (combustibles usés, déchets). Le combustible UOX envisagé est enrichi de telle sorte qu'il atteigne un taux d'irradiation de 46 GWj/t et 68 GWj/t. Le combustible UOX usé est retraité, et le retraitement standard consiste à séparer le plutonium afin de fabriquer un combustible MOX sur base d'uranium appauvri. La concentration du Pu dans le MOX est déterminée pour atteindre un taux d'irradiation du MOX de 46 et 68 GWj/t. L'impact du temps de refroidissement de l'UOX usé est étudié (5 à 30 ans), afin de quantifier l'impact de la disparition du ^{241}PU (fissile) par décroissance radioactive (T=14,3 ans). Un refroidissement de 30 ans demande à augmenter la teneur en Pu dans le MOX. L'241Am, avec une durée de vie de 432 ans, jour un rôle important dans le dimensionnement du site de stockage des déchets vitrifiés et dans leur radiotoxicité à long terme. Il est le candidat principal à la transmutation, et nous envisageons donc son recyclage dans le MOX, avec le plutonium. Cette stratégie permet de minimiser la puissance résiduelle et la radiotoxicité des verres, en laissant l'Am disponible dans les MOX usés pour une transmutation éventuelle future dans les réacteurs rapides. Nous avons étudié l'impact neutronique d'un tel recyclage. Le temps de refroidissement de l'UOX est encore plus sensible ici car l'241Am recyclé est un fort poison neutronique qui dégrade les performances du combustible (taux d'irradiation, coefficients de vide et de température). Néanmoins, à l'exception de quelques configurations, le recyclage de l'Am ne dégrade pas les coefficients de sûreté de base. Le réacteur MNSR du Ghana fonctionne aujourd'hui avec de l'uranium enrichi à 90,2% (HEU), et nous étudions ici la possibilité de le faire fonctionner avec de l'uranium enrichi à 12,5%, en passant d'un combustible sur base d'aluminium à un oxyde. Les simulations ont été menées avec le code MURE, et montrent que le cœur LEU peut-être irradié plus longtemps, mais demande d'intervenir plus tôt sur le pilotage en jouant sur la quantité de béryllium en cœur. Les flux de neutrons dans les canaux d'irradiation sont similaires pour les cœurs HEU et LEU, de même pour les coefficients de vide. Le combustible LEU usé présente cependant une radiotoxicité et une chaleur résiduelle plus élevée, du fait de la production plus importante de transuraniens pendant l'irradiation.

MOTS CLES: MURE; mono-recyclage; américium; plutonium; UOX; MOX; radiotoxicité; burnup; REP; MNSR; temps de refroidissement; durée de vie du cœur; HEU; LEU; méthode Monte Carlo; sûreté combustible nucléaire, déchets nucléaires.

INTRODUCTION

Le cycle du combustible représente la progression du combustible le long d'une chaîne comportant plusieurs étapes. L'amont du cycle consiste en la préparation du combustible (de la mine au réacteur), la période de service concerne la présence en réacteur, et l'aval du cycle concerne le retraitement, l'entreposage et le stockage des différentes matières (combustibles usés, déchets, …). Si le combustible usé n'est pas retraité, le cycle est appelé « cycle ouvert », ou « once-through », et le « cycle fermé » se réfère au cas où le combustible est multi-recyclé. Dans ce travail, on considère le cycle semi fermé français : le combustible UOX usé est retraité, séparé, de telle sorte que le plutonium est ré-utilisé sous forme de combustible MOX.

Deux types de réacteurs sont ici considérés.
1/ le mono-recyclage de l'américium issu des combustibles UOX usés des REP. Actuellement, tous les combustibles usés des REP sont d'abord entreposés dans des piscines de refroidissement près des centrales. Après quelques années de refroidissement, le combustible doit être transporté vers une usine de retraitement ou un centre de stockage pour les pays fonctionnant en cycle ouvert. Le retraitement est pratiqué en France et d'autres pays, et le stockage direct es combustibles usés, dans le cas du cycle ouvert, comme aux USA ou en Suède, n'a pas encore eu lieu. Dans les unités de retraitement, le combustible usé est séparé en trois parties : uranium, plutonium, qui peuvent être tout deux recyclés dans les REP, et les déchets contenant les produits de fission et les actinides mineurs (Np, Am, Cm). Le plutonium est recyclé sous forme de combustible MOX, sur une base d'uranium appauvri. Les déchets sont vitrifiés dans des colis destinés au stockage géologique. Enfin, les éléments de structure, dont les gaines, sont compactés et constituent les déchets de moyenne activité à vie longue. L'241Am contenu dans les verres est produit essentiellement pendant la période de refroidissement avant retraitement, par décroissance du 241Pu. L'241Am est responsable d'une puissance résiduelle élevée sur des périodes intermédiaires (100-500 ans), et influence fortement le dimensionnement du site de stockage géologique. Il serait donc intéressant de séparer l'américium du combustible usé afin de réduire la charge thermique des verres et leur radiotoxicité à long terme. L'uranium retraité peut quant à lui être ré-enrichi afin de produire un nouveau combustible, utilisable directement dans les REP. En France, environ 30% de l'uranium de retraitement est ainsi ré-utilisé, et alimente deux à trois réacteurs.
2/ Le MNSR (Miniature Neutron Source Reactor) au Ghana est spécifiquement conçu pour l'activation par flux de neutrons et la production d'isotopes. Beaucoup de réacteurs nucléaires sont utilisés pour la recherche et l'enseignement, et comme usine à neutrons pour des tests de matériaux sous irradiation ou production d'isotopes pour la médecine ou l'industrie. Ils sont plus petits que les réacteurs électrogènes, et beaucoup se trouvent sur des campus universitaires. Il y a environ 240 réacteurs de cette sorte dans le monde, répartis dans 56 pays. Certains fonctionnent avec de l'uranium hautement enrichi, et de nombreuses initiatives internationales incitent à les convertir à l'uranium faiblement enrichi, c'est-à-dire à moins de 20% en 235U. Depuis 1978, de nombreuses activités internationales concernant cette transition du combustible HEU au LEU, avec pour but ultime de faire disparaitre l'utilisation civile de l'uranium hautement enrichi. Mettre en place la conversion de tous les réacteurs du type MNSR serait un pas important dans cette direction.

OUTILS D'ANALYSE ET MÉTHODOLOGIE

Ce travail se concentre sur la simulation du combustible pendant le cycle : irradiation en Coeur, refroidissement, séparation et fabrication. Le comportement des neutrons dans le cœur est régi par l'équation de Boltzmann, qui peut être résolue analytiquement pour des problèmes très simplifiés. Pour ce travail, nous utilisons la méthode Monte Carlo pour calculer la neutronique d'un assemblage, grâce au code MCNP. Le code MURE (Monte Carlo Utility for Reactor Evolution) est écrit en C++, en programmation objet, et permet une grande flexibilité dans son utilisation. Nous l'utilisons pour calculer l'évolution du combustible pendant l'irradiation. La méthode Monte Carlo décrit le comportement d'une réacteur d'un point de vue statique. Le code MURE utilise alors les résultats de la simulation Monte Carlo statique pour calculer l'évolution du combustible pendant un temps donné. L'utilisateur choisit de recalculer les paramètres neutroniques du cœur régulièrement pour prendre en compte l'évolution du spectre de neutrons pendant l'irradiation. Ainsi, un calcul d'évolution est une succession de calculs Monte Carlo statiques et de calculs d'évolution. MURE contient une interface graphique qui permet d'analyser les résultats obtenus.

Le principe de la méthode Monte Carlo permet de traiter les sections efficaces neutroniques de façon continue en fonction de l'énergie. Entre deux interactions, l'énergie du neutrons ne change pas, et sa contribution au flux moyen dans le cellule considérée est donnée par $\frac{l(E)}{V}$, où l est la distance parcourue par le neutron entre ces deux interactions et V le volume de la cellule. Dans chaque cellule, le code Monte Carlo estime le flux intégré sur l'énergie, de même que le taux de réaction intégré sur l'énergie, toutes ces grandeurs étant normalisées par neutron de fission, on a donc, en appelant k me nombres de « parcours » neutroniques dans la cellule :

$$\Phi_c = \frac{1}{N_s} \frac{\sum_k l(E_k)\omega}{V} \qquad (4)$$

où is ω est le poids associés au neutron.

Les grandeurs fournies par MCNP doivent être normalisée par l'utilisateur afin de simuler la puissance souhaitée. Si ϕ^j est le flux fourni par MCNP, normalize par neutron de fission, on peut définir la puissance de l'assemblage normalisée par neutron de fission, note P_{MCNP}. Dans la pratique, on souhaite simuler une puissance de réacteur constante, et on doit donc renormaliser le flux fourni par MCNP. Le facteur de normalisation, noté α, est donné par

$$\alpha \equiv \frac{P_{user}}{1.6 \times 10^{-19} P_{MNCP}} = \frac{P_{user}}{1.6 \times 10^{-19} \sum_j \sum_i N_i^j \sigma_i^j \phi_{MCNP}^j \xi} \qquad (5)$$

où P_{user} est la puissance fixée par l'utilisateur, N_i^j le nombre de noyau i présents dans la cellule j. σ_i^j est la section efficace moyenne de fission du noyau I dans la cellule j. ϕ_{MCNP}^j est le flux fourni par MCNP dans la cellule j, et ξ est l'énergie moyenne délivrée par une fission du noyau i (~200 MeV).

Evolution des noyaux.
Le code MURE construit un arbre des noyaux qui consiste en un réseau de liens entre les noyaux voisins, représentant les réactions de décroissances et les réactions neutroniques. L'évolution est

calculée en résolvant les équations de Bateman entre deux calculs MCNP successifs. Dans chaque cellule évoluante, l'évolution des noayux est régie par :

$$\frac{dN_i}{dt} = \underbrace{-\sigma_i^{abs}\Phi N_i + \sum_{j \neq i} \sigma_{j \rightarrow i}\Phi N_j}_{reaction} \underbrace{- \lambda_i N_i + \sum_j \lambda_{j \rightarrow i} N_j}_{decay} \qquad (6)$$

où N_i est le nombre de noyaux *i*. $\sigma_i^{abs}\Phi$ le taux d'absorption moyen du noyau *i*, $\Phi\sigma_{j \rightarrow i}$ le taux de reaction produisant le noyau I à partir d'une reaction neutronique sur le noyau j, λ_i la constante de décroissance du noyau *i* et $\lambda_{j \rightarrow i}$ la constant de décroissance du noyau j qui produit I (et qui prend en compte les différents taux de branchement). Les deux premiers termes correspondent aux réactions neutroniques (capture, fission), et les deux derniers aux décroissances naturelles. A cause de l'évolution de la composition du combustible, le spectre en énergie évolue avec le temps, et les sections efficaces moyennes changent également. Il faut donc plutôt écrire les équation de Bateman sous la forme

$$\frac{dN_i}{dt} = \underbrace{-\sigma_i^{abs}(t)\Phi(t) N_i + \sum_{j \neq i} \sigma_{j \rightarrow i}(t)\Phi(t) N_j}_{reaction} \underbrace{- \lambda_i N_i + \sum_j \lambda_{j \rightarrow i} N_j}_{decay} \qquad (7)$$

Les sections efficaces moyennées sur le spectre neutronique sont calculées par MCNP :

$$\overline{\sigma_{x,i}} = \frac{\int \sigma_{x,i}(E)\phi(E)dE}{\int \phi(E)dE} \qquad (8)$$

x et *i* représentent le type de la réaction considérée et le noyau. L'intégration se fait sur toute la gamme en énergie (<20 MEV)
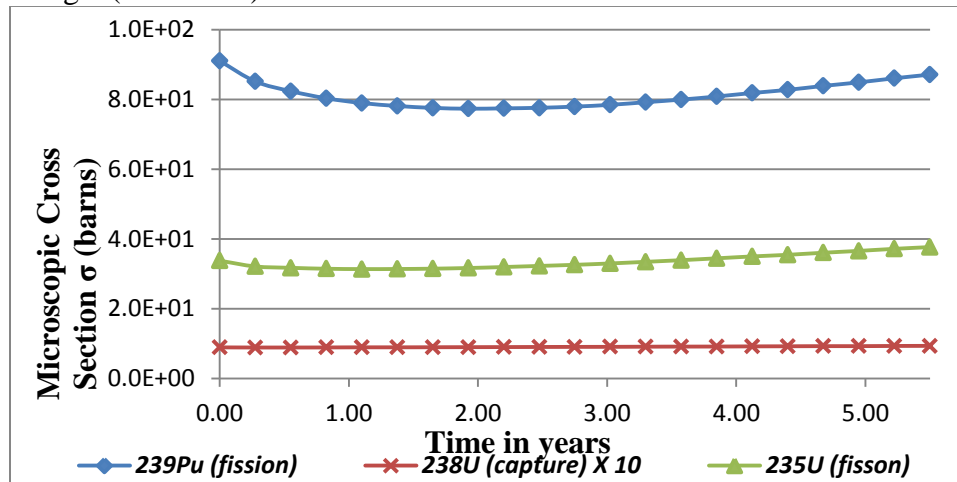
Figure 21 Evolution des sections efficaces microscopiques lors de l'évolution d'un combustible UOX jusqu'à 68 GWj/t.

L'évolution des sections efficaces microscopiques est un point clé de la simulation de l'évolution du combustible. Le calcul est effectué à chaque calcul MCNP durant l'évolution.

La section efficace d'un noyau donné dépend de la température du matériau. La figure 2 montre l'élargissement Doppler d'une résonance de l'238U pour différentes températures. Pour ce

travail, nous utilisons la librairie ENDFB6.8, et les sections efficaces à différentes température ont été produites à partir du code NJOY, dans la gamme 300K à 2000K (par pas de 100K).
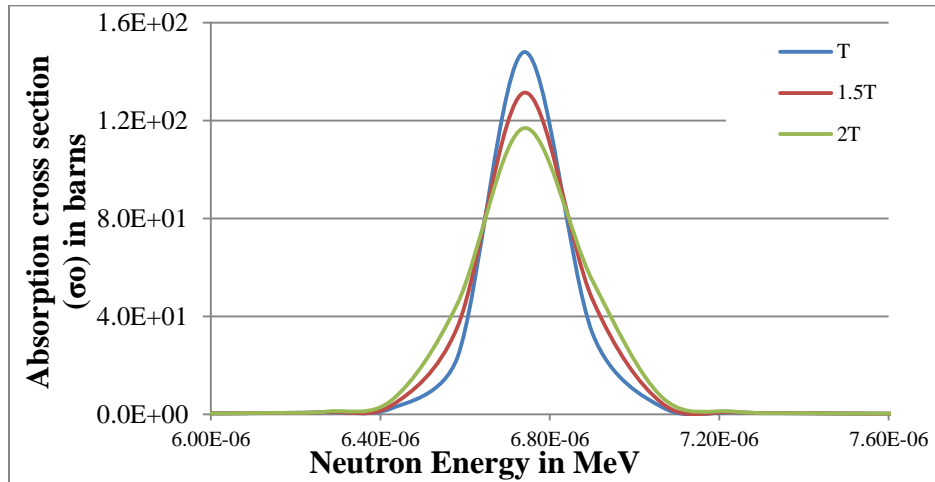
Figure 22 section efficace microscopique de capture de l'238U autour de T=1500K à l'énergie de
la première résonance.

A chaque fois que MCNP est appelé, la composition du combustible a change par réaction neutronique et décroissance. Au cours de l'évolution, MURE peut également prendre en compte des changements géométriques, de température, ou d'extraction.
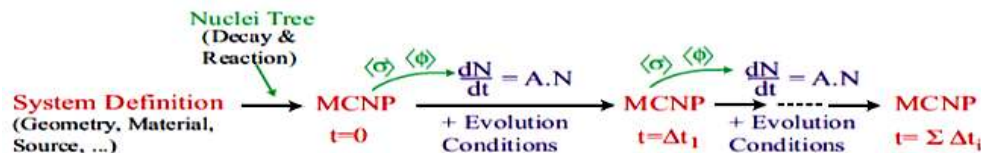
Figure 23 Schéma simplifié du principe d'évolution dans MURE [43].

Analyse du taux de combustion

Dans un combustible UOX standard, la matière fissile décroît avec le temps, les produits de fission s'accumulent, et des noyaux plus lourds que l'uranium sont produits par captures de neutrons successives. La réactivité intrinsèque du combustible décroît avec le temps. Le réacteur doit fonctionner à k =1, ce qui implique que le facteur de multiplication infini moyen des assemblages doit être supérieur à 1, en étant compensé par des poisons neutroniques. Il est possible d'irradier des combustibles jusqu'à des niveaux intrinsèques sous-critiques, en compensant cette sous-criticité par de nouveaux assemblages possédant un facteur k largement supérieur à 1. Cela implique un fractionnement du cœur du réacteur. On constate que l'évolution du k infini d'un assemblage UOX est linéaire, et on peut poser $k_\infty = k_\infty^o - \alpha t$. Appelons T la longueur d'un cycle d'irradiation et N le fractionnement du cœur, de telle sorte qu'un assemblage reste en cœur pendant un temps NT. Le réacteur doit être arrêté pour rechargement lorsque le k moyen des assemblages présents atteint 1,03 afin de prendre en compte les fuites d'un cœur réel. On obtient alors la condition suivante

$$T = \frac{2}{N+1} \frac{k_\infty^0 - k_\infty^{EOC}}{\alpha} \xrightarrow{N=1} \frac{k_\infty^0 - k_\infty^{EOC}}{\alpha} \qquad (9)$$

qui permet de calculer le temps d'irradiation, et donc le burn-up, d'un assemblage à ,aprtir du calcul de l'évolution du k infini d'un assemblage.

Le temps total de séjour en coeur (τ) est donné par

$$(\tau) = NT = \frac{2N}{N+1}\frac{k_\infty^0 - k_\infty^{EOC}}{\alpha} \xrightarrow[N\to\infty]{(NT)_{\max}} 2\frac{k_\infty^0 - k_\infty^{EOC}}{\alpha} \tag{10}$$
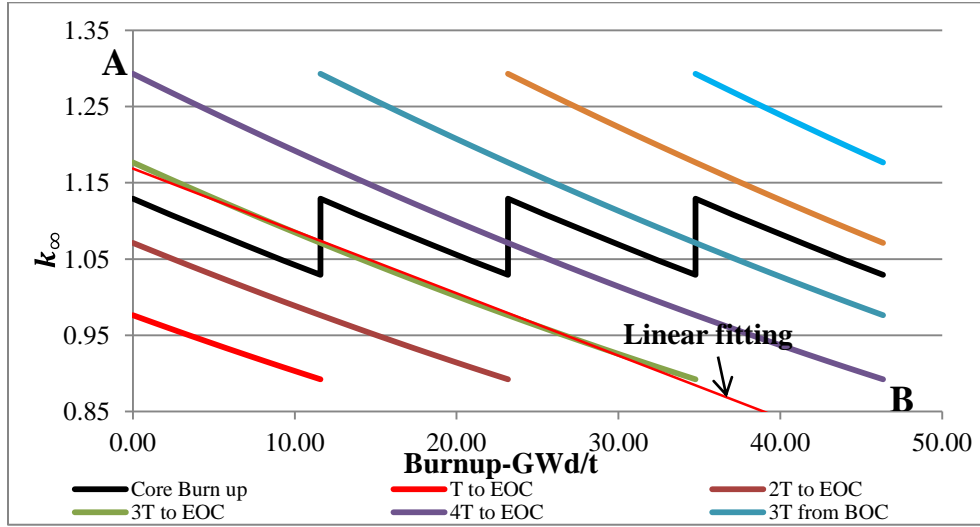
Figure 24 Illustration du calcul du burn-up en coeur à partir de l'évolution du k infini d'un assemblage pour un fractionnement de Coeur N=4 (UOX à 4.3%, N=4, k_∞^o =1.13 et k_∞^{EOC} = 1.03).

Dans le cas du MOX et MOXAm étudié ici, l'approximation liénaire n'est plus suffisante, et nous proposons une approximation quadratique $k_\infty = k_\infty^0 + \alpha t + \beta t^2$, et on obtient pour T :

$$T = -\frac{3}{2}\frac{\alpha}{\beta}\frac{(N+1)}{\Omega} \pm \left\{\left(\frac{3}{2}\frac{\alpha}{\beta}\frac{(N+1)}{\Omega}\right)^2 - \frac{6}{\Omega}\frac{K_\infty^0 - K_\infty^{eoc}}{\beta}\right\}^{\frac{1}{2}} \quad \text{où} \quad \Omega = \left(2N^2 + 3N + 1\right) \tag{11}$$

Pour β >0 et β < 0, le burnup est calculé par les équations (9) and (10) respectivement :

$$(\tau) = NT = -\frac{3}{2}\frac{\alpha}{\beta}\frac{N(N+1)}{\Omega} - \left\{\left(\frac{3}{2}\frac{\alpha}{\beta}\frac{N(N+1)}{\Omega}\right)^2 - \frac{N^2}{\Omega}\frac{6}{\beta}\left(K_\infty^0 - K_\infty^{eoc}\right)\right\}^{\frac{1}{2}} \xrightarrow[N\to\infty]{(NT)_{\max}} = -\frac{1}{2}\frac{\alpha}{\beta} - \left\{\left(\frac{1}{2}\frac{\alpha}{\beta}\right)^2 - 2\frac{K_\infty^0 - K_\infty^{eoc}}{\beta}\right\}^{\frac{1}{2}} \tag{12}$$

$$(\tau) = NT = -\frac{3}{2}\frac{\alpha}{\beta}\frac{N(N+1)}{\Omega} + \left\{\left(\frac{3}{2}\frac{\alpha}{\beta}\frac{N(N+1)}{\Omega}\right)^2 - \frac{N^2}{\Omega}\frac{6}{\beta}\left(K_\infty^0 - K_\infty^{eoc}\right)\right\}^{\frac{1}{2}} \xrightarrow[N\to\infty]{(NT)_{\max}} = -\frac{1}{2}\frac{\alpha}{\beta} + \left\{\left(\frac{1}{2}\frac{\alpha}{\beta}\right)^2 - 2\frac{K_\infty^0 - K_\infty^{eoc}}{\beta}\right\}^{\frac{1}{2}} \tag{13}$$

Table 3 Comparaison des approximations linéaire et quadratique pour un combustible UOX à différents enrichissements.

enrichissement UOX	linéaire		quadratique	
	Temps d'irradiation (années)	*Burnup (GWj/T)*	*Temps d'irradiation (années)*	*Burnup (GWj/T)*
2.0%	0.70	8.95	0.69	8.94
4.0%	3.14	40.38	3.22	41.41
6.0%	5.19	66.76	5.32	68.45
8.0%	7.06	90.86	7.25	93.32
10.0%	8.84	113.78	9.04	116.39
12.0%	10.55	135.78	10.82	139.33

Le tableau 1 montre des différences significatives entre les deux calculs, et valident ainsi la nécessité de passer à une approximation quadratique.

RADIOACTIVITE

Le processus de la radioactivité est aléatoire. Pour un noyau radioactif, la probabilité de décroître dans la seconde à venir est constante, et notée λ, ainsi la probabilité de décroître pendant time dt est λdt. On obtient donc l'équation d'évolution $dN = -N\lambda dt$. L'activité du noyau considéré, notée A, est le nombre de désintégration par seconde, l'activité totale d'un stock de noyau s'écrit donc :

$$A(t) = \sum_i A_i = \sum_i \lambda_i N_i(t) \tag{14}$$

RADIOTOXICITE

La radioactivité n'est pas suffisante pour décrire le risqué pris par un être humain lorsqu'il ingère une substance radioactive. Ce risque dépend en effet du type de radioactivité, de la forme chimique du composant ingéré, de l'énergie de la particule émise etc… Le concept de radiotoxicité par ingestion tente de quantifier ce risque en pondérant l'activité d'un noyau par un facteur de dose noté F, qui prend en compte l'ensemble des critères pertinents reliés au risque associé à l'ingestion d'un isotope radioactif. Elle s'exprime en Sievert (Sv).

Table 4 Périodes et facteurs de dose par ingestion pour quelques noyaux d'intérêts [58].

Nuclides	Life period (years)	F	Emission
Tc-99	2×10^5	0.64×10^{-9}	β-
I-129	1.6×10^7	0.11×10^{-6}	β-
Pu-238	88	0.23×10^{-6}	α
Pu-239	2.4×10^4	0.25×10^{-6}	α
Am-241	432	0.20×10^{-6}	α
Am-243	7.4×10^3	0.20×10^{-6}	α
Cm-244	18	0.16×10^{-6}	α

La radiotoxicité d'un stock de noyau i évolue avec le temps et s'écrit :

$$R_i(t) = F(i) \times \lambda_i N_i(t) \tag{15}$$

Ainsi, la radiotoxicité d'un stock de noyau s'écrit

$$R(t) = \sum_i f_i \lambda_i N_i(t) \tag{16}$$

Mono-recyclage de l'Am en réacteur REP

Dans ce travail, on considère le recyclage du Pu et de l'Am en REP, dans le but notamment de réduire la radiotoxicité des déchets issus du retraitement, ainsi que leur charge thermique.
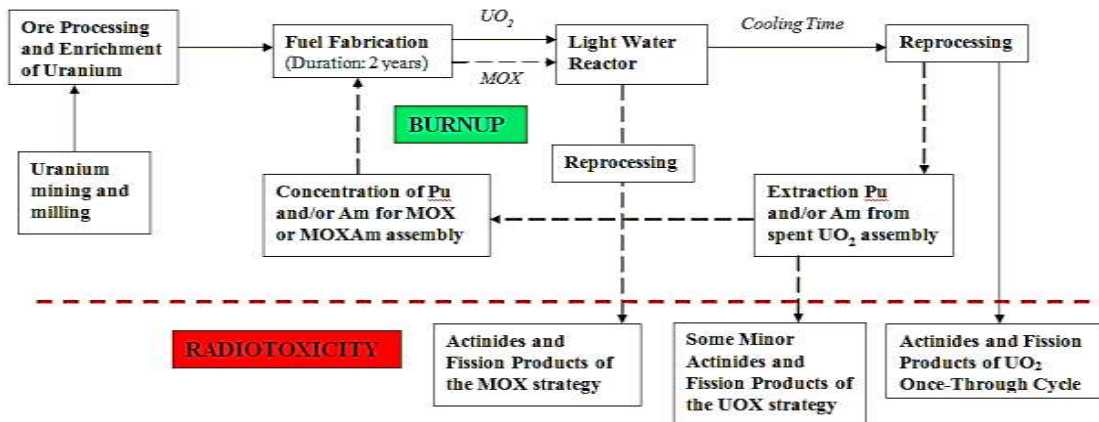
Figure 25 vision simlplifiée du cycle nucléaire UOX et MOX. Les lignes pointillées montrent le processus de recyclage du Pu et de l'Am.

Différents taux d'irradiation des UOX ont été simulés, et different temps de refroidissements avant retraitement ont été considérés. Après retraitement, un combustible MOX (U et Pu) ou MOXAm (U, Pu et Am) est fabriqué, l'uranium étant puisé dans les stocks d'uranium appauvri. Différents taux d'irradiation de ces combustibles sont envisagés, en jouant sur la concentration initiale en Pu (ou Pu+Am) dans le combustible.

La radiotoxicité du combustible usé et des verres issus du retraitement est analysée, et les différentes stratégies sont comparées. Il est important de noter que lorsque l'Am est recyclé, même si le spectre thermique n'est pas optimal pour sa transmutation en un seul passage, il reste disponible dans le combustible MOXAm usé, avec le Pu, pour une transmutation éventuelle future dans les réacteurs à neutrons rapides.

Un assemblage détaillé d'un réacteur REP a été simulé dans MURE. Les surfaces de cet assemblage sont réfléchissantes pour les neutrons, de telle sorte que nous simulons un système infini (voir tableau 3).

Table 5 Caractéristiques des assemblages REP simulés.

Materials	Paramètres
Number of fuel pins	264
Number of lattice points	17 X 17
Fuel material	UOX and MOX
U-235 Enrichment of UOX	variable for required BU
U-235 Enrichment of MOX	Depleted Uranium (0.25%)
Concentration MOX	variable for required BU
Fuel diameter	8.20mm
Clad material	Zircaloy
Clad diameter	9.50mm
Clad thickness	0.57mm
Distance between pins	12.60mm
Simulated Length of Fuel Pin	213.35mm
Power density	330W/cm^3
Moderator	H2O + 600ppm of Boron
Simulated Thermal Power	0.982MWth

Nous étudions également avec MURE les paramètres de sûreté de base (coefficients de vide, coefficients de température du combustible et du modérateur) en changeant les densités et les températures des sections efficaces utilisées.

Le combustible UOX usé est refroidi pendant 5 à 30 ans avant d'être retraité, afin d'étudier l'effet d'un long entreposage sur la production d'241Am par décroissance du 241Pu (période 14,32 années). Dans tous les cas, nous fixons à 2 ans la période nécessaire à la fabrication d'un nouveau combustible, période pendant laquelle le combustible continue d'évoluer par décroissance radioactive. La composition du nouveau combustible MOX ou MOXAm est alors définie afin d'atteindre des taux d'irradiation de 46 GWj/t et 68 GWj/t, avec ou sans l'Am issus de l'UOX usé.

Dans le seconde partie de ce travail, nous étudions le comportement neutronique du MNSR. Pour ce réacteur de recherche, le retraitement n'est pas considéré, et le combustible usé est considéré comme un déchet, destiné à être entreposé ou stocké. Les taux d'irradiation des deux combustibles envisagés (HEU et LEU) ont été simulés à l'aide de MURE. Le temps de vie du cœur est simulé à partir des conditions d'opération du MNSR utilisé comme réacteur de

recherche du Ghana (GHARR-1). La plupart des caractéristiques du cœur HEU ne changent pas lorsque l'on passe au cœur LEU, à l'exception des paramètres décrits dans le tableau 4.

Table 6 Différences entre les Cœur HEU et LEU du MNSR

Paramètre	HEU	LEU
Puissance thermique	30kW	34kW
combustible	U-Al disperse dans Al	UO_2
enrichissement	90.2%	12.5%
Nombre de crayons combustible	344	348
gaine	Aluminium	Zircaloy
U-235 chargé	~1kg	~1.357kg
Nombre de barres	6	2

Comme pour la simulation d'un assemblage REP, MURE est utilisé pour générer le fichier d'entrée à MCNP. Mais compte-tenu de la gtéométrie du cœur et de l'étude à mener, l'ensemble du cœur a été simulé, ainsi que tous les éléments de strcuture, sans utilisation de surface réfléchissantes. Puisque la gestion du combustible du MNSR est assurée par l'introduction au cours de l'irradiation de béryllium autour le cœur pour augmenter l'albebo neutronique et compenser la chute de réactivité, la simulation a été effectuée avec le béryllium introduit et toutes les barres de contrôle retirée.

Cela a été effectué pour estimer la durée de vie du cœur du MNSR à puissance nominale ou à la moitié de la puissance nominale, pour les combustibles HEU et LEU. Les paramètres de sûreté étudiés sont les mêmes que pour les REP, et la radiotoxicité du combustible usé est considérée à la fin de l'irradiation.

RÉSULTATS DU MONO-RECYCLAGE DE L'AMÉRICIUM

UOX Fuel Assembly

Différents enrichissements ont été étudiés pour les combustibles UOX, pour atteindre les taux d'irradiation de 46 GWj/t et 68 GWj/t, ce qui correspond à un enrichissement de 4,3% et 6,0% respectivement. A cause de la disparition du 241Pu pendant le refroidissement du combustible usé, avec une période de 14,32 ans, l'inventaire d'américium peut augmenter sensiblement, comme représenté sur la figure 6.
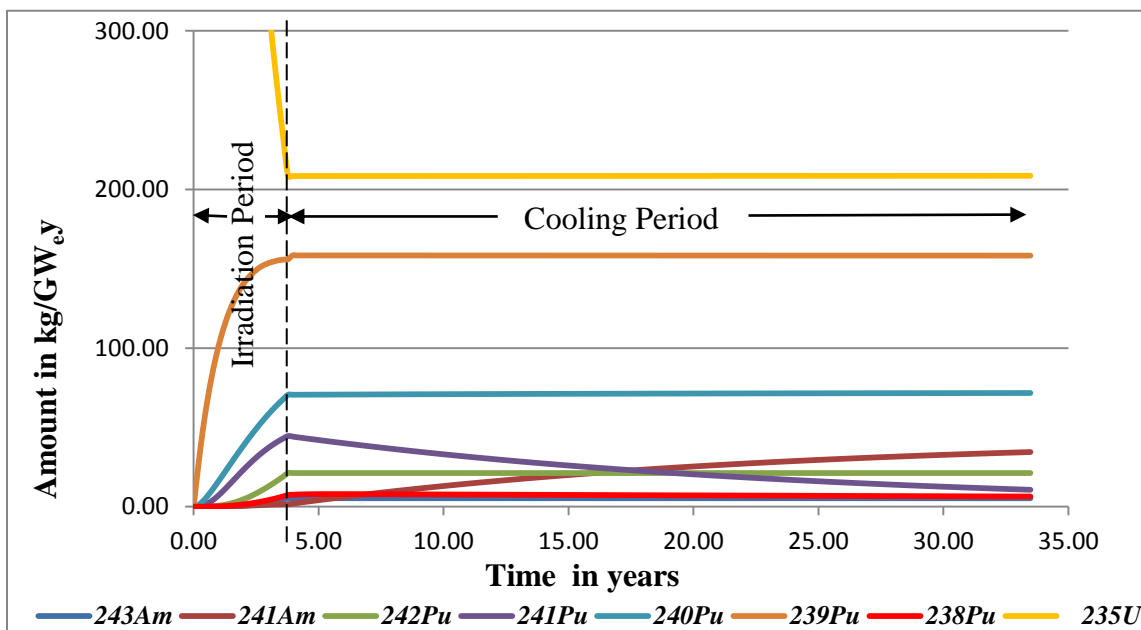
Figure 26 Evolution des principaux actinides pour un assemblage UOX (4,3%) pendant l'irradiation et le refroidissement du combustible usé.

L'accumulation de l'241Am pendant le refroidissement tend à augmenter la charge thermique des verres et leur radiotoxicité à long terme lorsque le retraitement est retardé. Environ 6,5% et 9,7% de l'uranium est consommé dans un combustible UOX qui atteint 46 GWj/t ou 68 GWj/t respectivement. Environ un quart de l'uranium consommé est converti en actinides plus lourd, principalement en plutonium. En passant de 46 à 68 GWj/t, la part de l'uranium converti en actinides passe de 27% à 24%, et la part de l'uranium converti en plutonium de 17% à 14%. Ainsi, la production d'actinides est réduite lorsque le combustible est conçu pour rester plus longtemps en réacteur.

Combustibles MOX

Le recyclage permet d'augmenter l'énergie produite à partir de l'uranium initial en faisant fissionner le plutonium en réacteur sous forme de combustible MOX [58].

Dans le but de comparer la stratégie de mono-recyclage de l'Am en REP, nous étudions également la stratégie standard de mono-recyclage du Pu telle qu'elle est pratiquée aujourd'hui, dans les mêmes conditions de simulation.
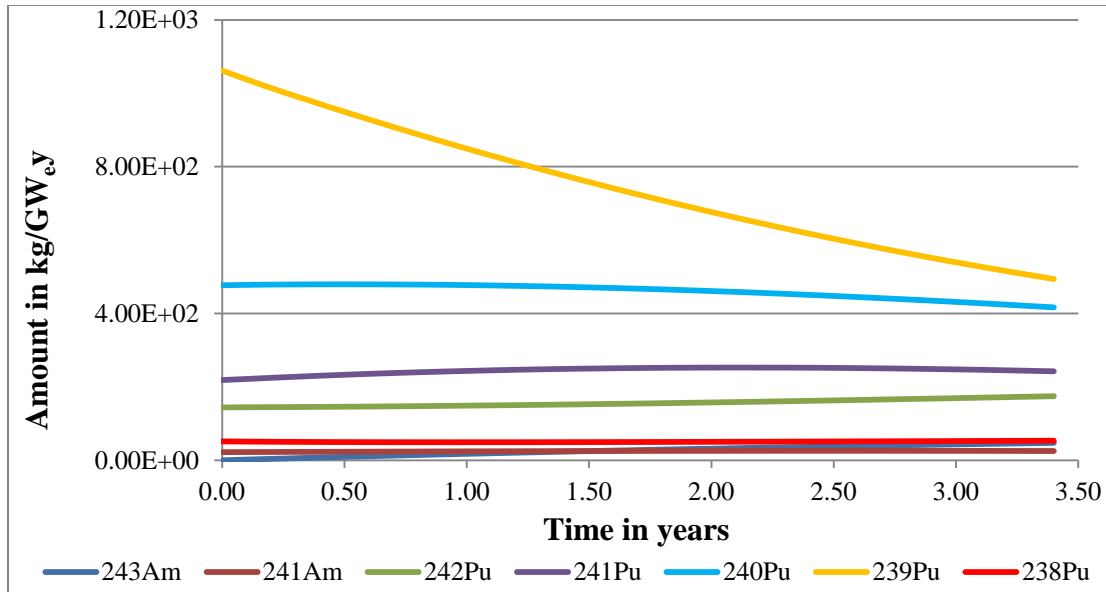
Figure 27 Evolution des principaux actinides pendant l'irradiation d'un combustible MOX fabriqué avec le Pu issu d'un UOX à 46 GWj/t.

Lorsque le temps de refroidissement de l'UOX est plus élevé, le plutonium est dégrade du fait de la disparition du 241Pu fissile, et sa concentration dans le combustible MOX doit augmenter.

Le combustible MOXAm

Le 241Pu a une section efficace de fission élevée, et l'241Am a une section efficace de capture élevée. Ainsi, le combustible MOXAm est encore plus pénalisé que le combustible MOX par un temps long de refroidissement des UOX avant retraitement. De plus, l'241Am émet, dans sa chaîne de décroissance, un gamma de haute énergie, qui complique le retraitement et la fabrication du combustible MOXAm.
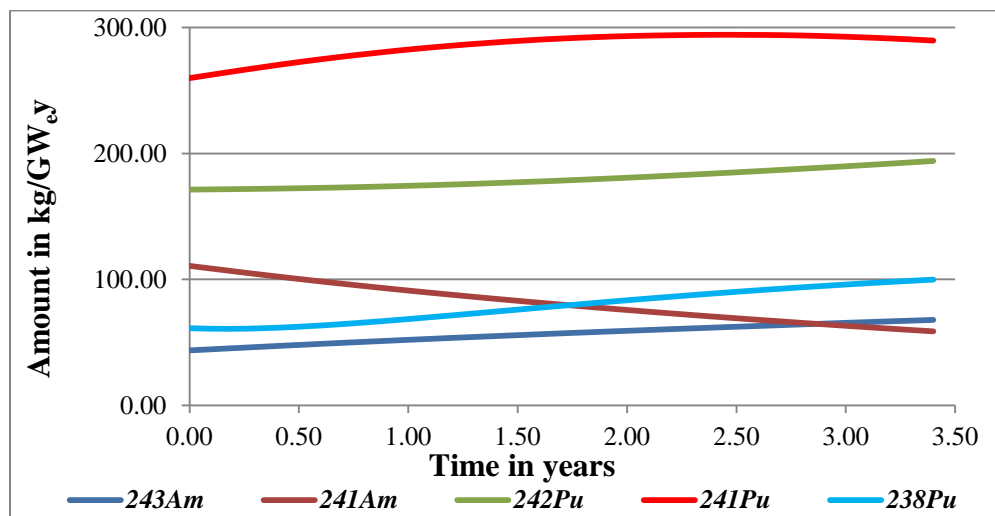

Figure 28 Evolution des principaux actinides d'un combustible MOXAm conçu pour atteindre 46GWj/t et fabriqué à partir d'un UOX refroidi 5 ans. On constate que l'241Am est transmuté pendant la phase d'irradiation, et le 241Pu continu à augmenter pendant l'irradiation.

Comparaison des stratégies de recyclage MOX ou MOXAm au cycle ouvert

Pour chaque recyclage, on calcule le facteur défini comme le nombre d'assemblages UOX à retraiter pour disposer du plutonium nécessaire à la fabrication d'un assemblage MOX. Ce facteur R est notamment utilisé pour normaliser les résultats sur la radiotoxicité totale du cycle. Le tableau 5 représente les principaux résultats obtenus pour les différentes configurations, où on peut mesurer l'impact du temps de refroidissement des UOX sur la teneur Pu des combustibles MOX, ainsi que l'impact de la présence de l'241Am, assez pénalisante lorsque le temps de refroidissement est élevé.

Table 7 Concentration de plutonium nécessaire pour atteindre les burn-up de 46 GWj/T et 68 GWj/t pour les combustibles MOX et MOXAm.

Taux d'irradiation des MOX GWd/t	concentration de Pu dans le MOX %		$R = \dfrac{MOX_{Assembly}}{UOX_{Assembly}}$	
	Cooling period of a spent UOX assembly after 46GWd/t			
	5 years	*30 years*	*5 years*	*30 years*
46	7.66	8.85	6.28	8.00
46 (with Am)	9.60	19.93	7.55	15.74
68	10.84	12.18	8.88	11.01
68 (with Am)	12.30	25.55	11.10	18.44

6.152Kg/GW$_e$.an and 8.915Kg/GW$_e$.an d'américium sont presents dans les UOX irradiés à 46 GWj/t et 68 GWj/t respectivement. Lorsque le temps de refroidissement augmente, ces valeurs augmentent, ce qui augmente la radiotoxicité des verres issus du retraitement.
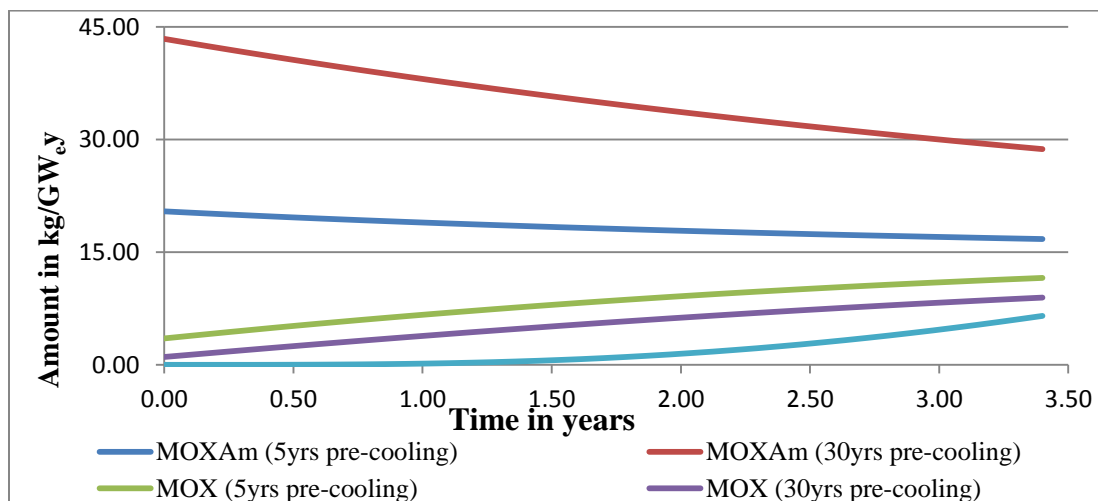

Figure 29 Evolution de la quantité d'américium dans le combustible MOX, selon les différentes stratégies envisagées, pour atteindre un taux d'irradiation de 46 GWj/t.

La figure 9 montre l'évolution de l'américium dans les différents combustibles envisagés. On y observe que les combustible MOXAm sont clairement incinérateurs d'américium, alors que les

combustibles MOX standards voient la quantité d'Am augmenter avec le temps. Même dans l'éventualité où les MOXAm n'étaient pas recyclés, le mono-recyclage de l'Am en REP aurait donc un impact positif sur la quantité totale d'Am mis aux déchets. Les concentrations d'Am en fin d'irradiation ne sont pas très éloignées entre les différents cas.

Radiotoxicité

La stratégie dominante aujourd'hui dans le monde pour la gestion du combustible usé est le cycle ouvert. Cette option est choisie ici comme option de référence pour comparer les radiotoxicités induites par les différentes stratégies envisagées dans ce travail. La figure 10 représente la radiotoxicité « par père » du combustible UOX usé (46 GWj/t) en détaillant la contribution des différents isotopes présents. Pendant le premier siècle, les produits de fission dominent la radiotoxicité, puis ce sont les différents isotopes du plutonium qui sont déterminants. Les actinides mineurs comme l'américium ont une contribution faible.
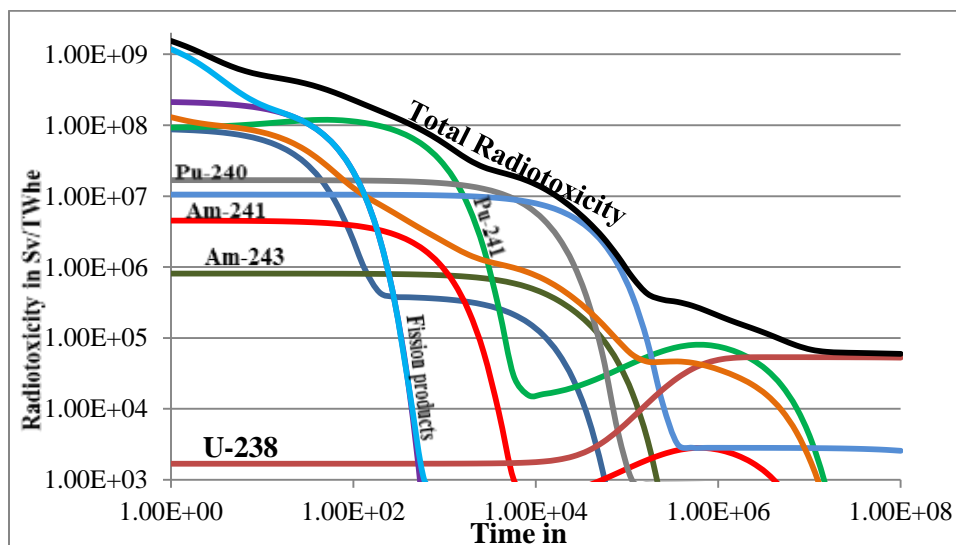
Figure 30 Radiotoxicité par père du combustible usé (UOX, 46 GWj/t) au déchargement

On constate également que lorsque le plutonium est extrait du combustible usé, l'241Am domine la radiotoxicité des verres. Sa contribution est plus élevée que sur la figure, puisque pendant la phase de refroidissement entre la décharge du combustible et la séparation, une partie importante de 241Pu sera devenu de l'241Am.

On trace sur la figure 11 la radiotoxicité des verres issus du recyclage du Pu ou du Pu+Am, et pour différent de refroidissement de l'UOX avant séparation.

Figure 31 Impact sur la radiotoxicité des verres du recyclage du Pu ou Pu+Am pour différent temps de refroidissement de l'UOX avant séparation.

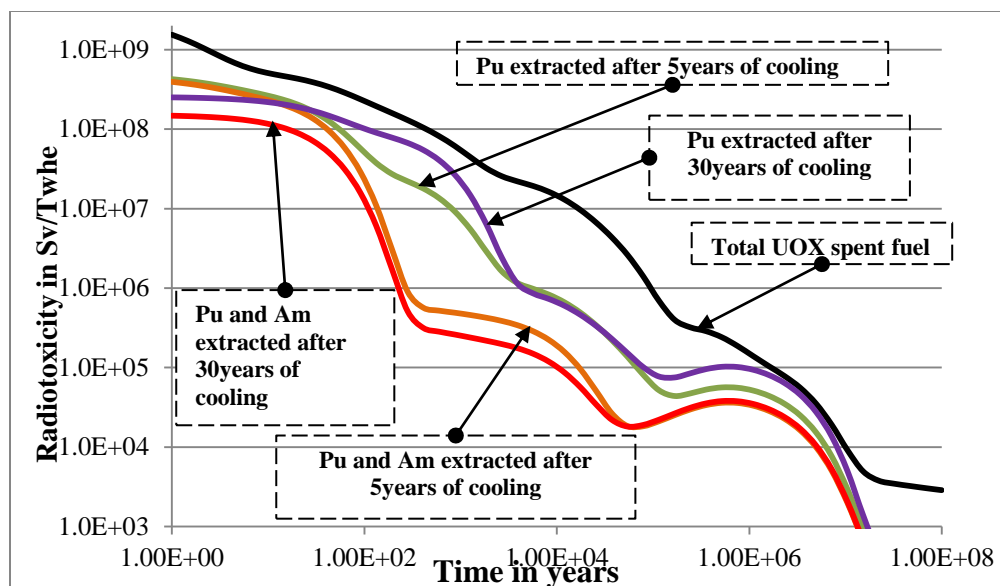Dans tous les cas, les pertes chimiques à la séparation sont prises à 10^{-3}. L'extraction de l'Am permet de réduire très significativement la radiotoxicité et la charge thermique des verres après 100 ans d'entreposage. Un long temps de refroidissement semble bénéfique dans le cas du recyclage de l'Am, ce qui est du à la décroissance du 244Cm, qui devient le 240Pu, recyclé dans le MOXAm. Cependant, comme il a été dit, un long temps de refroidissement dégrade sensiblement la qualité du combustible MOX, et encore plus du MOXAm, et peut le rendre impropre à l'utilisation en REP.

Les combustibles usés MOX ou MOXAm pourront être ré-utilisés pour démarrer d'autres réacteurs, mais pourraient être considérés comme déchets dans le cas notamment ou la filière nucléaire s'arrêtait. Dans ce cas, on peut comparer la radiotoxicité globale des différentes stratégies envisagées ici, c'est-à-dire incluant les verres issus du retraitement des UOX et les combustibles MOX ou MOXAm usés, en veillant à normaliser par le facteur R, représentant le nombre d'UOX nécessaire pour faire fonctionner un MOX, et par l'énergie totale produite par le cycle UOX+MOX (ou UOX + MOXAm). Dans le cas du mono-recyclage MOX, certains configurations où le burn-up du MOX est inférieur à celui de l'UOX, conduisent à une augmentation de la radiotoxicité par rapport au cycle ouvert, notamment lorsque le temps de refroidissement est très long, et où le 241Pu est surgénéré dans la phase MOX. A l'inverse, un MOX à 68GWj/T issu d'un UOX à 46 GWj/t après 30 ans de refroidissement ne change pas la radiotoxicité totale finale.

Dans le cas du MOXAm, réduire le temps d'irradiation et le temps de refroidissement tend à augmenter la radiotoxicité globale du cycle, principalement par le fait que l'Am ne peut être efficacement transmuté lorsque le temps d'irradiation est court. En règle général, la radiotoxicité globale du cycle n'est pas diminuée, du fait notamment des fortes concentrations de 244Cm dans le MOXAm usé. Cependant, les inventaires d'américium sont quant à eux réduits significativement.

Dans le cas où les assemblages usés étaient retraités pour en extraire le Pu avec ou sans les actinides mineurs, la stratégie de recyclage de l'Am en REP présenterait un avantage global significatif en termes de radiotoxicité de déchets vitrifiés.

Puissance résiduelle (stockage géologique)

La puissance résiduelle considérée ici est celle des déchets vitrifies et éventuellement des combustibles uses, produite par décroissance radioactive des noyaux, sur une période de quelques années à environ 1000 ans, qui est la période clé pour le dimensionnement d'un site de stockage géologique.

La figure 13 montre que l'impact de l'extraction de l'américium est très significatif comparé à un recyclage seul du plutonium. Les verres produits ont une chaleur résiduelle qui décroit très rapidement après une centaine d'année, ce qui laisse espérer des gains substantiels sur le dimensionnement d'un site de stockage, moyennant une période d'entreposage de quelques dizaines d'années.
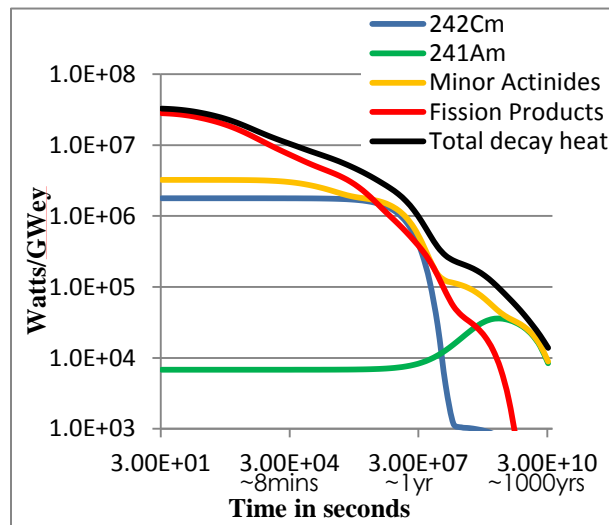

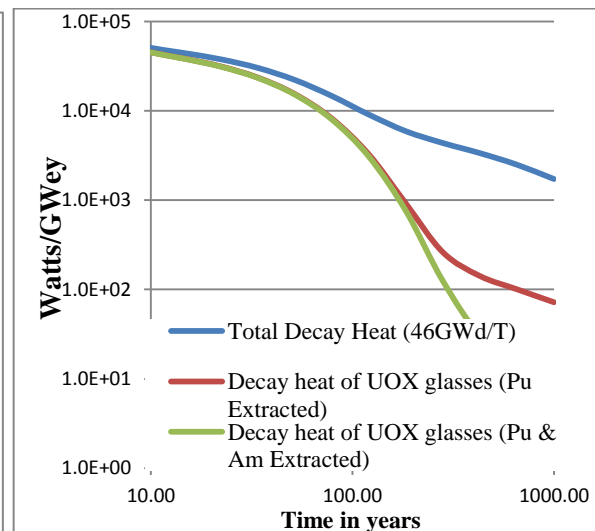**Figure 115** Puissance résiduelle d'un MOXAm usé (46GWj/t)

Figure 114 Impact de l'extraction d'actinides sur la puissance résiduelle des verres

Les actinides mineurs participent de façon non négligeable à la chaleur résiduelle d'un assemblage MOX usé après quelques années. Pour ce qui est des verres, l'extraction de l'Am permet de réduire sensiblement la puissance résiduelle sur des temps pertinents pour le dimensionnement du stockage géologique correspondant.

Coefficients de sûreté

Nous calculons ici les principaux coefficients de sûreté de base. Les contre-réactions neutroniques en fonction de la température ou de la perte du caloporteur sont nécessaires pour assurer la stabilité minimale d'un réacteur, sans pour autant être suffisantes. Sans ces contre-réactions, la moindre augmentation de puissance aurait un effet divergeant, en engendrant une hausse des températures, une baisse de la densité du caloporteur et une hausse de la puissance, conduisant à un accident de criticité.

Dans tous les cas étudiés, et notamment le recyclage de l'Am, les coefficients de vide restent négatifs. La présence d'Am, poison neutronique, demande à augmenter la proportion de

plutonium dans le cœur (d'autant plus que la présence d'241Am est corrélée à l'absence de 241Pu fissile). Ce faisant, on augmente la quantité de 240Pu et 242Pu, noyaux non fissiles avec un seuil de fission assez bas. On dégrade ainsi les coefficients de vide pour les cas les plus chargés en Am, c'est-à-dire pour le combustible MOXAm fabriqué après un long temps de refroidissement de l'UOX.

Globalement, il en est de même pour les coefficients de température – modérateur ou combustible – qui restent négatifs lorsque l'Am est recyclé. On note même que le recyclage de l'Am améliore le coefficient de température du modérateur par rapport au recyclage du Pu seul. Le tableau 6 donne les valeurs calculées des coefficients de température dans tous les cas étudiés. La valeur de référence est dk/dK = -4,473 10^{-6} (modérateur) et dk/dK = -1,953 10^{-6} (combustible) pour l'UOX (46GWj/t). Le coefficient de température du combustible reste dominé par l'élargissement Doppler des premières résonnances de l'238U, qui conduit à un effet Doppler négatif (résonance de capture).

Table 8 Coefficients de température modérateur et combustible des combustibles MOX et MOXAm.

Burn-up of MOX Assembly (GWd/t)	Temperature Coefficient ($\Delta k/\Delta K$) $\times 10^{-5}$							
	Sources of MOX and MOXAm fuel fabrication							
	5 years cooled spent 46GWd/t UOX		*30 years cooled spent 46GWd/t UOX*		*5 years cooled spent 68GWd/t UOX*		*30 years cooled spent 68GWd/t UOX*	
	Mod	Fuel	Mod	Fuel	Mod	Fuel	Mod	Fuel
46	-1.233	-2.277	-0.974	-2.169	-1.426	-2.183	-1.213	-2.119
46 (with Am)	-1.457	-2.075	-1.502	-1.608	-1.437	-1.932	-1.435	-0.949
68	-1.211	-2.274	-1.049	-2.065	-1.379	-2.238	-1.106	-2.013
68 (with Am)	-1.415	-2.019	-1.049	-2.065	-1.376	-1.859	-1.182	-1.392

RÉSULTATS DE LA CONVERSION DU COEUR DE MNSR

Le spectre de neutrons au début du cycle est modifié par le passage du combustible HEU au combustible LEU. Nous avons étudié en détail l'évolution de la réactivité et le taux d'irradiation accessible par ces deux combustibles, ainsi que les flux neutroniques obtenus dans les canaux d'irradiation. Pour ce travail, le cœur entier a été simulé, et non seulement l'assemblage comme précédemment.

Les puissances considérées sont 30 et 34 kW, correspondant à un niveau des régulateurs de réactivité à -7,5 mk pour le combustible HEU et -10,5mk pour le LEU. Le combustible LEU demande à anticiper la régulation de la réactivité par introduction de béryllium dans le réflecteur, par rapport au fonctionnement standard en HEU.

Nous avons considérés différents modes d'utilisation (puissance et gestion du cœur), et étudié la durée de vie du cœur. Le facteur keff est fixé à 1,0026 en début de cycle. Les cœurs HEU et LEU atteignent les mêmes burn-up, comme on peut le voir sur la figure 14. Cela rend les deux types de combustible tout à fait similaires en termes de potentiel d'irradiation.
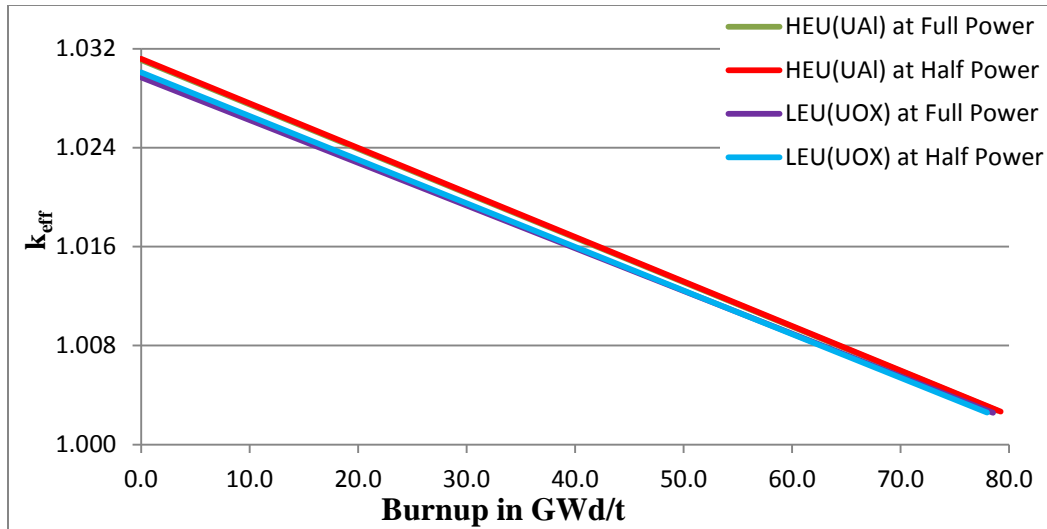
Figure 34 Evolution du facteur keff pour les combustibles HEU et LEU.

Nous avons enfin pris en compte le mode de fonctionnement du cœur, basé sur les données opérationnelles du réacteur GHARR-1 MNSR, c'est-à-dire 4h/jour à puissance divisée par deux, et 2h/j à pleine puissance. Le tableau 7 donne les principaux résultats obtenus, on on peut quantifier les légères différences entre les cœur HEU et LEU.

Table 9 Durée de vie des cœurs HEU et LEU en condition d'opération (4h/jour à puissance divisée par deux, et 2h/j à pleine puissance)

MNSR Burnup	HEU (90.2% UAl)				LEU (12.5% UOX)			
	Durée de vie simulée (jours)		Durée de vie opérationnelle (années)		Durée de vie simulée (jours)		Durée de vie opérationnelle (années)	
	P/2	*Pleine P.*	*P/2*	*Pleine P.*	*P/2*	*Pleine P.*	*P/2*	*Pleine P.*
Addition de Beryllium	117.2	75.6	3.06	3.96	109.6	50.4	2.87	2.64
Remplacement du coeur	5.3×10^3	2.6×10^3	138.55	135.94	6.2×10^3	3.1×10^3	162.08	160.08

FLUXE DANS LES CANAUX D'IRRADIATION

Le MNSR, comme la plupart des réacteurs de recherché, est conçu pour pouvoir utiliser un flux de neutrons afin d'irradier des matériaux. Puisque le MNSR est très largement utilisé pour des expériences d'activation, la connaissance du rapport des flux neutroniques dans les deux types de canaux d'irradiation (internes et externes) est un paramètre clé. Nous avons donc étudié ce point en détail pour le cœur transposé avec le combustible LEU. Les rapports de flux de neutrons moyens, pour une énergie de neutrons de 0.0001eV – 0.6.25eV est de 0.524 +/- 0.017 and 0.567 +/- 0.018 pour les cœurs HEU et LEU respectivement. Ce résultat est comparable avec les calculs antérieurs (Sogbadji et al., 2011), qui donnaient un rapport de 0,588.

RADIOTOXICITE DES COMBUSTIBLES HEU ET LEU USES

Il est également important de quantifier la radiotoxicité du combustible usé. La figure 15 montre une comparaison des combustibles usés dans différentes configurations.
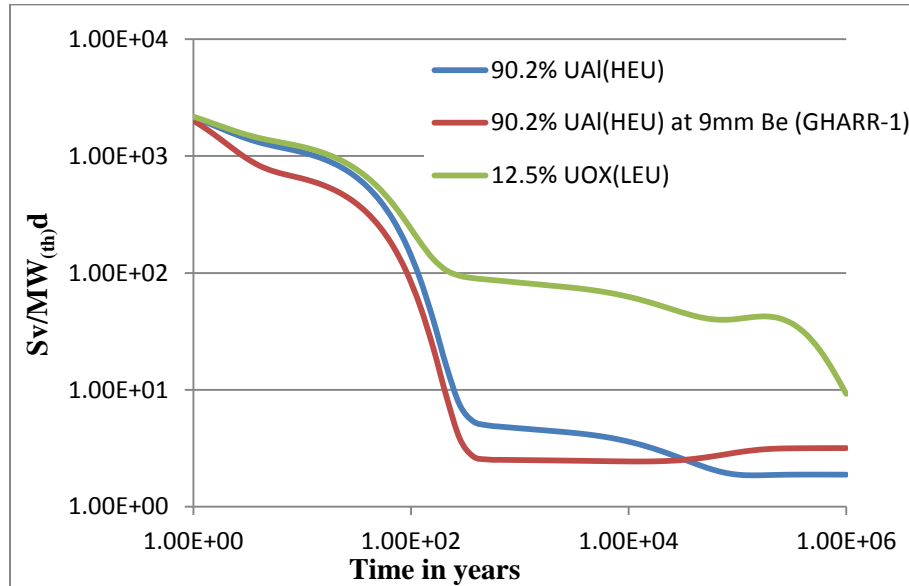

Figure 35 Comparaison de la radiotoxicité des combustibles uses pour les cas HEU et LEU, (réacteur GHARR-1), juste après la décharge du cœur.

Les produits de fission dominant la radiotoxicité du cœur, et notamment le 137Cs, pendant plusieurs dizaines d'années. La quantité de produits de fission est sensiblement la même pour les deux cœurs HEU et LEU, et la radiotoxicité des premières années est donc comparable. Au-delà, l'utilisation d'un combustible LEU conduit à une production accrue de plutonium et d'actinides plus lourds, ce qui tend à augmenter la radiotoxicité à long terme du combustible usé.

Considération de sûreté du MNSR

Nous avons comparé le comportement du coefficient de vide du modérateur pour les deux cœur HEU et LEU, ainsi que l'évolution de la puissance résiduelle après l'arrêt du cœur, qui joue un rôle de l'entreposage temporaire du combustible usé.
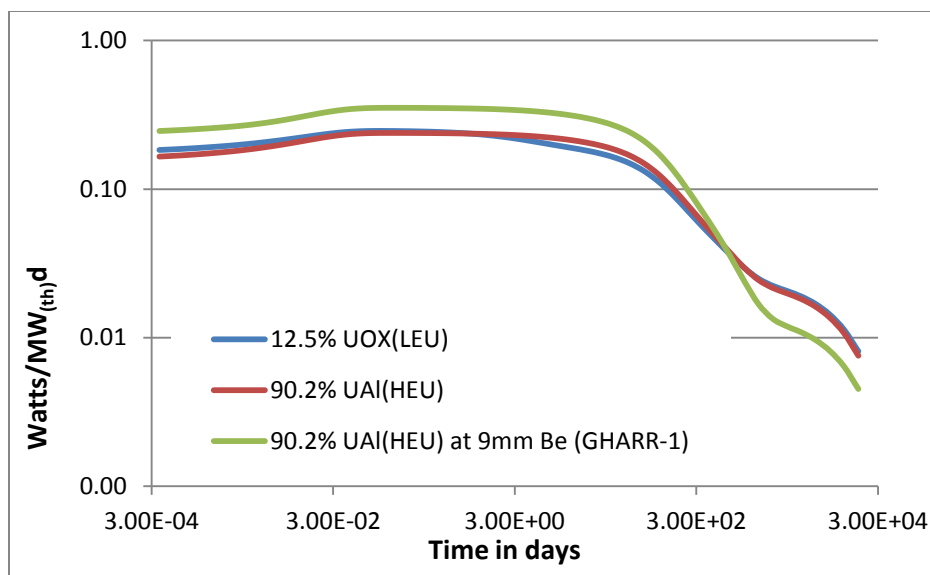
Figure 36 Comparaison de la puissance résiduelle des cœurs HEU et LEU, et du cœur actuel GHARR-1 HEU

Ici encore, les produits de fission dominant la puissance résiduelle. Le 144Ce est un contributeur important pendant les 2 années après l'arrêt du réacteur, puis le 137Cs joue un rôle important. Les deux cœurs HEU et LEU ont donc un comportement en termes de puissance résiduelle après leur durée de vie tout à fait similaires.

Coefficient de vide et de température
Du fait du caractère très compact de la zone fissile du MNSR, une modération par de l'eau et par un réflecteur en béryllium à proximité des crayons combustibles est utilisée. Ainsi, même avec une perte totale du caloporteur, il subsiste des neutrons thermiques dans le cœur du réacteur.

Les coefficients de température ont été calculés pour les deux cœurs. Le coefficient de température du cœur standard HEU est -5.12E-06 K^{-1}. On observe un changement significatif lorsque l'on passe au cœur LEU (-1.49E-05 K^{-1}), du fait de la présence beaucoup plus importante d'238U, qui joue un rôle majeur par élargissement Doppler des premières résonances de capture.

Le cœur HEU possède un coefficient de température du modérateur largement négatif de -4.00E-05 K^{-1}, qui permet de compenser son plus faible coefficient de température combustible. Pour le cœur LEU, le coefficient de température du modérateur est moins favorable mais ne change pas significativement le comportement de base du cœur. Cela est du à la présence d'238U dont la fission est favorisée lors d'une augmentation de température de l'eau induisant une diminution de sa densité.

CONCLUSIONS

Mono-Recyclage de l'Am en REP

Le mono-recyclage del'américium en REP permet de réduire très sensiblement la radiotoxicité à moyen terme des verres issus du retraitement des UOX, ainsi que leur puissance résiduelle, qui

joue un rôle majeur dans le dimensionnement d'un site de stockage. Nous avons également mené une comparaison des masses totales d'américium, et de la radiotoxicité globale des différentes stratégies, incluant les verres issus du retraitement des UOX, ainsi que les combustibles MOX ou MOXAm usés, qui devront être considérés comme des déchets dans le cas où le nucléaire s'arrêtait après ce premier recyclage. Le recyclage de l'Am eprmet dans tous les cas de réduire la quantité global d'Am produit, du fait d'une phase de transmutation en REP. Du point de vue de la radiotoxicité, elle est souvent augmentée, du fait notamment de la production supplémentaire de curium. Dans le cas où l'Am est recyclé, il reste disponible avec le plutonium, pour une transmutation éventuelle future, par exemple en réacteur rapide. Nous avons mis en évidence l'influence du temps de refroidissement des UOX sur ces paramètres, et globalement, un temps long est pénalisant, puisqu'il conduit à la disparition du 241Pu fissile, et à la production de l'Am241, poison neutronique.

Tous les combustibles étudiés, en fonction du burn-up vié, du temps de refroidissement, montrent un comportement satisfaisant du point des coefficients de base de sûreté, à l'exception de certains cas où l'UOX refroidit 30 ans avant le retraitement.

Ces études doivent être complétées par des études de sûreté plus poussées, couplant neutronique et thermo-hydrauliques, et d'un point de vue de la stratégie de mono-recyclage, les résultats obtenus pourraient être utilisés comme données d'entrée d'un code de scénario.

Conversion du cœur du MNSR

Même si le cœur LEU a une durée de vie plus élevée que le cœur initial de HEU, et consomme moins d'uranium, il est nécessaire d'anticiper l'introduction de béryllium pour compenser la chute de réactivité plus rapide. Les deux cœurs HEU et LEU montrent des rapports de flux de neutrons similaires dans les canaux d'irradiation, même si on observe une baisse de quelques % du flux thermalisé à l'intérieur et à l'extérieur des canaux pour le cœur LEU. La radiotoxicité du cœur en fin d'irradiation est plus élevée pour le combustible LEU, du fait de la présence plus importante d'238U. Concernant les coefficients de vide, ils sont négatifs pour les deux cas (HEU et LEU), malgré la présence de béryllium autour du cœur qui continue à ralentir les neutrons même en cas de perte de caloporteur. Puisque les barres de pilotages ne sont pas suffisantes pour obtenir une marge suffisante lors d'un arrêt de sûreté, il est recommandé pour le cœur LEU d'augmenter l'anti-réactivité des barres de régulation de réactivité de 3.0 mk.